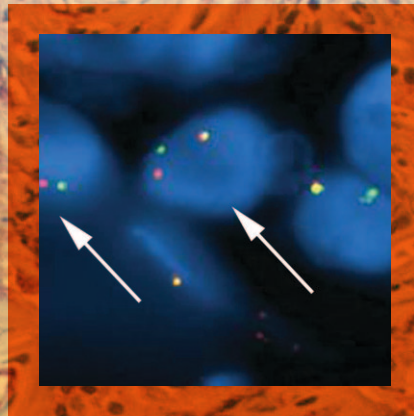
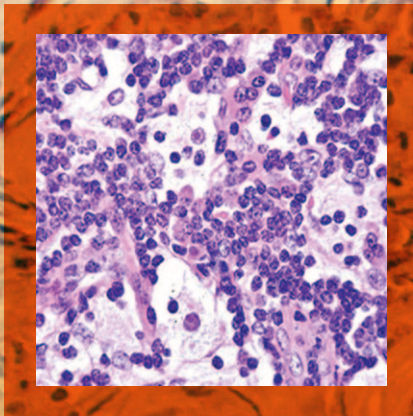


# HEAD AND NECK PATHOLOGY

Leon Barnes

Simion I. Chiosea

Raja R. Seethala



CONSULTANT PATHOLOGY

HEAD AND NECK  
PATHOLOGY

**Consultant Pathology Series**

David E. Elder, MB, ChB  
*Series Editor*

TUMORIGENIC MELANOCYTIC PROLIFERATIONS  
*David E Elder*

BRAIN TUMORS  
*Richard Prayson, Bette Kleinschmidt-DeMasters, and Mark L. Cohen*

HEAD AND NECK PATHOLOGY  
*Leon Barnes, Raja Seethala, and Simion Chiosea*

**Forthcoming Volumes in the Series**

THYROID PAPILLARY LESIONS  
*Virginia A. LiVolsi and Jennifer L. Hunt*

URINARY BLADDER DIAGNOSIS  
*Robert O. Petersen*

LIVER PATHOLOGY  
*Linda Ferrell and Sanjay Kakar*

CONSULTANT PATHOLOGY

VOLUME 3

HEAD AND NECK  
PATHOLOGY

Leon Barnes, MD

Professor of Pathology and Otolaryngology  
University of Pittsburgh School of Medicine  
Chief, Division of Head and Neck Pathology  
University of Pittsburgh Medical Center  
Professor of Oral and Maxillofacial Pathology  
University of Pittsburgh School of Dental Medicine  
Pittsburgh, Pennsylvania

Simion I. Chiosea, MD

Assistant Professor of Pathology  
University of Pittsburgh Medical Center  
Department of Pathology  
Presbyterian Hospital  
Pittsburgh, Pennsylvania

Raja R. Seethala, MD

Assistant Professor of Pathology and Otolaryngology  
University of Pittsburgh Medical Center  
Pittsburgh, Pennsylvania



**demos**MEDICAL

New York

Acquisitions Editor: Richard Winters  
Cover Design: Joe Tenerelli  
Compositor: Manila Typesetting Company  
Printer: Bang Printing

Visit our website at [www.demosmedpub.com](http://www.demosmedpub.com)

© 2011 Demos Medical Publishing, LLC. All rights reserved. This book is protected by copyright. No part of it may be reproduced, stored in a retrieval system, or transmitted in any form or by any means, electronic, mechanical, photocopying, recording, or otherwise, without the prior written permission of the publisher.

Medicine is an ever-changing science. Research and clinical experience are continually expanding our knowledge, in particular our understanding of proper treatment and drug therapy. The authors, editors, and publisher have made every effort to ensure that all information in this book is in accordance with the state of knowledge at the time of production of the book. Nevertheless, the authors, editors, and publisher are not responsible for errors or omissions or for any consequences from application of the information in this book and make no warranty, express or implied, with respect to the contents of the publication. Every reader should examine carefully the package inserts accompanying each drug and should carefully check whether the dosage schedules mentioned therein or the contraindications stated by the manufacturer differ from the statements made in this book. Such examination is particularly important with drugs that are either rarely used or have been newly released on the market.

#### Library of Congress Cataloging-in-Publication Data

Barnes, Leon, 1941-

Head and neck pathology / Leon Barnes, Simion I. Chiosea, Raja R. Seethala.

p. ; cm. -- (Consultant pathology ; 3)

Includes bibliographical references and index.

ISBN 978-1-933864-81-5

1. Head--Tumors--Histopathology--Case studies. 2. Neck--Tumors--Histopathology--Case studies. I. Chiosea, Simion I. II. Seethala, Raja R. III. Title. IV. Series: Consultant pathology series ; 3.

[DNLM: 1. Head and Neck Neoplasms--diagnosis--Case Reports. 2. Head--pathology--Case Reports. 3. Head and Neck Neoplasms--pathology--Case Reports. 4. Neck--pathology--Case Reports. WE 707]

RC280.H4B37 2011

616.99'491--dc22

2010039300

Special discounts on bulk quantities of Demos Medical Publishing books are available to corporations, professional associations, pharmaceutical companies, health care organizations, and other qualifying groups. For details, please contact:

Special Sales Department  
Demos Medical Publishing  
11 W. 42nd Street, 15th Floor  
New York, NY 10036  
Phone: 800-532-8663 or 212-683-0072  
Fax: 212-941-7842  
E-mail: [rsantana@demosmedpub.com](mailto:rsantana@demosmedpub.com)

---

# CONTENTS

<i>Series Foreword</i>	vii
<i>Preface</i>	ix
<i>Acknowledgments</i>	xi
<b>1. Squamous Cell Carcinoma—Variants</b>	<b>1</b>
1.1 Adenosquamous Carcinoma	3
1.2 Basaloid Squamous Cell Carcinoma	6
1.3 Hybrid Verrucous Carcinoma (Mixed Verrucous and Conventional Squamous Cell Carcinoma)	10
1.4 Spindle Cell Squamous Carcinoma	13
1.5 Verrucous Carcinoma—Papillary Keratosis	16
<b>2. Salivary Glands</b>	<b>19</b>
2.1 Acinic Cell Carcinoma	21
2.2 Adenoid Cystic Carcinoma With High-Grade Transformation	24
2.3 Chronic Sclerosing Sialadenitis (Kuttner Tumor)	27
2.4 Epithelial–Myoepithelial Carcinoma	30
2.5 Keratocystoma	33
2.6 Low-Grade Salivary Duct Carcinoma (Low-Grade Cribriform Cystadenocarcinoma)	35
2.7 Oncocytic Mucoepidermoid Carcinoma	38
2.8 Polymorphous Low-Grade Adenocarcinoma, Recurrent, With “Intermediate Grade” Progression	41
2.9 Salivary Duct Carcinoma	45
2.10 Salivary Gland Sebaceous Carcinoma	49
2.11 Sclerosing Polycystic Adenosis	52
2.12 Sialadenoma Papilliferum	56
<b>3. Sinonasal Tract—Nasopharynx</b>	<b>59</b>
3.1 Exophytic Schneiderian Papilloma	60
3.2 Nasopharyngeal Carcinoma	64
3.3 Respiratory Epithelial Adenomatoid Hamartoma—Inverted Papilloma	67
<b>4. Dental Lesions</b>	<b>71</b>
4.1 Calcifying Cystic Odontogenic Tumor	72
4.2 Calcifying Epithelial Odontogenic Tumor (Pindborg Tumor)	75

4.3	Dental Follicle–Dental Papilla–Myxoma	78
4.4	Glandular Odontogenic Cyst	82
4.5	Keratocystic Odontogenic Tumor (Odontogenic Keratocyst)	85
<b>5.</b>	<b>Neural-Neuroectodermal Lesions</b>	<b>89</b>
5.1	Craniopharyngioma	90
5.2	Malignant Peripheral Nerve Sheath Tumor	93
5.3	Middle Ear Adenoma–Paraganglioma–Otitis Media With Glandular Metaplasia	97
5.4	Mixed Olfactory Neuroblastoma–Adenocarcinoma	101
5.5	Mucosal Melanoma	104
5.6	Secretory Meningioma	107
<b>6.</b>	<b>Soft Tissue Tumors</b>	<b>111</b>
6.1	Angiosarcoma	112
6.2	Glomangiopericytoma—Solitary Fibrous Tumor	116
6.3	Inflammatory Myofibroblastic Tumor	120
6.4	Lobular Capillary Hemangioma	123
6.5	Synovial Sarcoma	126
<b>7.</b>	<b>Bone Tumors</b>	<b>129</b>
7.1	Central Giant Cell Granuloma	130
7.2	Chordoma	133
7.3	Ossifying Fibroma (Conventional Type)	136
<b>8.</b>	<b>Endocrine Tumors</b>	<b>139</b>
8.1	Carcinoma Metastatic to the Thyroid Gland	140
8.2	Mixed Medullary–Papillary Thyroid Carcinoma	145
8.3	Paraganglioma of Thyroid	149
8.4	Parathyroid Adenoma	152
<b>9.</b>	<b>Miscellaneous Lesions</b>	<b>155</b>
9.1	Branchial Cleft Cyst—Carcinoma	156
9.2	Eosinophilic Angiocentric Fibrosis	161
9.3	Follicular Dendritic Cell Sarcoma	165
9.4	Histoplasmosis	170
9.5	Median Rhomboid Glossitis	173
9.6	Rosai–Dorfman Disease–Rhinoscleroma	176
9.7	Wegener’s Granulomatosis	180
	<i>Index</i>	185

---

## SERIES FOREWORD

**D**iagnostic surgical pathology remains the gold standard for diagnosis of most tumors and many inflammatory conditions in most, if not all, organ systems. The power of the morphologic method is such that, in many instances, a glance at a thin section of tissue stained with two vegetable dyes is sufficient to determine with absolute certainty whether a patient should undergo a major procedure or not, or whether a patient is likely to live a healthy life or die of an inoperable tumor. In such cases, the diagnostic process is one of “gestalt,” a form of almost instantaneous pattern recognition that is similar to the recognition of faces, different brands of automobiles, or breeds of dogs. In other “difficult” cases, the diagnosis is not so obvious. In many of these cases, a diagnosis may be possible, but may be outside of the experience of the routine practitioner. In such a circumstance, it may be possible for a practitioner with more experience—a consultant—to make a diagnosis rather readily. In other cases, the problem may really not be suited to the histologic method. In these cases as well, a consultant may be invaluable in determining that it is simply not possible to make a reliable diagnosis with the materials available. In yet other cases, the diagnosis may be ambiguous, and again a consultant’s opinion can be important in establishing a differential diagnosis that may guide clinical investigation.

There are many fine consultants available to the practicing surgical pathology community. Many of them have authored textbooks, and many of them give presentations at national meetings. However, these materials can offer only a superficial insight into

the vast amount of knowledge that is embedded in these individuals’ cerebral cortices—and in their filing cabinets. This series represents an effort to enable the dissemination of this hitherto-inaccessible knowledge to the wider community. Our authors are individuals who have accumulated large collections of difficult cases and are willing to share their material and their knowledge. The cases are based on actual consultations, and the indications for the consultation, when available, are presented, because these are the records of the manner in which these cases presented themselves as being problematic. We have asked the consultants, when possible, to present their consultation letters in much the same form (albeit edited to some degree) as that in which they were first presented, because these represent the true records of the clinical encounter. In addition, we asked the authors to amplify upon these descriptions, with brief reference to the literature, and to richly illustrate the case reports with high-quality digital images. Images from books in the series, as well as additional images to amplify the presentation of the cases, will be made available on the website for downloading, study, and use in education. These images, in some cases, have been derived from virtual slides, which also may be made available in the future from a digital repository for their additional educational value.

*David E. Elder, MB, ChB, FRCPA  
Professor of Pathology and Laboratory Medicine  
Hospital of the University of Pennsylvania  
Philadelphia, Pennsylvania*





---

## PREFACE

The head and neck, arbitrarily defined as the area from the clavicles to the sella turcica, is the site of some of the most diverse and histologically complex tumors in the entire human body. Within this small, highly specialized region, one finds a remarkable range of tissues, including skin, mucosal surfaces, soft tissue, bone, lymph nodes, peripheral and central nervous system tissue, eyes, paraganglia, endocrine organs, salivary glands, and odontogenic structures. Adding to the problem, the biopsies are often small, frequently distorted, and difficult to orient for paraffin embedding, all of which impact on evaluation and diagnosis, even for experienced pathologists who deal with them on a daily basis.

With advancements in imaging and surgical techniques and the training of more and more head and neck/skull base surgeons, specimens from this area are on the increase as are our consultations. The division of Head and Neck-Endocrine Pathology at the University of Pittsburgh Medical Center currently receives approxi-

mately 1200 cases annually for diagnosis and/or second opinion. These cases range from common to extraordinary and serve as great teaching aids for our residents, fellows, and staff but otherwise lie dormant in our slide files.

To share their educational value and to more formally address some of the frequent questions raised by contributing pathologists, we have selected for this book 50 didactic cases from our consultation files for discussion and illustration. The cases were selected to illustrate the wide range of specimens seen in the head and neck and to address some of the more common, repetitive diagnostic problems that we have observed over the years. Since another book in the *Consultant Pathology Series* will be devoted to endocrine pathology, topics in this area have been curtailed to prevent duplication.

*Leon Barnes, MD*  
*Simion I. Chiosea, MD*  
*Raja R. Seethala, MD*



---

## ACKNOWLEDGMENTS

This book was made possible by the following clinicians and pathologists who graciously shared their interesting and challenging cases with us. To all of you, we extend our deep appreciation.

Dr. Sourav Ray, Mills Peninsula, California; Dr. Zenon Gibas, Longhorne, Pennsylvania; Dr. Isa Rose, University Kebangsaan Malaysia, Bangi Selangor, Malaysia; Dr. Jonas Johnson, Pittsburgh, Pennsylvania; Dr. Seungwon Kim, Pittsburgh, Pennsylvania; Dr. Carl Snyderman, Pittsburgh, Pennsylvania; Dr. Michael Venrick, Denver, Colorado; Dr. Lynnette Bornman, Columbus, Ohio; Dr. Jason Fancey, Aiken, South Carolina; Dr. Hrag Marganian, Anaheim, California; Dr. H. John Kraemer, Hollywood, Florida; Dr. Gregory Suslow, Dubois, Pennsylvania; Dr. Shaila Fernandes, Maumee, Ohio; Dr. George Yu, Hartford, Wisconsin; Dr. Asgher Zahid, Corning, New York; Dr. Kathryn Lane, Huntsville, Alabama; Dr. Barbara Ducatman, Morgantown, West Virginia; Dr. David Grossman, Troy, Michigan; Dr. John Loftis, Pittsburgh, Pennsylvania; Dr. Ralph Zade, Troy, Michigan; Dr. Edward McDade Jr., Orlando, Florida; Dr. Janis White, Clarksburgh, West Virginia; Dr. Warren White, Wilmington, North Carolina; Dr. Christopher Cold, Marshfield, Wisconsin; Dr. Jenne Lo, Urbana, Illinois; Dr. Jerry Kao, Oceanside, California; Dr. Bradford Halliday,

Scottsdale, Arizona; Dr. Ricardo Carrau, Pittsburgh, Pennsylvania; Dr. Damion Kistler, Oklahoma City, Oklahoma; Dr. Jack Causey II, Gulfport, Mississippi; Dr. Brian O'Hara, Philadelphia, Pennsylvania; Dr. Eugene Myers, Pittsburgh, Pennsylvania; Dr. Saukmal Khasnabis, Pittsburgh, Pennsylvania; Dr. Neirman Gokden, Little Rock, Arkansas; Dr. Paul Sagerman, Tuscon, Arizona; Dr. James D. Dollar, Charlotte, North Carolina; Dr. Chen-Chi Wang, Taichung, Taiwan; Dr. Gregory Suslow, Dubois, Pennsylvania; Dr. Nematollah Mirzabeigi, Monroeville, Pennsylvania; Dr. Mickey Myhre, Boise, Idaho; Dr. Zahid Asgher, Corning, New York; Dr. Steven P. Hodak, Pittsburgh, Pennsylvania; Dr. Owi Nandi, Aarau, Switzerland; Dr. Jeffrey Richmond, Erie, Pennsylvania; Dr. T. Brent Ponder, Toledo, Ohio; Dr. William E. Field II, Tempe, Arizona; Dr. William L. Chung, Pittsburgh, Pennsylvania.

We also wish to thank Ms. Linda Shab and Mr. Tom Bauer for providing many of the illustrations and Ms. Rae French and Mrs. Jenny Fullwood for secretarial support.

*Leon Barnes, MD*  
*Simion I. Chiosea, MD*  
*Raja R. Seethala, MD*



# 1 Squamous Cell Carcinoma—Variants

**M**ucosal biopsies of the head and neck are the most common specimens that we receive for second opinion. In most of these, consultation is requested for the evaluation of dysplastic biopsies that have been embedded tangentially (is there any evidence of invasion?) or for questions pertaining to histologic variants of squamous cell carcinoma (is this verrucous carcinoma?).

Because they are small and frequently distorted, tangential embedding is a common problem for everyone. Reembedding the specimen rarely resolves and often compounds the issue, and special stains, such as periodic acid-Schiff and laminin, to access breaches in the basement membranes, in our experience, are also largely ineffective. Our approach to this dilemma is to obtain multiple additional hematoxylin and eosin–stained sections at levels and, if the issue still exists, report the biopsy as “dysplasia with questionable superficial invasion.” The dysplasia should be graded and a comment added that “if there is any residual gross lesion, a repeat biopsy may be warranted and, if not, then close follow-up is recommended.”

There are 8 histologic variants of squamous cell carcinoma: conventional, verrucous, spindle cell, papillary, basaloid squamous, adenosquamous, adenoid, and lymphoepithelial. Of these, the two that we receive the most inquiries are verrucous and spindle cell.

The following comments may be helpful in evaluating these biopsies:

1. The keratinizing dysplasias (leukoplakia) are not always flat. Some are papillary and may be confused

with verrucous carcinoma (see “Verrucous Carcinoma” in this chapter).

2. Verrucous carcinoma may coexist with conventional squamous cell carcinoma. These are referred to as hybrid carcinomas, and the need to thoroughly evaluate all verrucous carcinomas microscopically for this possibility is emphasized. A biopsy that shows verrucous carcinoma but with some degree of dysplasia may be an early or incipient form of hybrid carcinoma (see “Hybrid Carcinoma” in this chapter).
3. A spindle cell lesion associated with dysplasia/carcinoma in situ of the overlying epithelium should be considered a spindle cell squamous carcinoma until proven otherwise. If suspected, do not depend on 1 epithelial marker to evaluate the spindle component. Multiple markers may be necessary, including cytokeratin (CK) 7, CK 20, pankeratin, CAM 5.2, CK 5/6, AE 1/3, epithelial membrane antigen, and p63 (see “Spindle Cell Squamous Carcinoma” in this chapter).
4. Papillary (exophytic) squamous carcinomas may be composed of keratinized or nonkeratinized epithelial cells. In the larynx, papillary nonkeratinized carcinoma can be difficult to distinguish from papillomas associated with recurrent respiratory papillomatosis. These papillomas are also predominantly, if not exclusively, nonkeratinized and often positive for human papillomavirus 6 or 11. They frequently exhibit basaloid (reserve) cell hyperplasia and occasionally mitoses in the lower one third of the epithelium. In papillary carcinoma, look for full-thickness epithelial disarray (dysplasia) and/or invasion and mitoses in all levels, some of which may be atypical.

5. Basaloid squamous carcinoma is a high-grade carcinoma composed of an invasive component of basaloid cells intimately associated with dysplasia, in situ and/or invasive squamous cell carcinoma. Small biopsies may contain only 1 component. The presence of well-demarcated islands of mitotically active basaloid cells with central necrosis adjacent to a mucosal surface should arouse suspicion of this tumor. Recuts may be helpful in identifying both elements (see “Basaloid Squamous Carcinoma” in this chapter).
6. Adenosquamous carcinoma and mucoepidermoid carcinoma (MEC) may be confused with each other. Mucoepidermoid carcinoma, even when high-grade, rarely shows keratinization or significant cellular pleomorphism and lacks a surface component of dysplasia or in situ carcinoma. Adenosquamous carcinoma, in turn, may show keratinization, cellular pleomorphism, and evidence of dysplasia and/or in situ carcinoma but lacks intermediate cells, as seen in MEC (see “Adenosquamous Carcinoma” in this chapter).
7. Adenoid squamous cell carcinoma (acantholytic carcinoma, pseudovascular carcinoma) may be confused with MEC or angiosarcoma. Adenoid squamous cell carcinoma, in contrast to MEC, lacks true glands and intermediate cells and is negative for mucin. Adenoid squamous cell carcinoma is distinguished from angiosarcoma by its strong affinity for CK and negative reaction for vascular markers.
8. Lymphoepithelial carcinoma (undifferentiated carcinoma, nasopharyngeal-type carcinoma) is seen not only in the nasopharynx but also occasionally in the base of the tongue, tonsil, sinonasal tract, and parotid gland. In the nasopharynx, it is almost always associated with the Epstein-Barr virus, whereas in other sites, the tumor is less often associated with this virus. More recent studies have shown that some of these tumors in the oropharynx (base of tongue, tonsil) are positive for the human papillomavirus and negative for the Epstein-Barr virus. Lymphoma, melanoma, and sinonasal undifferentiated carcinoma are included in the differential diagnosis.

### Selected Readings

1. Barnes L, Eveson JW, Reichart P, Sidransky D, eds. *World Health Organization Classification of Tumours. Pathology and Genetics of Head and Neck Tumours*. Lyon: IARC Press; 2005.
2. Stelow EB, Mills SE. Squamous cell carcinoma variants of the upper aerodigestive tract. *Am J Clin Pathol*. 2005;124(suppl 1): S96–109.
3. Wenig BM. Squamous cell carcinoma of the upper aerodigestive tract: precursors and problematic variants. *Mod Pathol*. 2002;15:229–254.

## 1.1

*Adenosquamous Carcinoma*

## CLINICAL INFORMATION

“An 84-year-old man presented with a 1.4-cm left erosive parasymphysial alveolar mandibular mass. Anterior segmental mandibulectomy and bilateral neck dissections were performed. This lesion has a mixed appearance, with more superficial areas resembling squamous cell carcinoma and deeper areas suggestive of a mucoepidermoid carcinoma. Preoperatively, the biopsy of the mass showed a superficially invasive squamous cell carcinoma. Also, the focus of metastatic carcinoma in one of the positive lymph nodes shows gland formation with columnar neoplastic cells. We have considered mucoepidermoid carcinoma, squamous cell carcinoma involving minor salivary glands, and adenosquamous carcinoma in our differential diagnosis.”

## OPINION

Microscopically, the neoplasm arises from the surface squamous epithelium rather than from the minor salivary glands. In situ squamous dysplastic changes (Figures 1.1.1 and 1.1.2) and invasive heavily keratinizing squamous cell carcinoma (Figure 1.1.3) are noted. The squamous cell carcinoma component is graded as moderately differentiated. The deeper part of the tumor shows glandular component (Figure 1.1.4). Importantly, the glandular component is well delineated from the squamous cell carcinoma. Mucicarmine highlights intracytoplasmic and intraluminal mucus (Figure 1.1.5). Metastatic foci show both squamous and glandular components. However, in some positive lymph nodes, the glandular component is predominant (Figures 1.1.6 and 1.1.7).

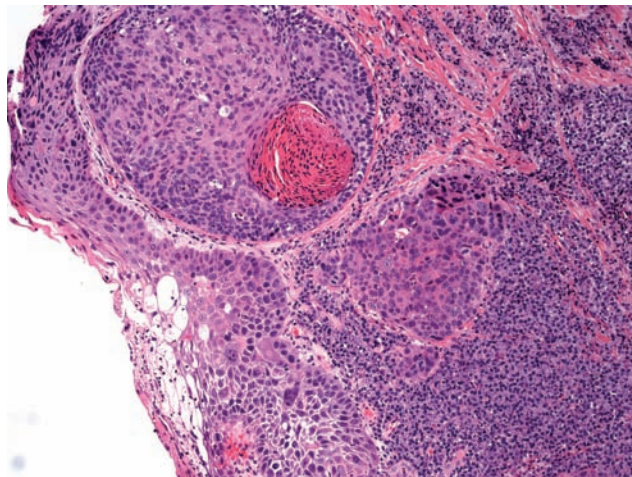


**FIGURE 1.1.1** Surface squamous dysplasia and superficial invasion, preoperative biopsy.

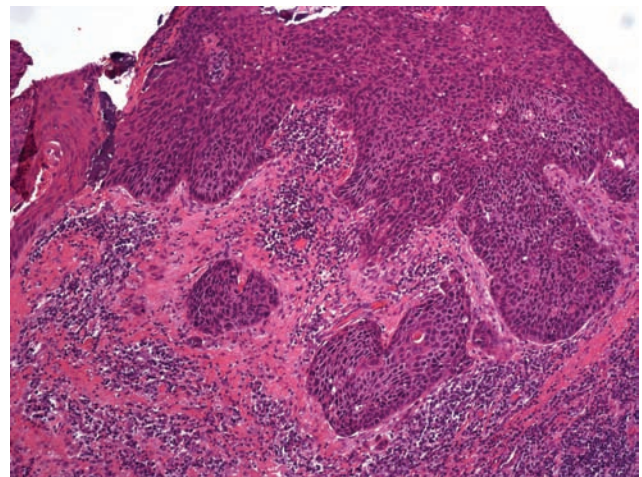


**FIGURE 1.1.2** Surface of the invasive squamous cell carcinoma, resection specimen.



## 1.1

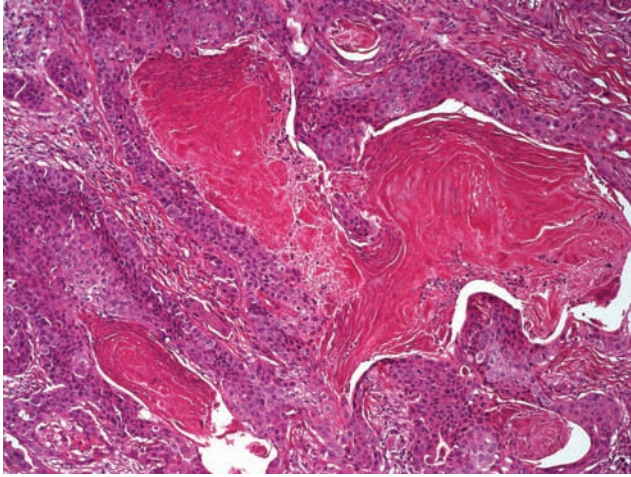


**FIGURE 1.1.3** Heavily keratinizing invasive squamous cell carcinoma, superficial part of the tumor.

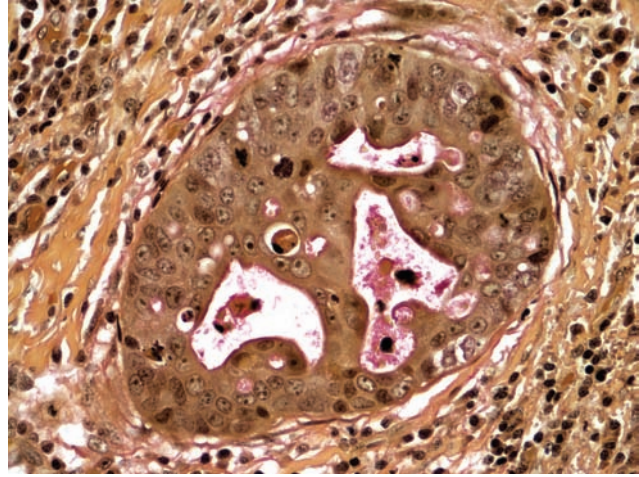


**FIGURE 1.1.5** Predominantly apical intraluminal and intracellular mucus secretions, mucicarmine.

### DIAGNOSIS

Left mandible, mandibulectomy, and bilateral neck dissections: Adenosquamous carcinoma with lymph node metastases.

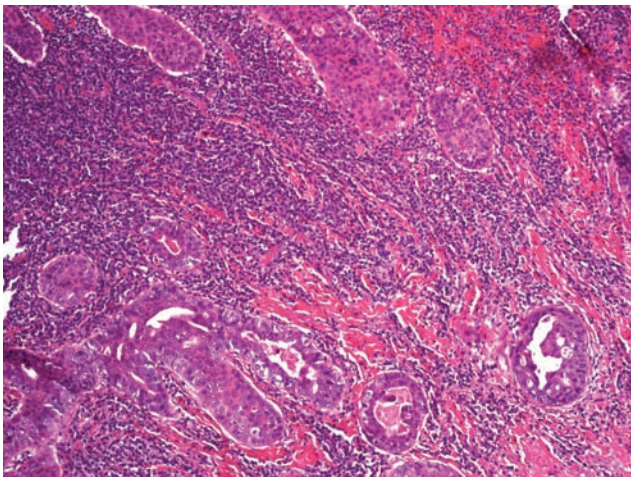


**FIGURE 1.1.4** Distinct glandular component, lower half of the field.

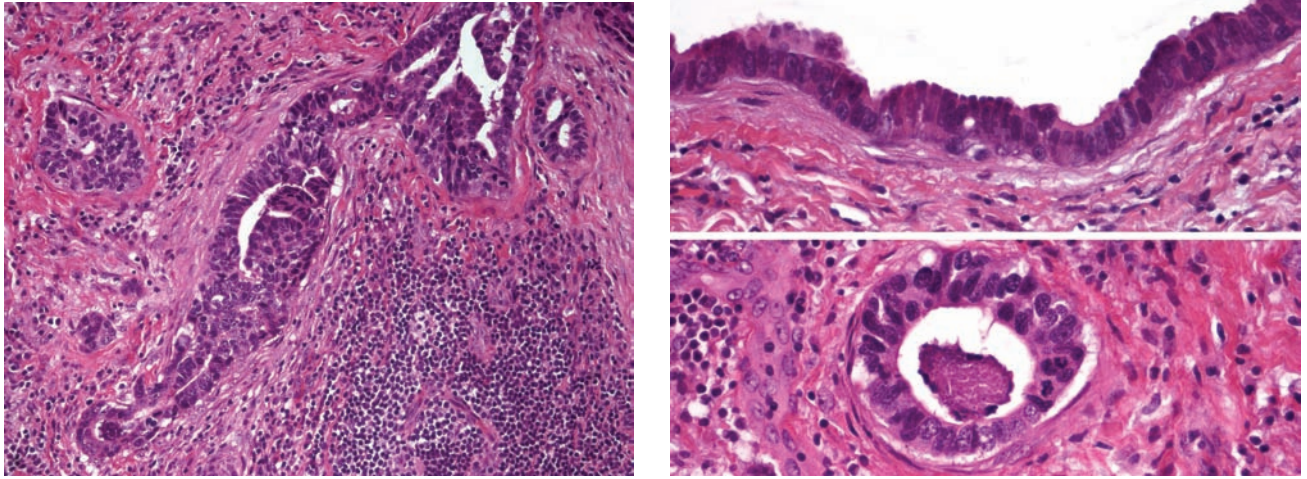
### COMMENT

We believe that the tumor is an adenosquamous carcinoma (AdSC). The diagnosis of AdSC is based on the presence of in situ dysplastic changes, heavy keratinization, and identification of 2 well-demarcated components of the tumor: squamous and glandular (1). Heavy keratinization is generally not seen in mucoepidermoid carcinomas (MECs). In addition, in MEC, glandular and epidermoid areas are intermingled, and randomly distributed within the tumor.

### DISCUSSION

The significance of distinguishing AdSC from MEC and squamous cell carcinoma is highlighted by the following:

- a. When compared to conventional squamous cell carcinomas, AdSC appears to have poorer prognosis (1). It is especially true when AdSC is compared to low-grade MEC.
- b. Metastatic AdSC with predominant glandular component may initiate erroneous search for a second primary adenocarcinoma.



**FIGURES 1.1.6 AND 1.1.7** Adenosquamous cell carcinoma metastatic to cervical lymph node. Areas with predominant glandular appearance.

### Reference

1. Alos L, Castillo M, Nadal A, et al. Adenosquamous carcinoma of the head and neck: criteria for diagnosis in a study of 12 cases. *Histopathology*. 2004;44(6):570–579.

## 1.2

*Basaloid Squamous Cell Carcinoma***CLINICAL INFORMATION**

“This is a 50-year-old man with a 3.8-cm tumor of the right tonsil and soft palate. I would appreciate your opinion.”

**OPINION**

Sections show a tumor composed of smooth contoured lobules of basaloid cells with focal central comedonecrosis (Figure 1.2.1). The cells have prominent large, round, vesicular nuclei with occasional nucleoli, and poorly defined pink cytoplasm (Figure 1.2.2). Mitoses are frequent. In some areas, the tumor contains small cystic spaces sometimes filled with amorphous, mucicarmine-negative material, creating a vague cribriform appearance (Figure 1.2.3). Other foci of the tumor contain extracellular eosinophilic

material arranged in hyaline cylinders, so-called hyalinoses (Figure 1.2.4). A small focus of conventional squamous cell carcinoma is seen adjacent to the basaloid component (Figure 1.2.5). The overlying squamous mucosa is ulcerated and, where intact, shows moderate dysplasia (Figure 1.2.6).

The tumor is strongly positive for p63 and variably positive for cytokeratins AE1/3 and Cam 5.2 (Figure 1.2.7).

**DIAGNOSIS**

Tumor, right tonsil, and soft palate: Basaloid squamous cell carcinoma.

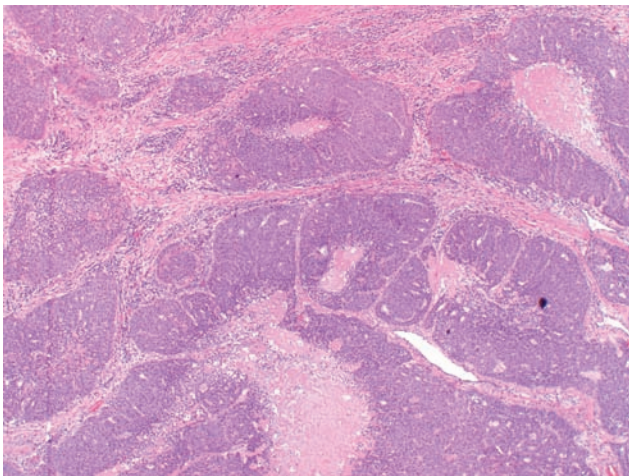


**FIGURE 1.2.1** Basaloid squamous cell carcinoma. Note the smooth contoured lobules of basaloid cells with central comedonecrosis.

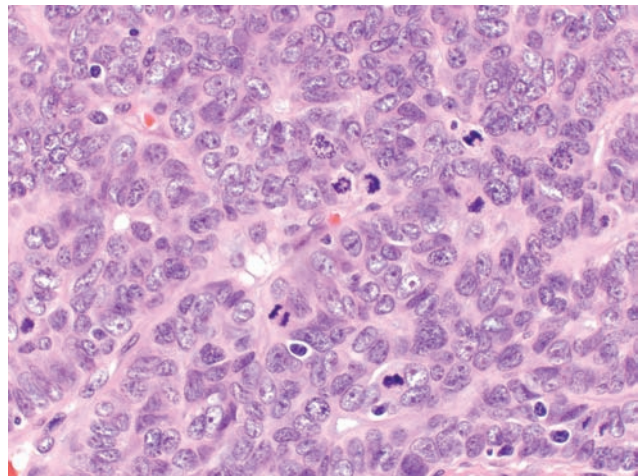


**FIGURE 1.2.2** Basaloid squamous cell carcinoma composed of large, round, vesicular nuclei with occasional nucleoli and frequent mitoses.

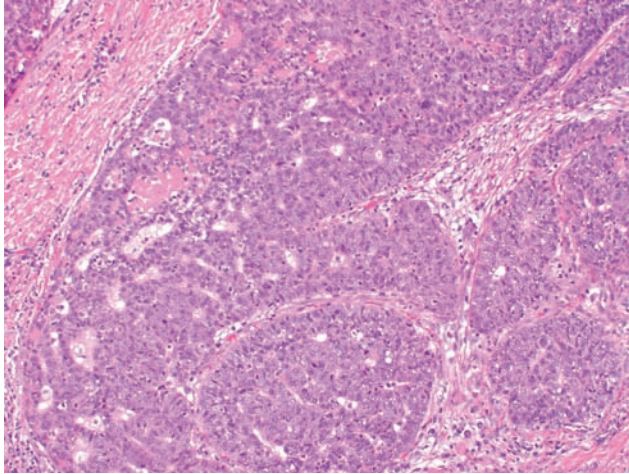


**FIGURE 1.2.3** Basaloid squamous cell carcinoma containing small cystic spaces creating a cribriform-like pattern. Compare with the cribriform pattern of ACC in Figure 1.2.10.

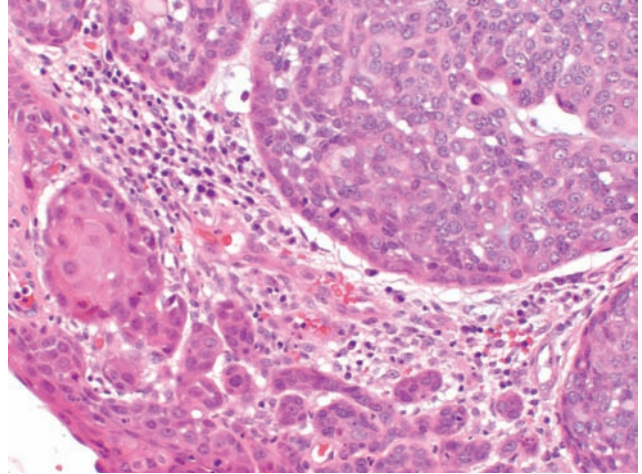


**FIGURE 1.2.5** Basaloid squamous cell carcinoma with small focus of conventional squamous cell carcinoma.

### DISCUSSION

Basaloid squamous cell carcinoma (BSCC) was first described in the head and neck in 1986 (1). Although an uncommon tumor, it is being recognized more frequently as pathologists become familiar with its appearance (2–6). It may originate in any mucosal site of the head and neck, especially the base of the

tongue, pyriform sinus, and supraglottic larynx. It occurs over a broad age range (27–88 years), with a mean of 63 years, and is more common in men (82% of all cases) (3).

Histologically, BSCC shows a biphasic pattern with basaloid and squamous elements, comedonecrosis, hyalinosis, and frequent mitoses. The squamous

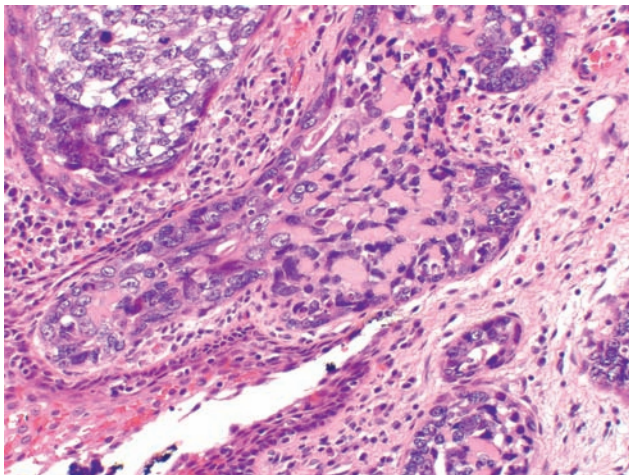


**FIGURE 1.2.4** Basaloid squamous cell carcinoma with tumor-associated hyaline cylinders (hyalinosis).

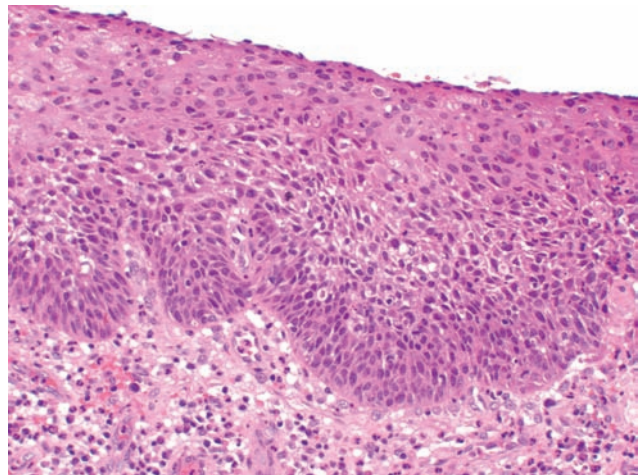


**FIGURE 1.2.6** Basaloid squamous cell carcinoma. Focus of moderate dysplasia of the overlying mucosa.

## 1.2

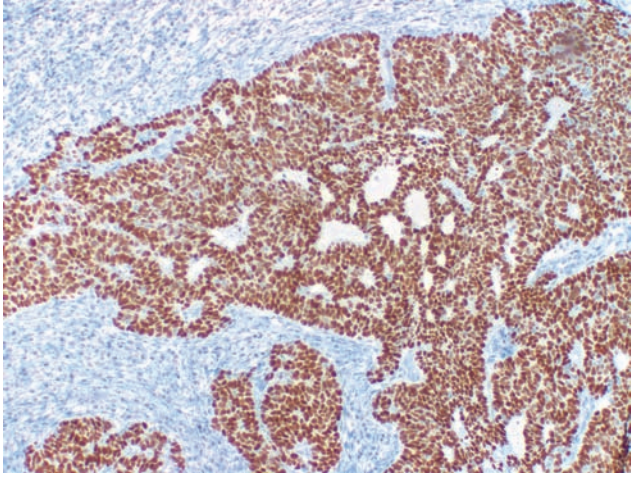


**FIGURE 1.2.7** Basaloid squamous cell carcinoma. The tumor is strongly positive for p63. Note the cribriform pattern that may result in confusion with ACC.

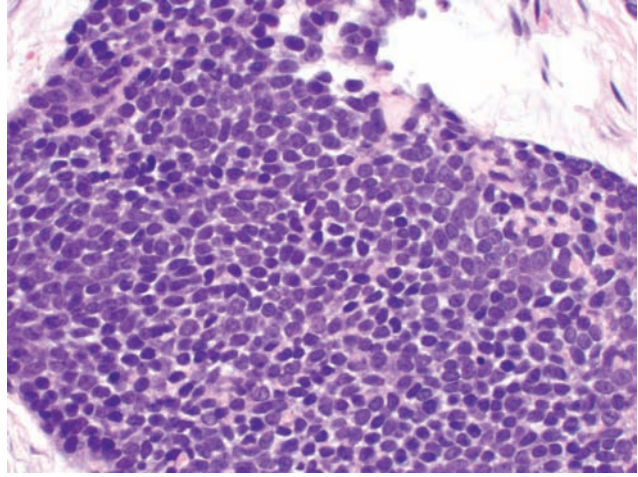


**FIGURE 1.2.9** Adenoid cystic carcinoma. The nuclei are small, hyperchromatic, and angulated. Note the absence of mitoses. Compare with the nuclei of BSCC shown in Figure 1.2.2.

component is generally small and often elusive. If there is extensive surface ulceration, as is common, only dysplastic changes may be seen. Some of the basaloid islands may also exhibit squamous differentiation, and when this occurs, the transition between the two components may be abrupt or show a zone of transition.

Basaloid squamous cell carcinomas may be associated with human papilloma virus 16 (HPV 16), with the frequency varying according to anatomic site. In one study, HPV 16 was observed in 76% of BSCCs of the oropharynx as opposed to 6% for those tumors arising in nonoropharyngeal sites (7).

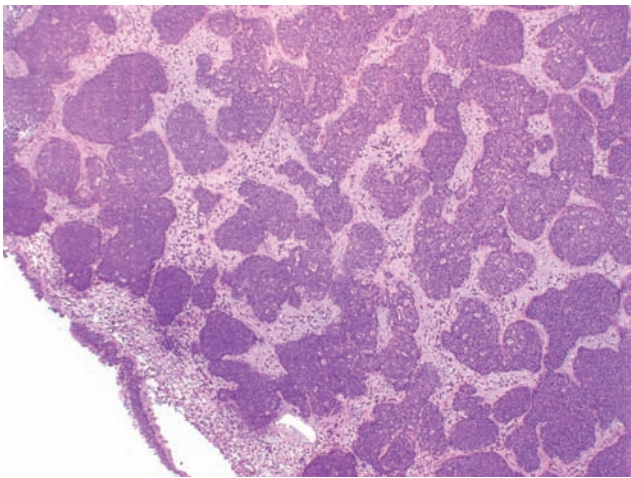


**FIGURE 1.2.8** Adenoid cystic carcinoma, solid variant. Note the absence of central necrosis of the tumor lobules. Compare with Figure 1.2.1.

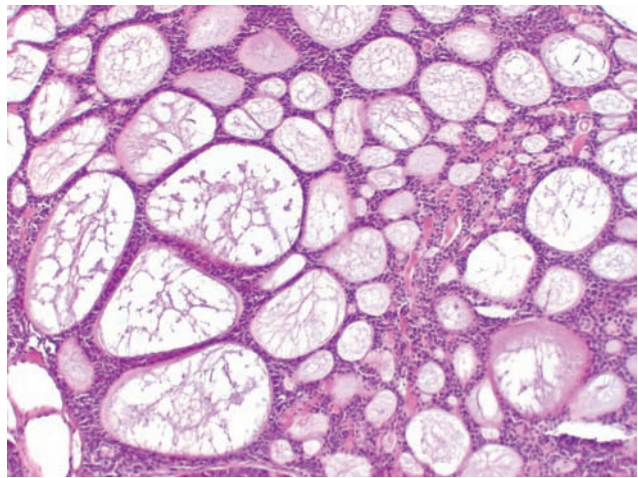


**FIGURE 1.2.10** Adenoid cystic carcinoma, cribriform pattern. If extensive, this pattern would be more in favor of ACC.

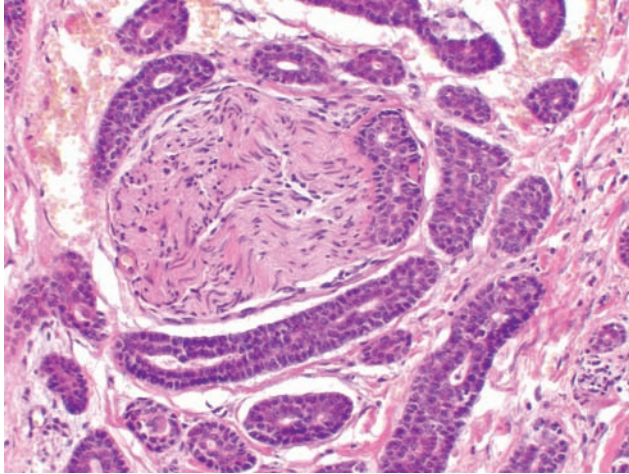


**FIGURE 1.2.11** Adenoid cystic carcinoma, perineural invasion. Extensive perineural invasion favors ACC.

The tumor is aggressive with frequent lymph node (65%) and distant metastasis (45%) to lungs, liver, and bones (3). Metastasis may be composed of basaloid, squamous, or both elements. In general, the basaloid component predominates.

At times, it may be difficult to separate BSCC from other tumors, especially the solid variant of adenoid cystic carcinoma (ACC). Clinical findings may be helpful in this instance. Adenoid cystic carcinoma is rarely associated with positive cervical lymph nodes, although this is common in BSCC. The solid variant of ACC generally shows little, if any, comedonecrosis and is composed of cells that are often small, hyperchromatic, and angulated with sparse mitotic activity (Figures 1.2.8 and 1.2.9). These find-

ings contrast with BSCC, which shows prominent comedonecrosis, round vesicular nuclei, and frequent mitoses. A prominent cribriform component and perineural invasion favor ACC (Figures 1.2.10 and 1.2.11). Adenoid cystic carcinoma also contains myoepithelial cells, which are absent in BSCC. C-kit is strongly positive in ACC and usually only focal or absent in BSCC.

### References

1. Wain SL, Kier R, Vollmer RT, Bossen EH. Basaloid-squamous carcinoma of the tongue, hypopharynx, and larynx: report of 10 cases. *Hum Pathol.* 1986;17(11):1158–1166.
2. Banks ER, Frierson HF Jr, Mills SE, George E, Zarbo RJ, Swanson PE. Basaloid squamous cell carcinoma of the head and neck. A clinicopathologic and immunohistochemical study of 40 cases. *Am J Surg Pathol.* 1992;16(10):939–946.
3. Raslan WF, Barnes L, Krause JR, Contis L, Killeen R, Kapadia SB. Basaloid squamous cell carcinoma of the head and neck: a clinicopathologic and flow cytometric study of 10 new cases with review of the English literature. *Am J Otolaryngol.* 1994;15(3):204–211.
4. Barnes L, Ferlito A, Altavilla G, MacMillan C, Rinaldo A, Doglioni C. Basaloid squamous cell carcinoma of the head and neck: clinicopathologic features and differential diagnosis. *Ann Otol Rhinol Laryngol.* 1996;105(1):75–82.
5. Paulino AF, Singh B, Shah JP, Huvos AG. Basaloid squamous cell carcinoma of the head and neck. *Laryngoscope.* 2000;110(9):1479–1482.
6. Ide F, Shimoyama T, Horie N, Kusama K. Basaloid squamous cell carcinoma of the oral mucosa: a new case and review of 45 cases in the literature. *Oral Oncol.* 2002;38(1):120–124.
7. Begum S, Westra WH. Basaloid squamous cell carcinoma of the head and neck is a mixed variant that can be further resolved by HPV status. *Am J Surg Pathol.* 2008;32(7):1044–1050.

## 1.3

## Hybrid Verrucous Carcinoma (Mixed Verrucous and Conventional Squamous Cell Carcinoma)

### CLINICAL INFORMATION

“The patient is a 55-year-old woman with a squamous proliferative lesion of the right maxillary area of the oral cavity. She is diabetic, hypertensive, and obese. She does not smoke. Your opinion will be appreciated.”

### OPINION

Sections show an exophytic, heavily keratinized proliferation of well-differentiated squamous cells with prominent bulbous rete pegs (Figures 1.3.1 and 1.3.2). The tumor has a pushing margin preceded by an intense stromal infiltrate of chronic inflammatory cells (Figure 1.3.3). Mitoses are sparse, and no keratohyaline granules are seen. These features are typical of verrucous carcinoma.

However, at the deep margin of the tumor, the cells become more pleomorphic, mitotically active, and infiltrate, which are characteristics of a conventional squamous cell carcinoma (Figures 1.3.4, 1.3.5, and 1.3.6). Transitional areas ranging from verrucous carcinoma to verrucous carcinoma with dysplasia to conventional squamous cell carcinoma are seen (Figure 1.3.3). At the tumor margin, an in situ component of both verrucous carcinoma and conventional squamous cell carcinoma is apparent (Figures 1.3.7 and 1.3.8).

About 60% to 70% of the tumor volume is verrucous carcinoma, and 30% to 40% conventional squamous cell carcinoma. No angiolymphatic or perineural invasion is seen.

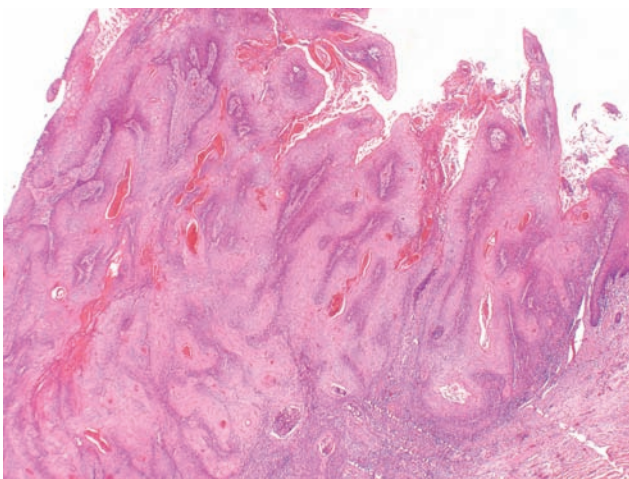


**FIGURE 1.3.1** Verrucous carcinomatous component. Tumor is exophytic, heavily keratinized, and composed of well-differentiated squamous cells.

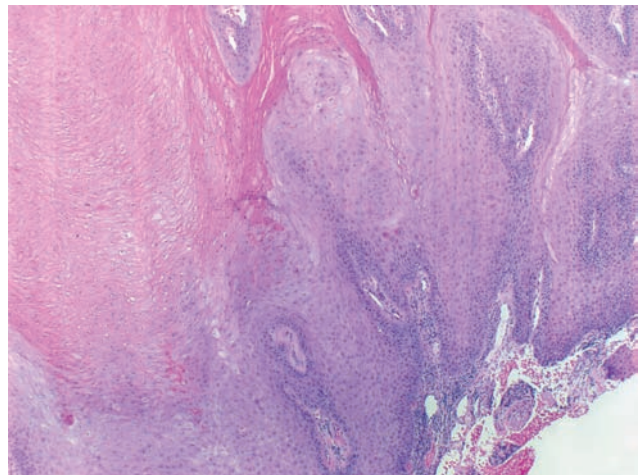


**FIGURE 1.3.2** Another higher-magnification view of the verrucous carcinoma component.

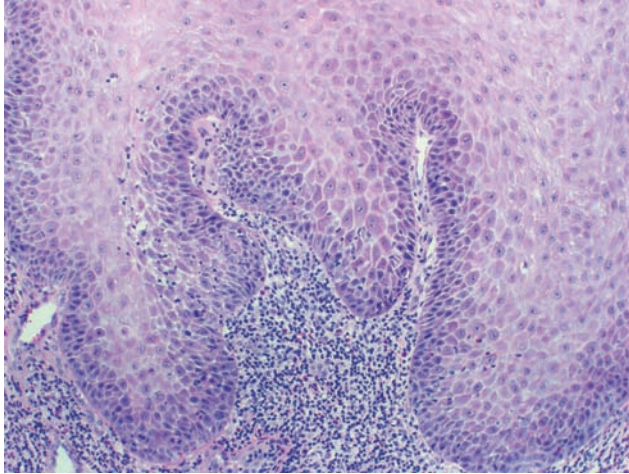


**FIGURE 1.3.3** Verrucous carcinomatous component showing mild dysplasia and a marked stromal inflammatory reaction.

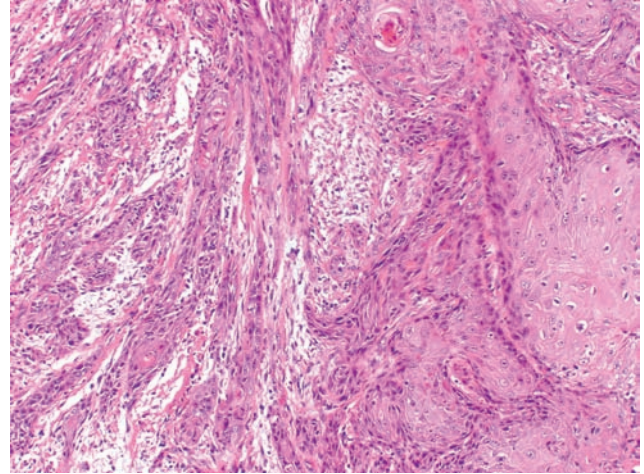


**FIGURE 1.3.5** Higher magnification of Figure 1.3.4.

#### DIAGNOSIS

Oral cavity, right maxillary area, excision: Hybrid carcinoma (mixed verrucous and conventional squamous cell carcinoma).

#### COMMENT

We believe that this lesion represents a hybrid carcinoma (HC)—a squamous cell carcinoma that has components of both verrucous carcinoma and conventional squamous cell carcinoma. The conventional squamous cell carcinoma is moderately differentiated and comprises about 30% to 40% of the tumor. No perineural or angiolymphatic invasion is seen.

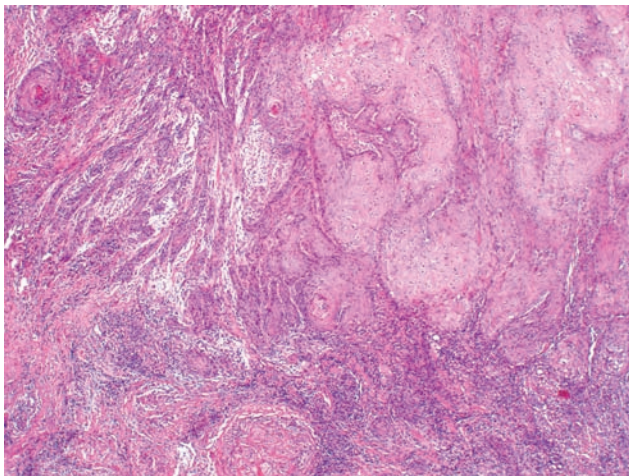


**FIGURE 1.3.4** Deep aspect of tumor showing both conventional squamous cell carcinoma on the left and verrucous carcinoma on the right.

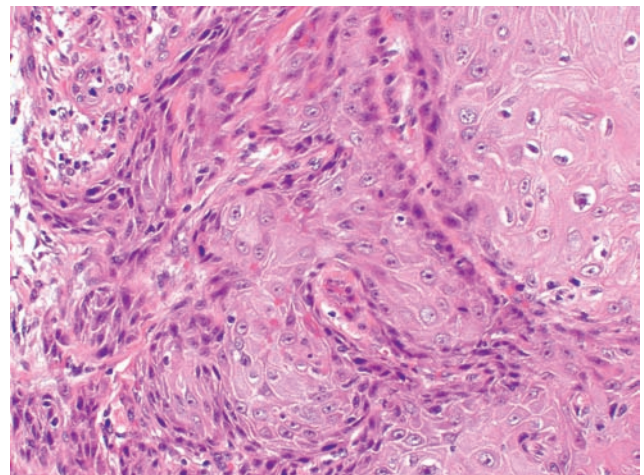


**FIGURE 1.3.6** Higher magnification of both Figures 1.3.5 and 1.3.6. Compare the pleomorphism of the conventional squamous cell carcinoma on the left with the bland appearance of the verrucous carcinoma on the right.



## 1.3

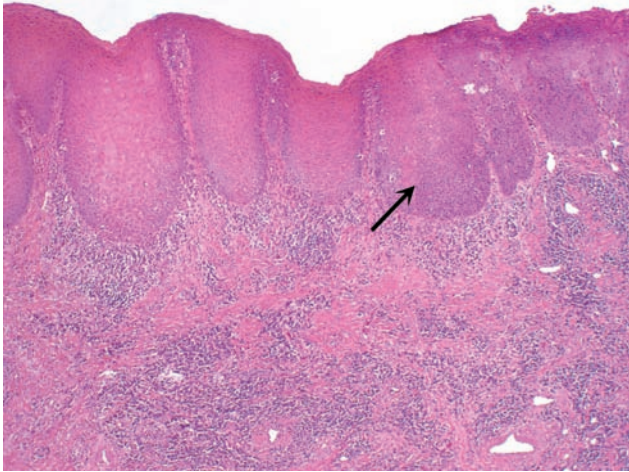


**FIGURE 1.3.7** In situ component of verrucous carcinoma on the left and conventional squamous cell carcinoma on the right. Note the abrupt transition between the two (arrow).

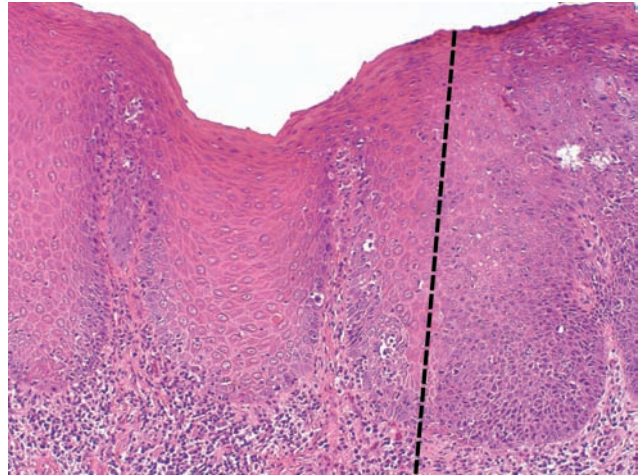


**FIGURE 1.3.8** Higher magnification of Figure 1.3.7. Again note the abrupt transition of the in situ verrucous carcinoma to the left of the dotted line and the in situ conventional squamous cell carcinoma to the right of the dotted line.

## DISCUSSION

Carcinomas composed of both verrucous carcinoma and conventional squamous cell carcinoma are referred to as HCs or hybrid verrucous squamous cell carcinomas (1–4). Although uncommon, they are being recognized more frequently. It is estimated that about 10% of all verrucous carcinomas of the larynx and 20% of all verrucous carcinomas of the oral cavity are hybrid, if thoroughly evaluated.

Grossly, these tumors usually resemble ordinary verrucous carcinoma. Microscopically, they range from those that are predominantly verrucous to those that are predominantly squamous, with gradation between these extremes. Accordingly, biopsies of HC may show only one or the other component. It is not uncommon to see a biopsy that resembles ordinary verrucous carcinoma but yet shows some degree of dysplasia (Figure 1.3.3). We sign out biopsies such as this as “verrucous carcinoma with dysplasia” and add the comment that the lesion might represent either an incipient or a nonrepresentative biopsy of an HC.

It is essential that all verrucous carcinomas be thoroughly evaluated. Failure to identify the con-

ventional squamous carcinoma portion within a verrucous lesion can result in inappropriate treatment, local recurrence, or metastatic disease (2).

Once the diagnosis of an HC carcinoma is made, it is also important to quantitate the 2 components and comment on prognostic variables, such as, “This 5-cm carcinoma is composed of 60% verrucous carcinoma and 40% conventional squamous cell carcinoma, moderately differentiated. No perineural or angiolymphatic invasion is seen. Margins of resection are free of tumor.”

## References

1. Medina JE, Dichtel W, Luna MA. Verrucous squamous-carcinoma of the oral cavity. A clinicopathologic study of 104 cases. *Arch Otolaryngol.* 1984;110:437–440.
2. Orvidas LJ, Olsen KD, Lewis JE, Suman VJ. Verrucous carcinoma of the larynx: a review of 53 patients. *Head Neck.* 1998;20:197–203.
3. Go JH, Oh YL, Ko YH. Hybrid verrucous squamous cell carcinoma of sinonasal tract: a case report. *J Korean Med Sci.* 1998;13:662–664.
4. Kato N, Onozuka T, Yasukawa K, Kimura K, Sasaki K. Penile hybrid verrucous-squamous carcinoma associated with a superficial inguinal lymph node metastasis. *Am J Dermatopathol.* 2000;22:339–343.

## 1.4

*Spindle Cell Squamous Carcinoma***CLINICAL INFORMATION**

“A 52-year-old man presented with a raised left vocal cord lesion. The patient is a smoker. We look forward to your interpretation and comments.”

**OPINION**

Histologic sections demonstrate an ulcerated polypoid mass (Figure 1.4.1). The surface of the mass is covered by fibrinopurulent exudate and granulation tissue (Figure 1.4.2). The base of the mass shows conventional squamous cell carcinoma (Figure 1.4.3). Further examination shows invasive squamous cell carcinoma and atypical spindle cells arising from the overlying carcinoma (Figure 1.4.4). Mitoses are present in both epithelial and spindle cells (Figure 1.4.5). Immunostain for cytokeratin 5/6 highlights scattered positive cells within the stroma (Fig. 1.4.6).

**DIAGNOSIS**

Left vocal cord lesion, excision:  
Ulcerated spindle cell squamous carcinoma.

**COMMENT**

The diagnosis of spindle cell squamous carcinoma (SCSC) is based on the combination of conventional squamous carcinoma with malignant spindle cells positive for cytokeratin 5/6.

**DISCUSSION**

Spindle cell carcinoma can be divided into 4 different entities: squamous cell carcinoma with reactive stroma, carcinosarcoma, collision tumor, and SCSC. In squamous cell carcinomas with reactive stroma, the

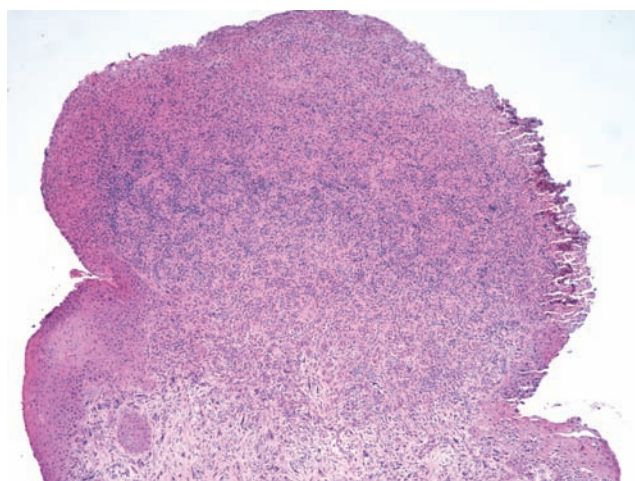


**FIGURE 1.4.1** Polypoid mass.

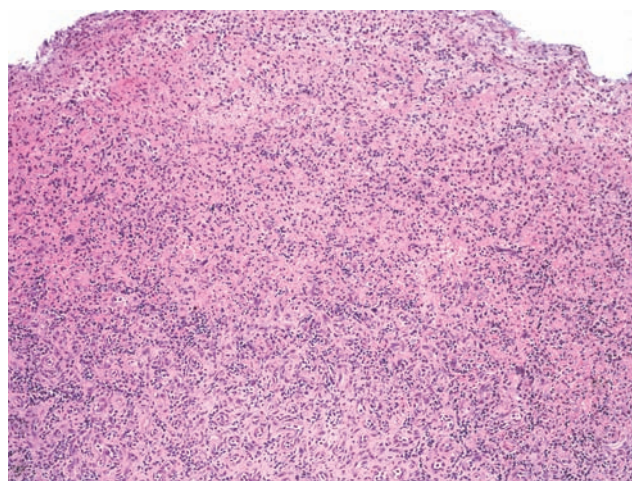


**FIGURE 1.4.2** Ulcerated surface of the tumor.

## 1.4

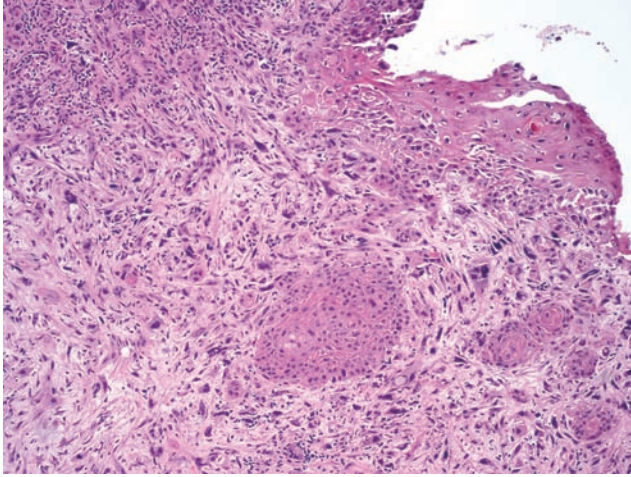


**FIGURE 1.4.3** Preserved squamous mucosa with conventional squamous carcinoma.

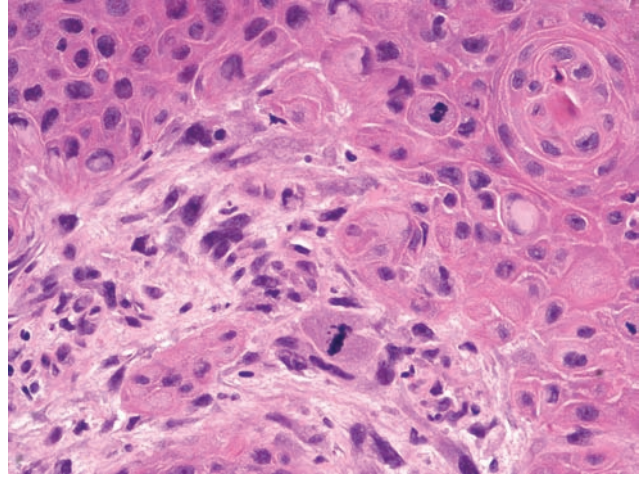


**FIGURE 1.4.5** Mitoses in epithelial and spindle cells. The spindle cells in this area are epithelioid but not nested.

spindle cells are bland or at most atypical, lack abnormal mitoses, and are uniformly negative for epithelial immunohistochemical markers. In addition, the border between carcinoma and stroma is sharp. Carcinosarcomas are characterized by foci of squamous cell carcinoma intermingled with heterologous elements of a sarcoma, for example, osteosarcoma (Fig. 1.4.7).

In rare cases when carcinomatous and sarcomatous elements are well delineated and are not intermingled, the diagnosis of “collision tumor” is favored.

Spindle cell squamous carcinoma is a variant of squamous cell carcinoma characterized by spindle cells, which mimic a true sarcoma but are epithelial in origin. The larynx, particularly the true vocal cord and the anterior commissure, is the most common

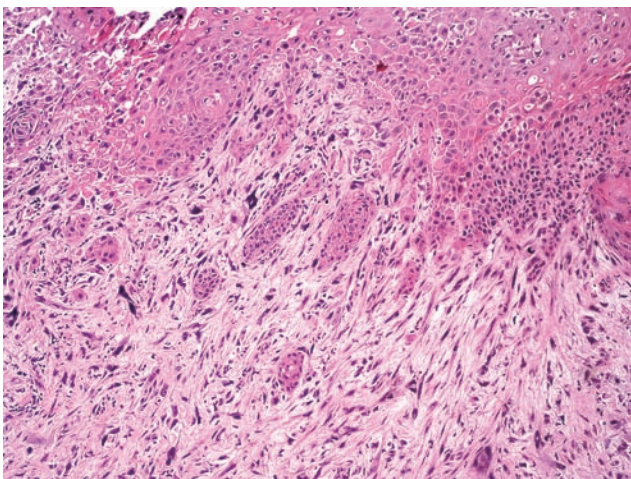


**FIGURE 1.4.4** The relationship between the recognizable squamous carcinoma and atypical spindle cells. Note the “streaming” of spindle cells from the overlying mucosa.

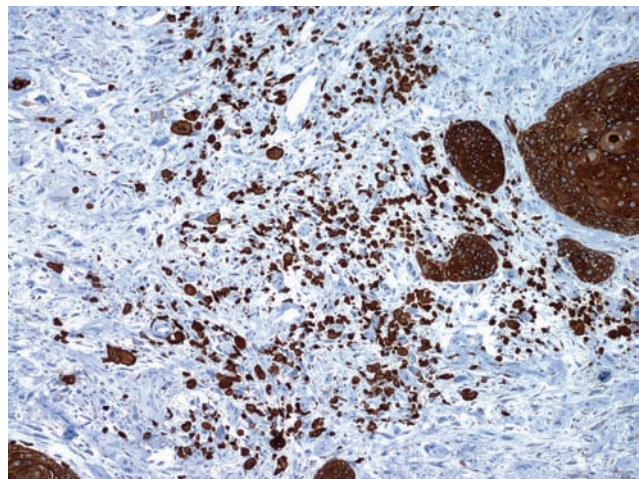


**FIGURE 1.4.6** Immunostain for cytokeratin 5/6.

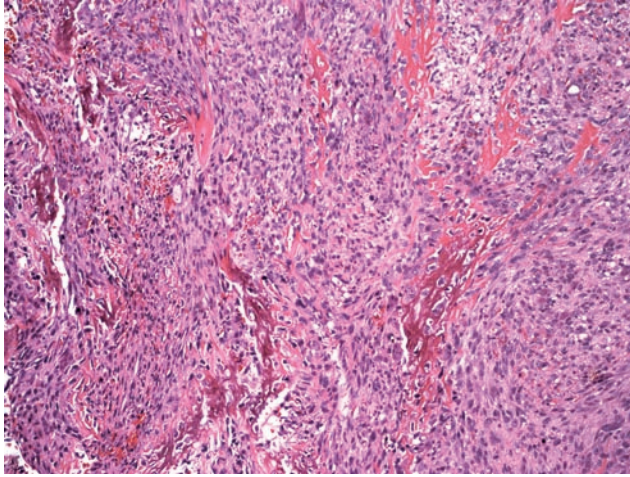


**FIGURE 1.4.7** Focus of osteosarcoma found in an SCSC. This combination is best designated as “carcinosarcoma.”

site of SCSC. About 80% of SCSCs are polypoid and affect men 50 to 80 years of age (1). About 70% of SCSCs are positive for at least 1 epithelial immunohistochemical marker (ie, cytokeratin AE1/3, cytokeratin 5/6, Cam5.2, or EMA) (1,2). About 60% of SCSCs are positive for p63 (3,4).

A diagnosis of SCSC may be challenging. First, when the ulcerated surface of the tumor is biopsied, one may render a benign diagnosis of “pyogenic granuloma/granulation tissue.” Even when rare atypical stromal cells are noted, the background of ulceration, inflammation, and vascular proliferation may still prompt the diagnosis of reactive “stromal atypia.”

Second, about two thirds of SCSCs are biphasic, that is, composed of a conventional squamous cell carcinoma and a spindle cell component (1,5). However, the remaining one third of SCSCs may be represented by spindle component only (so-called

monophasic SCSC), further complicating the diagnosis of carcinoma. Immunohistochemical studies may be helpful (see above).

Third, SCSC has to be distinguished from inflammatory myofibroblastic tumor (IMT) (6). Histologically, the mucosa overlying IMT lacks dysplasia, and the spindle cells are rather bland and without atypical mitoses (7). Immunohistochemically, myofibroblasts are focally positive for cytokeratin AE1/3 in about 60% of cases—this should not be interpreted as evidence of carcinoma (7). Exceptionally, in situ hybridization for *ALK* may be positive, confirming the diagnosis of IMT.

## References

1. Thompson LD, Wieneke JA, Miettinen M, Heffner DK. Spindle cell (sarcomatoid) carcinomas of the larynx: a clinicopathologic study of 187 cases. *Am J Surg Pathol*. 2002;26(2):153–170.
2. Lewis JE, Olsen KD, Sebo TJ. Spindle cell carcinoma of the larynx: review of 26 cases including DNA content and immunohistochemistry. *Hum Pathol*. 1997;28(6):664–673.
3. Dotto JE, Glusac EJ. p63 is a useful marker for cutaneous spindle cell squamous cell carcinoma. *J Cutan Pathol*. 2006;33(6):413–417.
4. Lewis JS, Ritter JH, El-Mofty S. Alternative epithelial markers in sarcomatoid carcinomas of the head and neck, lung, and bladder-p63, MOC-31, and TTF-1. *Mod Pathol*. 2005;18(11):1471–1481.
5. Zarbo RJ, Crissman JD, Venkat H, Weiss MA. Spindle-cell carcinoma of the upper aerodigestive tract mucosa. An immunohistologic and ultrastructural study of 18 biphasic tumors and comparison with seven monophasic spindle-cell tumors. *Am J Surg Pathol*. 1986;10(11):741–753.
6. Lewis JS. Spindle cell lesions—neoplastic or non-neoplastic? *Head Neck Pathol*. 2008;2(2):103–110.
7. Coffin CM, Watterson J, Priest JR, Dehner LP. Extrapulmonary inflammatory myofibroblastic tumor (inflammatory pseudotumor). A clinicopathologic and immunohistochemical study of 84 cases. *Am J Surg Pathol*. 1995;19(8):859–872.

## 1.5

*Verrucous Carcinoma—Papillary Keratosis***CLINICAL INFORMATION**

“Enclosed are slides of a right buccal mucosal lesion in a 63-year-old man. The slides show broad mildly atypical squamous nests that protrude into the lymphoid infiltrated submucosa. This raises a suspicion for squamous cell carcinoma. There is some atypia, with the differential diagnosis including that of a verrucous carcinoma or conventional squamous cell carcinoma. Your opinion would be appreciated.”

**OPINION**

A squamous mucosal lesion is covered by a thick scale of parakeratin and is composed of large, bulbous rete pegs that extend rather deeply into a marked

inflamed stroma (Figure 1.5.1). The cells are bland, free of mitotic activity, and exhibit random dyskeratosis (Figures 1.5.2 and 1.5.3). Keratohyalin granules are not observed.

**DIAGNOSIS**

Lesion, right buccal mucosa, biopsy: Verrucous carcinoma.

**COMMENT**

As indicated above, we believe that the microscopic findings are characteristic of verrucous carcinoma (VC).

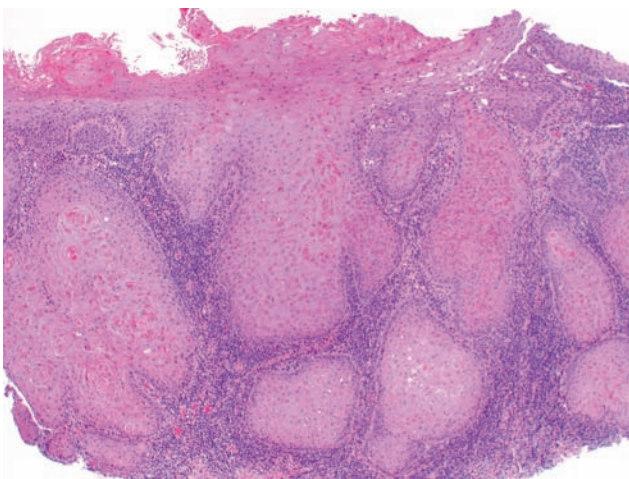


**FIGURE 1.5.1** Verrucous carcinoma. Note the large bulbous rete pegs, surface layer of parakeratin, and marked chronic inflammation.

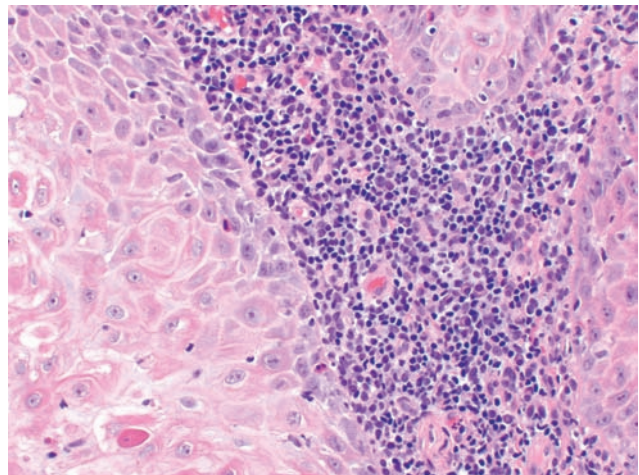


**FIGURE 1.5.2** Verrucous carcinoma. The tumor cells are cytologically bland.

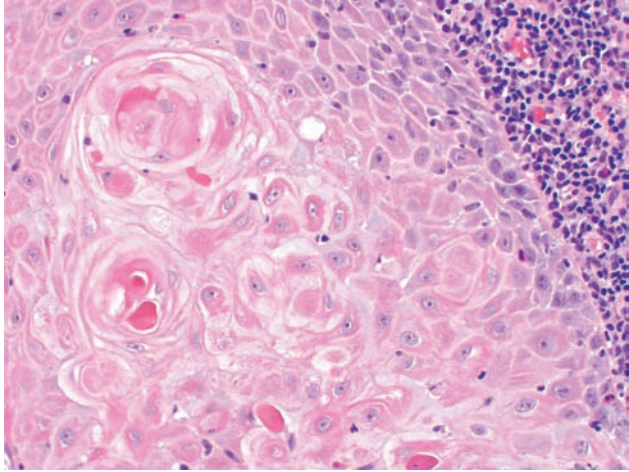


**FIGURE 1.5.3** Verrucous carcinoma. Higher magnification shows scattered dyskeratotic cells.

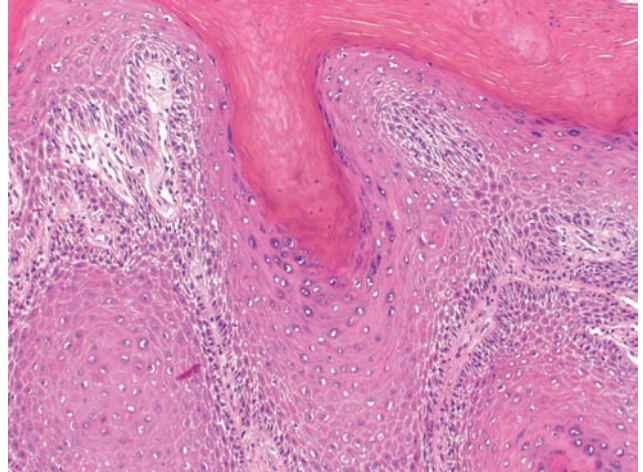


**FIGURE 1.5.5** Papillary keratosis with keratohyalin granules.

### DISCUSSION

The term *keratosis* is often used to describe mucosal lesions of the upper aerodigestive tract that show either a normal, atrophic, or hyperplastic squamous epithelium, with or without dysplasia, covered by a scale of orthokeratin or parakeratin (1). Although most keratoses are flat and localized, some are papil-

lary. These are referred to as papillary keratoses with or without dysplasia.

Distinguishing VC from papillary keratosis (PK) can be problematic, especially because biopsies tend to be small and difficult to orient and are often superficial and do not include the all-important epithelial-stromal interface (2–4).

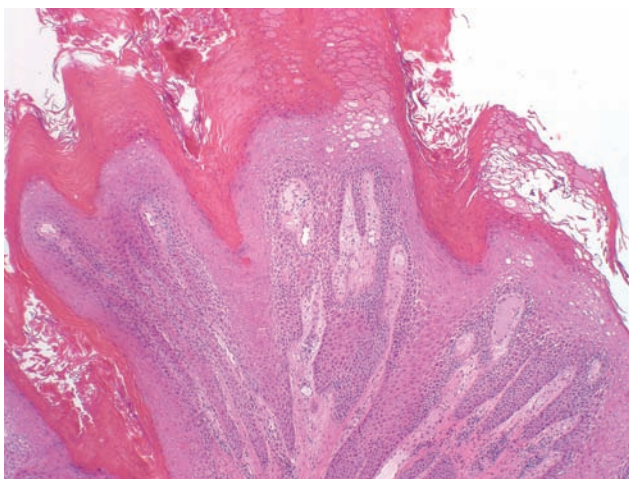


**FIGURE 1.5.4** Papillary keratosis with mild dysplasia. Note the elongated, pointy rete pegs with branching and lack of a significant inflammatory component.

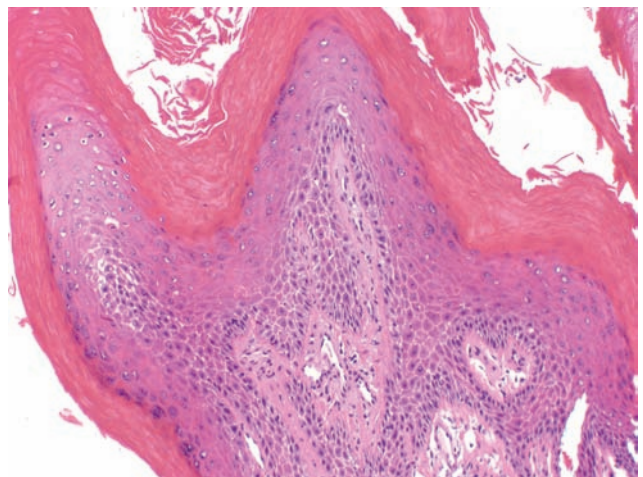


**FIGURE 1.5.6** Papillary keratosis. Higher magnification shows mild dysplasia.

## 1.5

The surface of most VCs is heavily keratinized and exophytic (wartlike). However, in small or early VCs, the surface may appear flat and nonpapillary (Figure 1.5.1). Microscopically, VC is composed of hyperplastic papillary fronds of cytologically bland epithelial cells and elongated, bulbous rete pegs that typically show little branching. Keratohyaline granules are sparse to absent. Mitoses are few and, if seen at all, tend to be concentrated in the basal region. The tumor has a pushing margin preceded by a chronic inflammatory infiltrate, which, in some cases, is so intense that it results in reactive enlargement of regional lymph nodes (Figure 1.5.1). Intralesional dyskeratotic cells, keratin pearls, and scattered stromal keratin granulomas are common (Figure 1.5.3). If the rete pegs do not extend beyond the adjacent intact normal squamous mucosa, some designate such lesions as “verrucous hyperplasia” (5).

Papillary keratosis (with or without dysplasia) can be distinguished from VC by the fact that the rete pegs in PK are thin, pointy, and often branched and the stroma is only mildly inflamed (Figure 1.5.4). Keratohyalin granules are also frequently observed (not always) in the epithelial cells just beneath the

keratin layer (Figure 1.5.5). Any degree of dysplasia is against the diagnosis of a pure VC and warrants consideration of PK with dysplasia (Figure 1.5.6). If a biopsy shows features of VC, as described above, but yet exhibits dysplasia, one should consider the possibility of an early or incipient hybrid carcinoma (mixed verrucous and conventional squamous cell carcinoma; see “Hybrid Carcinoma” case discussion in this book) (6,7).

### References

1. Barnes L. Diseases of the larynx, hypopharynx, and trachea. In: Barnes L, ed. *Surgical Pathology of the Head and Neck*. New York: Informa Healthcare; 2009:109–200.
2. Wenig BM. Squamous cell carcinoma of the upper aerodigestive tract: precursors and problematic variants. *Mod Pathol*. 2002;15:229–254.
3. Neville BW, Day TA. Oral cancer and precancerous lesions. *Ca Cancer J Clin*. 2002;52:195–215.
4. Stelow EB, Mills SE. Squamous cell carcinoma variants of the upper aerodigestive tract. *Am J Clin Pathol*. 2005;124(suppl 1): S96–S109.
5. Shear M, Pinborg JJ. Verrucous hyperplasia of the oral mucosa. *Cancer*. 1980;46:1855–1862.
6. Medina JE, Dichtel W, Luna MA. Verrucous squamous carcinoma of the oral cavity. A clinicopathologic study of 104 cases. *Arch Otolaryngol*. 1984;110:437–440.
7. Orvidas LJ, Olsen KD, Lewis JE, Suman VJ. Verrucous carcinoma of the larynx: a review of 53 patients. *Head Neck*. 1998;20:197–203.

---

## 2 Salivary Glands

The salivary glands consist of 3 pairs of major glands—parotid, submandibular, and sublingual—along with a myriad of minor glands distributed throughout the upper aerodigestive tract. Although lesions of the salivary glands are uncommon, the spectrum is wide, ranging from the following: congenital (aplasia), reactive (necrotizing sialometaplasia), metabolic (sialadenosis), autoimmune (Sjogren syndrome), inflammatory-infectious (chronic IgG4 sialadenitis), nonneoplastic (cysts), and neoplastic (pleomorphic adenoma).

In our consultation service, salivary glands are the second most frequent specimen that we receive for evaluation, exceeded only by a narrow margin by mucosal biopsies. Most of these are tumors and involve questions about classification. This is not unexpected

because these tumors are not only infrequent but 13 benign and 24 malignant primary epithelial neoplasms have been identified (see Table 2.1). The problem is further complicated by the fact that some of these neoplasms are of heterogenous composition that varies from field to field in the same lesion. Small biopsies, accordingly, can lead one astray.

In general, the probability of malignancy is inversely proportional to the volume of salivary tissue. Malignant neoplasms account for 15% to 30% of parotid tumors, 40% to 45% of submandibular tumors, 70% to 90% of sublingual tumors, and 50% of minor salivary tumors. A select group of entities, ranging from traditional to newly recognized, are presented in this section.



**TABLE 2.1** World Health Organization Histological Classification of Tumors of the Salivary Glands

Malignant epithelial tumors	Basal cell adenoma
Acinic cell carcinoma	Warthin tumor
Mucoepidermoid carcinoma	Oncocytoma
Adenoid cystic carcinoma	Canalicular adenoma
Polymorphous low-grade adenocarcinoma	Sebaceous adenoma
Epithelial-Myoepithelial carcinoma	Lymphadenoma
Clear cell carcinoma, not otherwise specified	Sebaceous
Basal cell adenocarcinoma	Nonsebaceous
Sebaceous carcinoma	Ductal papillomas
Sebaceous lymphadenocarcinoma	Inverted ductal papilloma
Cystadenocarcinoma	Intraductal papilloma
Low-grade cribriform cystadenocarcinoma	Sialadenoma papilliferum
Mucinous adenocarcinoma	Cystadenoma
Oncocytic carcinoma	
Salivary duct carcinoma	Soft tissue tumors
Adenocarcinoma, not otherwise specified	Hemangioma
Myoepithelial carcinoma	
Carcinoma ex pleomorphic adenoma	Hematolymphoid tumors
Carcinosarcoma	Hodgkin lymphoma
Metastasizing pleomorphic adenoma	Diffuse large B-cell lymphoma
Squamous cell carcinoma	Extranodal marginal zone B-cell lymphoma
Small cell carcinoma	
Large cell carcinoma	Secondary tumors
Lymphoepithelial carcinoma	
Sialoblastoma	
Benign epithelial tumors	
Pleomorphic adenoma	
Myoepithelioma	

(Barnes L, Eveson JW, Reichart P, Sidransky D. *World Health Organization Classification of Tumours. Pathology and Genetics. Head and Neck Tumours*. Lyon: IARC Press; 2005.)

### Selected Readings

- Zarbo RJ. Salivary gland neoplasia: a review for the practicing pathologist. *Mod Pathol*. 2002;15:298-323.
- Eveson JW, Nagao T. Diseases of the salivary glands. In: Barnes L, ed. *Surgical Pathology of the Head and Neck*. 3rd ed. New York: Informa Healthcare; 2009: 475-648.
- Ellis GL, Auclair PI. *Armed Forces Institute of Pathology Atlas of Tumor Pathology, Series 4, Tumors of the Salivary Glands*. Washington, DC: American Registry of Pathology; 2008.
- Barnes L, Eveson JW, Reichart P, Sidransky D. *World Health Organization Classification of Tumours. Pathology and Genetics. Head and Neck Tumours*. Lyon: IARC Press; 2005.

## 2.1

*Acinic Cell Carcinoma***CLINICAL INFORMATION**

“A 48-year-old woman presented with a left parotid cystic 2-cm mass. Is this an acinic cell carcinoma?”

**OPINION**

Histologic sections demonstrate a cystic lesion with a thick fibrous pseudocapsule (Figure 2.1.1). Most of the cyst lining is represented by a single layer of flat cells (Figure 2.1.2). Rare intracystic clusters of neoplastic cells are noted. Moderately enlarged cells with follicular growth pattern and eosinophilic cytoplasm surround the fibrotic stalks (Figure 2.1.3). Careful examination of periodic acid-Schiff stain with diastase (PASD) reveals rare enlarged zymogen granules (Figure 2.1.4).

**DIAGNOSIS**

Parotid gland, left parotidectomy: Acinic cell carcinoma, follicular, and papillary-cystic growth patterns.

**COMMENT**

The lack of increased number of classic basophilic zymogen granules makes this case particularly challenging. Constellation of smaller, fewer, and less basophilic zymogen granules is a known diagnostic dilemma with acinic cell carcinoma (ACC). This combination of histologic findings is more frequently encountered

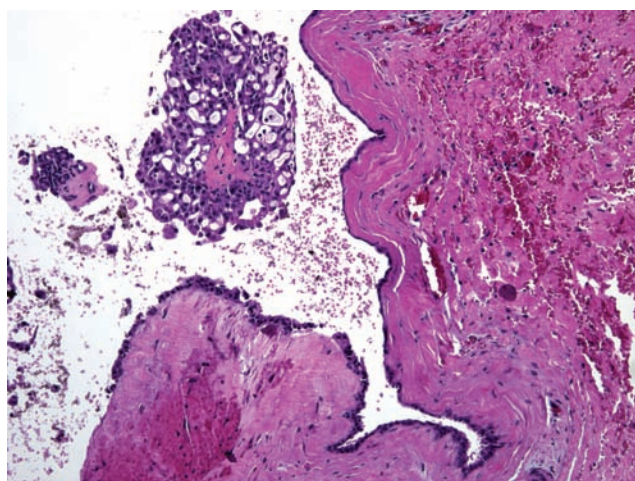


**FIGURE 2.1.1** Cystic lesion with thick fibrous pseudocapsule and clusters of neoplastic cells.

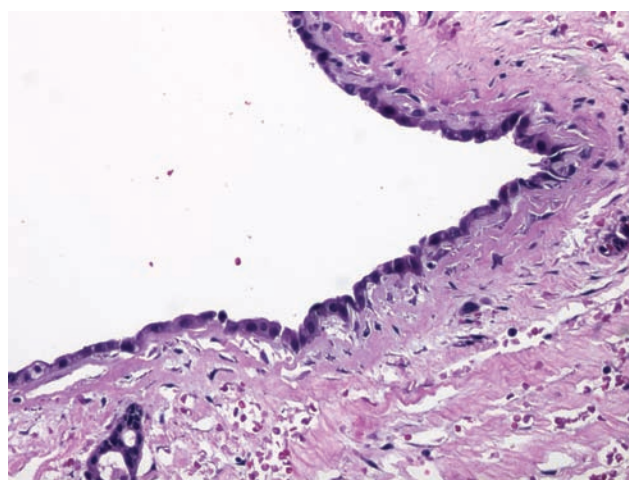


**FIGURE 2.1.2** Cyst lining—single layer of flat cells.

## 2.1

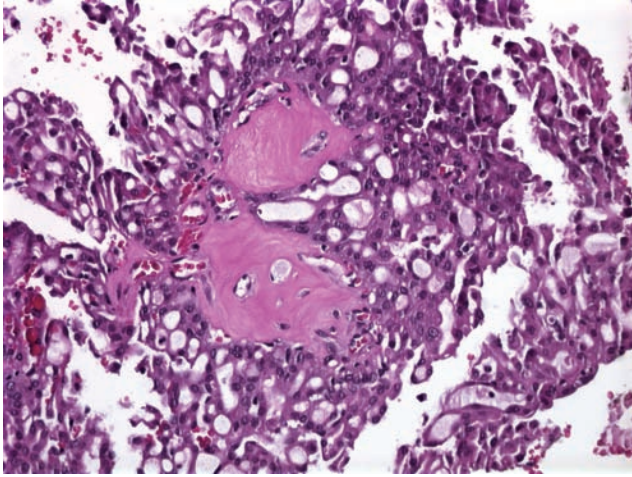


**FIGURE 2.1.3** Intracystic cluster of neoplastic cells. Note follicular growth pattern and eosinophilic cytoplasm.

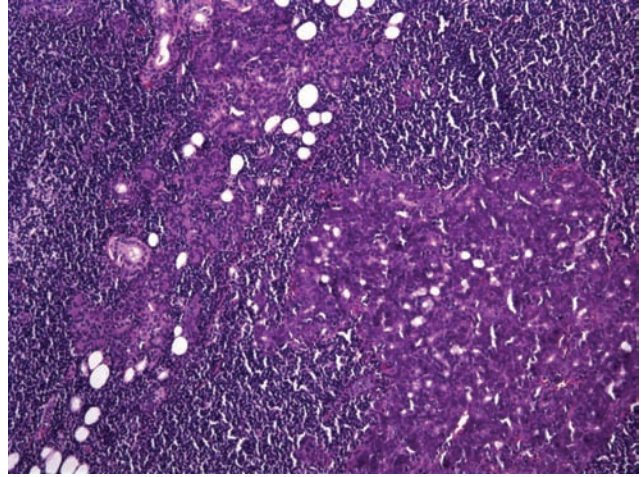


**FIGURE 2.1.5** Exuberant tumor-associated lymphoid infiltrate intimately admixed with ACC mimicking a metastatic process.

in ACCs arising in minor salivary glands. Demonstration of zymogen granules on PASD is diagnostic.

### DISCUSSION

This case illustrates diagnostic challenges posed by the papillary-cystic variant of ACC. Namely, the luminal epithelial proliferation may be extremely sparse, and

the lining may be just 1 cell thick or entirely absent when the cyst is ruptured. The cells with acinar differentiation are usually less numerous in the papillary-cystic variant than in the solid or follicular variants of ACC. It is prudent to entirely submit cystic salivary lesions for histologic evaluation. This approach may help to avoid “missing” the diagnosis of ACC.

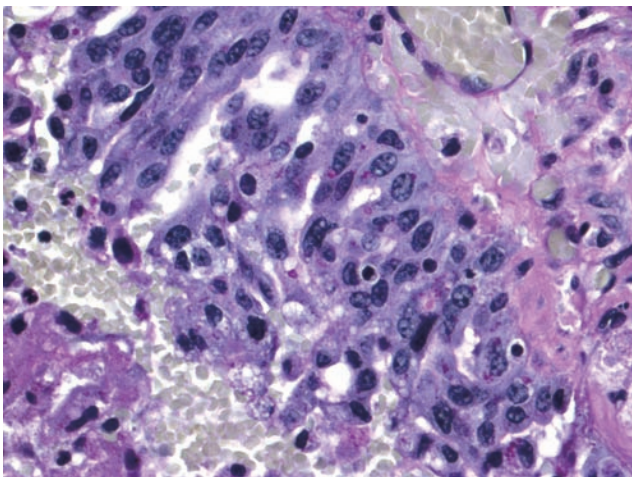


**FIGURE 2.1.4** Rare enlarged cytoplasmic zymogen granules as seen on PASD.

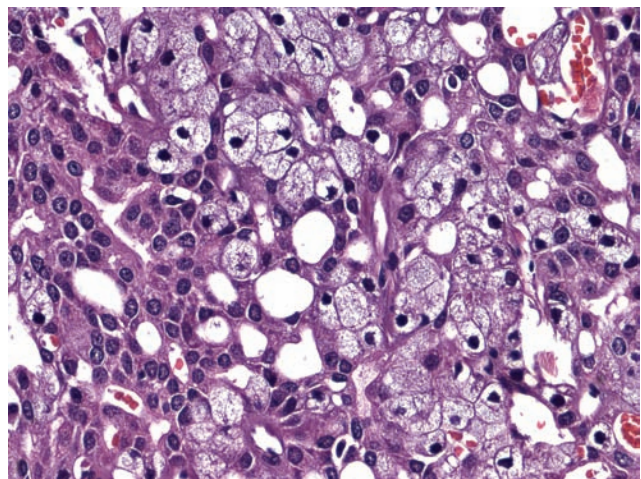


**FIGURE 2.1.6** Cell of acinic cell carcinoma with abundant finely vacuolated cytoplasm mimicking mucinous/sebaceous cells.

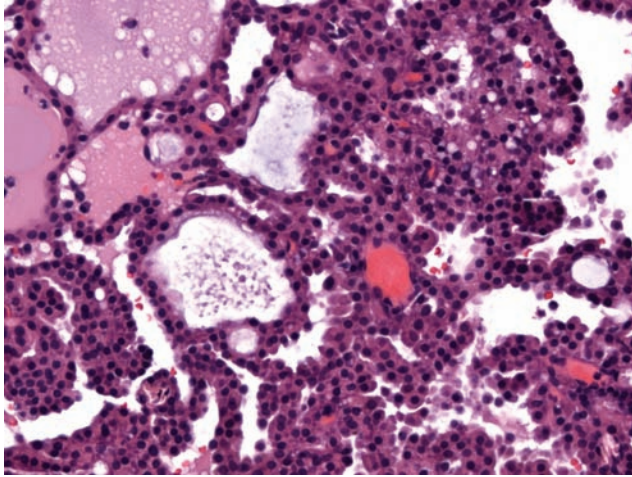


**FIGURE 2.1.7** Cuboidal intercalated duct-type cells with minimal to no acinic differentiation.

In addition, it may help one to render a more specific diagnosis of ACC rather than “cystadenocarcinoma, not otherwise specified.”

The prospective review of all ACC sent to us in consultation (1) over 1 academic year revealed 3 sources of difficulties in rendering this diagnosis.

First, exuberant tumor-associated lymphoid infiltrate sometimes seen in ACC raises the question of carcinoma metastatic to a lymph node (Figure 2.1.5) (2). Alternatively, when the focus of ACC is

small and more subtle, the possibility of salivary tissue inclusions within the lymph nodes is considered. However, benign salivary tissue inclusions are seen only in the (peri) parotid tissue and show both ducts and acini (3).

Next, the predominance of vacuolated mucous-like cells often prompts the consideration of mucoepidermoid carcinoma (Figure 2.1.6). However, in ACC, there is no squamoid differentiation on hematoxylin and eosin stain, and the lack of epidermoid cells can easily be confirmed by the negative p63 immunostain.

Finally, in some cases, nonspecific intercalated duct-type cells with minimal to no acinic differentiation are predominant (Figure 2.1.7). Finding zymogen granules on the PASD stain will lead to the correct diagnosis of ACC.

## References

1. Chiosea SI, Peel R, Barnes EL, Seethala RR. Salivary type tumors seen in consultation. *Virchows Arch.* 2009;454(4):457–466.
2. Auclair PL. Tumor-associated lymphoid proliferation in the parotid gland. A potential diagnostic pitfall. *Oral Surg Oral Med Oral Pathol.* 1994;77(1):19–26.
3. Martinez-Madrigal F, Micheau C. Histology of the major salivary glands. *Am J Surg Pathol.* 1989;13(10):879–899.

## 2.2

*Adenoid Cystic Carcinoma With High-Grade Transformation***CLINICAL INFORMATION**

“A 72-year-old man with a left maxillary mass and lymphadenopathy.”

**OPINION**

Microscopically, the tumor consists of two components. The first component is an infiltrative bilayered tubular proliferation composed of angulated hyperchromatic cells (Figure 2.2.1). The tumor nests are focally embedded in a myxoid acellular matrix. This component transitions (Figure 2.2.2) into a solid to cribriform proliferation of pleomorphic tumor cells with abundant comedonecrosis (Figure 2.2.3). Micropapillary growth is noted in the second component as well (Figure 2.2.4).

Immunohistochemically, these two components have different staining patterns. A p63 immunostain highlights the outer myoepithelial layer of the first component but is entirely negative in the second component (Figure 2.2.5). Conversely, a p53 immunostain is only faintly positive in the first component but diffusely strongly positive in the second component (Figure 2.2.6). A c-kit immunostain is positive in both components, whereas androgen receptor and Her-2/Neu are negative (not shown).

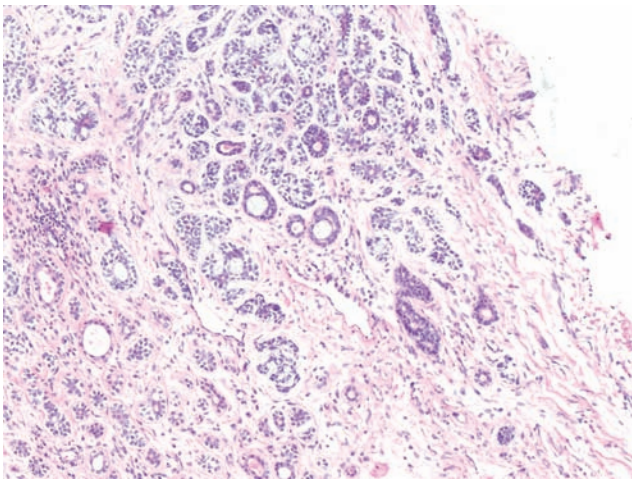


**FIGURE 2.2.1** Conventional tubular ACC component.

nostain highlights the outer myoepithelial layer of the first component but is entirely negative in the second component (Figure 2.2.5). Conversely, a p53 immunostain is only faintly positive in the first component but diffusely strongly positive in the second component (Figure 2.2.6). A c-kit immunostain is positive in both components, whereas androgen receptor and Her-2/Neu are negative (not shown).

**DIAGNOSIS**

Maxilla, left maxillectomy: Adenoid cystic carcinoma with high-grade transformation (dedifferentiated adenoid cystic carcinoma).

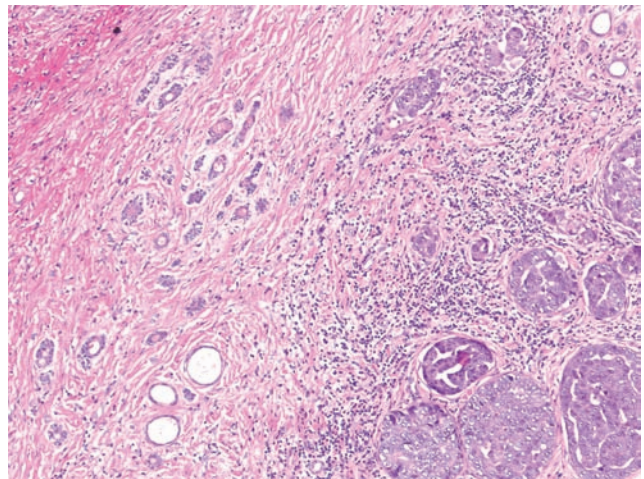


**FIGURE 2.2.2** Transition to a solid/pleomorphic component (right).

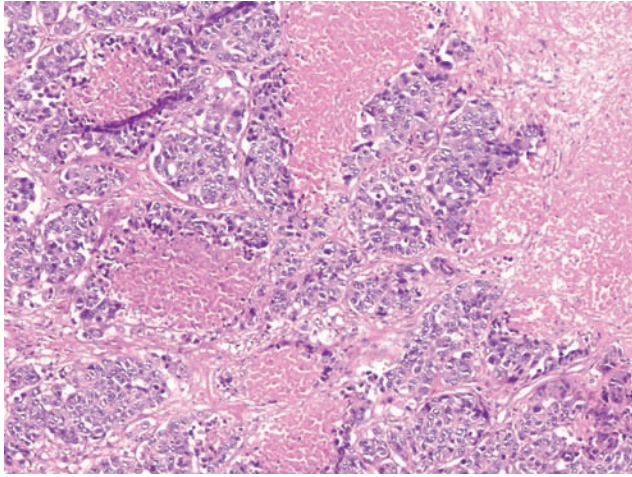


**FIGURE 2.2.3** Areas of comedonecrosis.

### COMMENT

This is an example of an adenoid cystic carcinoma with high-grade transformation (ACC-HGT). The diagnosis is established by the conventional monomorphic component, which is of the tubular pattern for ACC.

### DISCUSSION

Adenoid cystic carcinoma with high-grade transformation refers to the presence of a pleomorphic

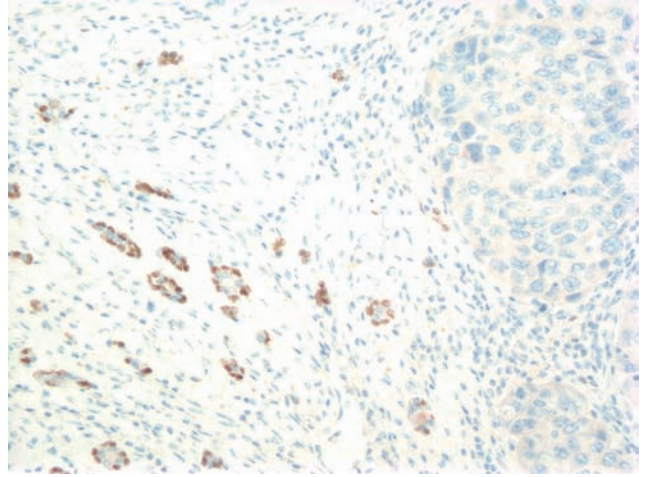


**FIGURE 2.2.5** p63 immunostaining showing an outer myoepithelial layer surrounding the conventional component (left) but not the transformed component (right).

mitotically active high-grade carcinoma component arising in an otherwise conventional ACC of any pattern/grade (1). These tumors have been historically described as dedifferentiated ACC as well (2).

The main differential diagnostic considerations include a carcinoma ex pleomorphic adenoma, dedifferentiated epithelial myoepithelial carcinoma, and ACC–salivary duct carcinoma hybrid tumor. Similar

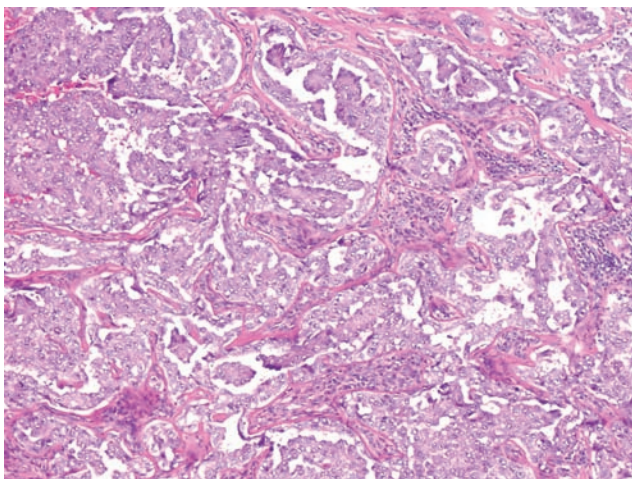


**FIGURE 2.2.4** Micropapillary growth.

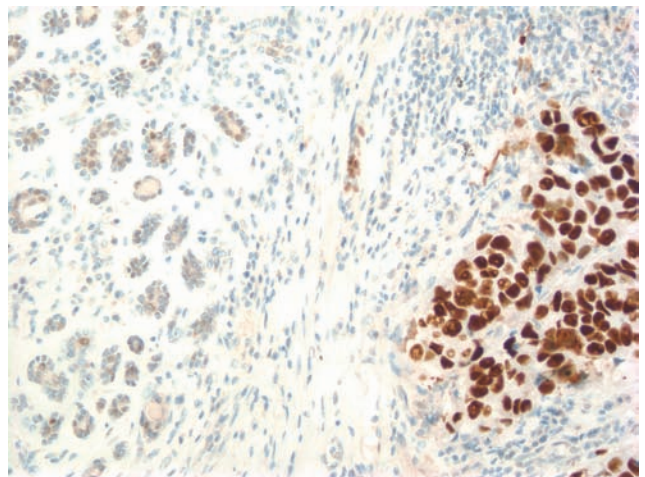


**FIGURE 2.2.6** p53 immunostaining showing strong reactivity in the transformed component (right).

## 2.2

to its pure counterpart, a salivary duct carcinoma hybrid would show positivity for androgen receptor and Her-2/Neu as well as prominent apocrine features with bright granular eosinophilic cytoplasm and peripical snouts. Distinguishing ACC-HGT from carcinoma ex pleomorphic adenoma and dedifferentiated epithelial-myoepithelial carcinoma rests mainly on the conventional lower-grade component rather than on the pleomorphic high-grade component. Identification of the classic features of ACC in the low-grade component, namely, the dark, monomorphic, angulated nuclei with scant cytoplasm arranged in a tubular, cribriform, and/or solid pattern, is necessary for the diagnosis of ACC-HGT.

Immunostains may also be of utility. The conventional component of ACC-HGT retains a biphasic phenotype—thus, the outer layer stains for myoepithelial markers (ie, p63 and smooth muscle actin) while the luminal component is cytokeratin-positive. In contrast, the transformed high-grade component loses its biphasic nature and is often only keratin-

positive. On the other hand, p53 alterations are frequent in ACC-HGT. Thus, the transformed component may be strongly immunopositive for this marker. Like conventional ACC, ACC-HGT is strongly c-kit-positive (1,2).

These tumors have an exceptionally poor prognosis with a median survival ranging from 12 to 36 months and may thus be even more aggressive than solid or “grade 3” ACC.

In addition, unlike conventional ACC, this tumor has a lymph node metastatic rate of greater than 50%. Thus, if a transformed component is found in an ACC, a neck dissection is likely warranted.

### References

1. Seethala RR, Hunt JL, Baloch ZW, Livolsi VA, Leon Barnes E. Adenoid cystic carcinoma with high-grade transformation: a report of 11 cases and a review of the literature. *Am J Surg Pathol.* 2007;31(11):1683–1694.
2. Cheuk W, Chan JK, Ngan RK. Dedifferentiation in adenoid cystic carcinoma of salivary gland: an uncommon complication associated with an accelerated clinical course. *Am J Surg Pathol.* 1999;23(4):465–472.

## 2.3

### Chronic Sclerosing Sialadenitis (Kuttner Tumor)

#### CLINICAL INFORMATION

“A 57-year-old man with a left submandibular mass.”

#### OPINION

On scanning magnification, the salivary gland is effaced by a densely sclerotic fibroinflammatory process that includes numerous lymphoid follicles (Figure 2.3.1). There is also a periductal accentuation of lymphoplasmacytic infiltrates (Figure 2.3.2). There is evidence of a lymphoplasmacytic obliterative phlebitis as highlighted by the elastic stain (Figures 2.3.3 and 2.3.4). There are also scattered areas of granulomatous inflammation (Figure 2.3.5). Stains for acid-fast and fungal organisms were negative. A kappa and lambda double immunostain overall shows polytypic

expression of light chain (Figure 2.3.6). An IgG4 immunostain shows more than 100 positive cells in 1 high-power field (Figure 2.3.7).

#### DIAGNOSIS

Submandibular gland, left excision: Chronic sclerosing sialadenitis (Kuttner tumor) with areas of superimposed necrobiotic granulomatous inflammation.

#### COMMENT

This is an example of chronic sclerosing sialadenitis (CSS). The diagnostic features include the characteristic dense fibroinflammatory infiltrate with periductal

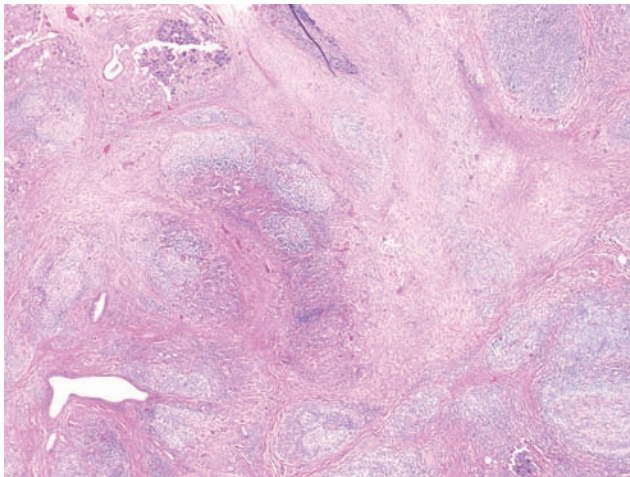


**FIGURE 2.3.1** Submandibular gland effaced by a fibroinflammatory process with lymphoid follicles.

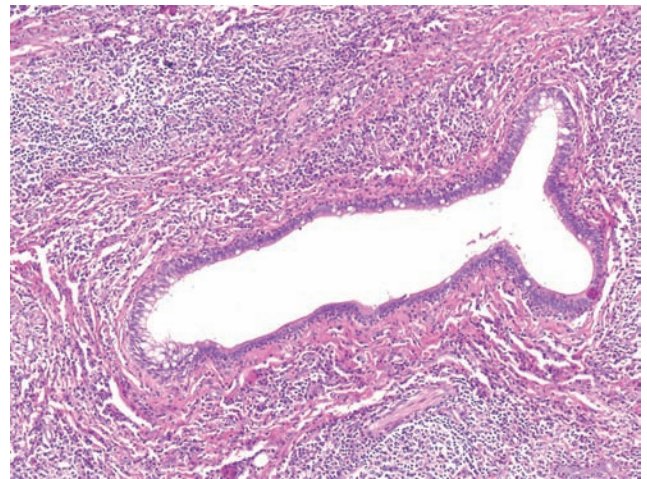


**FIGURE 2.3.2** Periductal lymphoplasmacytic infiltrates.



## 2.3

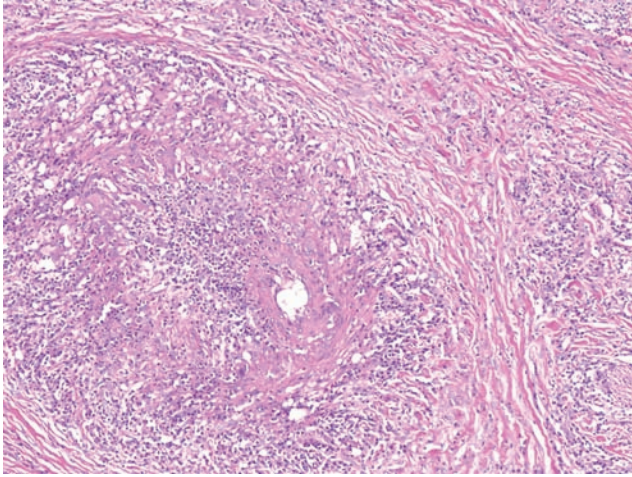


**FIGURE 2.3.3** Obliterative phlebitis.

accentuation, obliterative phlebitis, and an increased number of IgG4-positive plasma cells.

### DISCUSSION

Chronic sclerosing sialadenitis (also known as Kuttner tumor) refers to a pseudotumoral inflammatory process that typically involves the submandibular gland, although other mucoserous gland sites can be involved as well. Although historically this could be applied to any sclerosing inflammatory process of the

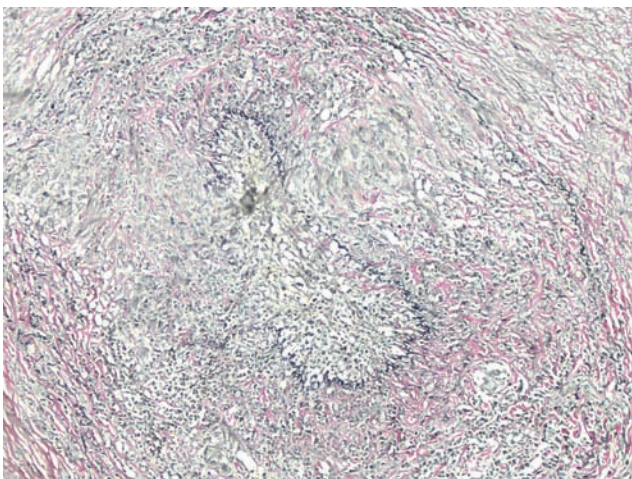


**FIGURE 2.3.4** Elastic stain highlighting elastic lamina.

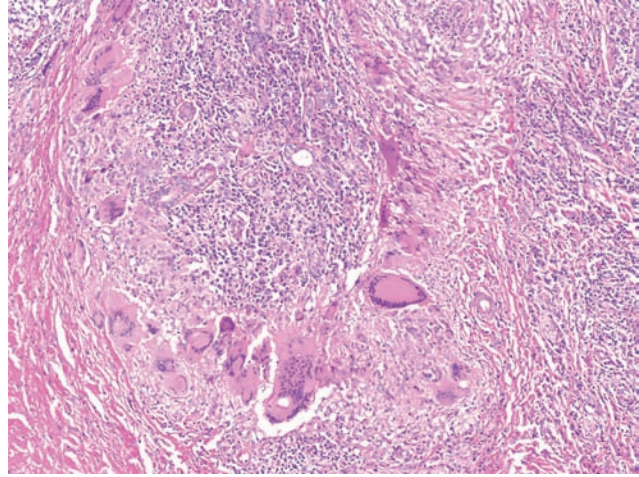


**FIGURE 2.3.5** Granulomatous inflammation occasionally seen.

salivary gland, more recently, it has become apparent that the prototypical CSS is actually an autoimmune disease process that is analogous to autoimmune pancreatitis (1).

The main differential diagnostic considerations include other forms of sialadenitis, lymphomas, and inflammatory myofibroblastic tumors. The presence of IgG4 plasma cell infiltrates (usually >50 cells per high-power field) and obliterative phlebitis is sufficient to exclude other forms of sialadenitis. In addi-

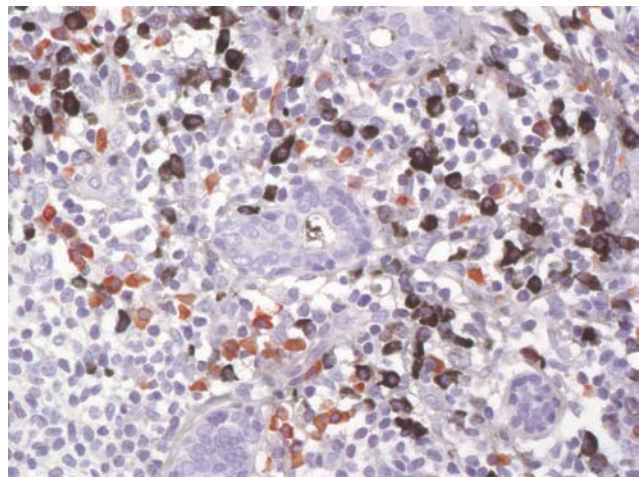


**FIGURE 2.3.6** Kappa (black) and lambda (red) showing no light chain restriction.

## 2.3

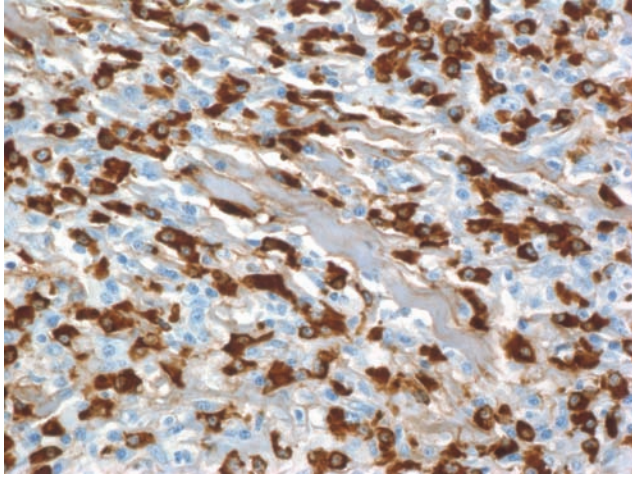


**FIGURE 2.3.7** Increased IgG4-positive plasma cell population.

tion, in post obstructive sialadenitis (ie, secondary to sialolithiasis), the sclerosis is less cellular and often more localized. In lymphoepithelial sialadenitis, the characteristic lymphoepithelial lesions will be present (1). Occasionally, the inflammation in CSS may be sufficiently dense to resemble a lymphoma or plasmacytoma; however, immunostains and ancillary studies may resolve this in most cases. Of note, unlike lymphoepithelial sialadenitis seen in Sjogren syndrome,

CSS has not been documented to progress to lymphoma. Inflammatory myofibroblastic tumors can be distinguished from CSS by the absence of IgG4 plasma cell infiltrates and obliterative phlebitis. In addition, inflammatory myofibroblastic tumors may harbor an *ALK* gene rearrangement (2).

Although CSS may be localized, it may also be a manifestation of a more generalized exocrinopathy that may include lung, breast, orbit, and/or pancreaticobiliary tree. In patients with systemic disease, serum IgG4 levels are often elevated as well. Some lesions have been noted to respond favorably to steroids or other immunosuppression (3).

### References

1. Kitagawa S, Zen Y, Harada K, Sasaki M, Sato Y, Minato H, et al. Abundant IgG4-positive plasma cell infiltration characterizes chronic sclerosing sialadenitis (Kuttner's tumor). *Am J Surg Pathol.* 2005;29(6):783–791.
2. Yamamoto H, Yamaguchi H, Aishima S, Oda Y, Kohashi K, Oshiro Y, et al. Inflammatory myofibroblastic tumor versus IgG4-related sclerosing disease and inflammatory pseudotumor: a comparative clinicopathologic study. *Am J Surg Pathol.* 2009;33(9):1330–1340.
3. Kamisawa T, Okamoto A. IgG4-related sclerosing disease. *World J Gastroenterol.* 2008;14(25):3948–3955.

## 2.4

*Epithelial–Myoepithelial Carcinoma***CLINICAL INFORMATION**

“A 65-year-old woman with a 1-cm left parotid mass.”

**OPINION**

Microscopically, the tumor consists of a solid encapsulated tumor with scattered foci of capsular penetration that extended only 1 mm beyond the capsule (Figure 2.4.1). The tumor is composed of nests of tumor cells with clear to pale eosinophilic cytoplasm. These nests are embedded in slightly myxoid stroma (Figure 2.4.2). Nuclei are round with vesicular chromatin and occasional prominent nuclei. Although the stroma is myxoid, no chondroid areas are noted. In addition, the tumor nests do not blend with the stroma and are instead distinct.

Immunostaining for cytokeratin highlights compressed tubules within the center of the tumor

nests (Figure 2.4.3). The outer abluminal layers of the tumor nests, however, are p63-positive (Figure 2.4.4). Within each tumor nest, these 2 cell types are distinctly organized with no transition.

**DIAGNOSIS**

Parotid, left parotidectomy: Epithelial-Myoepithelial carcinoma, minimally invasive.

**COMMENT**

This is an example of epithelial-myoepithelial carcinoma (EMCa) with predominance of myoepithelial component. Different cell populations are difficult to discern by light microscopy alone. However, the cytokeratin CAM 5.2 highlights the compressed duc-

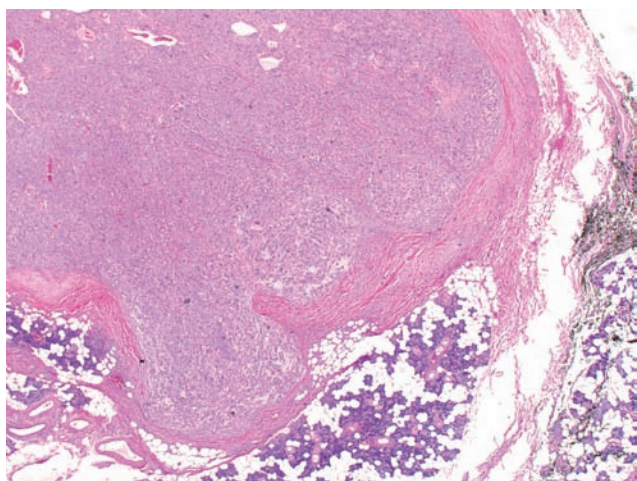


**FIGURE 2.4.1** Capsular invasion.

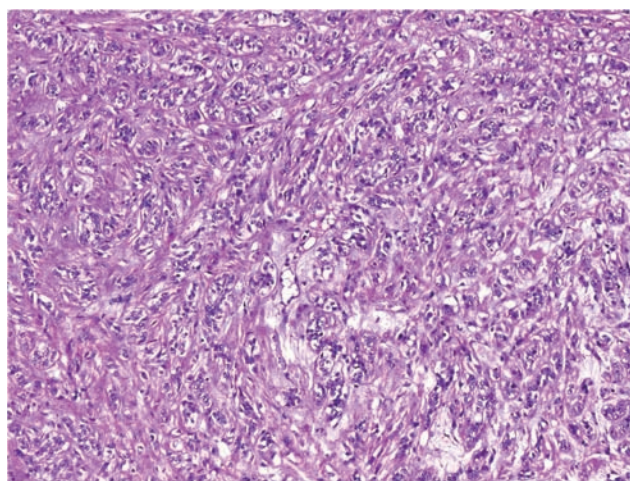


**FIGURE 2.4.2** Solid nests with a slightly myxoid stroma.

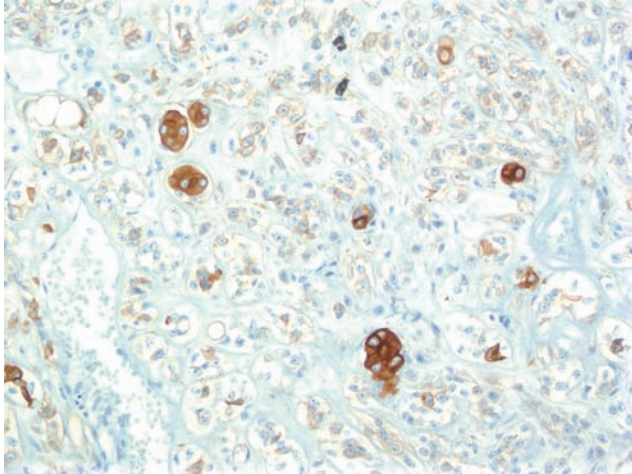


**FIGURE 2.4.3** Cytokeratin CAM 5.2 highlighting compressed ducts.

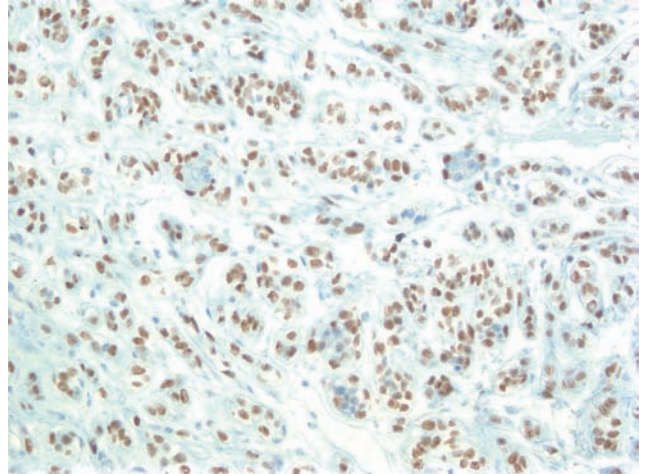


**FIGURE 2.4.4** A p63 immunostain highlighting the abluminal outer layers of tumor nests.

tal component supporting a biphasic nature to the tumor. The tumor is predominantly encapsulated; however, in few areas, it extends beyond the capsule (<1.5 mm).

### DISCUSSION

Epithelial-Myoepithelial carcinoma is quite rare and comprises only 1% to 2% of all salivary gland tumors. It most often occurs in the major salivary glands, but it also can occur at other mucoserous gland-rich sites (1). This tumor is morphologically identical to adenomyoepithelioma of the breast. However, in the head and neck regions, this tumor behaves as a low-grade malignancy with a considerable recurrence rate and capacity for metastasis. Histologically, EMCa is the prototypical biphasic tumor—comprised of an inner luminal layer with a ductal phenotype and an outer (abluminal) polygonal myoepithelial cell layer. Classically, the myoepithelial cell layer is of the clear cell type, although variant morphologies have been described.

The main differential diagnostic considerations include cellular pleomorphic adenoma, myoepithelioma/myoepithelial carcinoma, tubulotrabeular basal

cell adenoma/adenocarcinoma, and adenoid cystic carcinoma. These entities can be resolved based on architecture, cell constituents, and cytomorphologic features summarized below. Architecturally, cellular pleomorphic adenoma, myoepithelioma, and tubulotrabeular basal cell adenoma are noninvasive. In addition, myoepithelioma is a monophasic tumor that consists purely of myoepithelial cells and no ducts. Pleomorphic adenoma may resemble EMCa, but in addition to the noninvasive growth pattern, the outer myoepithelial cells tend to blend into the surrounding chondromyxoid stroma. In addition, the myoepithelial cells appear less plump and activated than in EMCa. Basal cell adenoma and adenocarcinoma, although also composed of ducts and myoepithelial cells, are characterized by palisading of the outermost layer of a tumor nest. In addition, although myoepithelial cells may be present in these tumors, they are not as prominent as in EMCa. Adenoid cystic carcinoma is also a biphasic tumor composed of epithelial cells and myoepithelial cells arranged in tubular, cribriform, and solid patterns. However, the characteristic nuclear features are hyperchromatic and angulated. In addition, adenoid cystic carcinoma has

## 2.4

a remarkable propensity to cleft from the basement membrane, a feature that is not seen in EMCa.

Occasionally, there is an overgrowth of the myoepithelial component obfuscating the biphasic nature of this tumor. Here, immunostains may be useful in highlighting the cell constituents. The outer myoepithelial layers are p63, actin, and calponin-positive, whereas the ductal components are typically positive for cytokeratins (usually low molecular weight) only.

The EMCa tumor behaves quite favorably, with a 5- and 10-year disease-specific survival in a recent series of 94% and 82%, respectively (2). Some cohorts suggest an even more aggressive behavior, but this may be a result of high-grade tumors (3). Recur-

rences, however, are usually late (median disease-free survival, ~11 years), indicating that patients should be followed up in the long term.

### References

1. Mantesso A, Loduca SV, Jaeger RG, Decio SP, Araujo VC. Analysis of epithelial-myoepithelial carcinoma based on the establishment of a novel cell line. *Oral Oncol.* 2003;39(5):453–458.
2. Seethala RR, Barnes EL, Hunt JL. Epithelial-Myoepithelial carcinoma: a review of the clinicopathologic spectrum and immunophenotypic characteristics in 61 tumors of the salivary glands and upper aerodigestive tract. *Am J Surg Pathol.* 2007;31(1):44–57.
3. Fonseca I, Soares J. Epithelial-Myoepithelial carcinoma. In: Barnes EL, Eveson JW, Reichart P, Sidransky D, eds. *World Health Organization Classification of Tumours: Pathology and Genetics. Head and Neck Tumours.* Lyon: IARC Press; 2005:225–226.

## 2.5

### *Keratocystoma*

#### CLINICAL INFORMATION

“This 16-year-old boy presented with a symptomatic 2-cm swelling of the right parotid gland of unknown duration. There was no lymphadenopathy. A superficial parotidectomy was performed. Your opinion of this most unusual case would be appreciated.”

#### OPINION

Sections show multiple, keratin-filled cysts lying in a fibrous, focally inflamed stroma (Figures 2.5.1, 2.5.2, and 2.5.3). The cysts are lined by a bland, hyperplastic squamous epithelium devoid of a granular cell layer and mucous cells (Figure 2.5.4). No cartilage or adnexal-type appendages are seen. Mitoses are sparse. In some areas, only small solid nests of squamous cells are observed (Figure 2.5.5). A mucicarmine stain is negative.

#### DIAGNOSIS

Lesion, right parotid gland, superficial parotidectomy: Keratocystoma.

#### COMMENT

This is a rare, recently described, benign entity referred to as a keratocystoma.

#### DISCUSSION

Only three cases of keratocystoma have been described, one in an 8-year-old girl and two in males 18 and 28 years of age (1,2). All occurred in the parotid gland and presented as asymptomatic masses up to 5-cm in greatest dimension. Whether it is a choristoma or a true

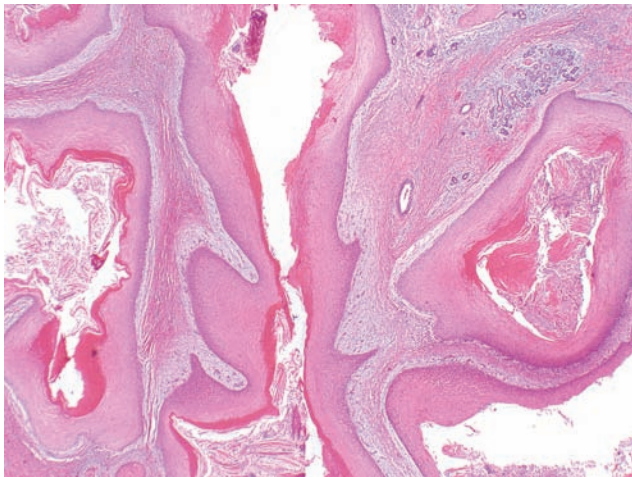


**FIGURE 2.5.1** Sections show multiple cysts lined by benign squamous epithelium and are filled with keratin.

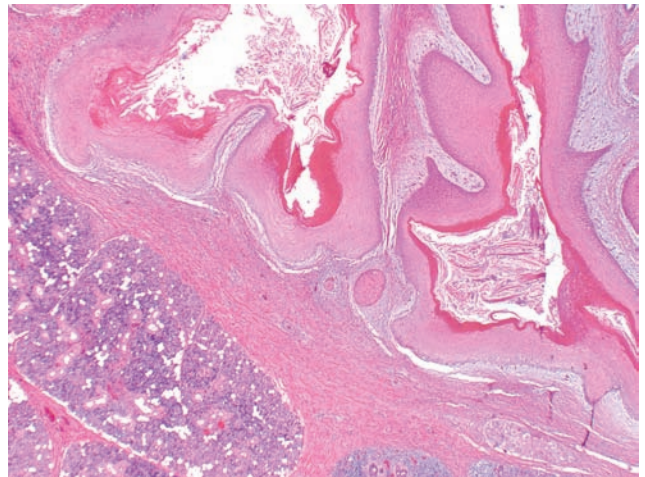


**FIGURE 2.5.2** Another view. Note the fibrotic stroma. Parotid tissue is apparent in the lower left.

## 2.5

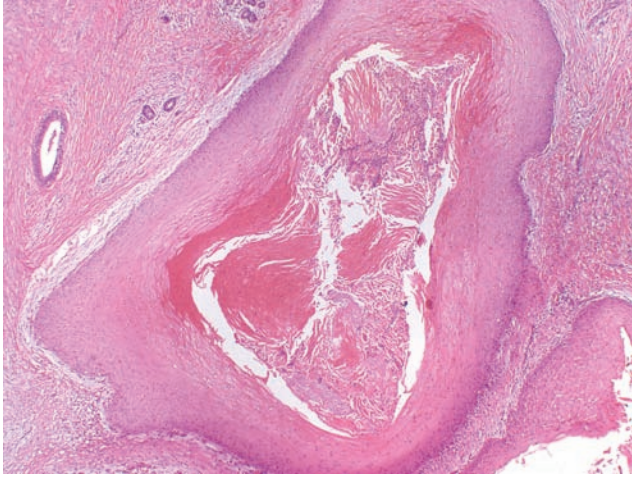


**FIGURE 2.5.3** Higher magnification. Note the absence of cartilage and adnexal-type appendages.

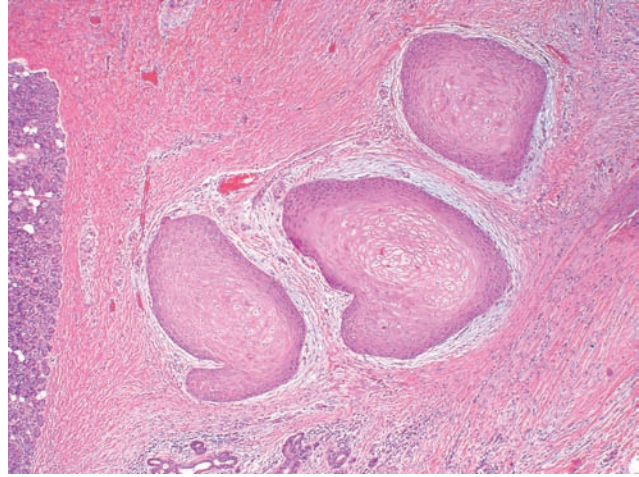


**FIGURE 2.5.5** Solid islands of squamous epithelium were also apparent.

cystic neoplasm is uncertain. None of the three patients has experienced recurrence after surgical excision.

The differential diagnosis includes a mucoepidermoid carcinoma, a squamous cell carcinoma, a pleomorphic adenoma with squamous elements, and a first branchial cleft abnormality.

The presence of extensive keratinization and absence of mucous and intermediate cells are against

a diagnosis of mucoepidermoid carcinoma. Pleomorphic adenoma is excluded by the absence of a significant ductal component, myoepithelial cells, and a chondromyxoid matrix.

First branchial cleft abnormalities are divided into type I and II variants. Type I resembles an epidermoid cyst and may present in the parotid gland; however, it is typically unicystic, not multicystic as in this case. Type II duplicates the external auditory canal and pinna and contains both cartilage and adnexal structures, which are absent in keratocystoma.

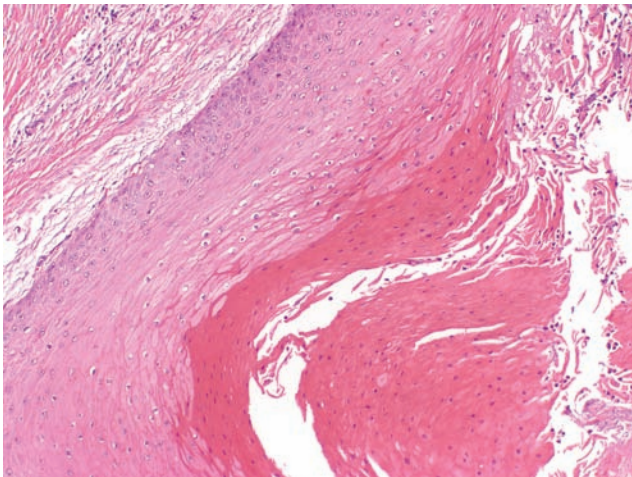


**FIGURE 2.5.4** The cysts are lined by benign squamous epithelium. No granular cell layer or mucous cells are seen.

### References

1. Seifert G, Donath K, Jautzke G. Unusual choristoma of the parotid gland in a girl. A possible trichoadenoma. *Virchows Arch.* 1999;434(4):355–359.
2. Nagao T, Serizawa H, Iwaya K, et al. Keratocystoma of the parotid gland: a report of two cases of an unusual pathologic entity. *Mod Pathol.* 2001;15:1005–1010.

## 2.6

## Low-Grade Salivary Duct Carcinoma (Low-Grade Cribriform Cystadenocarcinoma)

### CLINICAL INFORMATION

“A 68-year-old woman with a right parotid mass.”

### OPINION

Microscopically, the tumor consists of an unencapsulated, slightly permeative proliferation of tumor nests embedded in a sclerotic stroma (Figure 2.6.1). These nests show a solid to cribriform growth pattern with bland monomorphic nuclei and moderate amounts of cytoplasm (Figure 2.6.2). Other areas demonstrate nuclear enlargement with prominent nucleoli and oncocytic cytoplasm (Figure 2.6.3).

Immunohistochemically, the tumor cells are strongly positive for S100 (Figure 2.6.4) but negative for androgen receptor (Figure 2.6.5). A p63 immunostain highlights a delimiting basal layer surrounding many of the tumor nests (Figure 2.6.6).

### DIAGNOSIS

Parotid, right, biopsy: Low-grade salivary duct carcinoma (low-grade cribriform cystadenocarcinoma).

### COMMENT

This represents a low-grade salivary duct carcinoma (LGSDC). The World Health Organization recommends the designation “low-grade cribriform cystadenocarcinoma” to avoid confusion with conventional salivary duct carcinoma, which is a far more aggressive disease.

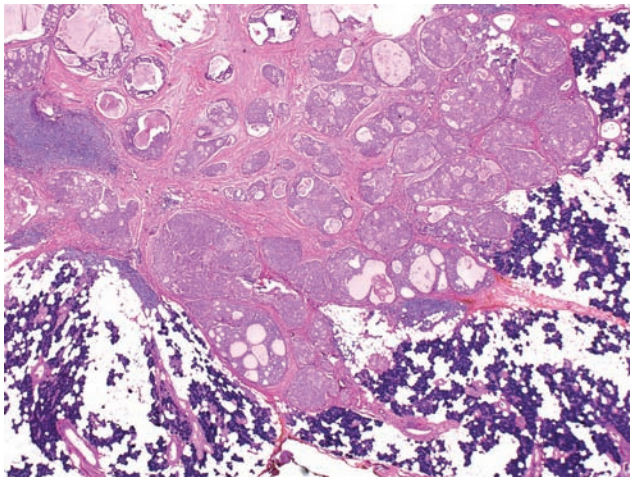


**FIGURE 2.6.1** Tumor focally permeating the parotid and demonstrating sclerotic stroma.

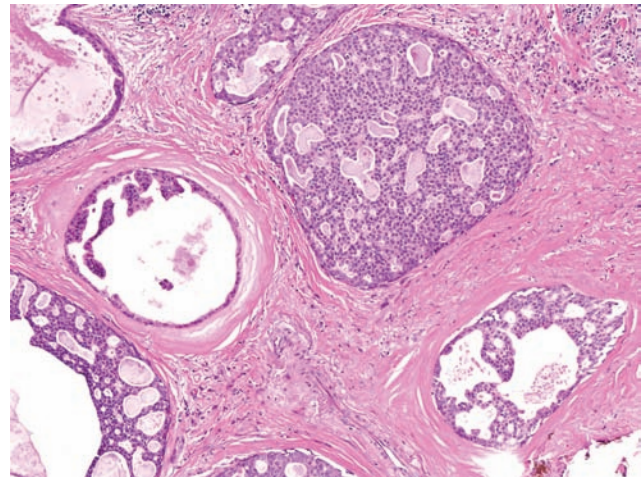


**FIGURE 2.6.2** Monomorphic tumor nests with cribriform growth cystic change and micropapillae.



## 2.6

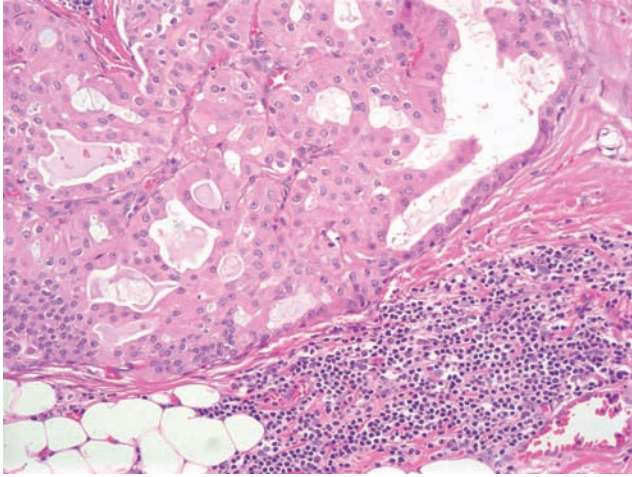


**FIGURE 2.6.3** Focal nuclear enlargement with oncocytic change.

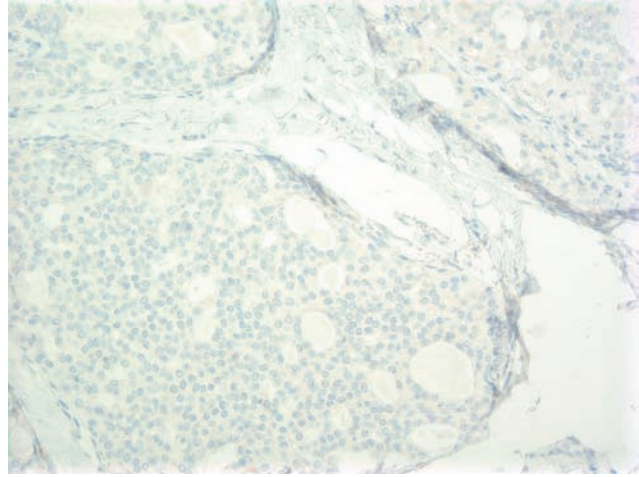


**FIGURE 2.6.5** Androgen receptor negativity.

## DISCUSSION

Low-grade salivary duct carcinoma is a rare low-grade salivary gland malignancy initially described by Delgado et al (1) that is predominantly a tumor of the sixth to seventh decade. This tumor almost always arises from the parotid gland. This tumor is typically composed of an unencapsulated solid to cribriform proliferation of bland tumor cells resembling low-grade ductal carcinoma in situ or atypical ductal hyperplasia of breast. Micropapillary and tubular

growth patterns may be seen as well. Cystic change is quite common, and subsequent hemosiderosis of the epithelium may be noted as well. Many of these tumors may show areas of moderate cytologic atypia and oncocytic change. Myoepithelial/Basal markers will demonstrate that most LGSDC are actually intraductal. Strong S100 immunoreactivity is essentially a defining feature (2).

The main differential diagnostic consideration includes conventional salivary duct carcinoma, par-

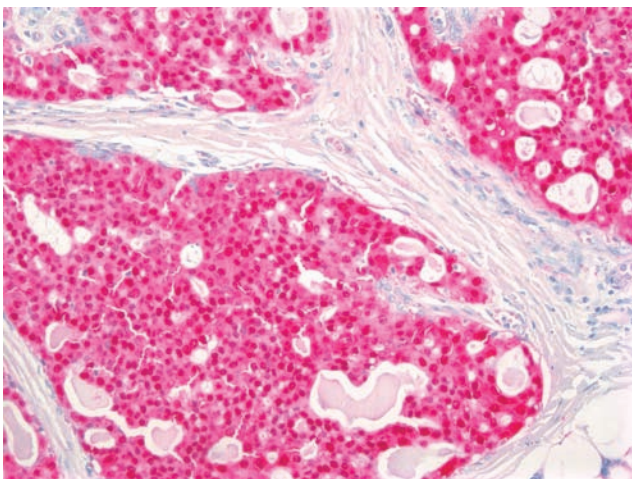


**FIGURE 2.6.4** Strong diffuse S100 positivity.

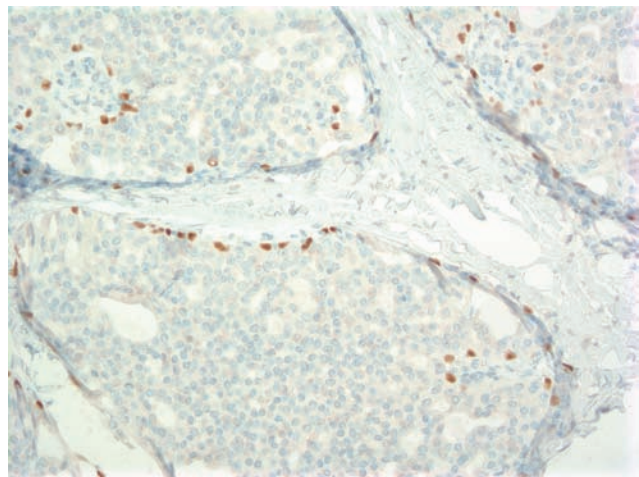


**FIGURE 2.6.6** p63 showing a partially delimiting myoepithelial layer around tumor nests.

ticularly the in situ type. Morphologically, however, conventional salivary duct carcinoma is fairly high grade even when in situ, often showing mitoses and comedonecrosis. Conventional salivary duct carcinomas also show apocrine features including granular vacuolated eosinophilic cytoplasm with decapitation secretions. Immunophenotypically, this is supported by the presence of GCDFP-15 and androgen receptor positivity+, features that are essentially absent in LGSDC. However, it must be noted that few tumors showing overlap between LGSDC and conventional salivary duct carcinoma have been described (3).

When LGSDC shows prominent cystic change, cystadenocarcinomas may also be considered in the differential diagnosis, and in fact, some previously described cystadenocarcinomas may be more appropriately classified as LGSDC. However, cystadenocarcinomas more frequently involve minor salivary gland sites. In addition, strictly speaking, cystadeno-

carcinomas should not have much cribriform growth and in contrast show a tendency for papillae formation. In addition, these tend to be more oncocytic than LGSDC. Finally, features such as columnar cells and absence of a delimiting myoepithelial layer are more frequent in cystadenocarcinomas (4).

### References

1. Delgado R, Klimstra D, Albores-Saavedra J. Low-grade salivary duct carcinoma. A distinctive variant with a low-grade histology and a predominant intraductal growth pattern. *Cancer*. 1996;78(5):958–967.
2. Brandwein-Gensler M, Hille J, Wang BY, Urken M, Gordon R, Wang LJ, et al. Low-grade salivary duct carcinoma: description of 16 cases. *Am J Surg Pathol*. 2004;28(8):1040–1044.
3. Weinreb I, Tabanda-Lichauco R, Van der Kwast T, Perez-Ordóñez B. Low-grade intraductal carcinoma of salivary gland: report of 3 cases with marked apocrine differentiation. *Am J Surg Pathol*. 2006;30(8):1014–1021.
4. Foss RD, Ellis GL, Auclair PL. Salivary gland cystadenocarcinomas. A clinicopathologic study of 57 cases. *Am J Surg Pathol*. 1996;20(12):1440–1447.

## 2.7

*Oncocytic Mucoepidermoid Carcinoma***CLINICAL INFORMATION**

“A 64-year-old woman with a 2-cm parotid mass.”

**OPINION**

Microscopically, the tumor consists of a macrocystic and microcystic mass surrounded by a prominent lymphoid stroma (Figure 2.7.1). Much of the cystic lesion is lined by oncocytic cuboidal to columnar epithelium (Figure 2.7.2). There are focal areas with stratification and architectural complexity, including more solid areas and basal layer hyperplasia (Figure 2.7.3). One area shows epidermoid and mucus cell differentiation (Figure 2.7.4).

A p63 immunostain shows areas of stratified basal/parabasal distribution of immunoreactivity that transitioned from simple basal/bilayered staining (Figure 2.7.5). Fluorescent in situ hybridization demon-

strated the presence of disruption at the *MAML* gene region on chromosome 11q21 indicative of a t(11;19) (q21;p13) translocation (Figure 2.7.6).

**DIAGNOSIS**

Parotid, right parotidectomy: Mucoepidermoid carcinoma, oncocytic variant, low-grade.

**COMMENT**

This represents a (oncocytic) low-grade mucoepidermoid carcinoma (OMEK). Although much of the cystic lesion is lined by oncocytic cuboidal to columnar epithelium, the areas of stratification, architectural complexity, epidermoid, and mucus cell differentiation support the above diagnosis. Although there is

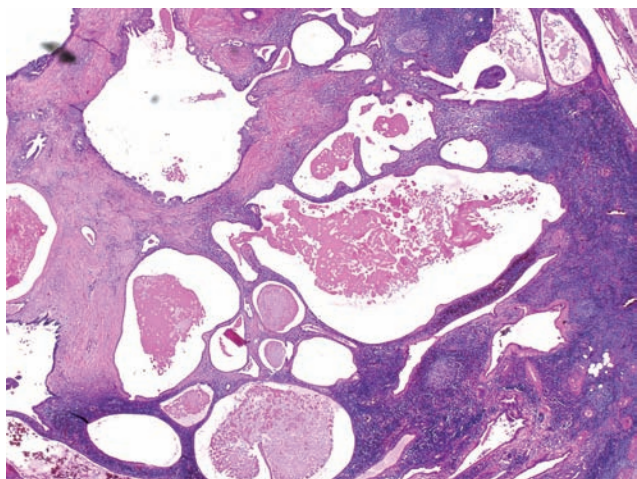


**FIGURE 2.7.1** Cystic tumor with prominent lymphoid stroma.

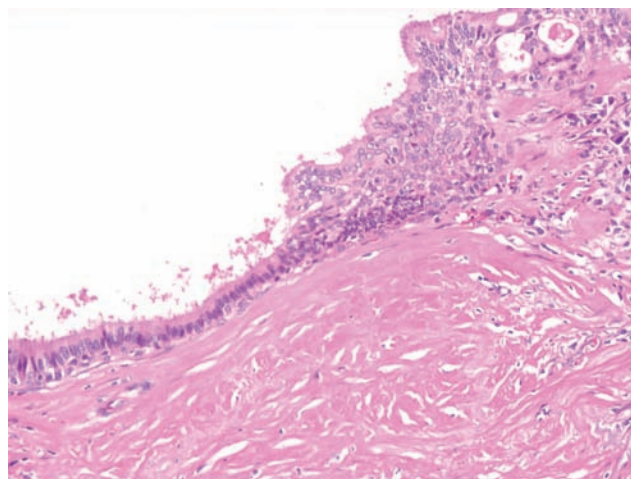


**FIGURE 2.7.2** Cysts are lined by oncocytic columnar epithelium.

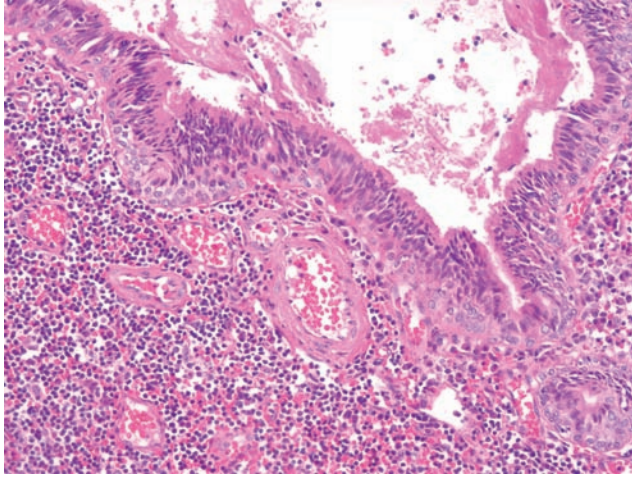


**FIGURE 2.7.3** Stratification and basal layer hyperplasia.

a prominent lymphoid stroma, which can be seen in a variety of lesions including mucoepidermoid carcinoma (MEC), in situ hybridization for MAML2 gene rearrangement is positive, a defining event in mucodepidermoid carcinoma.

### DISCUSSION

The OMEC comprises about 2% to 3% of all MEC. Similar to typical MEC, more than 75% occur in the parotid gland. Most tumors reported to date are typically low to intermediate-grade, although high-grade

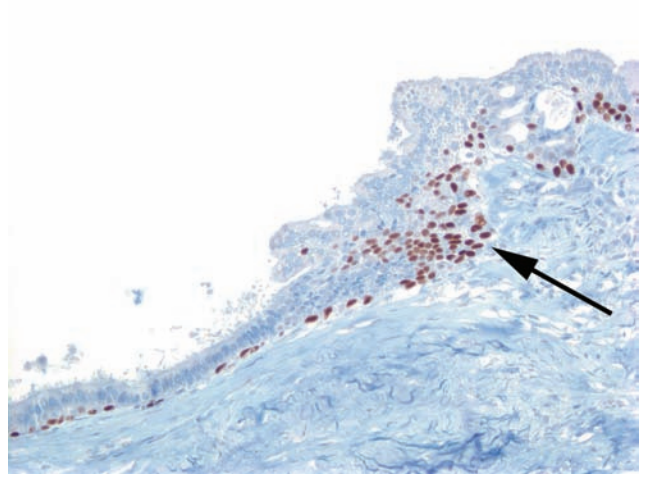


**FIGURE 2.7.5** p63 immunostain showing transition from bilayered appearance to a stratified appearance (arrow).

examples have been recently reported (1). The major differential diagnostic considerations include oncocytic cystadenoma and Warthin tumor for cystic low-grade OMEC, oncocytoma/oncocytic carcinoma for solid intermediate-grade OMEC, and perhaps salivary duct carcinoma for high-grade OMEC.

Low-grade OMECs often have oncocytic columnar cells and may even in areas show a bilayered appearance, resembling oncocytic cystadenoma and Warthin tumor, if there is lymphoid stroma. In addition, because these latter two may have scattered

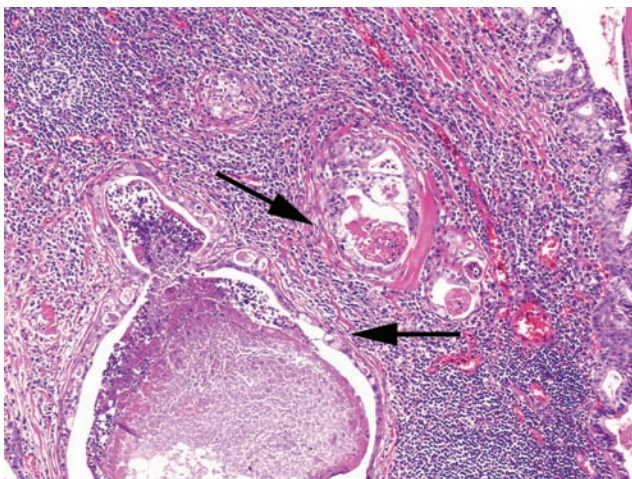


**FIGURE 2.7.4** Mucus cell differentiation (arrows).

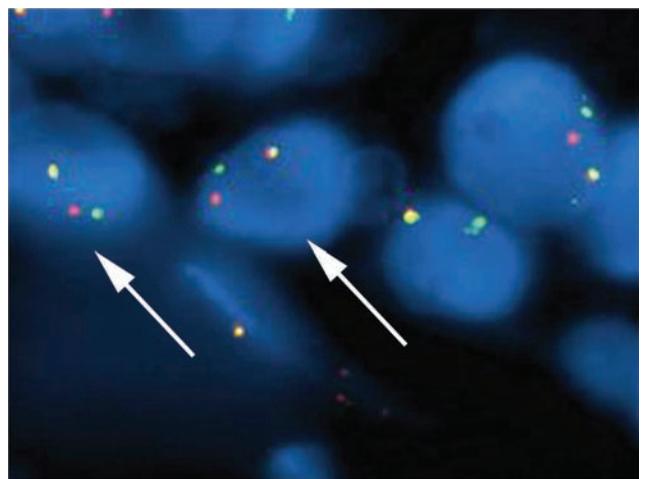


**FIGURE 2.7.6** Positivity for MAML2 disruption (arrows).

## 2.7

mucus cells, the diagnostic challenge is compounded further. Key distinguishing morphologic features of low-grade OMEC are the presence of architectural complexity, namely, solid areas, and more complex and coalescent papillary areas. On higher magnification, areas of stratification of columnar cells with tufting of underlying epidermoid-appearing cells are more common to OMEC. A mucicarmine stain will show some periapical mucin even in cells that do not appear to be mucus cells by light microscopy in OMEC. Immunostaining for p63 may also be of value particularly in the areas of epidermoid-appearing tufting because these foci will be diffusely positive in contrast to the consistent bilayered appearance of Warthin tumor and cystadenoma (1).

Despite these diagnostic criteria, some cases may be quite difficult. Here, molecular testing may become of use. Perhaps, the most dramatic advance in MEC pathogenesis is the characterization of the translocation, t(11;19) (q21;p13), which results in the fusion of the *MECT1* and *MAML2* genes. The *MECT1*-*MAML2* fusion protein appears to activate both Notch signaling targets and cAMP/CREB targets (2).

Despite what some authors claim, in our in-house experience, this translocation is entirely specific for MEC. In addition, with respect to OMEC, it is

identifiable in 70% to 80% of cases. As alluded to, the *MECT1*-*MAML2* translocation has been reported in some “Warthin tumors.” It has also been suggested that the Warthin tumor may represent a precursor for MEC (3). However, many of these translocation-positive “Warthin tumors” are not histopathologically well characterized, raising the possibility that these are merely MEC with a prominent lymphoid stroma. One group has reviewed their experience with the translocation in the Warthin tumor and found that on histologic review, the few translocation-positive “Warthin tumors” identified are more in keeping with MEC (4).

### References

1. Weinreb I, Seethala RR, Perez-Ordóñez B, Chetty R, Hoschar AP, Hunt JL. Oncocytic mucoepidermoid carcinoma: clinicopathologic description in a series of 12 cases. *Am J Surg Pathol*. 2009;33(3):409–416.
2. Tonon G, Modi S, Wu L, Kubo A, Coxon AB, Komiya T, et al. t(11;19)(q21;p13) translocation in mucoepidermoid carcinoma creates a novel fusion product that disrupts a Notch signaling pathway. *Nat Genet*. 2003;33(2):208–213.
3. Bell D, Luna MA, Weber RS, Kaye FJ, El-Naggar AK. *CRTC1/MAML2* fusion transcript in Warthin’s tumor and mucoepidermoid carcinoma: evidence for a common genetic association. *Genes Chromosomes Cancer*. 2008;47(4):309–314.
4. Fehr A, Roser K, Belge G, Loning T, Bullerdiek J. A closer look at Warthin tumors and the t(11;19). *Cancer Genet Cytogenet*. 2008;180(2):135–139.

## 2.8

## Polymorphous Low-Grade Adenocarcinoma, Recurrent, With “Intermediate Grade” Progression

### CLINICAL INFORMATION

“A 63-year-old woman with a multiply recurrent soft palate tumor, originally excised 18 years prior to presentation.”

### OPINION

Microscopically, the tumor consists of a multiple unencapsulated, solid tumor nodules in the submucosa (Figure 2.8.1).

The tumor is composed of a solid proliferation of a single population of cells with amphophilic cytoplasm and monomorphic ovoid nuclei with delicate, almost clear chromatin and focal tubule formation (Figure 2.8.2). In areas, there is slight pleomorphism and prominent nucleoli, although the delicate chromatin characteristics are retained (Figure 2.8.3). Hints of an acellular myxohyaline stroma are noted as well.

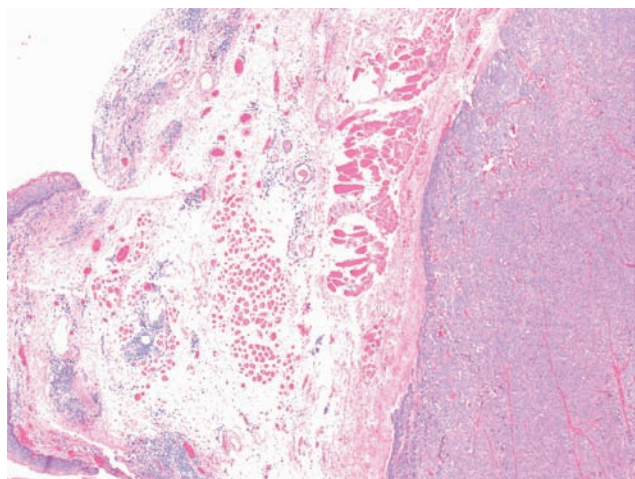


**FIGURE 2.8.1** Polymorphous low-grade adenocarcinoma submucosal nodule with solid growth.

Immunostaining for S100 is diffusely strongly positive in all tumor cells without any compartmental distribution (Figure 2.8.4). A p63 immunostain is negative (Figure 2.8.5).

On subsequent follow-up 20 months later, the patient developed several subcutaneous and pulmonary nodules (Figure 2.8.6). A fine-needle aspiration revealed tumor cells morphologically identical to the palate tumor (Figure 2.8.7).

### DIAGNOSIS

Soft palate, excision: Polymorphous low-grade adenocarcinoma, recurrent, with subsequent lung metastases.

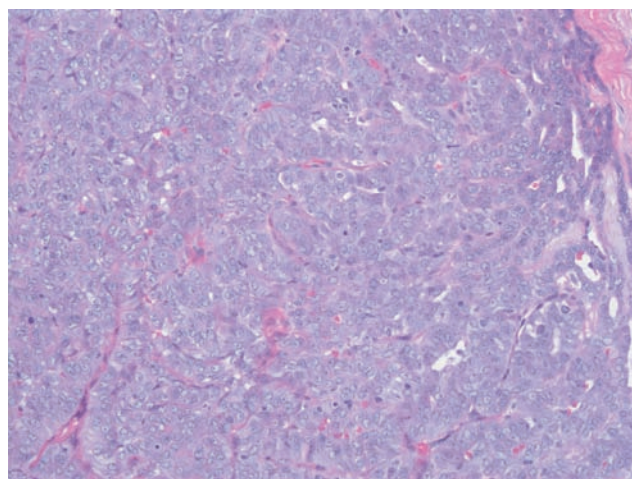


**FIGURE 2.8.2** Tumor cells are fairly monotonous with amphophilic cytoplasm. Focal tubule formation is seen (right).

## 2.8

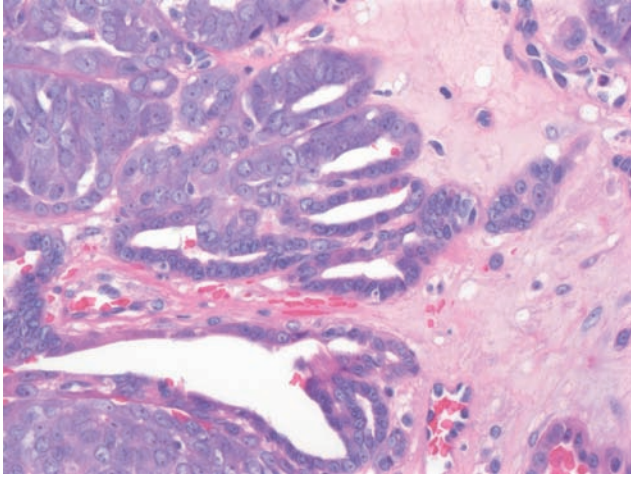


**FIGURE 2.8.3** Tumor nuclei are ovoid with slight pleomorphism. Chromatin is vesicular and almost “clear,” and prominent central nucleoli are noted.

**COMMENT**

This is an example of a recurrent polymorphous low-grade adenocarcinoma (PLGA). The tumor shows the characteristic nuclear features and staining profile. Of note, because this is a recurrent tumor, atypical or “intermediate-grade” features, such as focal pleomorphism and prominent nucleoli, can be seen. This case is also unusual in that distant metastases were identified.

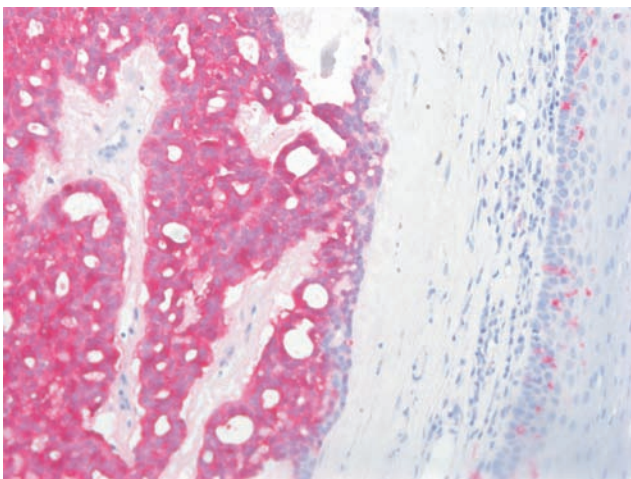


**FIGURE 2.8.4** S100 protein is diffusely strongly positive.

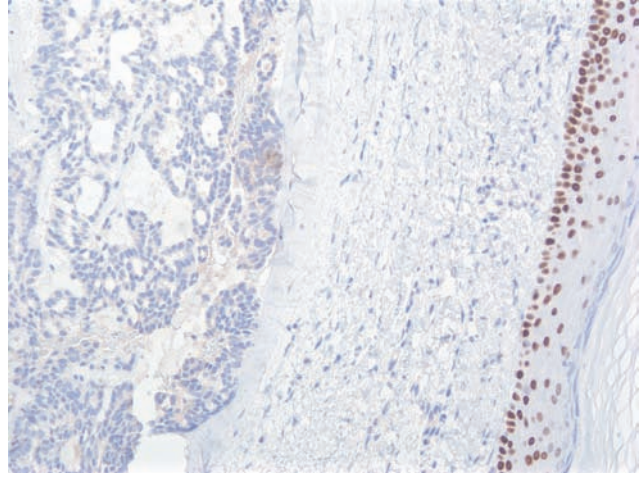


**FIGURE 2.8.5** P63 is negative (squamous mucosa on the right is an internal positive control).

**DISCUSSION**

Polymorphous low-grade adenocarcinoma is a term coined by Evans and Batsakis in 1984 (1) to characterize an uncommon low-grade malignancy of the minor salivary glands, although it has likely been described even earlier (2,3). Despite the indolent name, on long-term follow-up, the recurrence rate is fairly high at almost 33%. Nonetheless, distant metastases and disease-related deaths are still quite rare (4,5).

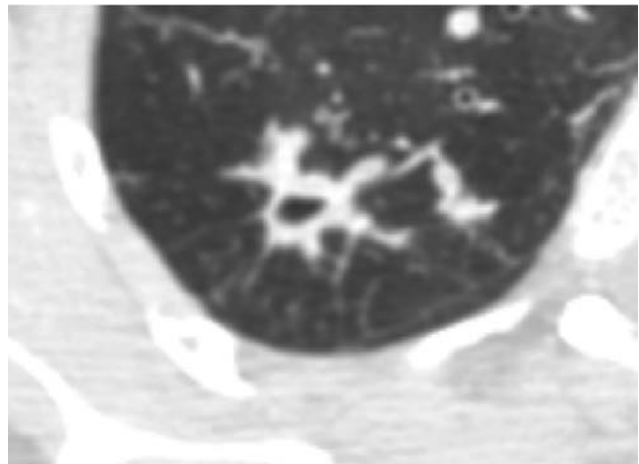


**FIGURE 2.8.6** Lung Computerized Tomogram demonstrating a nodule suspicious for metastasis.

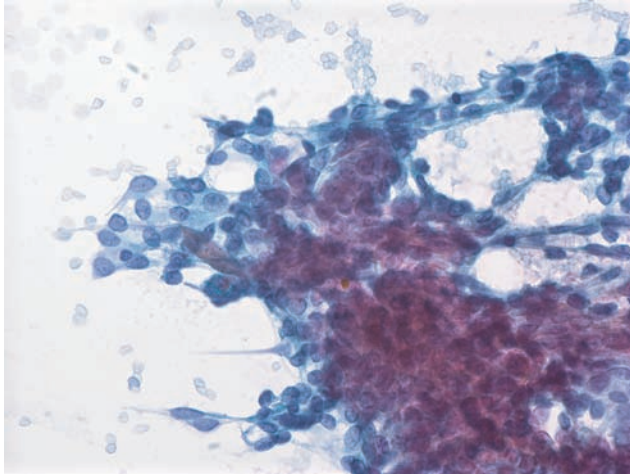


**FIGURE 2.8.7** Fine needle aspirate of this nodule shows tumor morphologically similar to the patient's palate tumor.

The tumor name is somewhat misleading; although the number of infiltrative patterns that this tumor can demonstrate is indeed very polymorphous, ranging from solid to tubular/cribriform, to papillary, cytologically this tumor is generally very monomorphic and actually phenotypically of only 1 cell type (ie, monophasic) (6). The cytonuclear features of this tumor are the key to recognition. Invariably, these tumor cells are composed of pale eosinophilic or amphophilic cytoplasm and contain ovoid nuclei with delicate, vesicular chromatin characteristics reminiscent of papillary thyroid carcinoma. The stroma is similar to that in many other salivary gland tumors and ranges from myxoid to hyaline reflective of ground substance deposition.

The main historical differential diagnostic consideration is adenoid cystic carcinoma because of the similar permeative growth patterns and matrix deposition (7). This is likely one of the most overrated diagnostic dilemmas in salivary gland tumor classification. Using modern morphologic criteria and given adequate material, this distinction is actually quite simple and does not require an extensive immunohistochemical panel as suggested in the literature (8).

Unlike PLGA, morphologically, adenoid cystic carcinoma is readily recognized by light microscopy as a biphasic tumor composed of inner ducts and abluminal myoepithelial cells. In contrast to the vesicular nuclei of PLGA, adenoid cystic carcinoma nuclei are small hyperchromatic and often angulated. In cases where this morphologic distinction is challenging, myoepithelial markers such as actin and p63 can highlight the biphasic nature of adenoid cystic carcinoma (8). In PLGA, when these are expressed, it is in a weak and patchy fashion in a random rather than compartmental distribution. In addition, PLGA is characteristically diffusely strongly positive for S100 protein, whereas adenoid cystic carcinoma is variable in its intensity and distribution. Markers such as c-kit and bcl-2 are unnecessary.

A similar approach can be taken in distinguishing PLGA from other biphasic low-grade adenocarcinomas, such as basal cell adenocarcinoma and epithelial myoepithelial carcinomas, which are now currently more relevant differential diagnostic considerations because they have cytomorphologic features that can overlap with PLGA (5). Myoepithelial carcinomas can occasionally show nuclear features that are very similar to PLGA, although true tubule formation is absent, and on immunostaining, the tumor cells are more consistently and diffusely p63 and actin-positive. Finally, adenocarcinoma not otherwise specified can resemble PLGA in growth pattern and is often S100 strongly positive; however, this designation should only be used if a tumor does not have the characteristic nuclear features of a PLGA.

Certain features have been identified as potential adverse prognosticators—namely, papillary predominant growth pattern and perhaps angiolymphatic invasion (4,5). However, perhaps more importantly, extrapalatal tumors, particularly of the base of the tongue, appear to behave in a more aggressive fashion as well (5). A subset of base of tongue tumors have



## 2.8

been suggested to be different entities, dubbed “cribriform adenocarcinomas of the tongue” altogether because of their cribriform growth predominance and propensity for lymph node metastases (9). However, there is no sufficient evidence to consider them separate tumors at this point.

Rarely, PLGA may progress to a high-grade adenocarcinoma with potentially lethal outcomes (10). Evidence for this can be seen in recurrent tumors, where “intermediate-grade features,” including slightly increased pleomorphism, prominent nucleoli, and mitotic activity, can be seen (5). Keys to recognition of these recurrent tumors with intermediate-grade features are the retention of chromatin clearing and ovoid nuclear contours. This threat of progression even in recurrences is argument for definitive resection with negative margins whenever possible.

### References

1. Evans HL, Batsakis JG. Polymorphous low-grade adenocarcinoma of minor salivary glands. A study of 14 cases of a distinctive neoplasm. *Cancer*. 1984;53(4):935–942.
2. Allen MS Jr, Fitz-Hugh GS, Marsh WL Jr. Low-grade papillary adenocarcinoma of the palate. *Cancer*. 1974;33(1):153–158.
3. Freedman PD, Lumerman H. Lobular carcinoma of intraoral minor salivary gland origin. Report of twelve cases. *Oral Surg Oral Med Oral Pathol*. 1983;56(2):157–166.
4. Evans HL, Luna MA. Polymorphous low-grade adenocarcinoma: a study of 40 cases with long-term follow-up and an evaluation of the importance of papillary areas. *Am J Surg Pathol*. 2000;24(10):1319–1328.
5. Seethala RR, Johnson JT, Barnes EL, Myers EN. Polymorphous low-grade adenocarcinoma: the University of Pittsburgh experience. *Arch Otolaryngol Head Neck Surg*. 2010;136(4):385–392.
6. Castle JT, Thompson LD, Frommelt RA, Wenig BM, Kessler HP. Polymorphous low-grade adenocarcinoma: a clinicopathologic study of 164 cases. *Cancer*. 1999;86(2):207–219.
7. el-Naggar AK, Huvos AG. Adenoid cystic carcinoma. In: Barnes EL, Eveson JW, Reichart P, Sidransky D, eds. *World Health Organization Classification of Tumours: Pathology and Genetics. Head and Neck Tumours*. Lyon: IARC Press; 2005:221–222.
8. Prasad ML, Barbacioru CC, Rawal YB, Husein O, Wen P. Hierarchical cluster analysis of myoepithelial/basal cell markers in adenoid cystic carcinoma and polymorphous low-grade adenocarcinoma. *Mod Pathol*. 2008;21(2):105–114.
9. Michal M, Skalova A, Simpson RH, Raslan WF, Curik R, Leivo I, et al. Cribriform adenocarcinoma of the tongue: a hitherto unrecognized type of adenocarcinoma characteristically occurring in the tongue. *Histopathology*. 1999;35(6):495–501.
10. Pelkey TJ, Mills SE. Histologic transformation of polymorphous low-grade adenocarcinoma of salivary gland. *Am J Clin Pathol*. 1999;111(6):785–791.

## 2.9

*Salivary Duct Carcinoma***CLINICAL INFORMATION**

“Enclosed are slides of a right submandibular gland tumor and right neck dissection from a 61-year-old man. As you can see, the gland is largely replaced by a high-grade adenocarcinoma with focal extension into skeletal muscle. Some of the lymph node metastases display papillary features with psammoma-like bodies. There is an apparent intraductal component that would be more suggestive of a primary salivary gland neoplasm, such as cystadenocarcinoma or possibly salivary duct carcinoma. Is this a primary tumor of salivary gland or does it represent a metastatic process?”

**OPINION**

Sections show submandibular gland and lymph nodes involved by a cytologically high-grade adenocarci-

noma, similar to infiltrating and intraductal breast carcinoma. Cribriform growth pattern, “comedo-type” necrosis, and intraductal involvement are seen (Figures 2.9.1 and 2.9.2). The tumor cells have abundant eosinophilic cytoplasm, large pleomorphic hyperchromatic nuclei, and numerous atypical mitotic figures (Figure 2.9.3). Focally, areas of comedo-type necrosis are calcified and simulate “psammoma-body”-type calcifications (Figures 2.9.4 and 2.9.5). Variable amounts of predominantly intracytoplasmic mucin can be seen (Figure 2.9.6). True goblet-type cells are not seen. The tumor is positive for androgen receptor (AR) (1) (Figure 2.9.7). P63 highlights “in situ/intraductal” component (Figure 2.9.8).

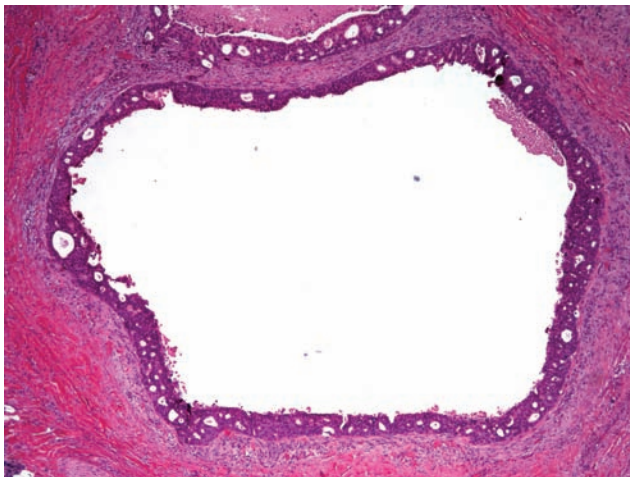


**FIGURE 2.9.1** Large duct involvement by SDC.

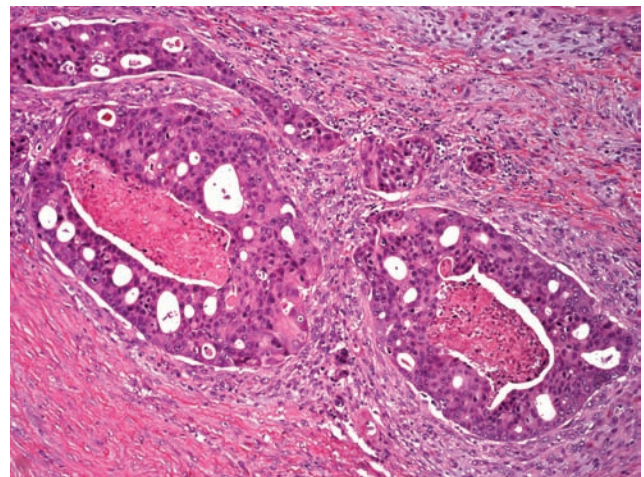


**FIGURE 2.9.2** Cribriform growth pattern and comedo-type necrosis.

## 2.9

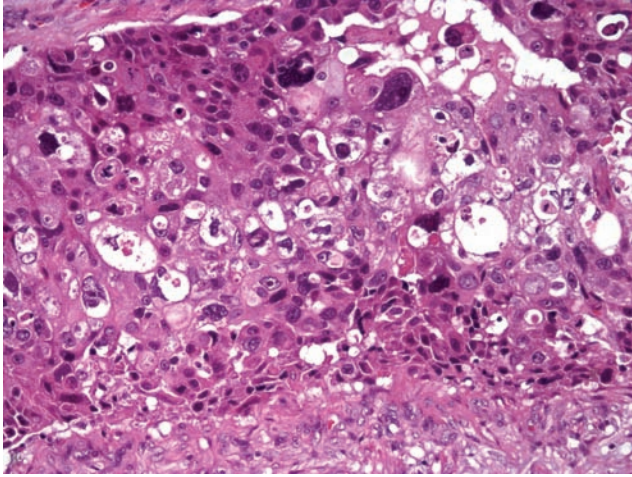


**FIGURE 2.9.3** High-grade cytology of SDC: Abundant eosinophilic cytoplasm, large irregular hyperchromatic nuclei.

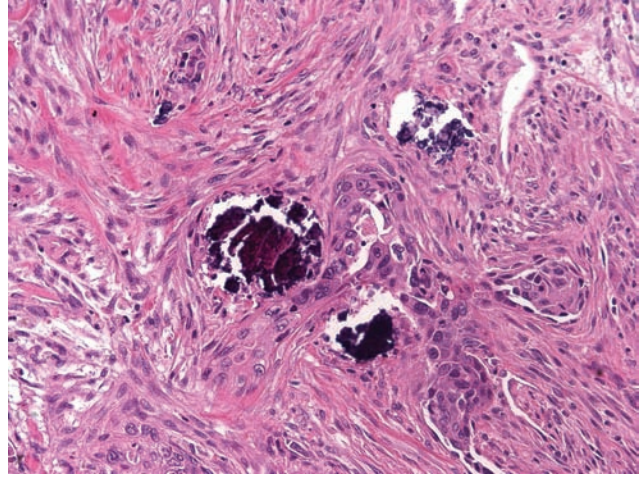


**FIGURE 2.9.5** Psammoma-body-like calcifications.

**DIAGNOSIS**

Right submandibular gland and lymph nodes, excision and dissection: Salivary duct carcinoma involving submandibular gland and metastatic to numerous lymph nodes. In situ component is identified. Perineural invasion is present.

**COMMENT**

We agree that this is a high-grade adenocarcinoma of the submandibular gland with metastases to the right neck lymph nodes. The presence of an in situ component and the involvement of regional lymph nodes are compatible with a submandibular primary. In addition, immunostains for prostate-specific antigen (PSA) and prostate acidic phosphatase (PAP) are negative, practically ruling out the possibility of metastatic prostate adenocarcinoma. The abundant

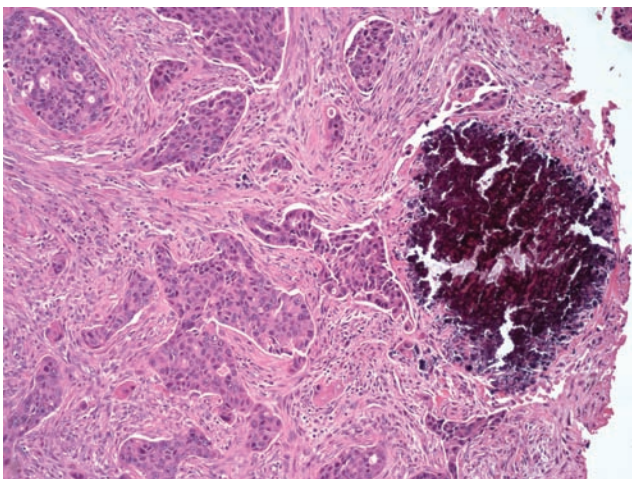


**FIGURE 2.9.4** Calcification of the necrotic foci.

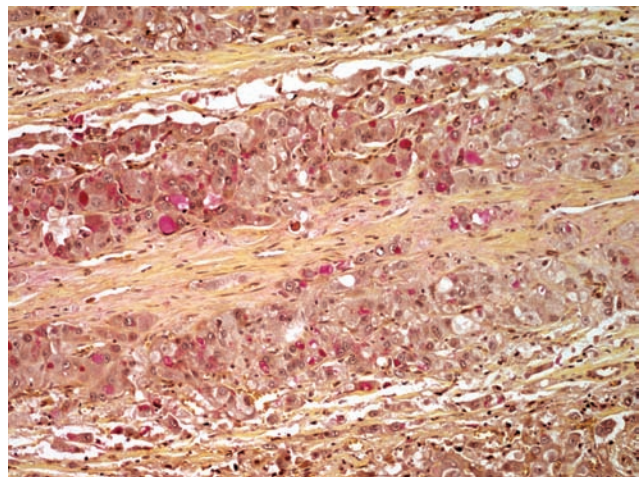


**FIGURE 2.9.6** Mucicarmine stain highlights predominantly intracellular mucin.

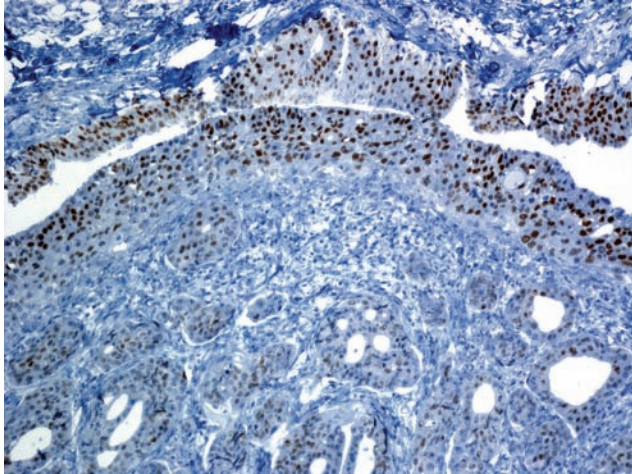


**FIGURE 2.9.7** Strongly positive AR in the intraductal component of SDC. Somewhat weaker AR expression in the infiltrating component of the SDC.

granular eosinophilic cytoplasm, cribriform growth pattern, and “comedo-type” necrosis, combined with the AR positivity, place this tumor in the salivary duct carcinoma (SDC) category.

A high-grade mucoepidermoid carcinoma (MEC) would be negative for AR and would show p63 reactivity in epidermoid cells.

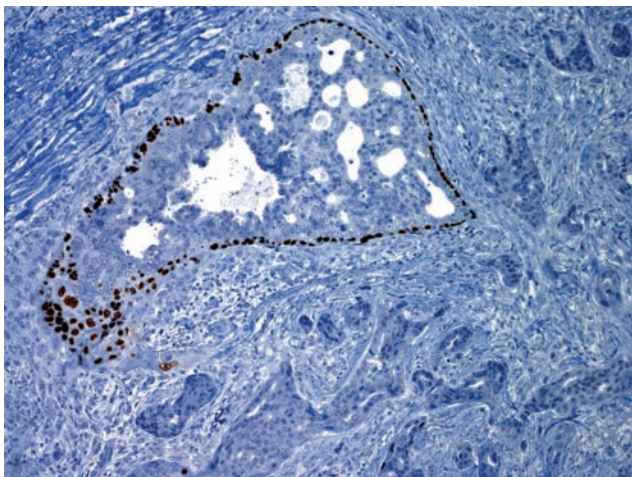


**FIGURE 2.9.8** p63 highlights residual basal/myoepithelial cells, accentuating the in situ component of SDC.



**FIGURE 2.9.9** An example of an “in-house” SDC, with minute foci of chalky comedo-type necrosis and extension to the overlying skin.

## DISCUSSION

Grossly, SDCs are firm, solid, and pink (“in-house” case, Figure 2.9.9). More extensive areas of comedo-type necrosis may be seen as white-grey chalky foci. Involvement of the overlying skin may be seen (Figure 2.9.9).

Salivary duct carcinoma is a rare high-grade epithelial malignancy. Review of our most recent consultation material (including ten cases of SDC in the 2007-2008 academic year) revealed that recognizing SDC is necessary to answer the following two most common questions: (1) Is it a metastasis or a carcinoma primary to the salivary gland? (2) If it is primary to the salivary gland, is it SDC, (cyst)adenocarcinoma, not otherwise specified, or a MEC?

The presence of the in situ component of SDC helps to distinguish it from metastatic prostatic adenocarcinoma in men and metastatic breast carcinoma in women. The in situ component is characterized by a smooth rounded contour and preserved residual layer of the myoepithelial cells. In larger ducts, foci of transition from normal to carcinomatous epithelium may be seen. Finally, p63 and other myoepithelial markers

## 2.9

are helpful in outlining an in situ component (Figure 2.9.8). Immunohistochemically, SDC expresses AR in 92.3% of cases and occasionally PAP (58.3%) and PSA (16.7%), indicating a close similarity with prostatic carcinoma (2). Adenocarcinomas of the AR+/PSA+/-/ PAP+/- phenotype remain diagnostically challenging because metastasis cannot be ruled out with confidence. In addition, metastatic SDC should be considered when no prostatic primary is found (3). In women, while considering the possibility of breast carcinoma metastatic to the neck, one should remember that 6% and 1.3% of SDC express progesterone and estrogen receptors, respectively (2).

Unlike SDC, MEC consists of a heterogeneous cell population, including basal, epidermoid (highlighted by p63), and mucinous cells. Mucoepidermoid carcinoma lacks a cribriform growth pattern and does not show comedo-type necrosis. Finally, a significant subset of MEC is characterized by MECT1-MAML2 t(11;19)(q21;p13) translocation (4). A rare mucin-rich variant of SDC has been described, occasionally even resembling colloid carcinoma of the breast (5).

Importantly, in most SDCs, mucin is intracellular rather than intraluminal/intracystic (Figure 2.9.6).

Unlike SDC, cystadenocarcinomas are cytologically low-grade tumors with true columnar/mucinous cells and abundant intraluminal/intracystic mucin. Cystadenocarcinomas rarely show cribriform growth pattern or comedo-type necrosis.

### References

1. Kapadia SB, Barnes L. Expression of androgen receptor, gross cystic disease fluid protein, and CD44 in salivary duct carcinoma. *Mod Pathol.* 1998;11(11):1033–1038.
2. Fan CY, Wang J, Barnes EL. Expression of androgen receptor and prostatic specific markers in salivary duct carcinoma: an immunohistochemical analysis of 13 cases and review of the literature. *Am J Surg Pathol.* 2000;24(4):579–586.
3. James GK, Pudek M, Berean KW, Diamandis EP, Archibald BL. Salivary duct carcinoma secreting prostate-specific antigen. *Am J Clin Pathol.* 1996;106(2):242–247.
4. Okabe M, Miyabe S, Nagatsuka H, Terada A, Hanai N, Yokoi M, et al. MECT1-MAML2 fusion transcript defines a favorable subset of mucoepidermoid carcinoma. *Clin Cancer Res.* 2006;12(13):3902–3907.
5. Simpson RH, Prasad AR, Lewis JE, Skalova A, David L. Mucin-rich variant of salivary duct carcinoma: a clinicopathologic and immunohistochemical study of four cases. *Am J Surg Pathol.* 2003;27(8):1070–1079.

## 2.10

*Salivary Gland Sebaceous Carcinoma***CLINICAL INFORMATION**

“A 75-year-old man with a large right parotid mass.”

**OPINION**

Microscopically, the tumor consists of a solid infiltrative mass within a highly fibrous stroma (Figure 2.10.1). On higher magnification, tumor cells are plump and polygonal with clear, microvacuolated cytoplasm. Nuclei are pleomorphic with prominent central nucleoli (Figure 2.10.2). Perineural invasion is identified (Figure 2.10.3). The tumor is positive for epithelial membrane antigen (Figure 2.10.4), p63 (Figure 2.10.5), and p53 but negative for androgen receptor. The mucicarmine is negative (Figure 2.10.6), and the fluorescent in situ hybridization for *MAML2* gene rearrangements is negative (Figure 2.10.7). On the skin overlying the parotid lesion, there is a small

superficially invasive squamous cell carcinoma that shows no connection with the parotid mass (Figure 2.10.8). The keratinizing nested squamous cell carcinoma is morphologically distinct from the parotid lesion (Figure 2.10.9).

**DIAGNOSIS**

Parotid and skin, right parotidectomy and skin excision:

- Sebaceous carcinoma, poorly differentiated, parotid
- Separate focus of cutaneous superficially invasive squamous cell carcinoma.

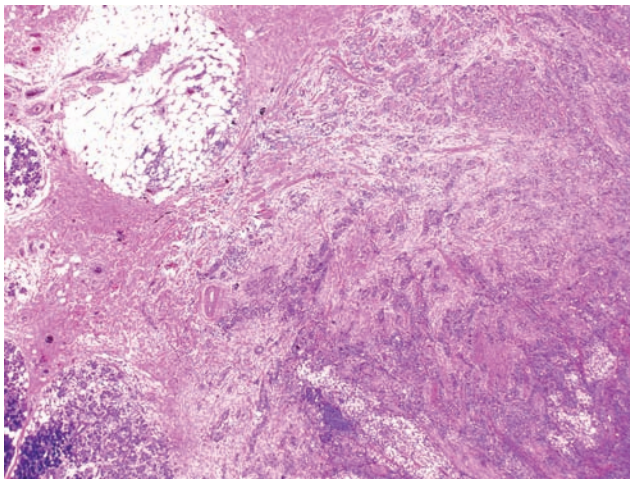


**FIGURE 2.10.1** Infiltrative solid tumor.

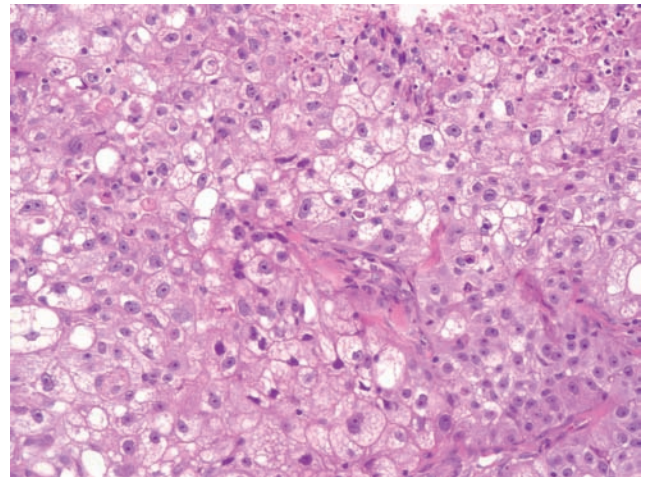


**FIGURE 2.10.2** Cells with clear vacuolated cytoplasm and pleomorphic nuclei with prominent nucleoli.

## 2.10

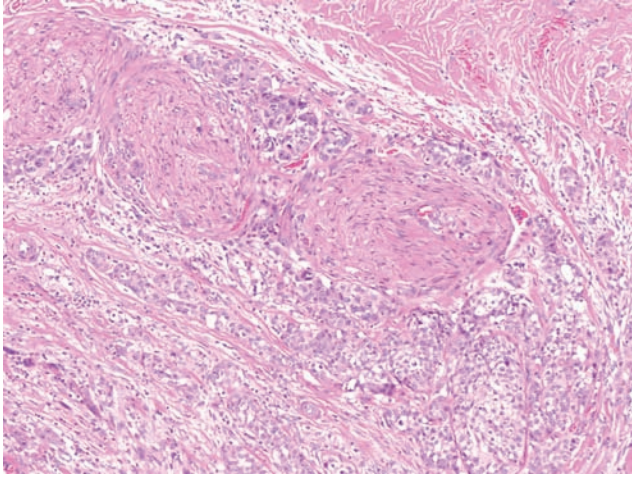


FIGURE 2.10.3 Perineural invasion.

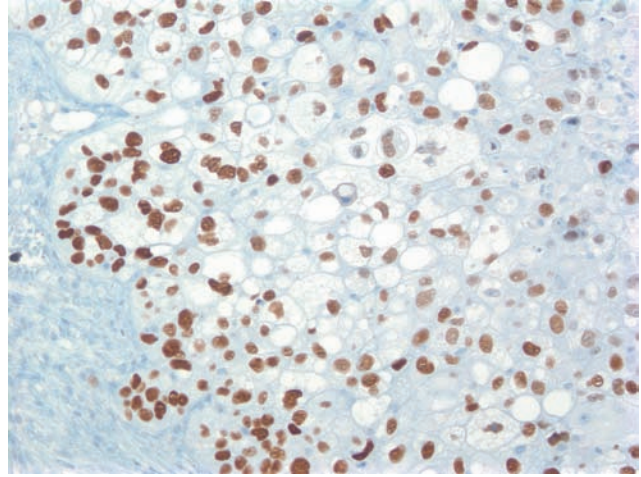


FIGURE 2.10.5 P63 is positive.

## COMMENT

This is an example of a sebaceous carcinoma that is likely of salivary gland origin rather than of skin adnexal origin. The challenge of classifying this tumor is further compounded by the presence of a cutaneous squamous cell carcinoma. However, the small size of the skin lesion, the spatial separation, and the morphologic differences here suggest that these are separate tumors.

## DISCUSSION

Sebaceous carcinoma of salivary gland origin is extremely rare. There is a bimodal age distribution peaking in the third decade and the seventh to eighth decade. More than 90% occur in the parotid. Unlike cutaneous adnexal sebaceous carcinomas, those of the salivary gland do not appear to be part of the Muir-Torre syndrome. In support of this, DNA mismatch repair proteins are retained (1,2).

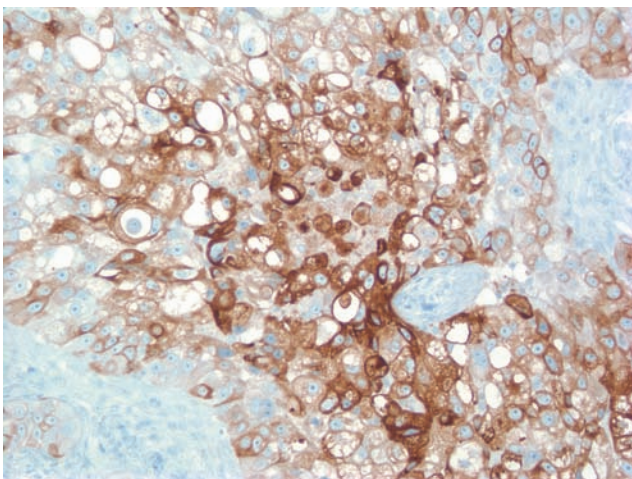


FIGURE 2.10.4 Epithelial membrane antigen is positive.

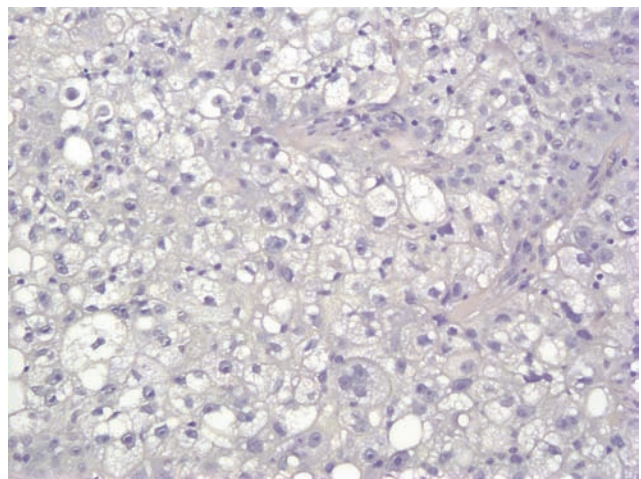
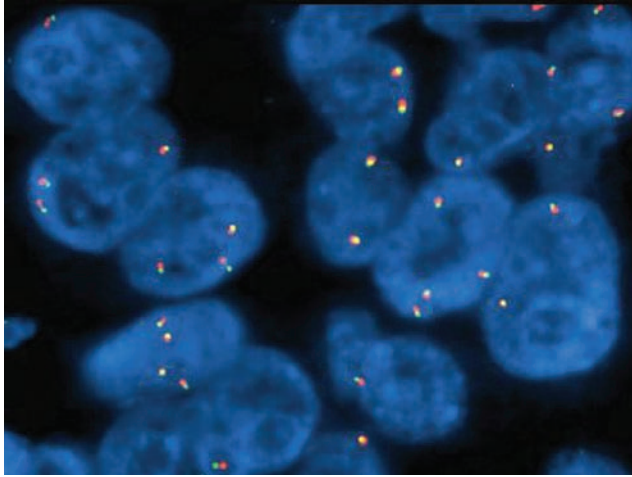
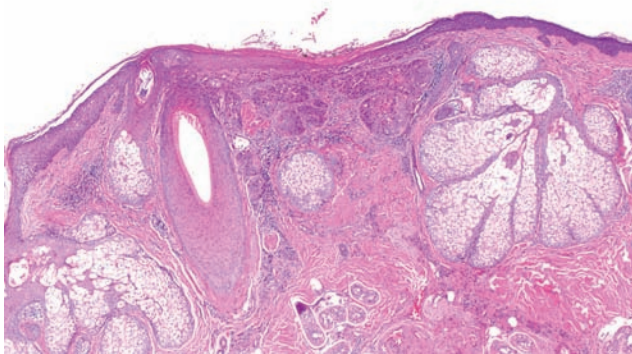


FIGURE 2.10.6 Mucicarmine is negative.



**FIGURE 2.10.7** MAML2 FISH using breakapart probes shows intact signals (red and green close together) in all cells and is thus negative for a rearrangement. Polysomy (greater than two signals per cell) is present in many cells.

Differential diagnostic considerations encompass both skin and parotid lesions. It is difficult to distinguish a skin sebaceous carcinoma from a parotid sebaceous carcinoma. One useful distinguishing feature is the location of the majority of the tumor. In addition, unlike cutaneous sebaceous carcinomas, those of the parotid are typically androgen receptor-negative (3). Other entities in the differential diagnosis include clear cell muco dermoid carcinoma and its



**FIGURE 2.10.8** A separate superficially invasive squamous cell carcinoma (SCC) of the skin.

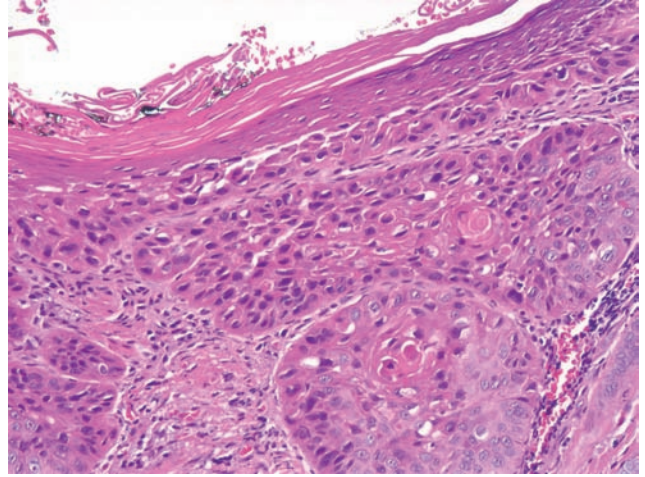


**FIGURE 2.10.9** Keratinizing morphology is distinct from the parotid mass.

cutaneous counterpart, hidradenocarcinoma. However, sebaceous carcinomas are negative for mucicarmine and do not harbor the t(11;19) MECT-MAML2 translocation seen in mucoepidermoid carcinoma and hidradenocarcinomas (4,5).

## References

1. Gnepp DR. Malignant sebaceous tumors. In: Barnes EL, Eveson JW, Reichart P, Sidransky D, eds. *Pathology and Genetics: Head and Neck Tumors*. Lyons: IARC; 2005.
2. Batsakis JG, el-Naggar AK. Sebaceous lesions of salivary glands and oral cavity. *Ann Otol Rhinol Laryngol*. 1990;99 (5 Pt 1):416–418.
3. Shinozaki A, Nagao T, Endo H, Kato N, Hirokawa M, Mizobuchi K, et al. Sebaceous epithelial-myoepithelial carcinoma of the salivary gland: clinicopathologic and immunohistochemical analysis of 6 cases of a new histologic variant. *Am J Surg Pathol*. 2008;32(6):913–923.
4. Kazakov DV, Ivan D, Kutzner H, Spagnolo DV, Grossmann P, Vanecek T, et al. Cutaneous hidradenocarcinoma: a clinicopathological, immunohistochemical, and molecular biologic study of 14 cases, including Her2/neu gene expression/amplification, TP53 gene mutation analysis, and t(11;19) translocation. *Am J Dermatopathol*. 2009;31(3):236–247.
5. Martins C, Cavaco B, Tonon G, Kaye FJ, Soares J, Fonseca I. A study of MECT1-MAML2 in mucoepidermoid carcinoma and Warthin's tumor of salivary glands. *J Mol Diagn*. 2004;6(3):205–210.



## 2.11

*Sclerosing Polycystic Adenosis***CLINICAL INFORMATION**

“This 63-year-old woman has had a history of a right parotid mass for 5 years. There is no lymphadenopathy. The lesion was excised and presents an unusual histology. We would appreciate your opinion.”

**OPINION**

Sections show a well-circumscribed fibrolipomatous lesion containing epithelial cells with both ductal and acinar differentiation arranged in a lobular as well as a diffuse pattern (Figures 2.11.1, 2.11.2, 2.11.3, and 2.11.4). Ducts, often dilated or cystic, are lined by epithelium that varies from atrophic, to hyperplastic, to cribriform (Figures 2.11.5 and 2.11.6). Some ducts are lined by cells with an apocrine, mucous, or squamoid appearance (Figures 2.11.6, 2.11.7, 2.11.8, and 2.11.9). In a few areas, the ducts are distended by cells

with uniform, bland, mitotically inactive nuclei surrounded by a peripheral layer of myoepithelial cells. Acini often contain large, eosinophilic, zymogen-like granules (Figure 2.11.10).

The ratio of ductal-acinar components to stroma is highly variable, with some parts of the tumor being mainly fibrous to those that are more epithelial. Closely packed glands similar to sclerosing adenosis of the breast are common, as well as sparse areas of chronic inflammation (Figures 2.11.11 and 2.11.12).

The ducts and acini are positive for cytokeratins (AE1/3 and CAM 5.2) and variably positive for epithelial membrane antigen and S100 protein and are surrounded by a layer of myoepithelial cells. In a few areas, the epithelial cells are weakly positive for estrogen and progesterone receptors.

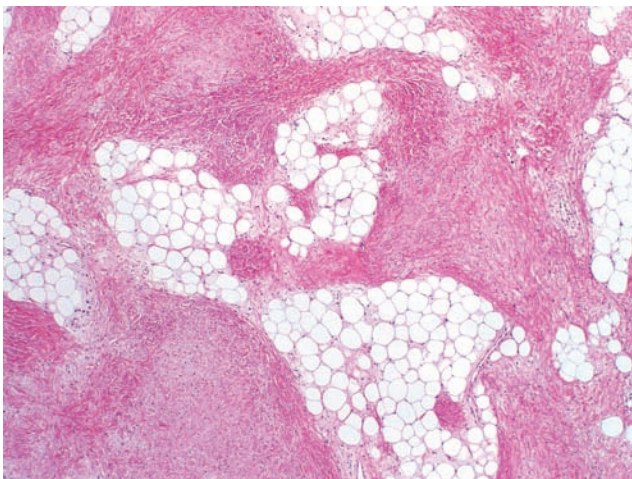


**FIGURE 2.11.1** Area composed of fibrolipomatous tissue devoid of an epithelial component.

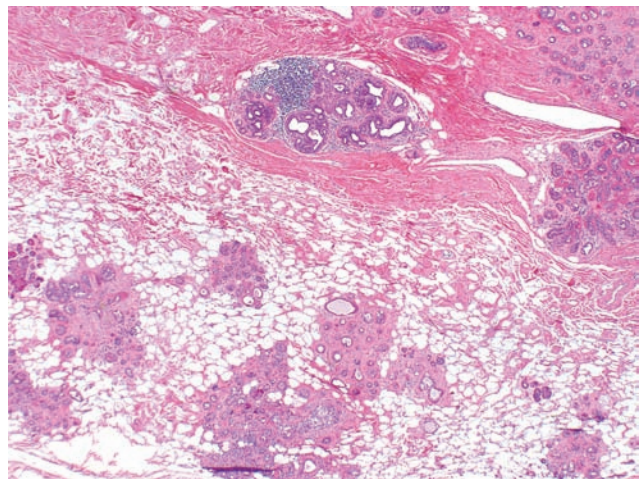


**FIGURE 2.11.2** Another area composed of well-defined lobules of salivary ducts and acini.

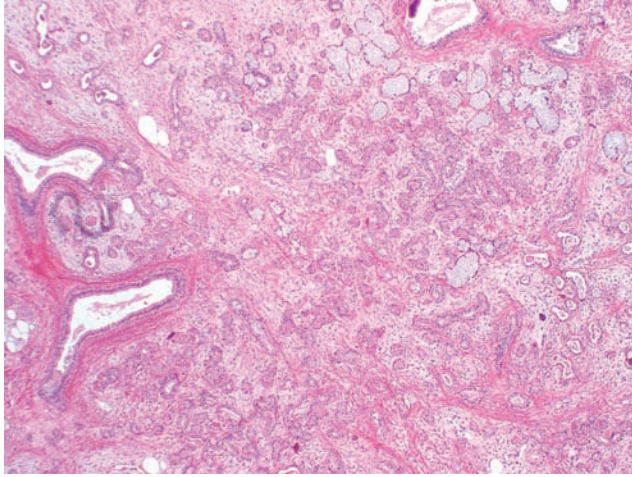


**FIGURE 2.11.3** In some areas, the proliferation of ducts and acini is more diffuse.

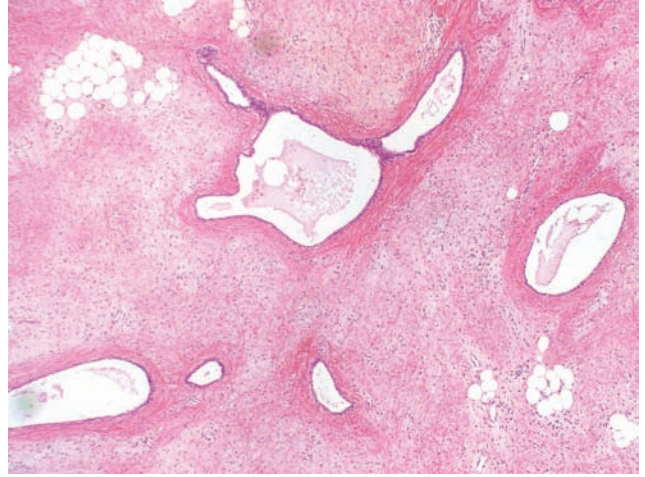


**FIGURE 2.11.5** Some ducts are cystically dilated and lined by atrophic epithelium.

#### DIAGNOSIS

Lesion of right parotid gland: Sclerosing polycystic adenosis.

#### COMMENT

Sclerosing polycystic adenosis (SPA) is a recently described entity that is regarded as the salivary equiv-

alent of fibrocystic disease—sclerosing adenosis of the breast. Simple excision is usually curative.

#### DISCUSSION

Sclerosing polycystic adenosis is a rare salivary disorder first described by Smith et al in 1996 (1). Although regarded as the salivary homolog of fibrocystic disease—sclerosing adenosis of the breast, a few cases have shown ductal epithelial atypia/dysplasia,

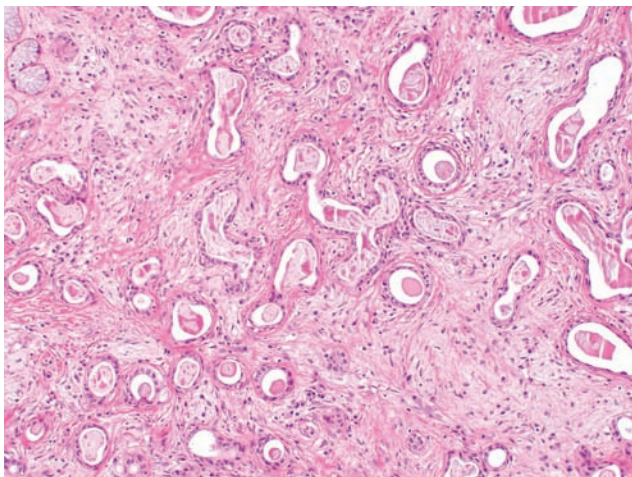


**FIGURE 2.11.4** High-power view of ducts with luminal secretions.

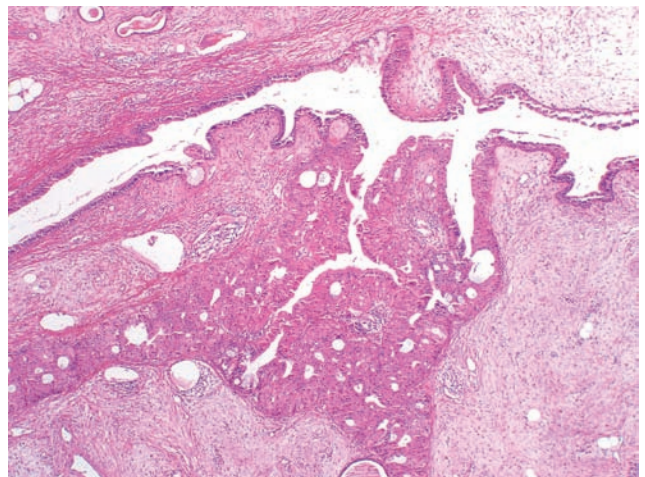


**FIGURE 2.11.6** A duct lined by hyperplastic, apocrine type cells.

## 2.11

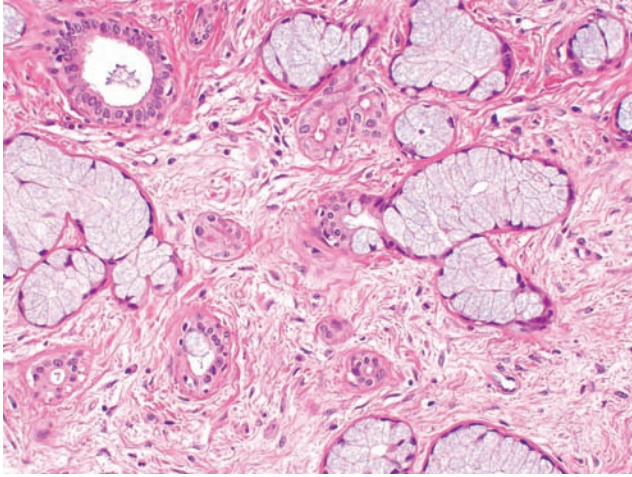


**FIGURE 2.11.7** Some ducts and acini are lined by mucous cells.

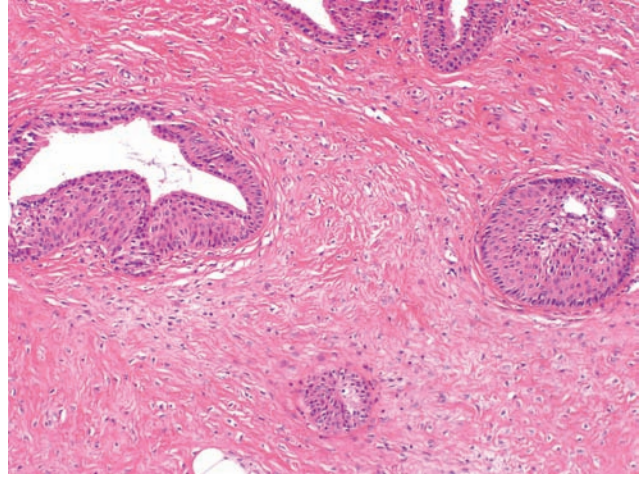


**FIGURE 2.11.9** Ducts with squamous metaplasia.

carcinoma in situ, and/or clonality, raising the possibility that it may even be a neoplasm (2,3).

Sclerosing polycystic adenosis occurs over a broad age range (mean, 41 years; range, 9–84 years) and is slightly more common in females (58%). It arises most often in the parotid gland but has also been described in the submandibular and minor salivary glands (hard palate, buccal mucosa, and floor of mouth).

The differential diagnosis might include polycystic (dysgenetic) disease, chronic sclerosing sialadenitis, and possibly even carcinoma.

Polycystic (dysgenetic) disease is a rare developmental disorder consisting of a diffuse, honeycombed, lattice work of cysts with inspissated secretions replacing normal salivary parenchyma with only rare residual acini. Unlike SPA, fibrosis is not prominent, and ductal/acinar proliferation is absent.

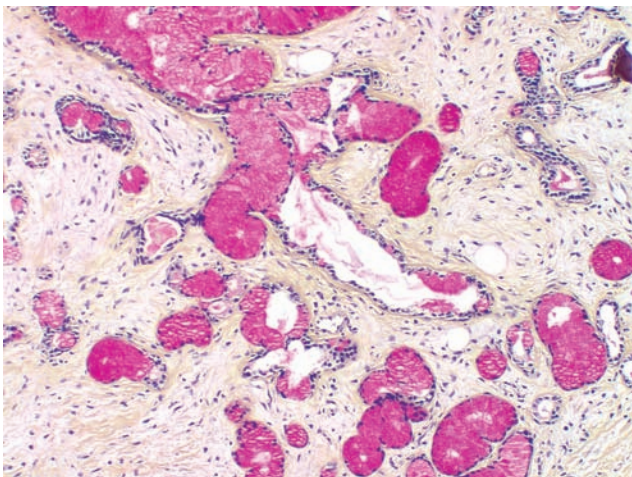


**FIGURE 2.11.8** A mucicarmine stain confirms the mucous content of the cells shown in Figure 2.11.7.

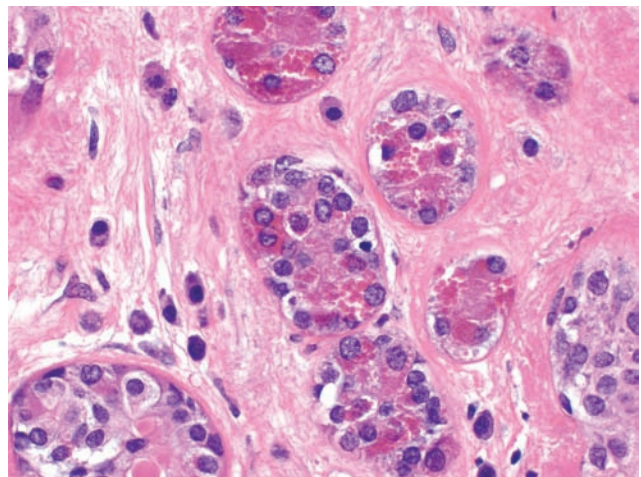


**FIGURE 2.11.10** Acini containing eosinophilic zymogen-like granules.

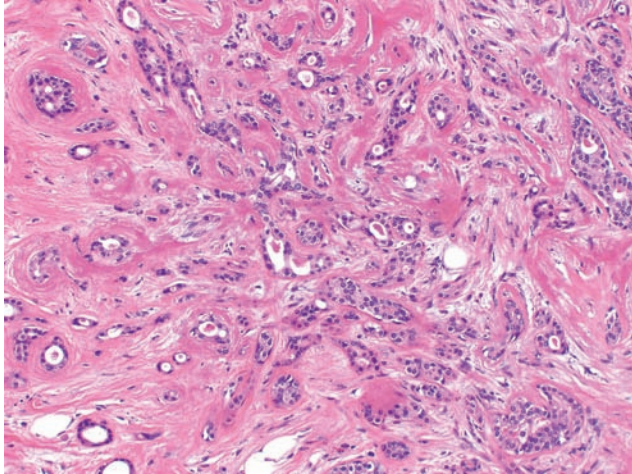


**FIGURE 2.11.11** Area of sclerosing adenosis.

Chronic sclerosing sialadenitis, also sometimes referred to as Kuttner tumor, mainly affects the submandibular gland rather than the parotid gland and is characterized by extensive fibrosis and chronic inflammation with a large component of IgG4 plasma cells. Unlike SPA, ductal/acinar proliferation is not seen.

Because of the adenosis and occasional ductal atypia/dysplasia, SPA might be mistaken for a carcinoma. Overall lobular architecture, prominent peripheral layer of myoepithelial cells around the ducts and acini, and lack of invasion are features against a carcinoma but do not exclude focal in situ changes observed in a few cases of SPAs.

Although simple surgical excision is usually curative, 10% to 20% of patients may develop one or more local recurrences, usually after an interval of 4

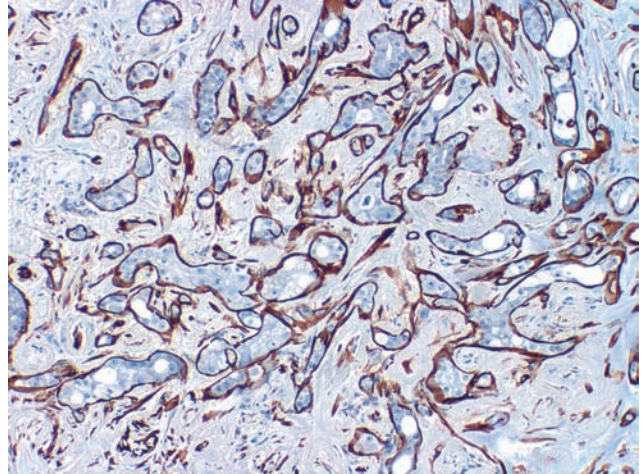


**FIGURE 2.11.12** A calponin stain of sclerosing adenosis shown in Figure 2.11.11 demonstrates a layer of myoepithelial cells around each duct.

or more years. The histology of the recurrent tumor has been similar to that of the primary. No patient has so far developed metastasis or died of the disease.

### References

1. Smith BC, Ellis GL, Slater LJ, Foss RD. Sclerosing polycystic adenosis of major salivary glands. A clinicopathologic analysis of nine cases. *Am J Surg Pathol.* 1996;20:161–170.
2. Skalova A, Michal M, Simpson RH, Starek I, Pradna J, Pfaltz M. Sclerosing polycystic adenosis of parotid gland with dysplasia and ductal carcinoma in situ. Report of three cases with immunohistochemical and ultrastructural examination. *Virchows Arch.* 2002;440:29–35.
3. Gnepp DR, Wang LJ, Brandwein-Gensler M, Slootweg P, Gill M, Hille J. Sclerosing polycystic adenosis of the salivary gland: a report of 16 cases. *Am J Surg Pathol.* 2006;30:154–164.

## 2.12

*Sialadenoma Papilliferum*

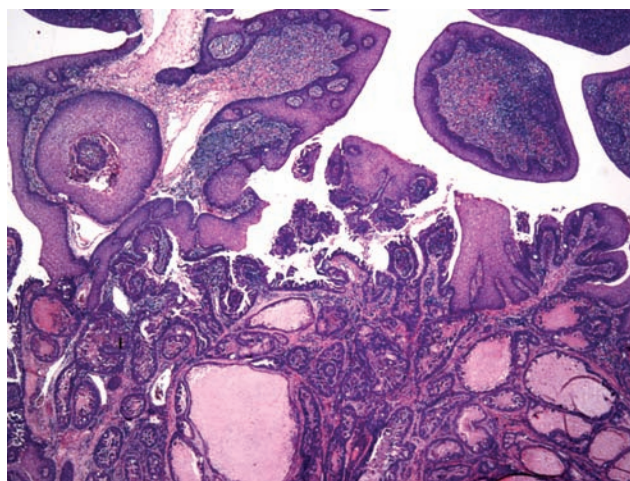
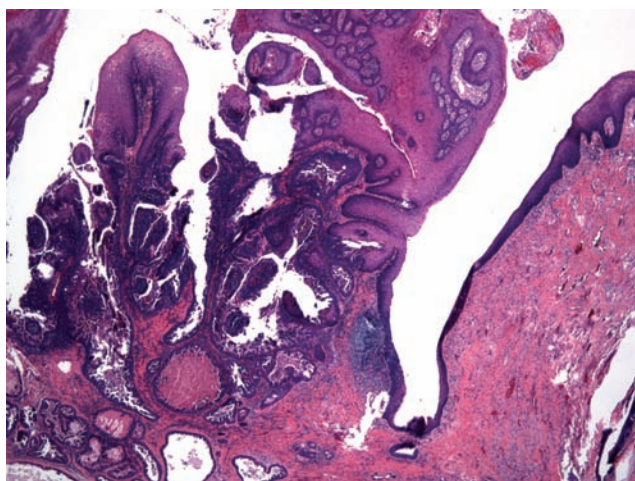
## CLINICAL INFORMATION

“This is a firm fungating base of tongue mass in a 61-year-old man. The patient has no prior significant medical history. The specimen is a 2.1-cm excisional biopsy of a firm, white exophytic base of tongue mass. The lesion shows some features of sialadenoma papilliferum; however, it is quite large and shows a haphazard infiltrative architecture near its base. I am concerned about a low-grade adenocarcinoma. At the time of intraoperative consultation, the differential diagnosis included invasive squamous cell carcinoma, mucoepidermoid carcinoma, or other carcinomas of the minor salivary gland origin.”

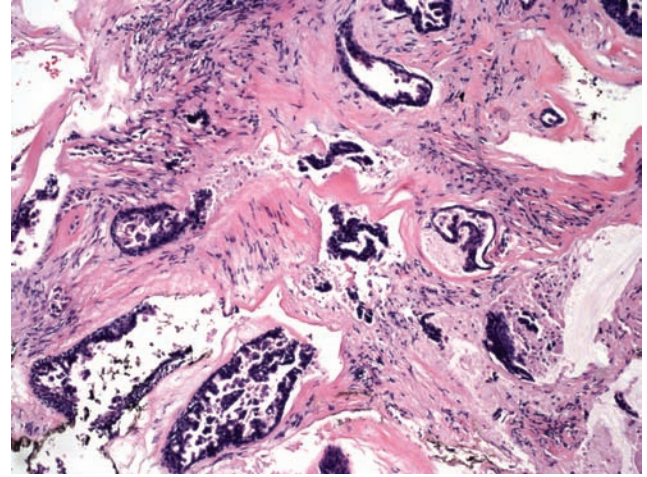
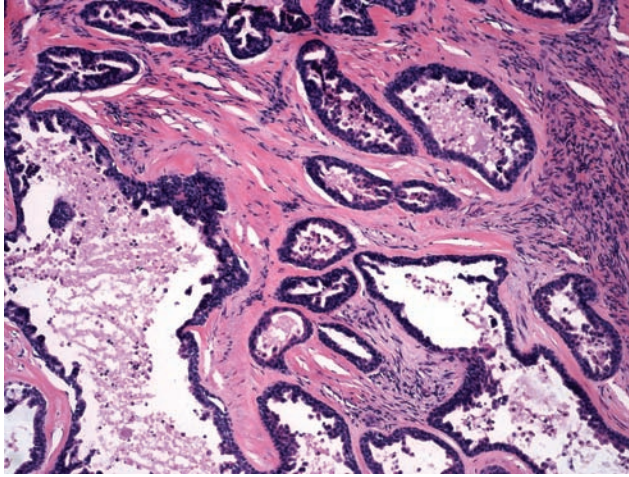
## OPINION

Sections show a lesion with an exophytic squamous papillary surface (Figures 2.12.1 and 2.12.2) and

an apparently infiltrative base (Figures 2.12.3 and 2.12.4). Because the lesion extends to the resection edge, it is difficult to appreciate whether it is circumscribed or encapsulated. Papillary stalks are lined by acanthotic nonkeratinizing squamous epithelium resembling squamous papilloma at low magnification (Figures 2.12.1 and 2.12.2). Immediately adjacent to the squamous epithelium, there is glandular component (Figure 2.12.5). The glands are distended and angulated, and some appear “broken.” Intraductal micropapillary proliferations and mucoid debris with numerous intraluminal neutrophils are noted. Most of the ducts are connected to the surface (Figure 2.12.2). The ductular epithelium is composed of two layers—inner columnar and basal cells (Figure 2.12.6). A moderate predominantly plasmacytoid infiltrate is apparent in the stroma (Figure 2.12.7).



FIGURES 2.12.1 AND 2.12.2 Papillary surface of the SP.



FIGURES 2.12.3 AND 2.12.4 Distended irregular glands at the base of the SP.

#### DIAGNOSIS

Base of tongue, excision: Sialadenoma papilliferum with marked acute inflammation.

#### COMMENT

We believe the lesion is benign and represents a sialadenoma papilliferum (SP). This lesion shows focally exuberant micropapillary growth pattern. Although

we were not involved in the gross evaluation of this specimen, the lesion appears to focally extend to one of the margins. For this reason, local recurrence may be an issue in the future. In the literature, of about 20 cases with available follow-up, 2 cases were reported to recur within 3 years (1,2).

#### DISCUSSION

Sialadenoma papilliferum is a rare benign salivary-type neoplasm. It most likely arises from the excretory

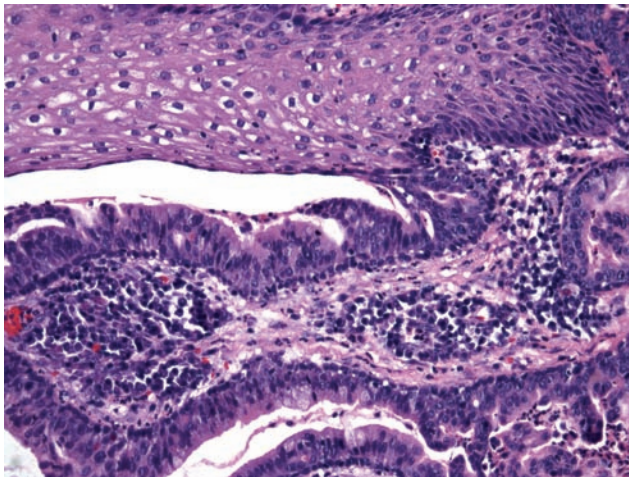


FIGURE 2.12.5 Abrupt transition between squamous epithelium and glandular component.

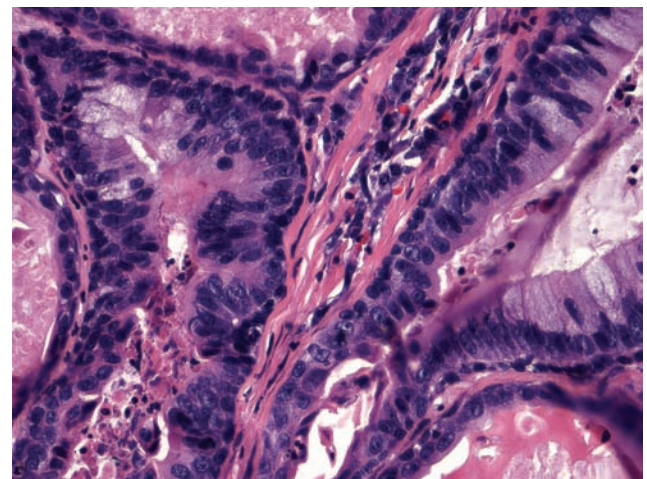
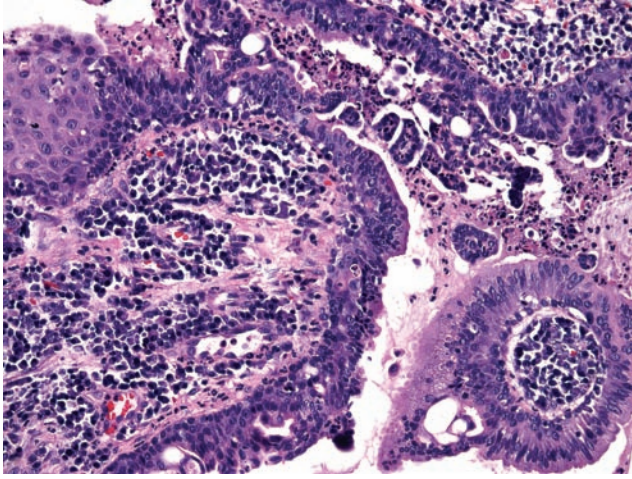


FIGURE 2.12.6 Double-layered ductal epithelium.

## 2.12



**FIGURE 2.12.7** Predominantly plasmacytoid stromal infiltrate.

ducts of the minor salivary glands. At the time of preparation of this report, 61 cases were described in the English literature (most are summarized in Brannon et al (3) and Pires et al (4)). The great majority of SP develops at the border between the hard and soft palate. Buccal mucosa is the second most common site, and the base of tongue is a rather unique location for SP. Sialadenoma papilliferum presents as a slowly growing exophytic mass and clinically is most commonly thought to be a squamous papilloma or a verrucous carcinoma. The key diagnostic feature of an SP is the combination of 2 components: (1) exophytic superficial papillomatous squamous component and (2) underlying ductal proliferation composed of luminal columnar cells and basal cells. The presence of the glandular component differentiates SP from a routine squamous papilloma. In addition, further diagnostic considerations include inverted ductal papilloma and an intraductal mucoepidermoid carcinoma. Inverted ductal papillo-

mas have an endophytic growth pattern and are usually submucosal. Initially, SP and mucoepidermoid carcinomas may appear to be composed of the same cellular elements: squamous and glandular.

However, in mucoepidermoid carcinomas, these elements are intermixed, and in SP, they are quite distinct: squamous—superficial, and glandular—endophytic. In addition, one could rely on the double-layered nature of the ductal component in SP and on specific molecular changes in the mucoepidermoid carcinoma (see “Salivary Duct Carcinoma” discussion).

Recently, the first case of an SP with a confirmed malignant component was reported (5). This tumor included an SP and areas of epithelial-myoepithelial carcinoma with high-grade component metastatic to the lung and cervical vertebrae. In addition, severe dysplasia/carcinoma in situ in the squamous component of the SP is a known occurrence (6).

### References

1. Pimentel MT, Lopez Amado M, Garcia Sarandeses A. Recurrent sialadenoma papilliferum of the buccal mucosa. *J Laryngol Otol.* 1995;109(8):787–790.
2. Rennie JS, MacDonald DG, Critchlow HA. Sialadenoma papilliferum. A case report and review of the literature. *Int J Oral Surg.* 1984;13(5):452–454.
3. Brannon RB, Sciubba JJ, Giuliani M. Ductal papillomas of salivary gland origin: a report of 19 cases and a review of the literature. *Oral Surg Oral Med Oral Pathol Oral Radiol Endod.* 2001;92(1):68–77.
4. Pires FR, Pringle GA, de Almeida OP, Chen SY. Intra-oral minor salivary gland tumors: a clinicopathological study of 546 cases. *Oral Oncol.* 2007;43(5):463–470.
5. Shimoda M, Kameyama K, Morinaga S, Tanaka Y, Hashiguchi K, Shimada M, et al. Malignant transformation of sialadenoma papilliferum of the palate: a case report. *Virchows Arch.* 2004;445(6):641–646.
6. Ponniah I. A rare case of sialadenoma papilliferum with epithelial dysplasia and carcinoma in situ. *Oral Surg Oral Med Oral Pathol Oral Radiol Endod.* 2007;104(2):e27–e29.

### 3 Sinonasal Tract—Nasopharynx

The sinonasal tract and nasopharynx are encased in bone and lined by 3 types of epithelium: Ectodermally derived ciliated respiratory mucosa (Schneiderian membrane) and neuroectodermally derived olfactory mucosa in the sinonasal tract, and endodermally respiratory and squamous mucosa in the nasopharynx. It is therefore not surprising that some of the most unusual and unique tumors of the head and neck are found in this location.

Knowledge of the presenting signs and symptoms, laterality, site of occurrence, and imaging studies are of immense value in evaluating these specimens. Although virtually any condition of the sinonasal tract and nasopharynx can manifest with nasal obstruction and epistaxis, pain and neurologic disturbances always arouse suspicion of malignancy. Unilateral lesions are also of more concern than those that are bilateral because they are more often neoplastic as opposed to bilateral lesions, which tend to be bland or inflammatory (ie, chronic polypoid rhinosinusitis).

Site of origin can focus the differentiation diagnosis. For instance, angiofibroma predilects the

nasopharynx, the exophytic Schneiderian papilloma the nasal septum, the inverted papilloma the lateral nasal wall–ethmoid sinus region, the olfactory neuroblastoma the cribriform plate, the hamartomas the nasal septum, and the adenocarcinomas the ethmoid sinus.

Imaging studies are essential in further clarifying the site of origin and the extent of disease. One must remember that in the relatively enclosed osseous framework of the sinonasal tract and nasopharynx, any lesion, including ordinary sinonasal polyps, may cause bone erosion. Frank bone destruction, on the other hand, is obviously a sign of a more aggressive condition. Awareness of the imaging findings can also be very helpful in the evaluation of lesions that are histologically borderline malignant.

#### Selected Readings

1. Barnes L. Diseases of the nasal cavity, paranasal sinuses, and nasopharynx. In: *Surgical Pathology of the Head and Neck*. 3rd ed. New York: Informa Healthcare; 2009:343–422.
2. Barnes L, Eveson JW, Reichart P, Sidransky. *World Health Organization Classification of Tumours. Pathology and Genetics, Head and Neck Tumours*. Lyon: IARC Press; 2005.



## 3.1

*Exophytic Schneiderian Papilloma***CLINICAL INFORMATION**

“Enclosed please find slides of a left nasal cavity tumor from a 56-year-old man. The tumor seems to be compatible with a sinonasal Schneiderian papilloma. Focal squamous atypia and mitoses are seen. I would appreciate your opinion.”

**OPINION**

Sections show an exophytic mucosal lesion composed of fibrovascular cores covered primarily by a hyperplastic, nonkeratinizing squamous epithelium with interspersed ciliated respiratory epithelium, mucous (goblet) cells, and microcysts (Figures 3.1.1, 3.1.2, 3.1.3, and 3.1.4). Focally, the epithelium is keratinized with an overlying scale of parakeratin (Figures 3.1.5 and 3.1.6). Few mitoses are apparent in the basal

layer of the epithelium but no dysplasia. Mucoserous (minor salivary) glands and cartilage are not seen, nor is there any unequivocal evidence of an inverted growth pattern.

**DIAGNOSIS**

Lesion left nasal cavity, biopsy: Schneiderian papilloma (see comment).

**COMMENT**

As indicated above, I believe this is a Schneiderian papilloma. The papilloma has an exophytic pattern as typically seen in Schneiderian papillomas arising from

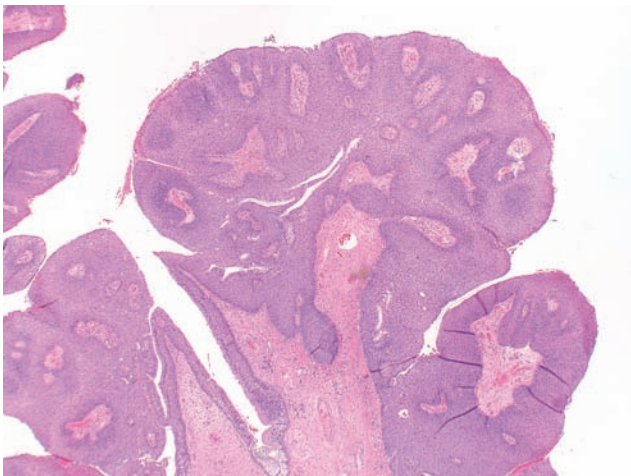


**FIGURE 3.1.1** Exophytic Schneiderian papilloma, low magnification. Note the exophytic growth and essential absence of surface keratin.

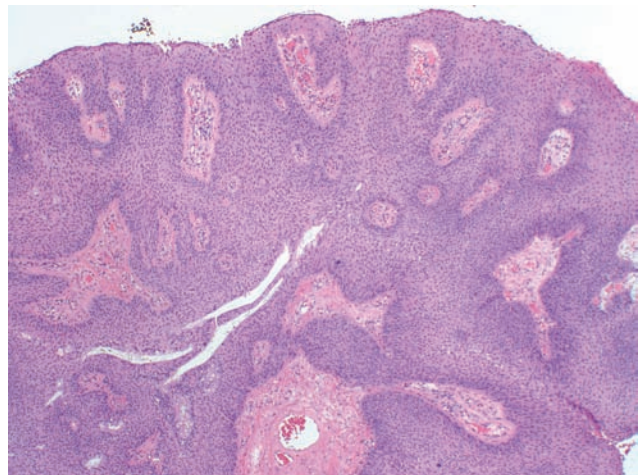


**FIGURE 3.1.2** Exophytic Schneiderian papilloma composed of nonkeratinized squamous epithelium.

3.1

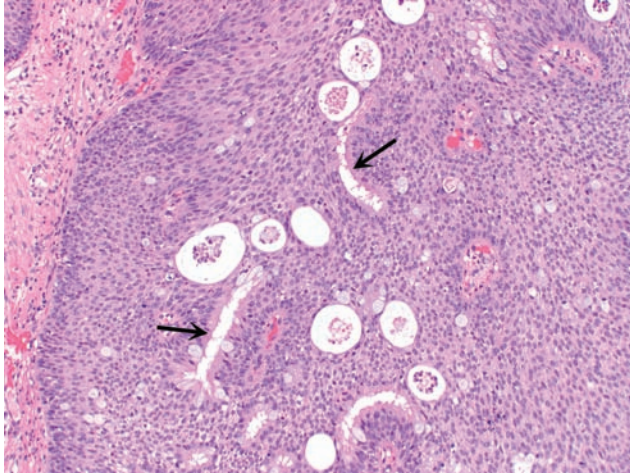


**FIGURE 3.1.3** Exophytic Schneiderian papilloma. Note the small foci of interspersed ciliated, respiratory epithelium (arrows) and small cysts.

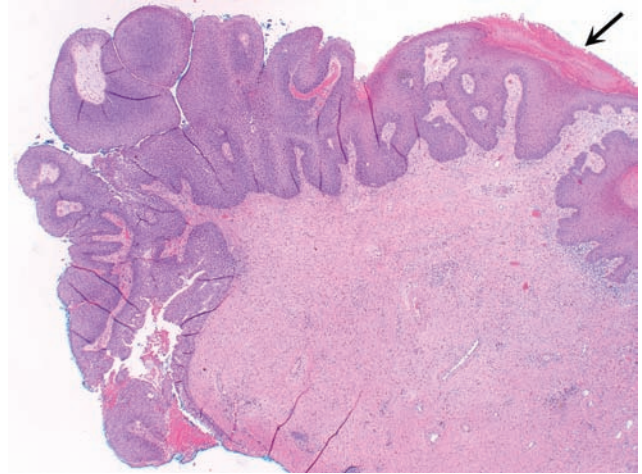


**FIGURE 3.1.5** Exophytic Schneiderian papilloma showing focal surface keratinization (arrow).

the nasal septum. In some instances, inverted papillomas may also have a focal exophytic component. If this is the entire lesion, I would call it an exophytic Schneiderian papilloma (ESP). If there is any residual lesion in the patient, the distinction between the 2 papillomas rests on thorough examination of the resected lesion as well as on the presumed site of origin (septum versus lateral nasal wall).

### DISCUSSION

The ectodermally derived respiratory mucosa that lines the sinonasal tract, so-called Schneiderian membrane, gives rise to 3 morphologically distinct papillomas. These are referred to as the ESP, the inverted Schneiderian papilloma (ISP), and the oncocytic Schneiderian papilloma (OSP) (1).

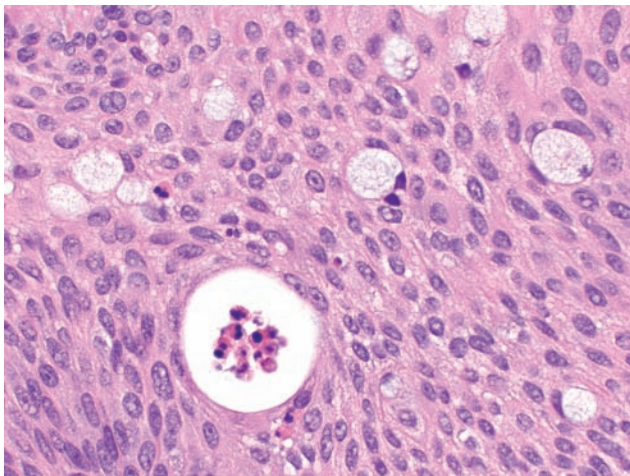


**FIGURE 3.1.4** Exophytic Schneiderian papilloma. Higher magnification shows residual mucous (goblet) cells and a small cyst.

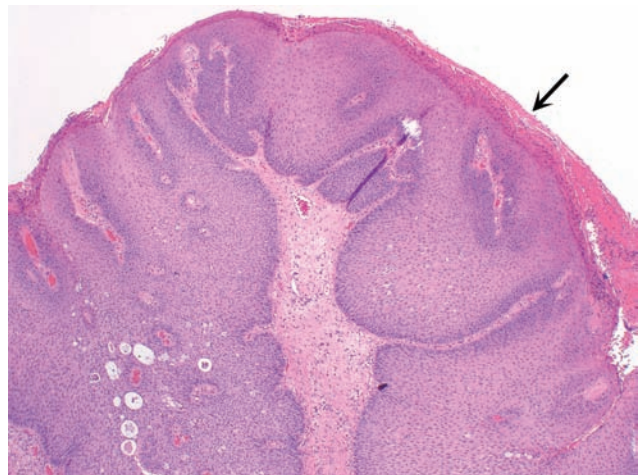


**FIGURE 3.1.6** Another view of Figure 3.1.5. Although focally keratinized (arrow), the presence of residual mucous (goblet) cells and cysts readily identify this lesion as an ESP rather than a cutaneous papilloma.

### 3.1

The ESP arises almost exclusively from the lower, anterior nasal septum; rarely exceeds 2-cm; and has little to no malignant potential. The ISP arises primarily from the lateral nasal wall in the vicinity of the middle turbinate-ethmoid sinus area, rarely from the nasal septum. It may then extend into the nasal cavity and/or one or more of the ipsilateral paranasal sinuses. The OSP arises in areas similar to the ISP. In contrast to the ESP, the ISP and OSP may be associated with malignancy in about 5% to 15% of cases (2).

On small biopsies, it may be difficult to distinguish an ESP from an ISP, especially because some ISPs may exhibit a focal papillary surface. The site of origin (septum vs lateral nasal wall) may be helpful. A prominent inverted pattern of growth eliminates ESP from consideration (Figure 3.1.7). If the biopsy is small and without defining features, the generic term *Schneiderian papilloma of uncertain type* is appropriate.

Because ESPs arise from the lower anterior nasal septum and may project into the nasal vestibule (the area just inside the nostril covered by skin), they must also be distinguished from a variety of cutaneous papillomas that arise in this area. Although ESPs

have little, if any, malignant potential, failure to recognize and treat them adequately often results in local recurrence and more extensive spread along the nasal septum. Most cutaneous papilloma (verruca vulgaris, seborrheic keratosis, etc) are heavily keratinized (Figure 3.1.8). The lack of significant surface keratinization and the presence of mucous cells (accentuated by a mucicarmine stain) and ciliated and/or “transitional” epithelium as seen in ESPs readily allow one to discriminate between an ESP and a cutaneous papilloma. Although not an integral component of ESPs, the presence of cartilage and mucoserous (minor salivary) glands in the adjacent nonpapillomatous tissue should always suggest a nasal mucosal rather than a cutaneous origin. Likewise, numerous pilosebaceous units and sweat glands are more consistent with a lesion of cutaneous origin (3).

Some ESPs, however, may show focal surface keratinization, especially if the lesion is irritated (“nose picker”) or the lesion is exceptionally large, protrudes into the nasal vestibule, and is exposed to the drying effect of ambient air (Figures 3.1.5 and 3.1.6).



**FIGURE 3.1.7** Inverted Schneiderian papilloma. The epithelial proliferation is inward rather than exophytic.

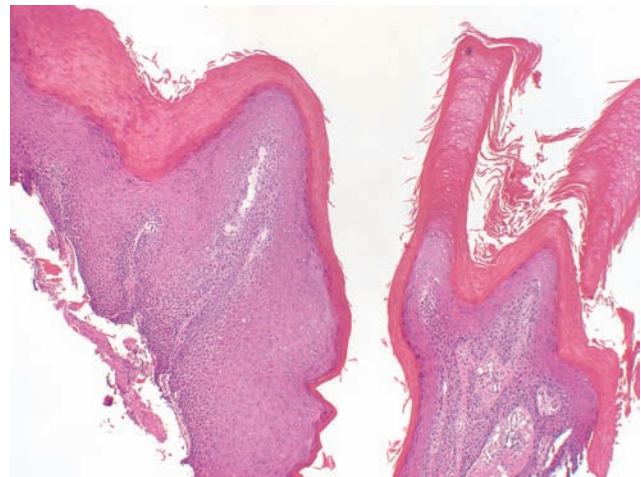


**FIGURE 3.1.8** Shave biopsy of a nonspecific keratinized cutaneous squamous papilloma of the nasal vestibule. Note the prominent surface layer of keratin and lack of mucous (goblet) cells and cysts.

**References**

1. Barnes, L. Schneiderian papillomas and non-salivary glandular neoplasms of the head and neck. *Mod Pathol.* 2002;15:279–297.
2. Barnes L, Peel RL. Fungiform papilloma versus cutaneous papilloma of nasal vestibule. In: Barnes L, Peel RL, eds. *Head and Neck Pathology. A Text/Atlas of Differential Diagnosis.* New York: Igaku-Shoin; 1990:58–59.
3. Barnes L, Tse LLY, Hunt JL. Schneiderian papillomas. In: Barnes L, Eveson JW, Reichart P, Sidransky D, eds. *World Health Organization Classification of Tumours, Pathology and Genetics, Head and Neck Tumours.* Lyon: IARC Press; 2005: 28–32.

## 3.2

*Nasopharyngeal Carcinoma***CLINICAL INFORMATION**

“This 46-year-old man presents with a mass in the nasopharynx. It has an exophytic appearance. Your opinion would be greatly appreciated.”

**OPINION**

Sections show a papillary neoplasm with broad fibrovascular cores covered by multilayers of epithelial cells with poorly defined cytoplasm and large vesicular nuclei with prominent nucleoli (Figures 3.2.1, 3.2.2, and 3.2.3). Mitoses are frequent, and intratumoral lymphocytes are sparse. The tumor appears predominantly in situ with only 1 or 2 areas of questionable superficial invasion of the stroma.

The cells are strongly positive for cytokeratin 5/6 and CAM 5.2 and exhibit full-thickness nuclear

staining for p53 (Figure 3.2.4). The tumor is also strongly positive on in situ hybridization for the Epstein-Barr virus (EB) (Figure 3.2.5).

**DIAGNOSIS**

Mass in nasopharynx, biopsy: Papillary nasopharyngeal carcinoma, nonkeratinizing undifferentiated type, predominantly in situ with areas of questionable superficial invasion.

**COMMENT**

I believe this is an uncommon variant of papillary nasopharyngeal carcinoma. In support of this are the large vesicular nuclei with prominent nucleoli and strong positivity for the EB on in situ hybridization.

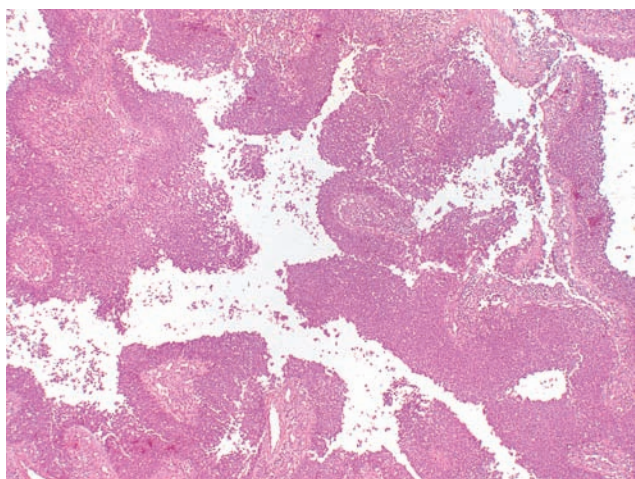


**FIGURE 3.2.1** Low-power view showing papillary configuration.

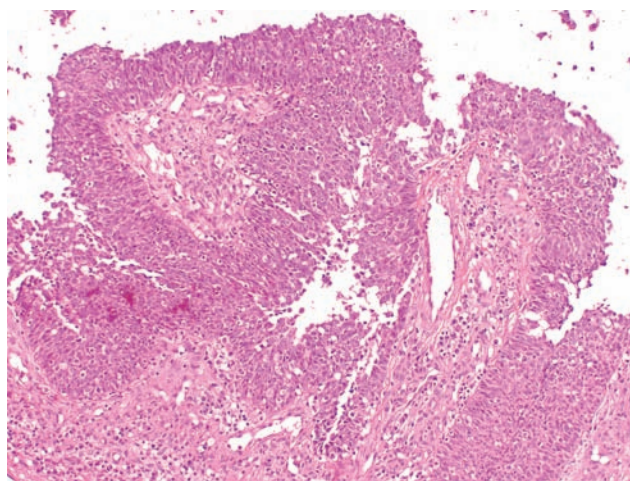


**FIGURE 3.2.2** The tumor has broad fibrovascular cores.

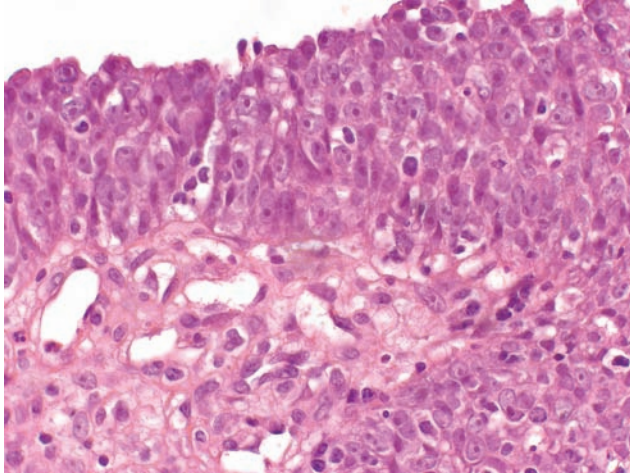


**FIGURE 3.2.3** The overlying epithelium is composed of multiple layers of cells with round, vesicular nuclei and prominent nucleoli.

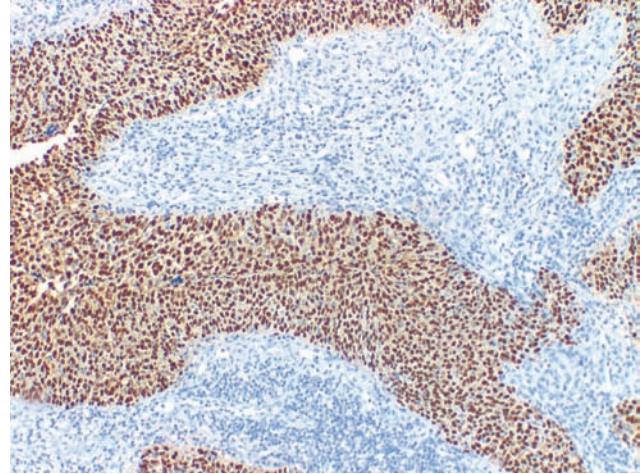


**FIGURE 3.2.5** The tumor is strongly positive for the EB (in situ hybridization).

### DISCUSSION

The World Health Organization classifies nasopharyngeal carcinoma into three major categories (Table 3.2.1) (1). Keratinizing squamous cell carcinoma is a squamous cell carcinoma that, by definition, shows evidence of keratinization (keratin pearls, dyskeratotic cells, and/or intercellular bridges). It is uncommon below the age of 40–years, has a weak association with

the EB, and has the worst prognosis (overall 20%–40% 5-year survival rate). The basaloid squamous cell carcinoma is the least-common variant (1). Preliminary data indicate that it may be less aggressive than basaloid squamous cell carcinoma occurring in other head and neck sites and that some cases, particularly those from Asia, are associated with the EB.

The nonkeratinizing carcinoma, especially the undifferentiated type, is the most common variant of nasopharyngeal carcinoma. It occurs in all ages, including children; has a strong relationship with the EB; and has the best prognosis (overall 65% 5-year survival rate).

The differentiated variant of nonkeratinizing carcinoma has cells with poorly defined cytoplasm

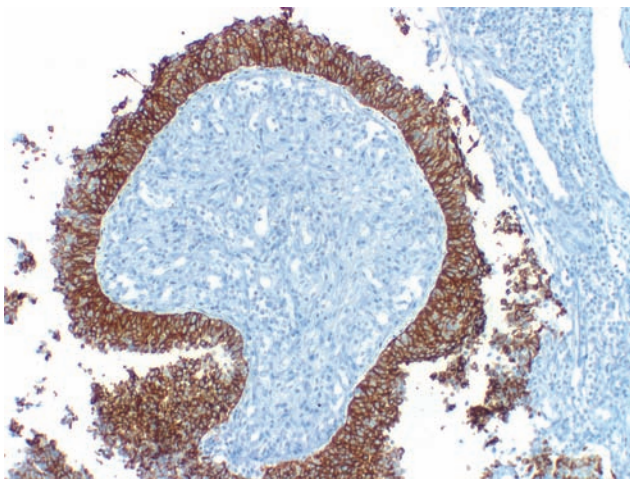


**FIGURE 3.2.4** The tumor cells are strongly positive for cytokeratin 5/6.

**TABLE 3.2.1** The World Health Organization Classification of Nasopharyngeal Carcinoma

- |   |
|---|
| 1. Keratinizing squamous cell carcinoma |
| 2. Nonkeratinizing carcinoma            |
| A. Differentiated                       |
| B. Undifferentiated                     |
| 3. Basaloid squamous cell carcinoma     |

## 3.2

and rather uniform hyperchromatic nuclei devoid of nucleoli. Overall, it resembles a transitional cell and/or urothelial carcinoma.

The undifferentiated variant is characterized by tumor cells with large vesicular nuclei and prominent nucleoli. Lymphocytes, often numerous, can be seen permeating both nonkeratinizing variants. The undifferentiated variant may grow as syncytial aggregates of tumor cells (Regaud pattern), individual cells with admixed lymphocytes (Schmincke pattern), or rarely as a spindle cell or papillary tumor.

The differential diagnosis includes a primary lymphoepithelial carcinoma of the sinonasal tract and sinonasal undifferentiated carcinoma (SNUC). Both

lymphoepithelial carcinoma and undifferentiated carcinoma of the nasopharynx share the same histology, and both are positive for EB. In this instance, only the location (nasopharynx vs paranasal sinus) may allow one to distinguish between the two.

-Barr status is also helpful in excluding SNUC because SNUCs, except for rare cases from Asians, are negative for this virus.

### Reference

1. Chan JKC, Pilch BZ, Bray F, et al. Nasopharyngeal carcinoma. In: Barnes L, Eveson JW, Reichart P, Sidransky D, eds. *World Health Organization Classification of Tumours, Pathology and Genetics, Head and Neck Tumours*. Lyon: IARC Press; 2005:85–97.

## 3.3

## Respiratory Epithelial Adenomatoid Hamartoma—Inverted Papilloma

### CLINICAL INFORMATION

“This patient is a 47-year-old man with nasal congestion, loss of his sense of smell, and difficulty breathing. Multiple polyps were found in both nares. A CT scan showed complete opacification of both nasal cavities, the anterior and posterior ethmoid sinuses, and mucosal thickening of both maxillary sinuses. Could this be an inverted papilloma or even a well differentiated adenocarcinoma?”

### OPINION

Sections show a polypoid lesion composed of dispersed glands lined by several layers of bland, ciliated respiratory epithelium (Figures 3.3.1, 3.3.2, and 3.3.3). Each gland is surrounded by a thick collagenized basement membrane (Figure 3.3.3). Many of the

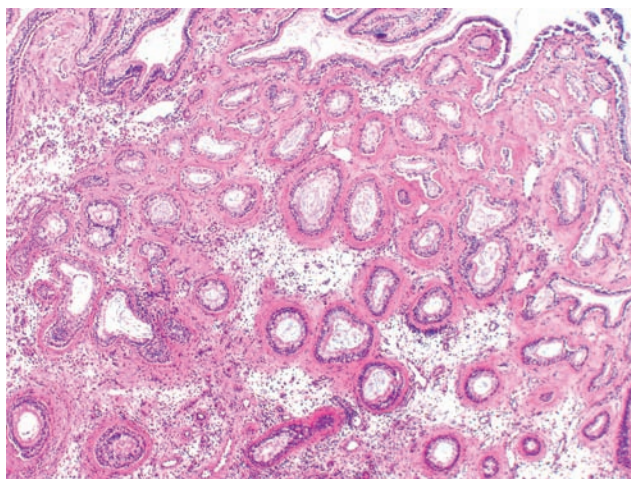


**FIGURE 3.3.1** Respiratory epithelial adenomatoid hamartoma. Note the polypoid appearance and numerous glands surrounded by thick, hyalinized basement membranes.

glands contain mucoid secretions. The intervening stroma varies from fibrous to myxoid and contains chronic inflammatory cells as well as small lobules of mucoserous (minor salivary) glands.

### DIAGNOSIS

Tissue from right nasal cavity: Respiratory epithelial adenomatoid hamartoma.

### COMMENT

Respiratory epithelial adenomatoid hamartoma (REAH) is a recently recognized entity that is often confused with an inverted Schneiderian papilloma or even a well-differentiated adenocarcinoma. Simple excision is curative.

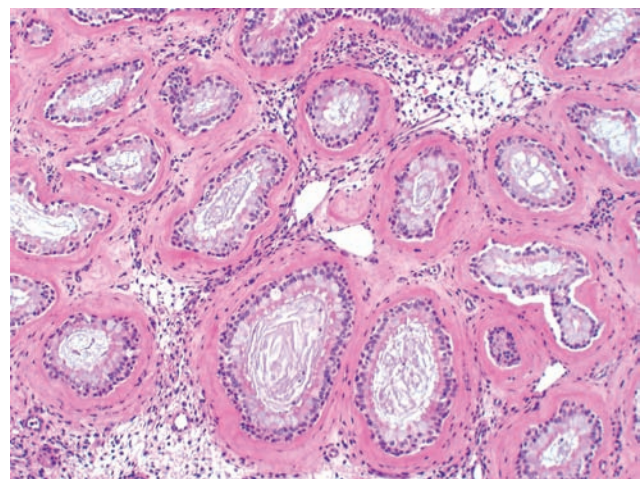


**FIGURE 3.3.2** Higher magnification of Figure 3.3.1.



## 3.3

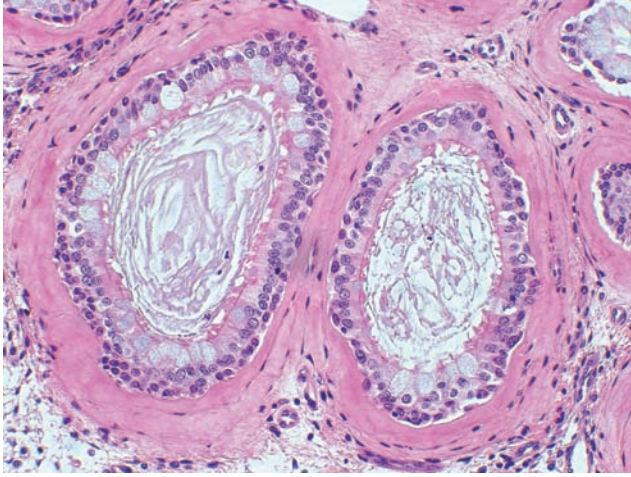


**FIGURE 3.3.3** Respiratory epithelial adenomatoid hamartoma. The glands are lined by a “thin” layer of ciliated respiratory epithelium. Compare the thickness of the epithelial lining with the “thick” multilayered epithelium seen in IPs (Figure 3.3.8).

## DISCUSSION

Respiratory epithelial adenomatoid hamartoma is an uncommon, recently described entity. Of 31 REAHs reported by Wenig and Heffner (1), 27 occurred in men and 4 in women who ranged in age from 27 to 81 years (median, 58 years). Most were unilateral and arose from the nasal cavity (22 cases, 71%), particu-

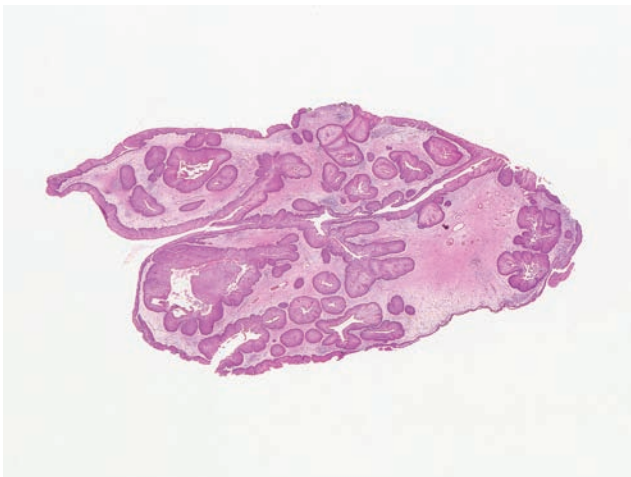


**FIGURE 3.3.4** Low-power view of an IP showing the typical endophytic pattern of growth.



**FIGURE 3.3.5** Inverted papilloma composed of sharply demarcated islands of squamous epithelium.

larly the posterior nasal septum and to a lesser extent along the lateral nasal wall, middle meatus, and inferior turbinate. A few, however, were bilateral. The remaining cases occurred in the paranasal sinuses and nasopharynx. Nasal stuffiness, obstruction, epistaxis, and chronic rhinosinusitis are the most common manifestations.

Respiratory epithelial adenomatoid hamartomas are typically polypoid or exophytic, rubbery, tan-white to red-brown, and range up to 5.0-cm in

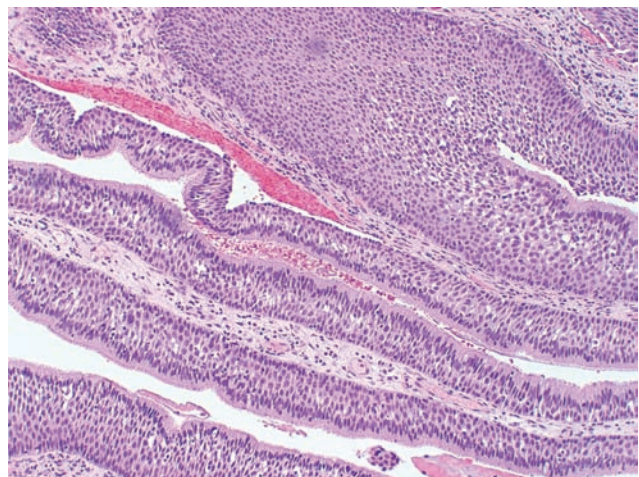


**FIGURE 3.3.6** Some IPs are composed of both squamous and respiratory epithelium.

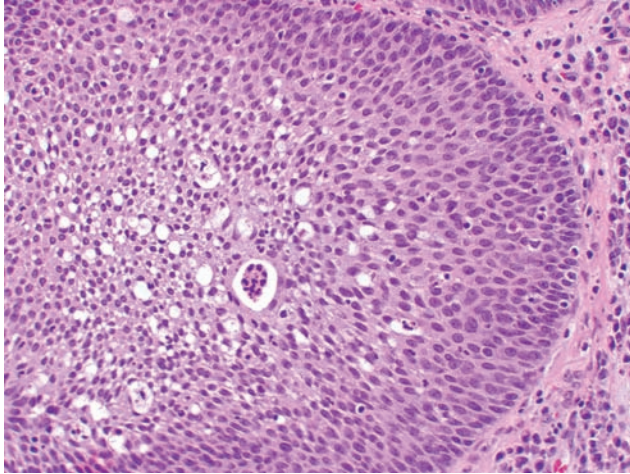


**FIGURE 3.3.7** Squamous epithelium in an IP. The epithelium is bland, and the basement membrane is thin.

greatest dimension. Histologically, they are composed of small- to medium-sized, round to oval glands lined by ciliated respiratory epithelium, often with admixed mucin-secreting (goblet) cells (Figures 3.3.1, 3.3.2, and 3.3.3). The glands arise from invagination of the surface epithelium into the lamina propria and, consequently, often maintain direct continuity with the surface. The glands are characteristically surrounded by thick, eosinophilic basement membranes. The

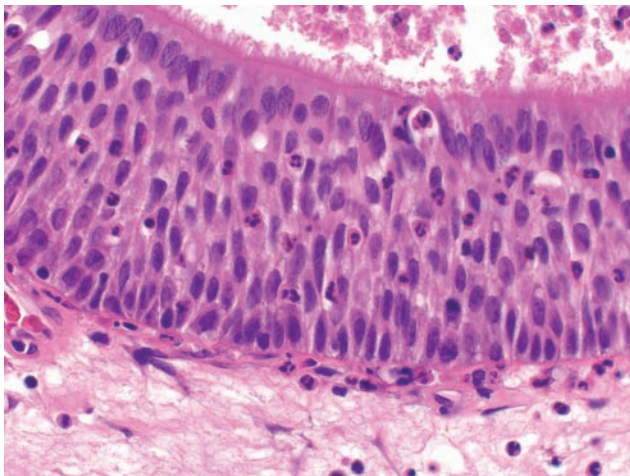


**FIGURE 3.3.8** Respiratory epithelium in an IP. Note the multilayered appearance and epithelial transmigration of neutrophils.

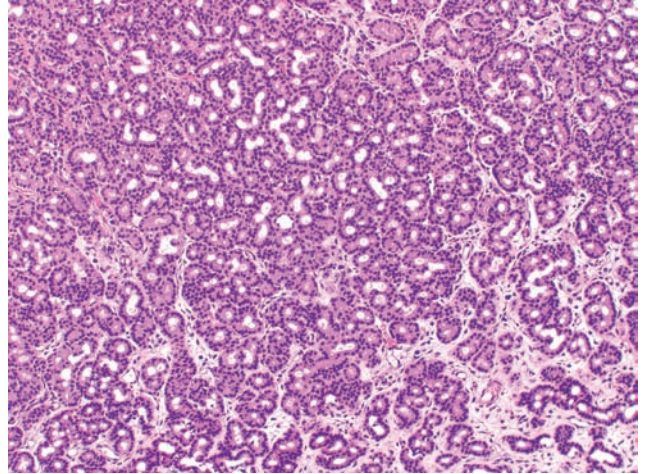


**FIGURE 3.3.9** Well-differentiated adenocarcinoma of the sinonasal tract.

stroma is well vascularized, edematous, or fibrous and contains scattered chronic inflammatory cells and, occasionally, mucoserous (minor salivary) glands arranged in a typical lobular configuration. A few may also harbor chondro-osseous foci.

Respiratory epithelial adenomatoid hamartomas are most often confused with ordinary sinonasal

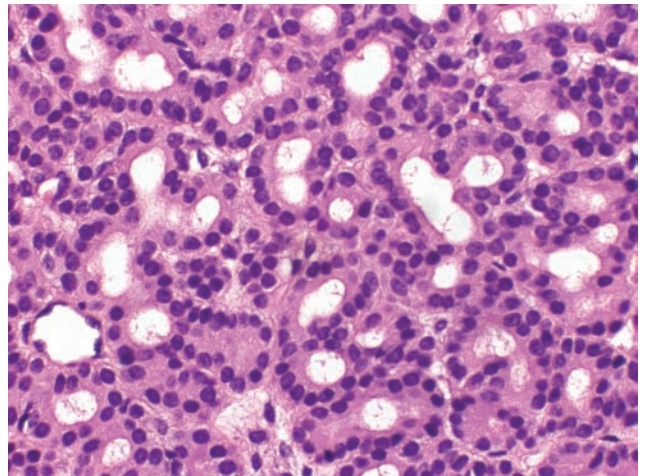


**FIGURE 3.3.10** Higher magnification of Figure 3.3.9. Note the back-to-back arrangement of nonciliated glands and that the glands are lined only by a single layer of epithelial cells devoid of a peripheral component of basal/myoepithelial cells.

### 3.3

polyps, inverted papillomas (IPs), and adenocarcinoma (2). The glands in sinonasal polyps are of the mucoserous (minor salivary) type as opposed to the ciliated respiratory epithelial-lined glands in REAH.

In contrast to REAHs, which occur primarily on the nasal septum, IPs characteristically arise from the lateral nasal wall in the region of the middle turbinate-ethmoid sinus and often extend secondarily into the sinuses (3). Isolated lesions of the paranasal sinuses without nasal involvement, however, do occur.

Inverted papillomas are composed of hyperplastic islands of squamous and/or respiratory epithelium, often permeated by neutrophils (Figures 3.3.4, 3.3.5, 3.3.6, 3.3.7, and 3.3.8). The basement membranes around the epithelial islands are thin and delicate, not thick and hyalinized as seen in REAH (Figure 3.3.7). The ciliated epithelium in IPs is multilayered (thick) as opposed to the “thin” rather attenuated respiratory epithelium that lines the glands in REAH (Figure 3.3.8). Mucoserous (minor salivary) glands are sparse to absent in IP and often prominent in REAH.

Adenocarcinoma may arise from the mucosa or mucoserous (minor salivary) glands and vary from well to poorly differentiated. They are characterized by a back-to-back arrangement of glands devoid of cilia, mitotic activity, occasional nuclear pleomorphism, necrosis, desmoplastic stromal reaction, and/or absence of a peripheral layer of basal/myoepithelial cells. These features are not seen in REAH (Figures 3.3.9 and 3.3.10) (4).

#### References

1. Wenig BM, Heffner DK. Respiratory epithelial adenomatoid hamartomas of the sinonasal tract and nasopharynx: a clinicopathologic study of 31 cases. *Ann Otol Rhinol Laryngol*. 1995;104:639–645.
2. Sangoi AR, Berry G. Respiratory epithelial adenomatoid hamartoma: diagnostic pitfalls with emphasis on differential diagnosis. *Adv Anat Pathol*. 2007;14:11–16.
3. Barnes L. Schneiderian papillomas and nonsalivary glandular neoplasms of the head and neck. *Mod Pathol*. 2002;15:279–297.
4. Ozolek JA, Barnes L, Hunt JL. Basal/myoepithelial cells in chronic sinusitis, respiratory epithelial adenomatoid hamartoma, inverted papilloma, and intestinal-type and nonintestinal-type sinonasal adenocarcinoma: an immunohistochemical study. *Arch Pathol Lab Med*. 2007;131:530–537.

---

## 4 Dental Lesions

A basic understanding of normal odontogenesis is essential in evaluating lesions of the jaws and oral soft tissues. In many instances, the “hematoxylin and eosin (H & E)” section alone is nondiagnostic and must be supplemented with knowledge of the clinical and radiographic (imaging) studies. This is especially so in evaluating cysts of the jaws where the H & E section may show only a “cyst lined by stratified squamous epithelium.” To further classify such lesions, one must have additional information. Is the cyst associated with an impacted, unerupted, or previously extracted tooth or did it occur in a non-tooth-bearing area of the jaw? Is the tooth viable, that is, does it react

to thermal or electrical stimulation? What is the relationship or location of the cyst to a tooth? Does it occur at the apex of the tooth or is it laterally located?

### Selected Readings

1. Regezi JA. Odontogenic cysts, odontogenic tumors, fibroosseous, and giant cell lesions of the jaws. *Mod Pathol.* 2002; 15:331–341.
2. Barnes L, Eveson JW, Richart P, Sidransky. *World Health Organization Classification of Tumours. Pathology and Genetics. Head and Neck Tumors.* Lyon: IARC Press; 2005.
3. Budnick SD, Barnes L. Cysts and cyst-like lesions of the oral cavity, jaws and neck, In: Barnes L, ed. *Surgical Pathology of the Head and Neck.* 3rd ed. New York: Informa Healthcare; 2009:1163–1195.

## 4.1

*Calcifying Cystic Odontogenic Tumor***CLINICAL INFORMATION**

“A 41-year-old man presented with a gingival mass in the area of teeth #22 and #23. The lesion has the appearance of an odontogenic tumor. The initial low-power impression is of an adenoid basal-type carcinoma. Your opinion regarding the classification of this tumor is appreciated.”

**OPINION**

The biopsy consists of several small fragments. One fragment shows minute area of basaloid proliferation connected to the hyperplastic squamous mucosa (Figure 4.1.1). The second fragment consists of congested vessels, moderate inflammatory infiltrate, and a nodule of basaloid cells with trabecular/plexiform

and cribriform growth pattern (Figure 4.1.2). Close examination of this fragment shows epithelial nests with peripheral palisading, which is characteristic of the ameloblastic epithelium (Figure 4.1.3). The island in the upper left corner is further characterized by central loosely arranged cells, resembling stellate reticulum. So far, ameloblastoma is the leading diagnostic possibility. However, another fragment shows cells with abundant eosinophilic cytoplasm without nuclei, that is, ghost cells (Figure 4.1.4). Ghost cells at different maturation stages and foci of calcification are identified (Figure 4.1.5). The involvement of the bone by the tumor (Figure 4.1.6) raises the possibility of an intraosseous origin.

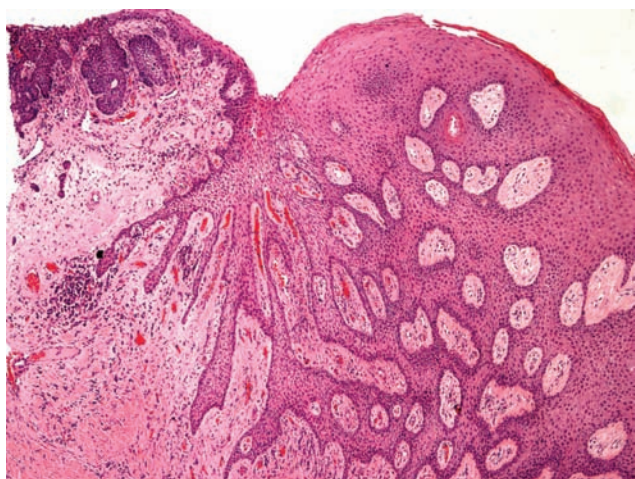


**FIGURE 4.1.1** Basaloid proliferation (upper left) connected to the hyperplastic squamous mucosa.

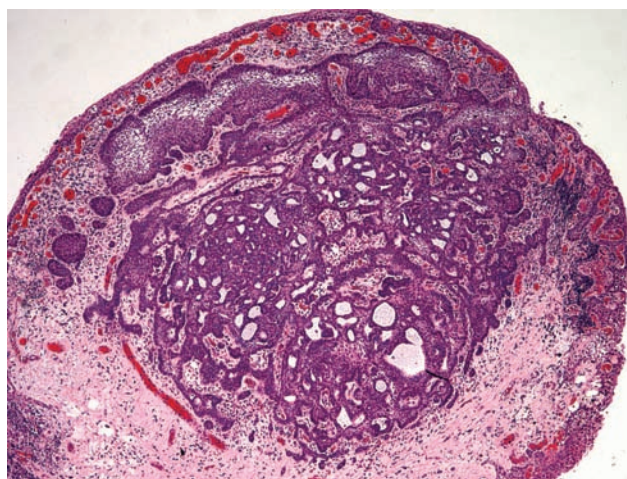


**FIGURE 4.1.2** Trabecular and cribriform proliferation of basaloid cells.

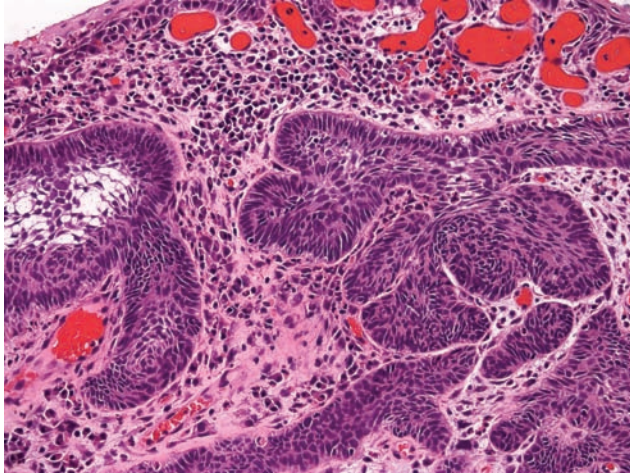


**FIGURE 4.1.3** Peripheral palisading of basaloid epithelium. Note loose arrangement of central cells in the left upper corner.

#### DIAGNOSIS

Gingiva, area of teeth #22 and #23, biopsy: Calcifying cystic odontogenic tumor.

#### COMMENT

The biopsy is diagnostic of a calcifying cystic odontogenic tumor (CCOT). Calcifying cystic odontogenic

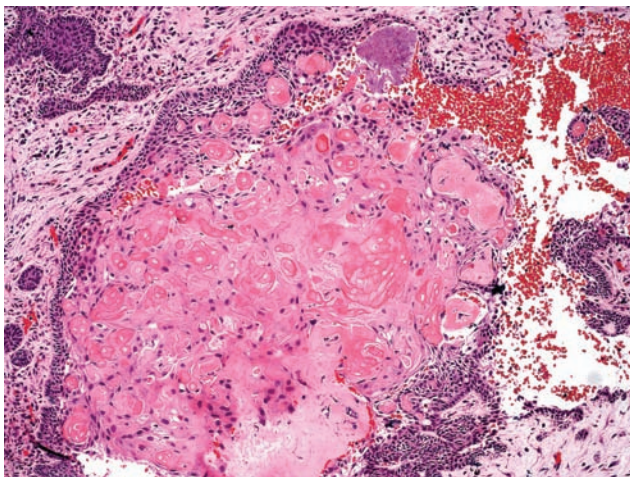


**FIGURE 4.1.4** Ghost cells.

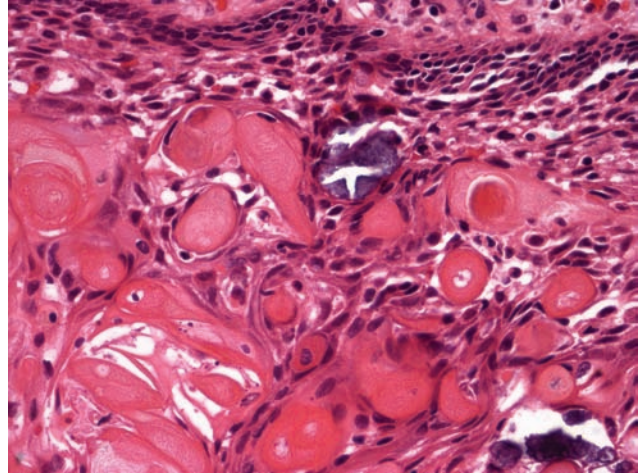


**FIGURE 4.1.5** Ghost cells in different stages of maturation and foci of calcification.

tumor is also known as calcifying odontogenic cyst and Gorlin cyst. The World Health Organization working group recommends the term CCOT (1).

#### DISCUSSION

Calcifying cystic odontogenic tumor comprises 1% to 4.6% of all benign odontogenic tumors (2). About 80% of CCOTs are intraosseous, with the remainder arising within the mucosa (3). Radiographically,

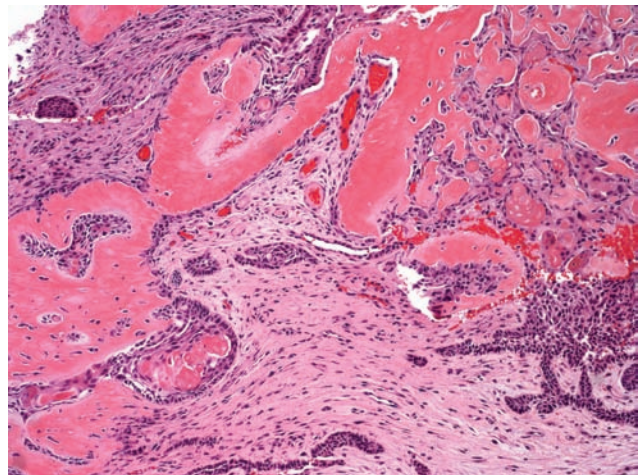


**FIGURE 4.1.6** Bone fragments with tumor, suggesting a possible intraosseous component.

## 4.1

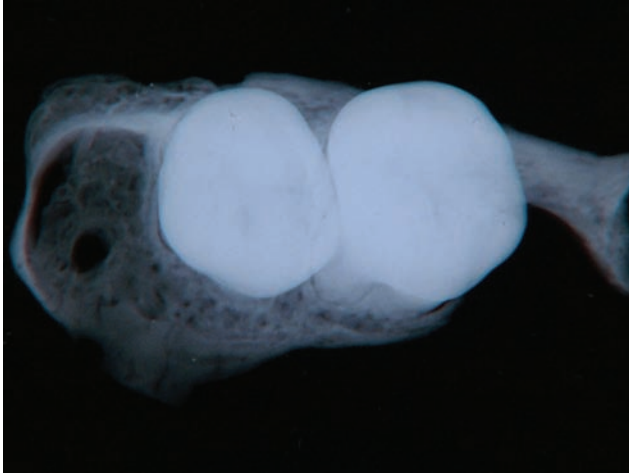


**FIGURE 4.1.7** Image of another intraosseous cystic CCOT—radiolucent lesion with well-defined border.

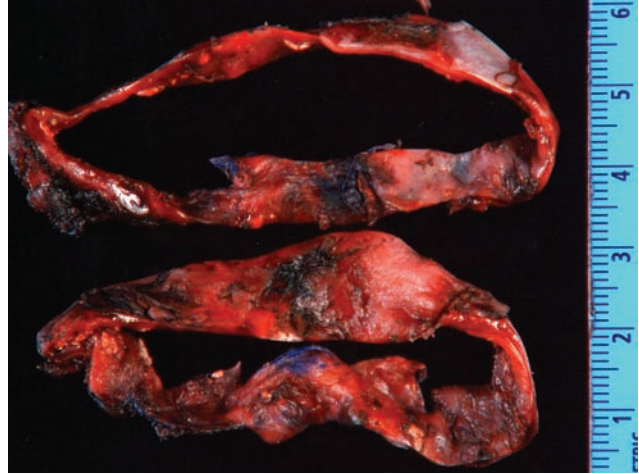


**FIGURE 4.1.8** Gross presentation of an intraosseous CCOT—thin-walled unilocular cyst.

intraosseous CCOTs present as multilocular radiolucencies with well-circumscribed borders (Figure 4.1.7, another case). An apparent multilocular appearance in this case is probably caused by the intracystic radiopaque material, since, grossly, the lesion is unilocular (Figure 4.1.8).

Calcifying cystic odontogenic tumor is frequently associated with several other odontogenic tumors (eg, ameloblastoma, odontoma, odontogenic adenomatoid tumor). The CCOT must be distinguished from the ameloblastoma and calcifying epithelial odontogenic tumor (also known as Pindborg tumor). Importantly, calcification is not found in ameloblastoma, and ghost cells are significantly less prominent. Both the ameloblastoma and the calcifying epithelial odontogenic tumor have a more aggressive clinical course. There-

fore, although enucleation is the appropriate surgical treatment for CCOT, ameloblastomas require excision with adequate margins. Finally, the importance of differentiating CCOT from ameloblastoma is highlighted by the lack of reported instances of malignant transformation of the CCOT.

### References

1. Barnes L, Eveson J, Reichart P, Sidransky D, eds. *Pathology and Genetics of head and Neck Tumours*. Lyon: IARC Press; 2005.
2. Daley TD, Wysocki GP, Pringle GA. Relative incidence of odontogenic tumors and oral and jaw cysts in a Canadian population. *Oral Surg Oral Med Oral Pathol*. 1994;77(3): 276–280.
3. Hong SP, Ellis GL, Hartman KS. Calcifying odontogenic cyst. A review of ninety-two cases with reevaluation of their nature as cysts or neoplasms, the nature of ghost cells, and subclassification. *Oral Surg Oral Med Oral Pathol*. 1991;72(1):56–64.

## 4.2

### *Calcifying Epithelial Odontogenic Tumor (Pindborg Tumor)*

#### CLINICAL INFORMATION

“A 78-year-old man with an expansile right maxillary mass.”

#### OPINION

Microscopically, the tumor consists of an abundant thick, “waxy,” acellular, eosinophilic to amphophilic matrix with interspersed cords of tumor cells (Figure 4.2.1). The tumor appears to invade the bone in areas (Figure 4.2.2). Focal lamellar calcifications are noted within the matrix (Figure 4.2.3). The tumor cells are eosinophilic and squamoid-appearing with some pleomorphism but no mitoses or necrosis (Figure 4.2.4). The stroma is congophilic (Figure 4.2.5) and shows “apple-green” birefringence (Figure 4.2.6).

#### DIAGNOSIS

Maxillary sinus, right, biopsy: Calcifying epithelial odontogenic tumor (Pindborg tumor).

#### COMMENT

This represents a calcifying epithelial odontogenic tumor (CEOT), also known as a “Pindborg” tumor in reference to the author who first described this entity (1). This is a typically indolent nonmetastasizing tumor of presumed odontogenic origin. The presence of eosinophilic polygonal, squamoid-appearing cells embedded in a dense amyloid stroma defines this entity. Larger, long-standing lesions demonstrate

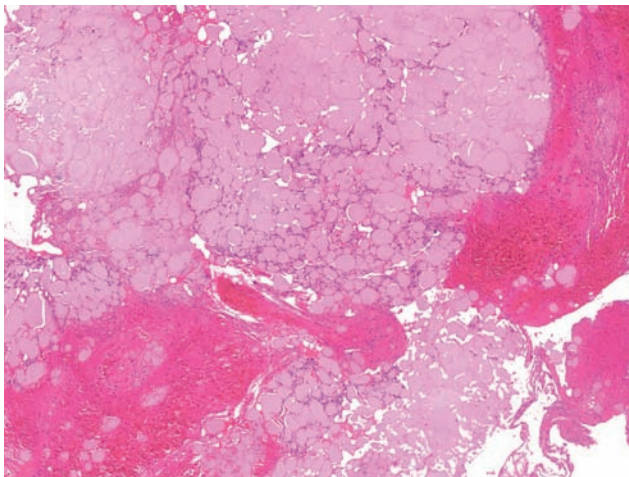


**FIGURE 4.2.1** Tumor showing abundant waxy eosinophilic matrix.

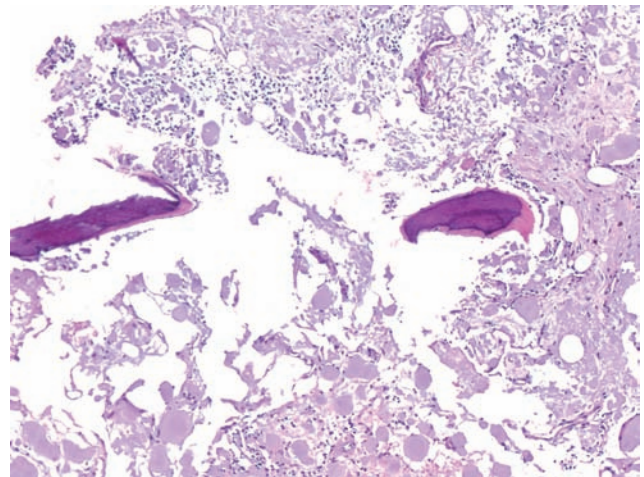


**FIGURE 4.2.2** Tumor invading bone; matrix is more amphophilic.



## 4.2

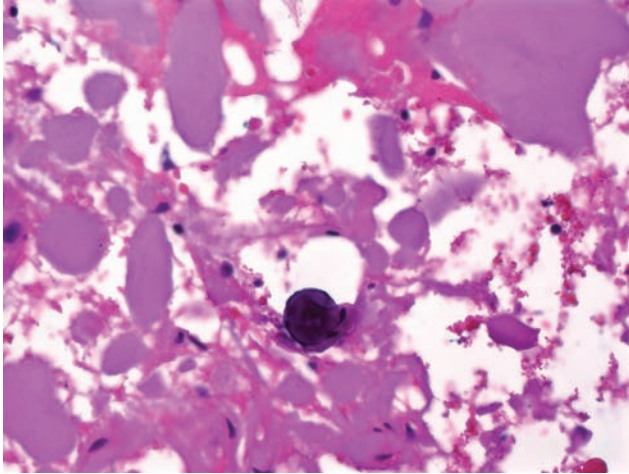


FIGURE 4.2.3 Lamellar calcification.

calcification of matrix in a lamellar fashion resulting in the characteristic “Liesegang ring-like” calcifications often seen in this tumor. In this particular case, calcification was only focal with minimal lamellation.

#### DISCUSSION

Calcifying epithelial odontogenic tumor is a rare odontogenic tumor of adulthood that constitutes 1% to 2% of odontogenic tumors. Most CEOTs are intraosseous (central) with a mandibular predomi-

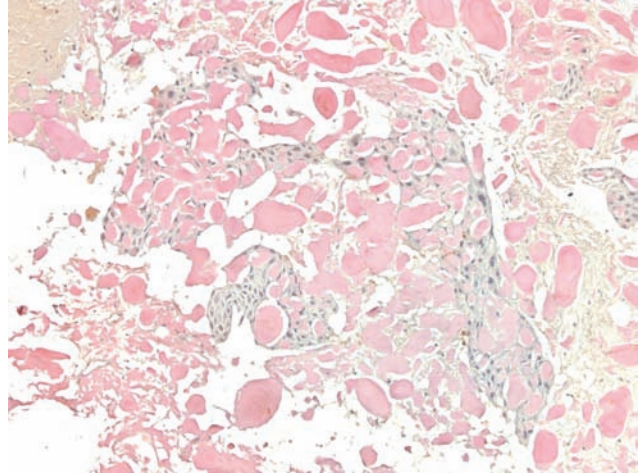


FIGURE 4.2.5 Matrix congophilia.

nance of 2:1. These tumors are characterized by a proliferation of eosinophilic polygonal cells that are arranged in cords or sheets that may show a squamoid appearance. Varying degrees of amyloid matrix and calcification may be present. The beta pleated sheet component of the amyloid in CEOT is not well characterized, and most immunohistochemical assessments of this component are likely plagued by artifacts. A more multimodal sophisticated approach has identified a novel protein as the proposed amyloido-

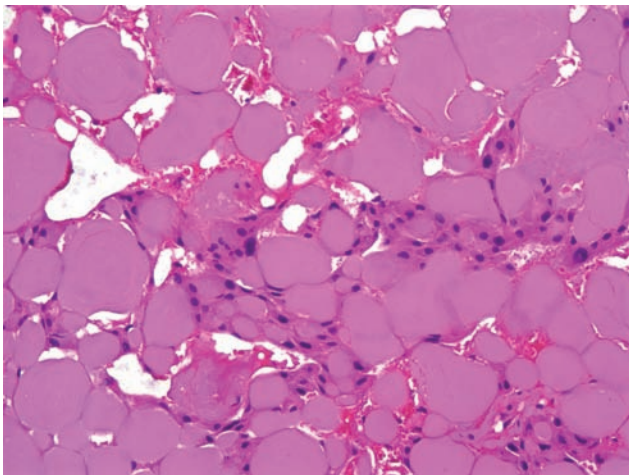


FIGURE 4.2.4 Eosinophilic and squamoid-appearing cells with mild pleomorphism.

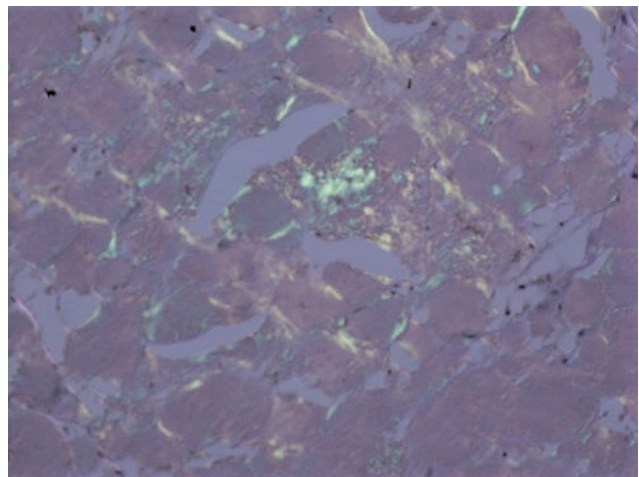


FIGURE 4.2.6 Apple-green birefringence.

genic component (2). Almost two thirds are associated with an unerupted tooth or odontoma. Variants include clear cell CEOT, CEOT with Langerhan cells, and mixed CEOT/adenomatoid odontogenic tumor (3). Maxillary tumors are more locally aggressive than mandibular tumors, although malignant CEOTs are exceptionally rare (4).

The diagnosis of CEOT is usually fairly straightforward. The main differential diagnostic considerations when the stroma is prominent include matrix-producing salivary gland tumors, such as adenoid cystic carcinoma, myoepithelioma, and pleomorphic adenoma. However, although myxohyaline, the salivary gland tumor matrix is not as refractile as the amyloid and shows no congophilia or birefringence under polarized light. In addition, the cell constituents show duct formation in the case of adenoid cystic carcinoma and pleomorphic adenomas. Although a myoepithelial subpopulation may be seen in CEOT (3), it is not as pervasive as in the matrix-producing salivary gland tumors.

On the other end of the spectrum, more cellular CEOT may be mistaken for squamous cell carcinoma or an intermediate/high-grade mucoepidermoid carcinoma (MEC). However, although CEOT may show pleomorphism, they will not show mitoses and necrosis and typically will not show keratinization as seen in squamous cell carcinoma. In addition, CEOT will not show mucosal surface dysplasia. Calcifying epithelial

odontogenic tumor can be distinguished from MEC by the absence of mucus cells. In addition, cysts are not as common in CEOT as they are in MEC (5).

Odontogenic tumors with morphologic overlap with CEOT include adenomatoid odontogenic tumor (which may be seen with CEOT as a mixed tumor) and calcifying cystic odontogenic tumor/dentinogenic ghost cell tumors. Adenomatoid odontogenic tumors have true duct structures and areas with a “whorling” pattern, unlike pure CEOT. Although the calcifying cystic odontogenic tumor/dentinogenic ghost cell tumors category often has calcifications resembling those of CEOT, the tumor cells are more epidermoid-appearing and nonviable ghost cells are characteristic.

## References

1. Pindborg JJ. A calcifying epithelial odontogenic tumor. *Cancer*. 1958;11(4):838–843.
2. Solomon A, Murphy CL, Weaver K, Weiss DT, Hrcic R, Eulitz M, et al. Calcifying epithelial odontogenic (Pindborg) tumor-associated amyloid consists of a novel human protein. *J Lab Clin Med*. 2003;142(5):348–355.
3. Philipsen HP, Reichart PA. Calcifying epithelial odontogenic tumour: biological profile based on 181 cases from the literature. *Oral Oncol*. 2000;36(1):17–26.
4. Veness MJ, Morgan G, Collins AP, Walker DM. Calcifying epithelial odontogenic (Pindborg) tumor with malignant transformation and metastatic spread. *Head Neck*. 2001;23(8):692–696.
5. Makos CP, Nikolaidou AJ. Calcifying epithelial odontogenic tumour or Pindborg’s tumour: features and behaviour in relation to a case. *Int Dent J*. 2004;54(6):457–460.

## 4.3

*Dental Follicle–Dental Papilla–Myxoma***CLINICAL INFORMATION**

“This tissue was removed from a 13-year-old boy from the anterior mandibular area in association with an unerupted supernumerary tooth. Clinically, this was felt to be a cyst. My working diagnosis is an odontogenic myxoma. Your interpretation of this lesion is appreciated.”

**OPINION**

The specimen consists of islands of odontogenic epithelium lying in a fibrous matrix with myxoid change (Figure 4.3.1). The epithelial islands are surrounded by a dense layer of collagen and are well demarcated from the stroma (Figure 4.3.2). Small specks of calcific debris are sometimes apparent.

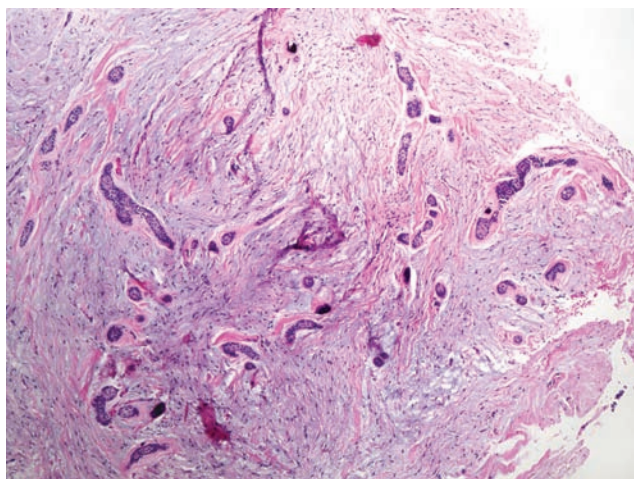


**FIGURE 4.3.1** Dental follicle containing numerous odontogenic rests lying in a fibromyxoid matrix.

**DIAGNOSIS**

Tissue from anterior mandible, excision: Dental follicle with odontogenic rests and myxoid stromal changes.

**COMMENT**

It is my understanding that the microscopic slide contains the entire specimen. Based on its association with an unerupted, supernumerary tooth, small size, circumscription, and histologic appearance, I believe this is a dental follicle with myxoid change rather than an odontogenic myxoma.

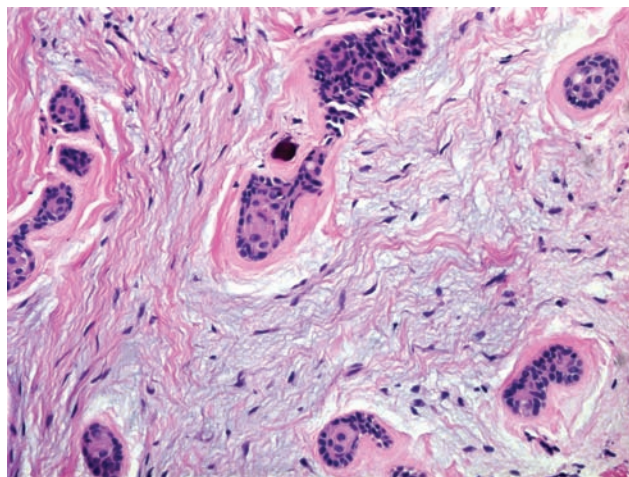


**FIGURE 4.3.2** High-power view of dental follicle in Figure 4.3.1. The odontogenic rests are each surrounded by a dense layer of collagen. Note the myxoid stromal changes.



**FIGURE 4.3.3** Panorex view of a dental follicle associated with unerupted mandibular molar teeth. Note the thin (<3 mm), uniform radiolucency around the crown of one of the teeth (arrow) (Panorex courtesy of Dr Bobby Collins, University of Pittsburgh School of Dental Medicine).

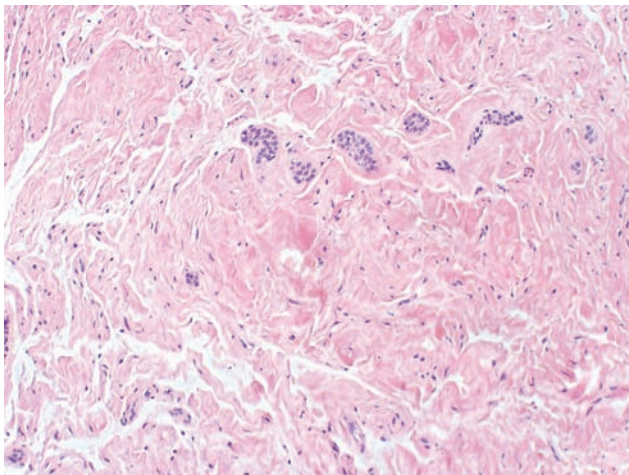


**FIGURE 4.3.4** Dental follicle. Note the odontogenic rests and uniform fibrous matrix without myxoid change.

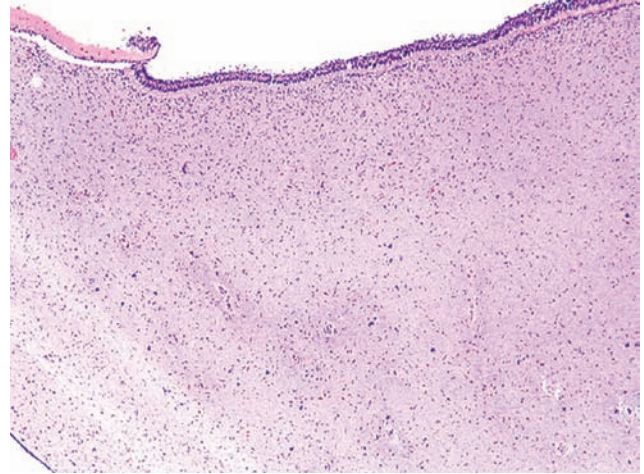


**FIGURE 4.3.5** Dental papilla composed of a uniform myxoid matrix with a surface epithelial layer. Odontogenic rests are not seen in this case. Note the sharp borders.

### DISCUSSION

The dental follicle and dental papilla are normal components of odontogenesis (tooth development) that are occasionally removed during surgical extraction of developing or impacted teeth. Their importance lies in the fact that pathologists who are unfamiliar with these structures may mistake them for more significant

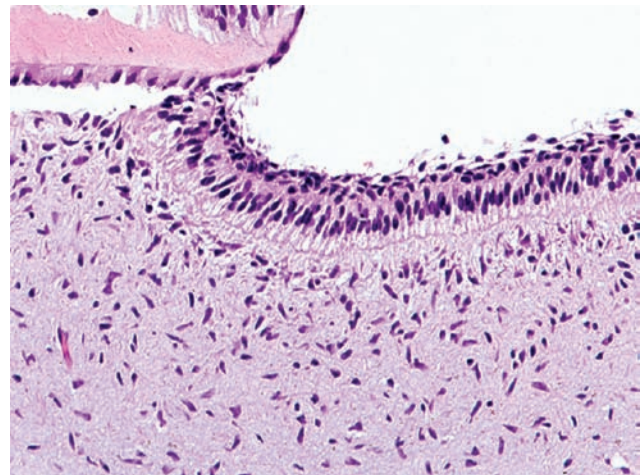


**FIGURE 4.3.6** High-power view of the dental papilla in Figure 4.3.5. Note the surface epithelial component and small amount of pink dentinoid material (upper left corner).

## 4.3

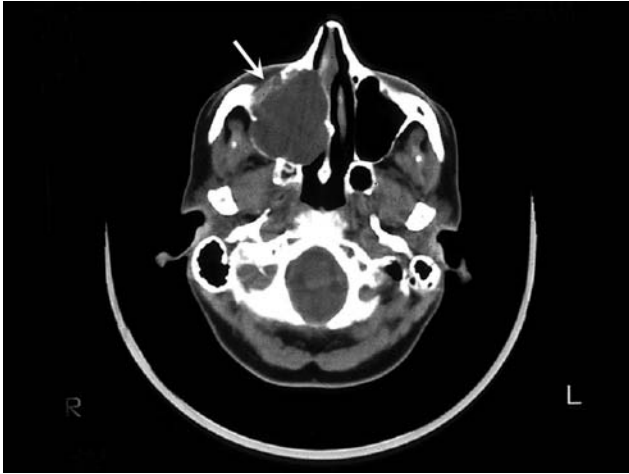


**FIGURE 4.3.7** Image of an odontogenic myxoma of right maxillary sinus. Note the large size and focal destruction of the anterior bony wall of the sinus (arrow).

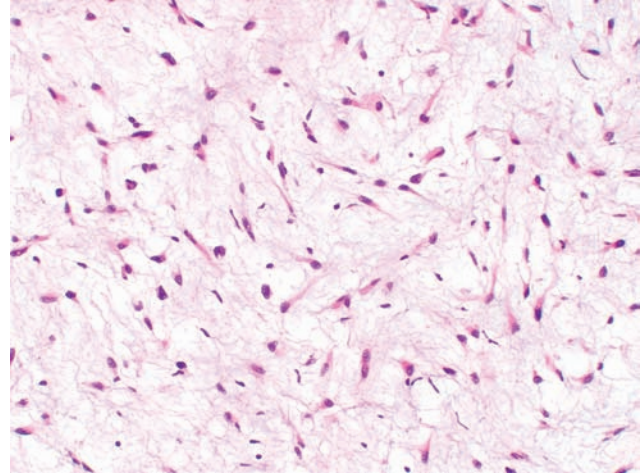


**FIGURE 4.3.9** Odontogenic myxoma composed of a hypocellular myxoid matrix. Compare with Figures 4.3.5 and 4.3.6.

lesions, particularly an odontogenic fibroma, a dentigerous cyst, or an odontogenic myxoma (1–3).

The dental follicle ultimately gives rise to the periodontal ligament and is typically associated with an unerupted tooth, especially a mandibular or maxillary third molar. On a Panorex radiograph, it pres-

ents as a uniform semicircular radiolucency (<3 mm in width) around the crown of an unerupted tooth (Figure 4.3.3). It is composed of a collagenous fibrous matrix often with myxoid change and is lined, in about half the cases, by a reduced enamel epithelium, which varies from columnar to cuboidal to attenuated squamous or even respiratory (1) (Figures 4.3.1 and 4.3.4). Small calcific deposits are not uncommon.

The dental follicle is most often confused with an odontogenic fibroma or a dentigerous cyst and, occasionally, even an odontogenic myxoma because of stromal myxoid changes. Distinguishing a dental follicle from an odontogenic fibroma is not always possible by histology alone and may require clinical and radiologic confirmation. Odontogenic fibromas are larger than dental follicles, and on imaging, they are radiolucent, less symmetric, and often have sclerotic borders (2). In contrast to dental follicles, the odontogenic fibroma lacks an epithelial lining and usually contains more odontogenic rests.

A dentigerous cyst, by definition, is a cyst associated with the crown of an unerupted tooth, usually a mandibular molar. The distinction between a



**FIGURE 4.3.8** Gross specimen obtained from the odontogenic myxoma shown in Figure 4.3.7. Note the large size.

dentigerous cyst and a dental follicle with an epithelial lining can at times be very subjective (4). Dentigerous cysts, however, tend to be larger than dental follicles, and on Panorex radiographs, the radiolucency around the crown of the unerupted tooth is irregular (not symmetrical as seen in dental follicles) and is usually greater than 4 mm in thickness (Figure 4.3.3). The epithelial lining of a dentigerous cyst varies from cuboidal to squamous but is usually more “squamoid” and thicker than that of a dental follicle. Some cysts may also be inflamed.

Dental follicles with myxoid stromal changes may also be confused with an odontogenic myxoma but can be distinguished by the features noted below.

The dental papilla is the precursor of the pulp and dentin of the tooth. Histologically, it is composed of a well-circumscribed, less than 1.5-cm mass of myxoid tissue often lined by odontoblasts (cuboidal to columnar cells) (Figures 4.3.5 and 4.3.6).

The odontoblasts give rise to the dentin, and not infrequently, small amounts of eosinophilic den-

toid matrix may be seen in a dental papilla (Figure 4.3.6).

The dental papilla is most often confused with an odontogenic myxoma. Both are composed of a myxoid matrix; however, the odontogenic myxoma is larger, generally not associated with an unerupted tooth, and histologically is poorly circumscribed and lacks an epithelial lining (5) (Figures 4.3.7, 4.3.8, and 4.3.9). Odontogenic myxoma may or may not contain odontogenic rests.

## References

1. Kim J, Ellis GL. Dental follicular tissue: Misinterpretation as odontogenic tumors. *J Oral Maxillofac Surg.* 1993;51:762–767.
2. Suarez PA, Batsakis JG, El-Naggar AK. Don't confuse dental soft tissues with odontogenic tumors. *Ann Otol Rhinol Laryngol.* 1996;105:490–494.
3. Fellegara G, Mody K, Kuhn E, Rosai J. Normal dental papilla simulating odontogenic myxoma. *Int J Surg Pathol.* 2007;15:282–285.
4. Slater LJ. Dentigerous cyst versus dental follicle. *Br J Oral Maxillofac Surg.* 2000;38:402 (Commentary).
5. Kaffe I, Naor H, Buchner A. Clinical and radiological features of odontogenic myxoma of the jaws. *Dentomaxillofac Radiol.* 1997;26:299–303.

## 4.4

*Glandular Odontogenic Cyst***CLINICAL INFORMATION**

“A 39-year-old man with a left mandibular cyst associated with impacted teeth.”

**OPINION**

Microscopically, the cyst was unilocular and contained hemorrhage and acellular debris including cholesterol crystals (Figure 4.4.1). The lining was composed of a bland squamous epithelium with areas of plaque-like thickening (Figure 4.4.2). In some areas, the most superficial layers of the cyst lining consisted of an eosinophilic cuboidal epithelium (Figure 4.4.3). In other areas, scattered mucus cells were identified as well (Figure 4.4.4). Some regions of the cyst, however, demonstrated a ciliated columnar lining (Figure 4.4.5) and even intraepithelial ductular lumina (Figure 4.4.6).

**DIAGNOSIS**

Maxillary sinus, right, biopsy: Glandular odontogenic cyst.

**COMMENT**

This is a glandular odontogenic cyst (GLOC), also previously known as sialo-odontogenic cyst. The GLOC is a locally aggressive cyst composed of nonsquamous elements ranging from cilia to mucus cells to intraepithelial ducts.

**DISCUSSION**

The GLOC is a very rare odontogenic cyst comprising 0.01% to 0.2% of all jaw cysts that was described

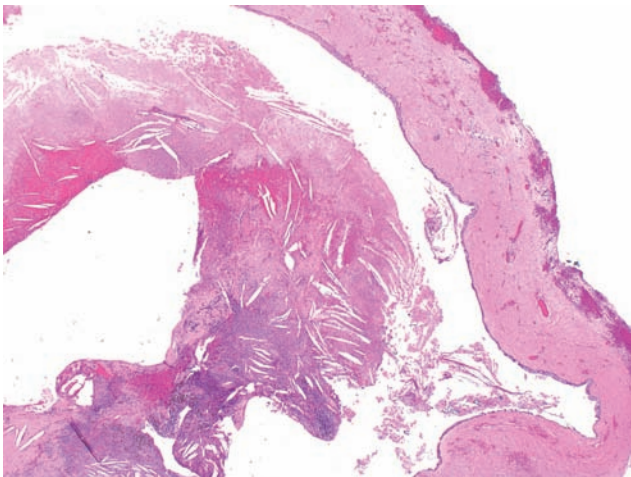


**FIGURE 4.4.1** Unicystic tumor with intracystic hemorrhage, debris, and cholesterol crystals.

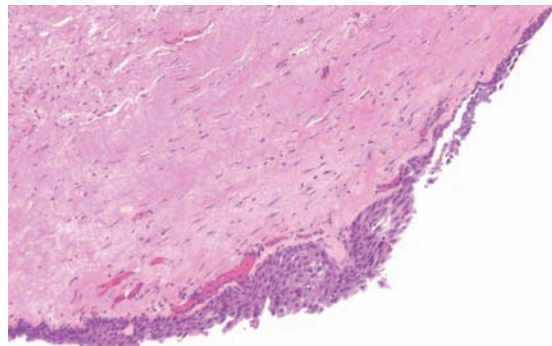


**FIGURE 4.4.2** Squamous epithelium with focal plaque-like thickening.

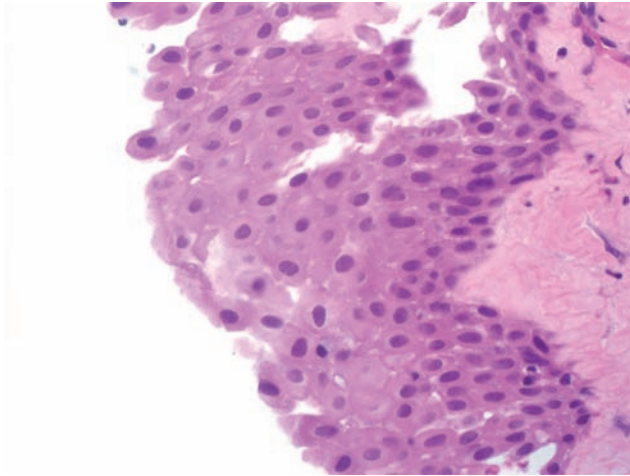


**FIGURE 4.4.3** The epithelium has a superficial eosinophilic cuboidal layer.

by Gardner et al (1) fairly recently in 1988 (2,3). It presents most frequently in the fourth to fifth decades, and roughly 70% occur in the mandible, occasionally associated with impacted teeth, tooth displacement, and rarely tooth resorption. It may be unilocular or multilocular, and aggressive features such as cortical thinning or breakthrough are fairly common (3).

The GLOC may show some overlap with dentigerous cysts, which may occasionally show mucus cells

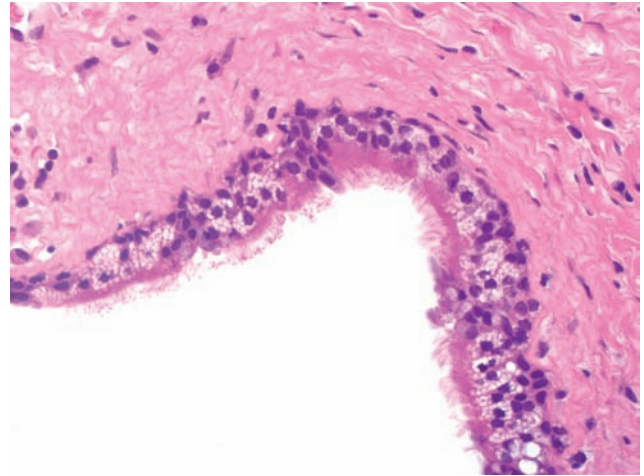


**FIGURE 4.4.5** Areas of ciliated epithelium are present.

and cilia, as well as lateral periodontal cyst, which is also characterized by plaque-like epithelial thickenings. However, neither of these lesions is radiographically as aggressive as GLOC. In addition, the lateral periodontal cyst has a characteristic location between teeth. Finally, several criteria are proposed for inclusion into the GLOC category and exclusion of other entities: (1) epithelial plaques, often with whorled epithelium; (2) intraepithelial glandular spaces; (3) superficial eosinophilic cuboidal cells; (4) ciliated

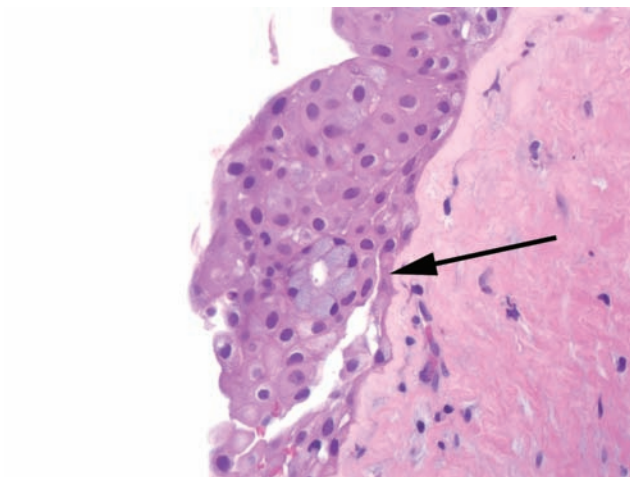


**FIGURE 4.4.4** Intraepithelial mucus cells are noted (arrow).

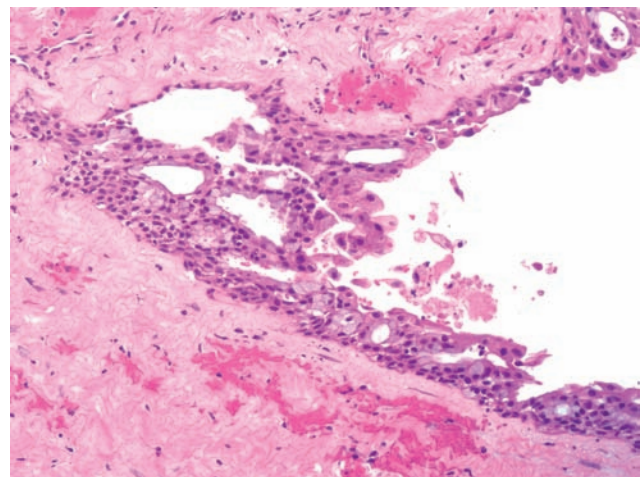


**FIGURE 4.4.6** Intraepithelial ductule formation is noted. The lumina are often lined by mucus cells.



## 4.4

cells; and (5) mucus cells. Thus, having at least four of these criteria can be useful in histologically distinguishing GLOC from these other two entities (4).

At the other end of the spectrum, the main diagnostic consideration includes central or intraosseous mucoepidermoid carcinoma (CMEC). This is an entity that is typically low-grade and thus often cystic. Radiographically, it has a similar appearance and distribution to GLOC. The clinical outcome is similar, except that few cases have been reported to result in lymph node metastases or even death (5). Histologically, the differences can actually be quite subtle because both lesions may have squamoid, mucinous, and eosinophilic cuboidal cells. However, in CMEC, the eosinophilic cells when present are simply modified intermediate cells and will not be at the surface but rather at the center of epithelial proliferation. In addition, intraepithelial gland formation and ciliated cells are not particularly common in CMEC (2). Finally, although GLOC will have epithelial plaque-like areas and whorling, CMEC, in areas of epithelial proliferation, will show a more papillary tufting into the cyst lumina with the tips lined by mucus cells.

The outcome for GLOC is variable with recurrence rates ranging from 25% to 55%. Higher recurrence rates are noted with simple curettage; thus, excision or curettage with chemical cautery is recommended (2,3). Although GLOC and CMEC may potentially be related, documentation of malignant transformation of GLOC has not been described to date.

### References

1. Gardner DG, Kessler HP, Morency R, Schaffner DL. The glandular odontogenic cyst: an apparent entity. *J Oral Pathol.* 1988;17(8):359–366.
2. Krishnamurthy A, Sherlin HJ, Ramalingam K, Natesan A, Premkumar P, Ramani P, et al. Glandular odontogenic cyst: report of two cases and review of literature. *Head Neck Pathol.* 2009;3(2):153–158.
3. Kaplan I, Anavi Y, Hirshberg A. Glandular odontogenic cyst: a challenge in diagnosis and treatment. *Oral Dis.* 2008;14(7):575–581.
4. Kaplan I, Anavi Y, Manor R, Sulkes J, Calderon S. The use of molecular markers as an aid in the diagnosis of glandular odontogenic cyst. *Oral Oncol.* 2005;41(9):895–902.
5. Browand BC, Waldron CA. Central mucoepidermoid tumors of the jaws. Report of nine cases and review of the literature. *Oral Surg Oral Med Oral Pathol.* 1975;40(5):631–643.

## 4.5

*Keratocystic Odontogenic Tumor (Odontogenic Keratocyst)***CLINICAL INFORMATION**

“55-year-old woman presented with a left mandibular bone lesion in the #20-#19 area. The histologic sections consist of portions of a cyst wall with parakeratotic and orthokeratotic squamous lining. The cyst wall has mixed acute and chronic inflammatory infiltrate and underlying granulation tissue. Sections appear to represent an ‘odontogenic orthokeratinized keratocyst.’”

**OPINION**

Histologic sections demonstrate a characteristic parakeratinized corrugated squamous lining (Figure 4.5.1). The lack of rete ridges and palisading basal layer is noted. The cyst contains desquamated “free” keratin (Figure 4.5.2). In some areas, characteristic histo-

logic features are obscured by an intense inflammatory process (Figures 4.5.3–4.5.5). Areas remote from the main cyst and adjacent to the skeletal muscle are involved by the cyst (Figure 4.5.6).

**DIAGNOSIS**

Mandible, left, “#20-#19 area,” excision: Keratocystic odontogenic tumor (odontogenic keratocyst) with chronic inflammation.

**COMMENT**

We agree with your diagnosis of odontogenic keratocyst. The World Health Organization working group now recommends the term *keratocystic odontogenic*

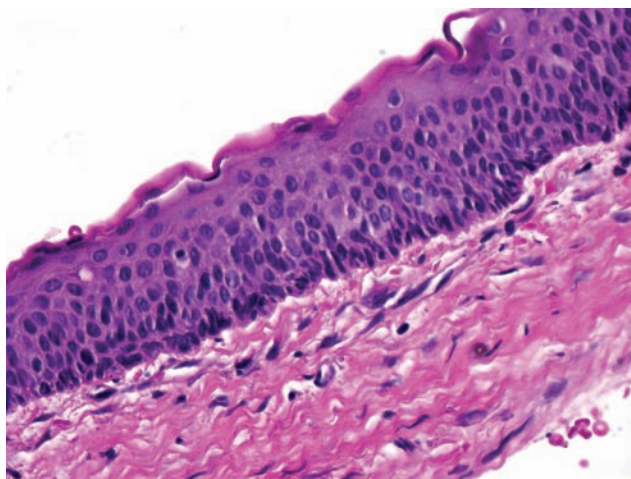


**FIGURE 4.5.1** Keratocystic odontogenic tumor. A 9-cell-thick parakeratinized corrugated squamous lining with palisaded basal cells and without rete ridges.

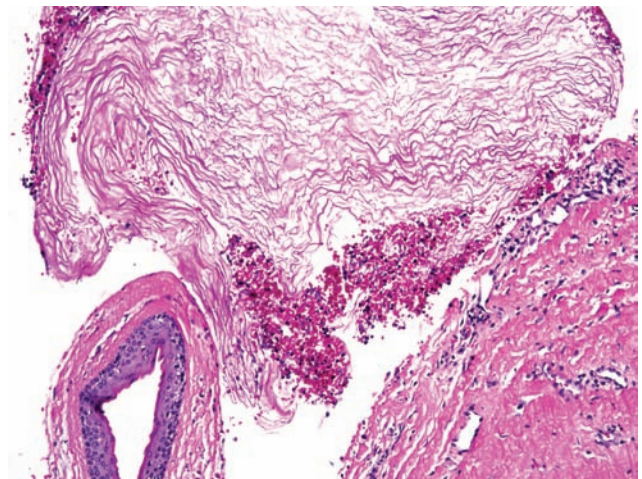


**FIGURE 4.5.2** Note desquamated keratin in the cavity.

## 4.5

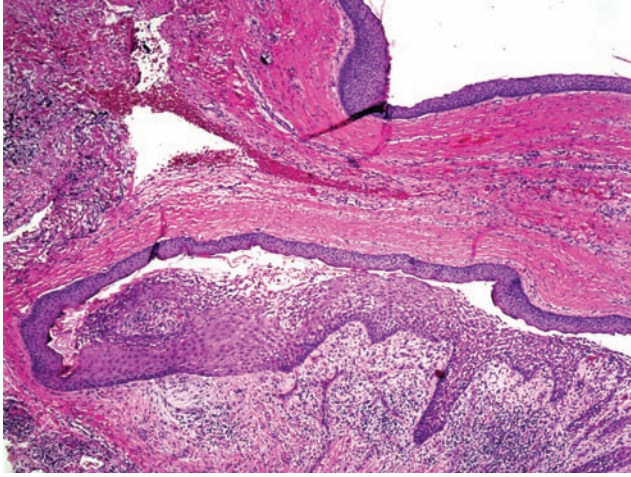


**FIGURE 4.5.3** Inflamed KCOT. Although squamous lining is still preserved, the characteristic KCOT features are lost. In the lower half of the illustrated field, the surface does not appear corrugated and some rete ridges can be seen.

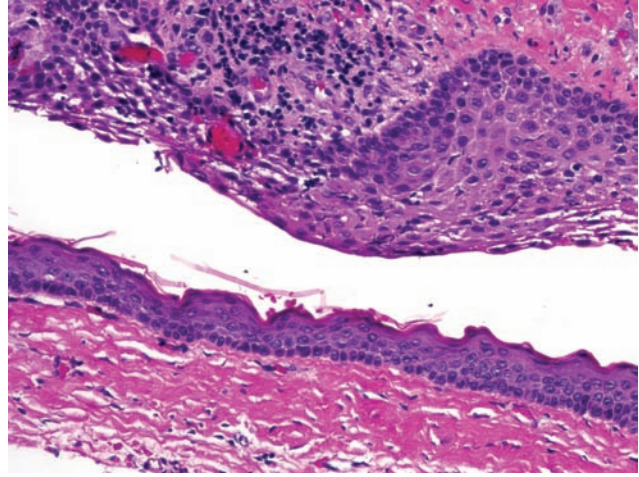


**FIGURE 4.5.5** Loss of epithelial lining in inflamed areas (upper left corner). Typical KCOT features in the lower half of the field.

tumor (KCOT) to better reflect its neoplastic nature and potential for locally aggressive behavior (1).

## DISCUSSION

The KCOT is a benign cyst with a local recurrence rate of up to 29%, usually within 2 years after initial surgical intervention (1). True malignant transforma-

tion to a squamous cell carcinoma is rare (2). Peripheral palisading of the basal nuclei and corrugated parakeratosis (not orthokeratosis) are important histopathologic features of KCOT. Mandibular cysts lined by orthokeratinizing squamous epithelium are unrelated to KCOT and are not associated with the inherited nevoid basal cell carcinoma syndrome.

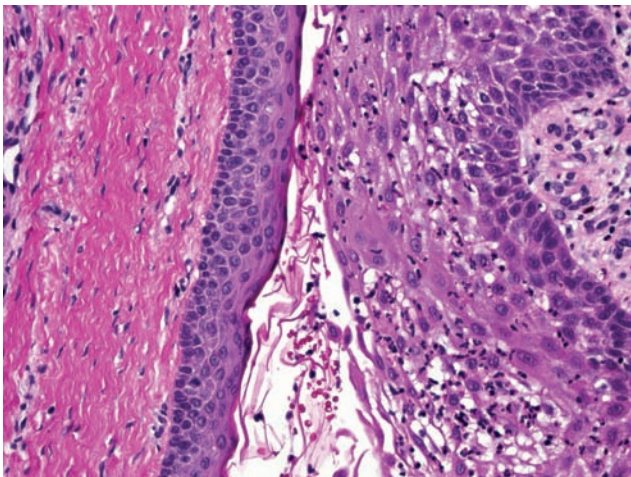


**FIGURE 4.5.4** Inflamed KCOT. A side-by-side illustration of KCOT features in areas spared of inflammation.

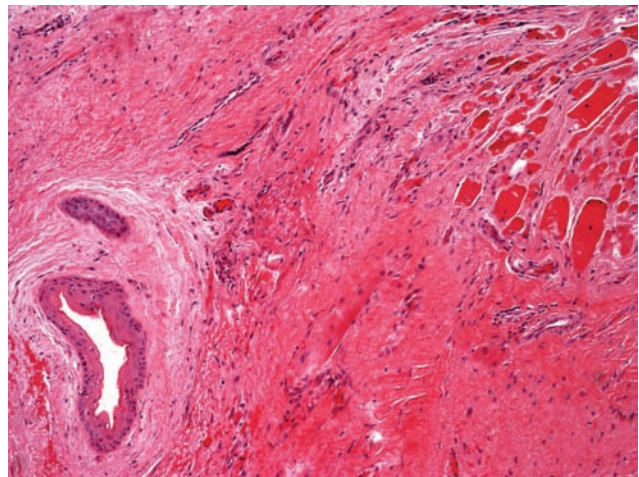


**FIGURE 4.5.6** Keratocystic odontogenic tumor involving soft tissue. Note skeletal muscle in the upper right corner.

The marked chronic inflammation is known to mask the diagnostic features of KCOT. When inflammation is prominent, it is often difficult to classify odontogenic cysts without the benefit of radiographic studies and the knowledge of the viability of the teeth and relationship of the cyst to teeth.

The more unusual feature seen in odontogenic cysts is the presence of ciliated cells. Ciliated epithelium has been described in a variety of odontogenic cysts, particularly of the maxilla, and may either represent a periapical/radicular, dentigerous cyst with ciliated metaplasia (3) or a nasopalatine duct cyst.

With a prior history of trauma or surgery, a traumatic inclusion cyst with entrapped respiratory epithelium enters the differential diagnosis.

### References

1. Madras J, Lapointe H. Keratocystic odontogenic tumour: reclassification of the odontogenic keratocyst from cyst to tumour. *J Can Dent Assoc.* 2008;74(2):165–165h.
2. MacLeod RI, Soames JV. Squamous cell carcinoma arising in an odontogenic keratocyst. *Br J Oral Maxillofac Surg.* 1988;26(1):52–57.
3. Takeda Y, Oikawa Y, Furuya I, Satoh M, Yamamoto H. Mucous and ciliated cell metaplasia in epithelial linings of odontogenic inflammatory and developmental cysts. *J Oral Sci.* 2005;47(2):77–81.



## 5 Neural-Neuroectodermal Lesions

Tumors of neural or neuroectodermal origin are common in the head and neck. Most of the neural lesions are easily recognized, whereas those of neuroectodermal origin tend to be more problematic. Many of the latter tumors fall under the proverbial umbrella term of *small round cell neoplasms*, and of all biopsies of the head and neck, these are the ones more susceptible to distortion and crush artifact.

Most of the neuroectodermal neoplasms are found in the supraglottic larynx or sinonasal tract. In the larynx, most are either carcinoid, atypical carcinoid, small cell carcinoma, paraganglioma, or metastatic small cell carcinoma (usually from the lung). In the sinonasal tract, the differential diagnosis includes virtually all small round cell neoplasms, including those mentioned in the larynx, as well lymphoma, melanoma, olfactory neuroblastoma, Ewing sarcoma–peripheral neuroectodermal tumor, extramedullary plasmacytoma, ectopic or invasive pituitary adenoma, granulocytic sarcoma, rhabdomyosarcoma, sinonasal undifferentiated carcinoma, and lymphoepithelial carcinoma (list not intended to be complete).

Hematoxylin and eosin–stained sections are often nondiagnostic but may offer a few clues to

the correct diagnosis. For instance, nonhemosiderin pigment suggests a melanoma; scattered cells with eosinophilic cytoplasm might indicate melanoma, extramedullary plasmacytoma, myeloid sarcoma, or rhabdomyosarcoma; neurofibrillary matrix and Homer-Wright rosettes support an olfactory neuroblastoma; and extensive necrosis and mitoses raise the possibility of a sinonasal undifferentiated carcinoma.

If the differential diagnosis cannot be narrowed by the initial hematoxylin and eosin section, then a “shotgun” approach using many immunohistochemical stains to rule out the above list of differential diagnoses may be necessary, supplemented occasionally by molecular-genetics studies.

A spectrum of neural and neuroectodermal cases are presented in this section.

### Selected Readings

1. Wang BY, Zagzag D, Nonaka D. Tumors of the nervous system. In: Barnes L, ed. *Surgical Pathology of the Head and Neck*. 3rd ed. New York: Informa Healthcare; 2009: 669–771.
2. Mills SE. Neuroectodermal neoplasms of the head and neck with emphasis on neuroendocrine carcinomas. *Mod Pathol*. 2002;15:264–278.
3. Wenig BM. Undifferentiated malignant neoplasms of the sinonasal tract. *Arch Pathol Lab Med*. 2009;133:699–712.

## 5.1

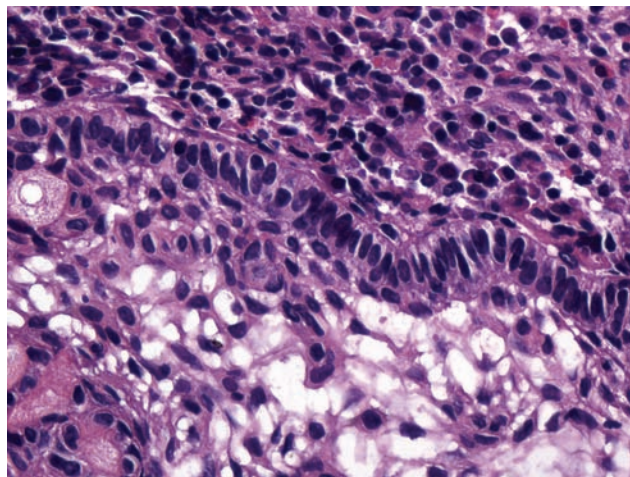
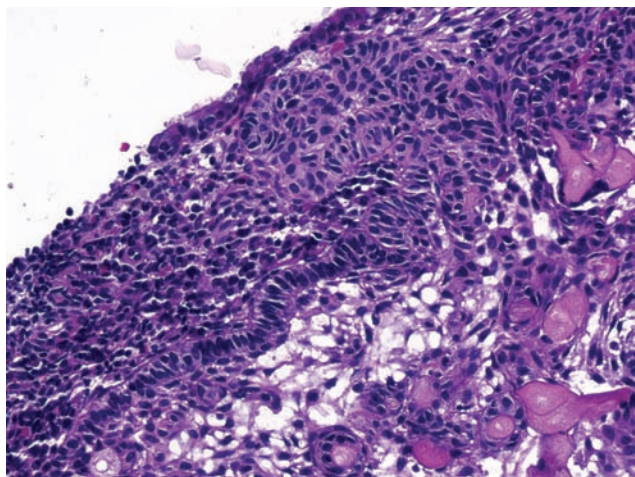
*Craniopharyngioma***CLINICAL INFORMATION**

“A 50-year-old woman of Asian descent presented with an exophytic small nasopharyngeal mass based in the posterior nasal septum. The 0.3-cm biopsy may represent the majority of the mass. The patient spent part of her life in China and has an older sister diagnosed with an aggressive nasopharyngeal carcinoma in the past.”

**OPINION**

Underlying an unremarkable respiratory epithelium of the nasopharynx, there is a rim of palisading basaloid columnar cells (Figures 5.1.1 and 5.1.2). The aggregates of eosinophilic plump polygonal keratinocytes with ghost nuclei are surrounded by loosely arranged stellate cells (stellate reticulum) (Figure 5.1.3). The

nodules of “wet keratin” may remotely resemble squamous pearls. However, aggregates of wet keratin lack the keratohyaline granules, show ghost nuclei, and are composed of plump rather than flat keratinocytes. Although palisading basaloid cells show no well-developed subnuclear vacuoles, the overall appearance is that of an adamantinomatous epithelium (Figure 5.1.2). In addition, there is a focus of solid growth pattern and oval to spindle cells (Figure 5.1.4). Focal calcification is noted (Figure 5.1.5). There is no evidence of cystic change, necrosis, nuclear pleomorphism, or atypical mitoses. Central nervous system tissue is absent. The tumor cells are positive for cytokeratin 5/6 (Figure 5.1.6) and p63 (Figure 5.1.7). Both cytokeratin 5/6 and p63 immunostains highlight the trabecular/linear arrangement of the tumor cells.



**FIGURES 5.1.1 AND 5.1.2** Respiratory nasopharyngeal mucosa with palisading columnar cells and loosely arranged stellate cells. Plasmacytoid infiltrate seen in the upper half of Figure 5.1.2 is a normal component of the nasopharyngeal mucosa.

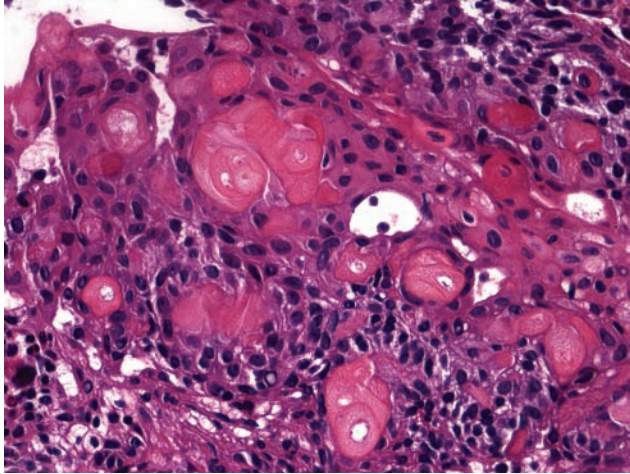


**FIGURE 5.1.3** Nodules of wet keratin. The keratinocytes are plump and show ghost nuclei. This is in contrast to the flat, flaky keratin seen in epidermoid cysts and keratinizing squamous cell carcinomas. Note the absence of keratohyaline granules.

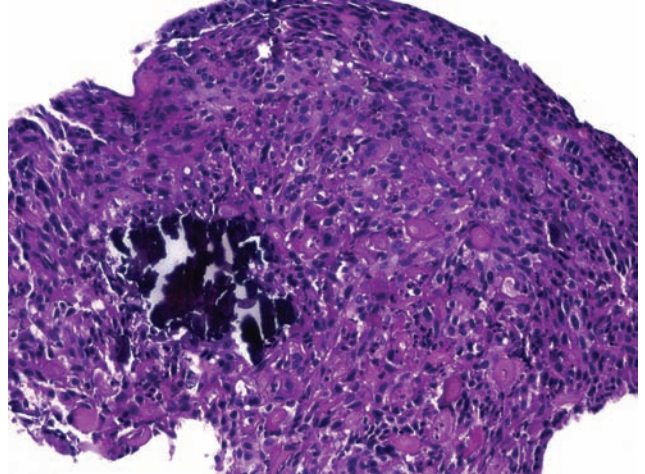


**FIGURE 5.1.5** Focus of calcification.

#### COMMENT

We believe this lesion represents a craniopharyngioma (CP). Without the benefit of imaging studies, we are not sure whether it is primary in the nasopharynx (infraselar nasopharyngeal CP) or an extension from an intracranial process.

Given the family history and clinical concern for nasopharyngeal carcinoma, we performed in situ hybridization for Epstein-Barr virus, and it is negative.

#### DIAGNOSIS

Nasopharyngeal mass, biopsy: Craniopharyngioma.

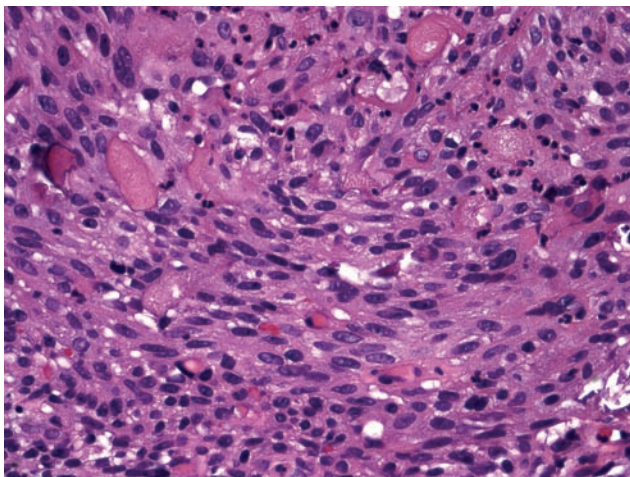


**FIGURE 5.1.4** Area of the solid growth.

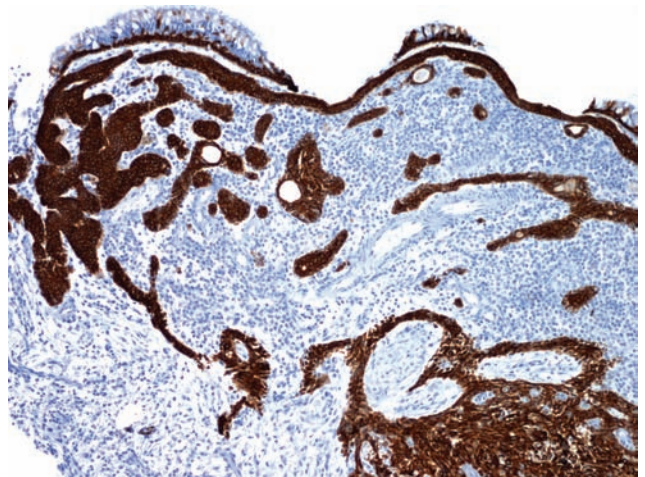


**FIGURE 5.1.6** Immunostain for cytokeratin 5/6 highlights trabecular arrangement of the tumor cells.



## 5.1

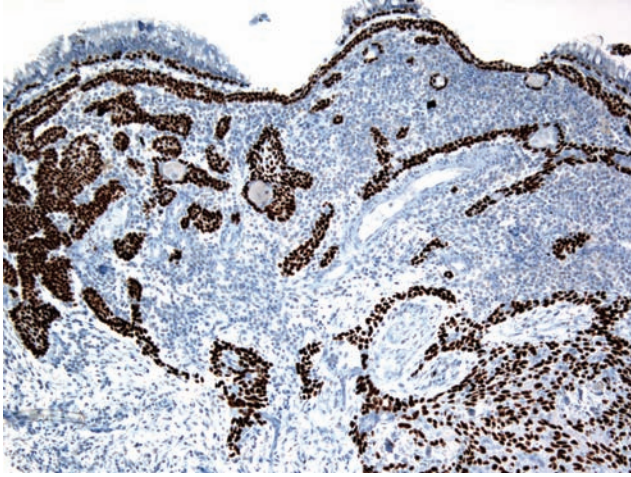


**FIGURE 5.1.7** Craniopharyngioma cells are positive for p63.

### DISCUSSION

The histologic differential diagnosis includes an ameloblastoma and a solid component of the calcifying cystic odontogenic tumor. Several histologic features distinguishing ameloblastoma from CP have been described (1). For instance, the presence of dystrophic calcification favors the diagnosis of CP over ameloblastoma. However, without imaging studies, this differential diagnosis is difficult and, most likely, of no clinical value. Odontogenic classification of CP have been proposed: adamantinomatous and calcifying cystic odontogenic tumor–like subtypes of CP were similar in their clinical presentation (2). The

common embryologic origin of CP, ameloblastoma, and some odontogenic cysts is further supported by the report of CP with tooth structures (3).

Only about 20 cases of infrasellar CPs have been reported to date (4–7). Ectopic odontogenic epithelium is the most likely origin of the adamantinomatous type of nasopharyngeal CP. Rathke cleft cyst gives rise to the squamous (papillary) type of CP.

### References

1. Gorlin RJ, Chaudhry AP. The ameloblastoma and the craniopharyngioma; their similarities and differences. *Oral Surg Oral Med Oral Pathol.* 1959;12(2):199–205.
2. Paulus W, Stockel C, Krauss J, Sorensen N, Roggendorf W. Odontogenic classification of craniopharyngiomas: a clinicopathological study of 54 cases. *Histopathology.* 1997;30(2):172–176.
3. Seemayer TA, Blundell JS, Wiglesworth FW. Pituitary craniopharyngioma with tooth formation. *Cancer.* 1972;29(2):423–430.
4. Ahsan F, Rashid H, Chapman A, Ah-See KW. Infrasellar craniopharyngioma presenting as epistaxis, excised via Denker's medial maxillectomy approach. *J Laryngol Otol.* 2004;118(11):895–898.
5. Byrne MN, Sessions DG. Nasopharyngeal craniopharyngioma. Case report and literature review. *Ann Otol Rhinol Laryngol.* 1990;99(8):633–639.
6. Chakrabarty A, Mitchell P, Bridges LR. Craniopharyngioma invading the nasal and paranasal spaces, and presenting as nasal obstruction. *Br J Neurosurg.* 1998;12(4):361–363.
7. Hwang KR, Lee JY, Byun JY, Hong HS, Koh ES. Infrasellar craniopharyngioma originating from the pterygopalatine fossa with invasion to the maxillary sinus. *Br J Oral Maxillofac Surg.* 2009;47(5):422–424.

## 5.2

*Malignant Peripheral Nerve Sheath Tumor***CLINICAL INFORMATION**

“A 54-year-old woman with a left parapharyngeal space mass tumor. Seven years subsequent to resection showed local recurrence and liver metastasis.”

**OPINION**

Microscopically, the tumor is well demarcated, demonstrating a thin pseudocapsule. There are alternating cellular areas and collagenous areas with areas of stag-horn vasculature (Figure 5.2.1). Many of the cellular areas are composed of bland spindle cells with “wavy” nuclei within a collagenized stroma (Figure 5.2.2). However, other areas show a plump, more epithelioid appearance (Figure 5.2.3). Mitoses were noted at up to 8 per 10 high-power fields (Figure 5.2.4). Scat-

tered throughout the tumor were areas of geographic necrosis (Figure 5.2.5), and embolization material was noted within large vessels (Figure 5.2.6).

Immunohistochemically, the tumor was focally positive for S100 (Figure 5.2.7), positive for CD34 (Figure 5.2.8), and positive for type IV collagen (Figure 5.2.9). The tumor was negative for bcl-2 (Figure 5.2.10) as well as cytokeratin, p63, and melanocytic markers.

**DIAGNOSIS**

Parapharyngeal, left, excision: Malignant peripheral nerve sheath tumor, embolized.

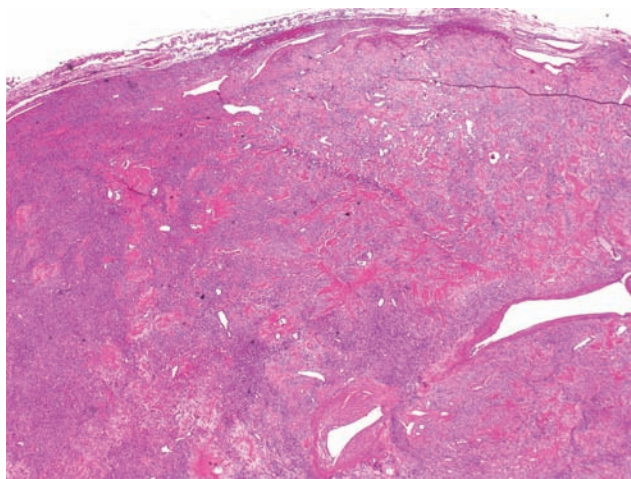


**FIGURE 5.2.1** Well-circumscribed pseudoencapsulated tumor with alternating cellular and collagenous areas. Vessels are staghorn in appearance.

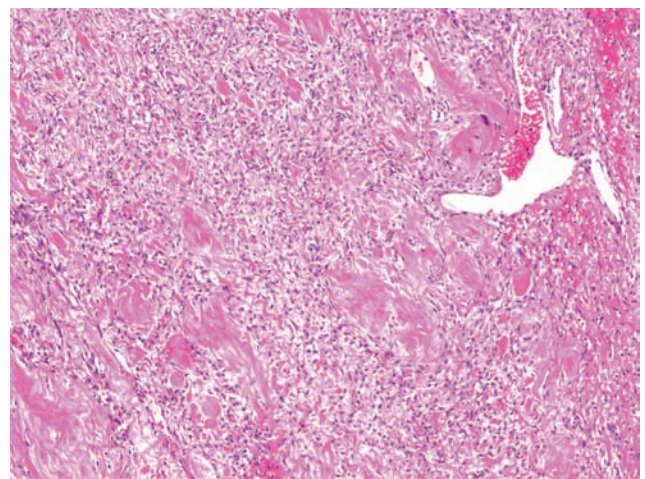


**FIGURE 5.2.2** Areas of spindled morphology and “wavy nuclei” with collagenized stroma.

## 5.2

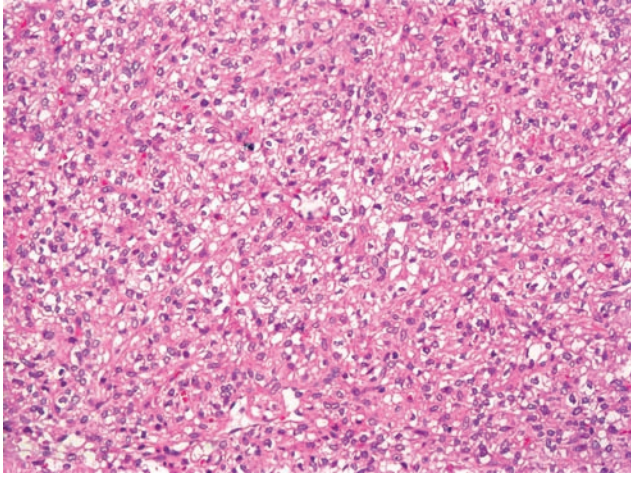


FIGURE 5.2.3 Areas with more epithelioid morphology.

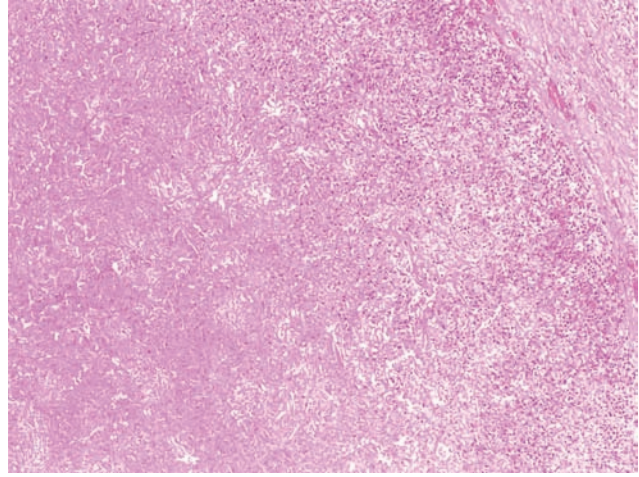


FIGURE 5.2.5 Areas of geographic necrosis.

## COMMENT

This represents a malignant peripheral nerve sheath tumor (MPNST). This tumor shows a morphologic spectrum ranging from spindled to epithelioid to sclerotic. Although the CD34 immunoreactivity is unusual, the patchy S100 reactivity and type IV collagen positivity are supportive.

Parapharyngeal MPNST is extremely rare. Occasionally these occur in the setting of neurofibromatosis, but we see no plexiform growth or benign neurofibroma areas to suggest this. Some MPNSTs are

postulated to arise from schwannomas, but again, we see no evidence of benign schwannoma.

## DISCUSSION

Malignant peripheral nerve sheath tumor comprises only 2% to 14% of all head and neck sarcomas (1). Head and neck MPNST most commonly arise in the soft tissue of the neck or sinonasal tract (1,2). Although benign nerve sheath tumors (schwannoma and neurofibroma) are among the three most common parapharyngeal space tumors (along with paragangliomas and

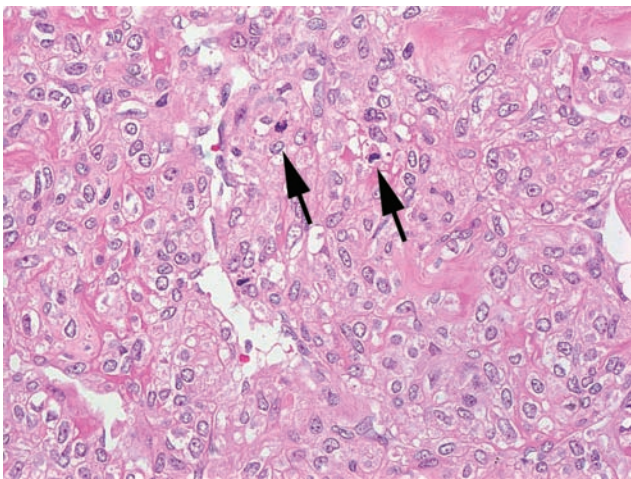


FIGURE 5.2.4 Mitotic activity (arrows).

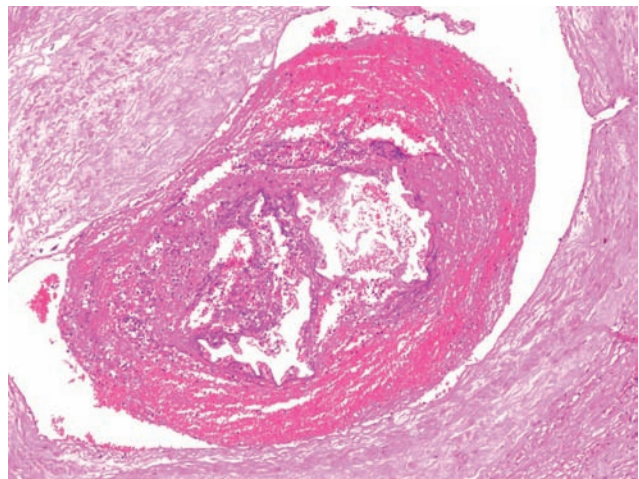
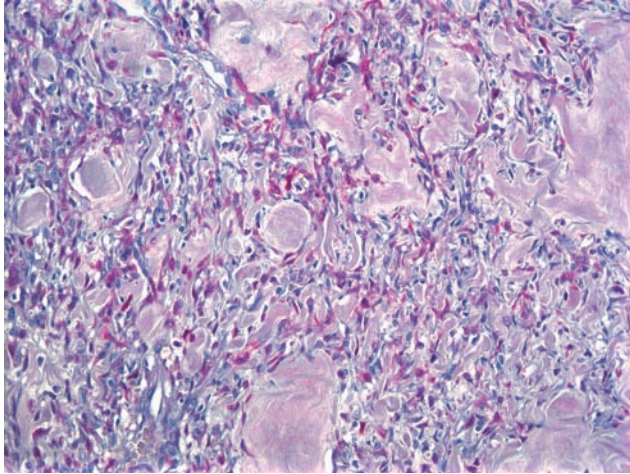
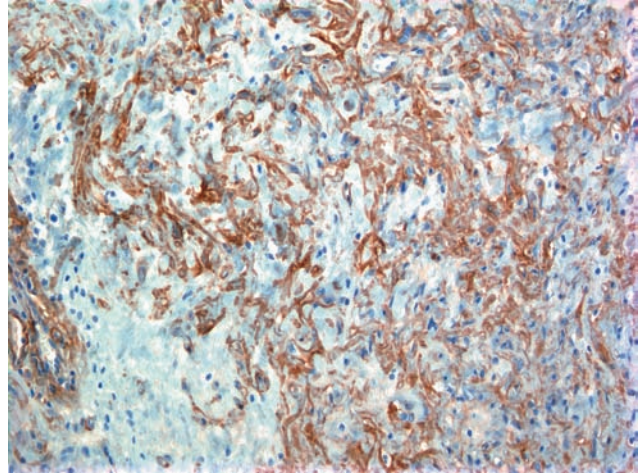


FIGURE 5.2.6 Embolization material.



**FIGURE 5.2.7** S100 patchy immunoreactivity.



**FIGURE 5.2.9** Collagen IV positivity.

pleomorphic adenomas), MPNST presenting as a parapharyngeal space mass is extremely rare, with two reported cases of MPNST with rhabdomyosarcomatous differentiation (Triton tumors) (3,4) and one reported case in the setting of neurofibromatosis type I (5).

Malignant peripheral nerve sheath tumor of the head and neck may be particularly challenging because of the variety of tumor types that need to be considered in the differential diagnosis, which include melanoma, salivary gland myoepithelial tumors, and other sarcoma types. In addition, variant morphology,

particularly epithelioid and rhabdomyoblastic morphology, is fairly common in MPNST of the head and neck, further adding to the difficulty.

It may be difficult to confirm a malignant peripheral nerve sheath phenotype by immunohistochemistry because S100 may be very patchy. In fact, diffuse staining, although possible in MPNST (particularly the epithelioid type), should invoke the diagnosis of melanoma until proven otherwise (with a broad panel of melanocytic markers) (1). Ultrastructurally, these tumors will show reduplication and

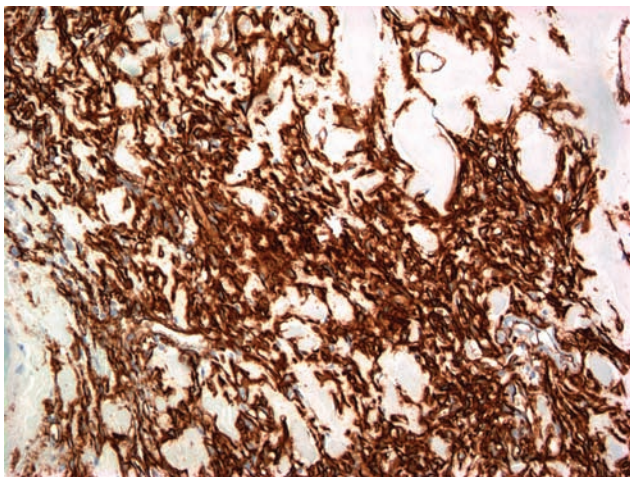


**FIGURE 5.2.8** CD34 diffuse positivity.

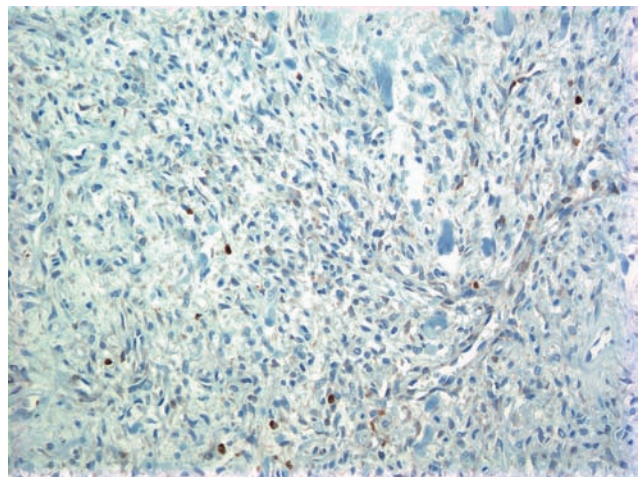


**FIGURE 5.2.10** Bcl-2 negativity.

## 5.2

thickening of the external lamina. Thus, an immunophenotypic correlate to this finding is increased type IV collagen or laminin staining around tumor cells (6). Malignant peripheral nerve sheath tumors are variably positive for actin and CD34, and in the case of Triton tumors, they may be positive for desmin and myogenin as well.

The main differential diagnostic considerations for malignant spindle cell tumors of the head and neck sites always include spindle cell (sarcomatoid) squamous carcinoma, myoepithelial carcinoma, and melanoma. Thus, immunostains for keratins, p63, muscle markers, and other melanocytic markers (ie, HMB-45, melan-A) are necessary before considering a true sarcoma.

This particular case, because of the heavy collagenization, the hemangiopericytoma-like staghorn vasculature, and the CD34 immunoreactivity, raised the differential diagnosis of solitary fibrous tumor. However, solitary fibrous tumors are S100-negative. In addition, solitary fibrous tumors are almost invariably bcl-2-positive, and this particular case was negative. Although the fibrosis in this case may have been secondary to the embolization, a “fibroblastic

MPNST” variant that is strongly CD34-positive has been described (7).

### References

1. Thompson LDR, Fanburgh-Smith JC. Malignant soft tissue tumors. In: Barnes EL, Eveson JW, Reichart P, Sidransky D, eds. *Pathology and Genetics: Head and Neck Tumors*. Lyons: IARC; 2005.
2. Vege DS, Chinoy RF, Ganesh B, Parikh DM. Malignant peripheral nerve sheath tumors of the head and neck: a clinicopathological study. *J Surg Oncol*. 1994;55(2):100–103.
3. Oysu C, Aslan I, Bilgic B, Yazicioglu E. Malignant triton tumour of the parapharyngeal space. *J Laryngol Otol*. 2001;115(7):573–575.
4. Yang BB, Jiang H, Chang HY. Malignant triton tumour of the parapharyngeal space: a case arising from the cervical sympathetic nerve. *J Laryngol Otol*. 2008;122(5):531–534.
5. Sabesan T, Hussein K, Ilankovan V. Malignant peripheral nerve sheath tumour of the parapharyngeal space in a patient with neurofibromatosis type 1. *Br J Oral Maxillofac Surg*. 2008;46(7):585–587.
6. Huang HY, Park N, Erlandson RA, Antonescu CR. Immunohistochemical and ultrastructural comparative study of external lamina structure in 31 cases of cellular, classical, and melanotic schwannomas. *Appl Immunohistochem Mol Morphol*. 2004;12(1):50–58.
7. Houreih MA, Eyden B, Deolekar M, Banerjee S. A case of fibroblastic low-grade malignant peripheral nerve sheath tumor—a true neurofibrosarcoma. *Ultrastruct Pathol*. 2007; 31(5):347–356.

## 5.3

## Middle Ear Adenoma–Paraganglioma–Otitis Media With Glandular Metaplasia

### CLINICAL INFORMATION

“This 66-year-old woman presents with a recurrent lesion of the right middle ear. The lesion was biopsied several years ago and was diagnosed as a paraganglioma.”

### OPINION

Sections show a glandular neoplasm lying in a fibrous stroma covered by a keratinized squamous epithelium (Figure 5.3.1). The glands are closely packed with a “back-to-back” appearance (Figure 5.3.2). Cells lining the glands have pale pink cytoplasm with centrally located nuclei, whereas those at the periphery of the tumor islands are more columnar and tend to palisade. Mitoses, necrosis, and a zellballen pattern

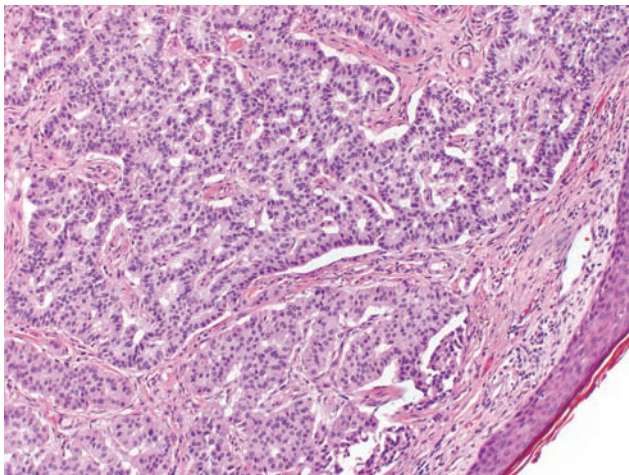


**FIGURE 5.3.1** Middle ear adenoma composed of numerous back-to-back glands. Some tumors, however, may contain few, if any, glands and are composed of only large sheets, small clusters, and/or cords of tumor cells.

are not seen, and there is no connection of the tumor to the overlying squamous epithelium. The tumor is strongly positive for synaptophysin and cytokeratin (Figures 5.3.3 and 5.3.4).

### DIAGNOSIS

Recurrent lesion of the right middle ear, excision: Middle ear adenoma.

### COMMENT

As indicated above, we believe this is a middle ear adenoma (MEA) and not a paraganglioma. The fact that the tumor is positive for cytokeratin supports this diagnosis; paragangliomas are negative for this stain.

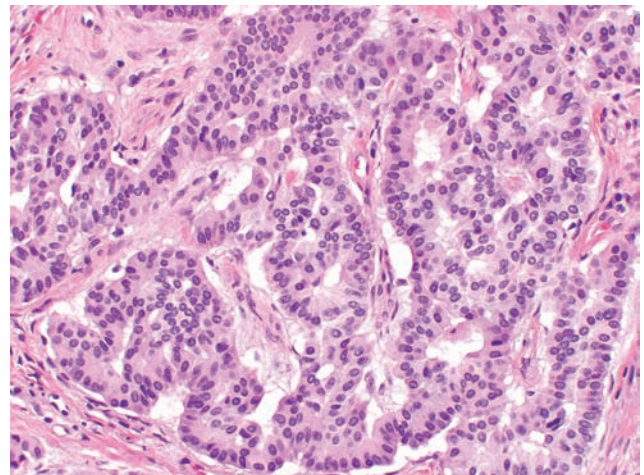


**FIGURE 5.3.2** Middle ear adenoma. Higher magnification of Figure 5.3.1 showing uniform cells free of mitoses.

## 5.3

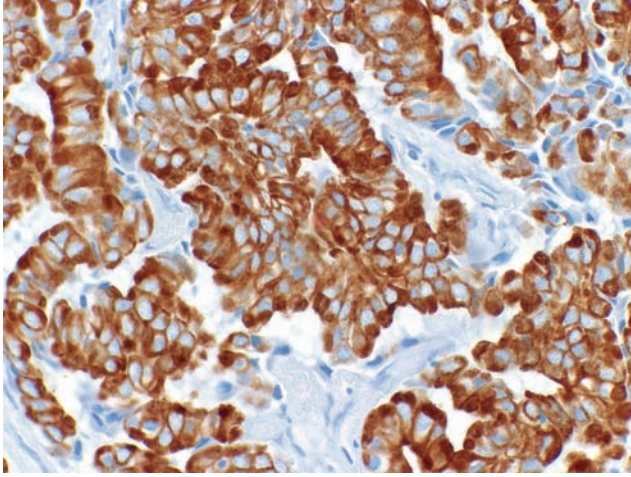


**FIGURE 5.3.3** Middle ear adenomas are positive for synaptophysin.

Middle ear adenomas are also known as neuroendocrine adenomas and carcinoids. Although they are generally regarded as benign, 15% to 20% have developed local recurrence and, in rare instances, have even metastasized, indicating that they should be regarded as low-grade or potentially malignant neoplasms.

## DISCUSSION

Tumors of the middle ear with glandular and/or neuroendocrine differentiation are the subject of ongoing

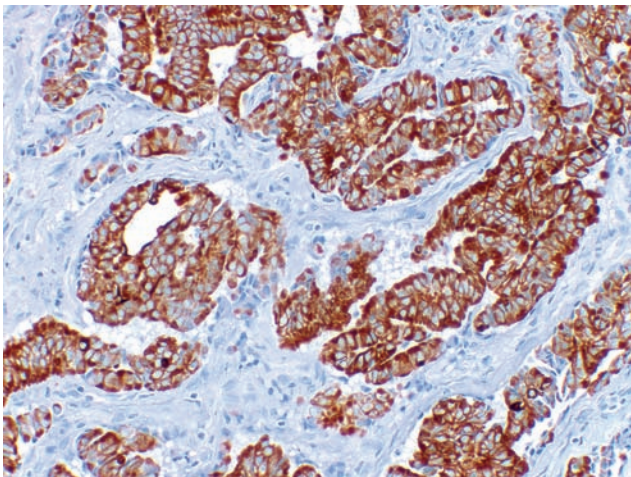


**FIGURE 5.3.4** Middle ear adenomas are positive for cytokeratin.

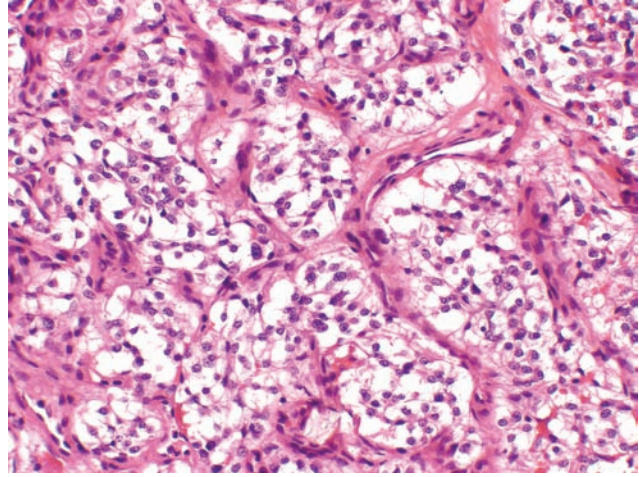


**FIGURE 5.3.5** Jugulotympanic paraganglioma. Note the Zellballen pattern and absence of glands.

controversy regarding their terminology and biological behavior (1–4). Although originally described under the rubric MEA, subsequent studies have shown that most, if not all, exhibit either focal or diffuse neuroendocrine differentiation prompting the use of additional terms, including *MEA with neuroendocrine differentiation*, *neuroendocrine adenoma*, and *carcinoid* (1–4). The most recent edition of the World Health Organization book on classification of head and neck tumors, however, continues to endorse the term MEA (2).

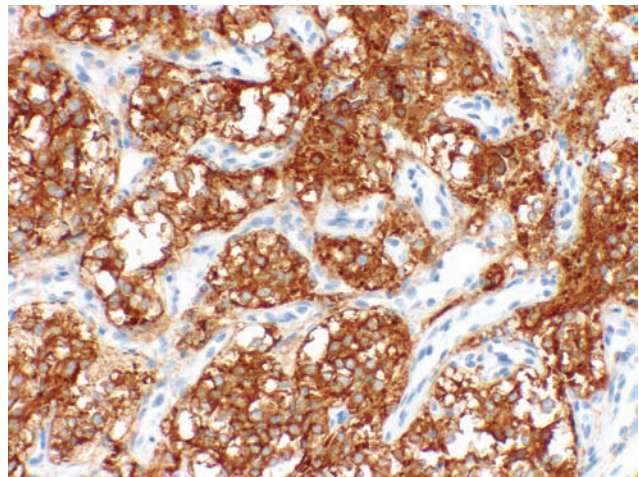


**FIGURE 5.3.6** Jugulotympanic paragangliomas are positive for synaptophysin.

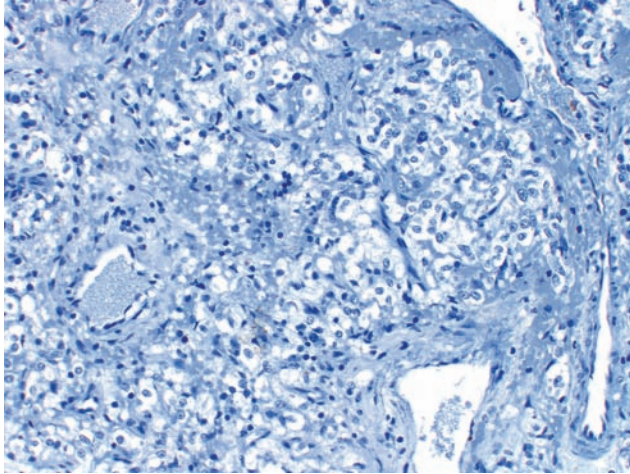


**FIGURE 5.3.7** Jugulotympanic paragangliomas are negative for cytokeratin.

These tumors are treated by surgical excision and typically pursue a benign, uneventful course. Local recurrence, however, develops in 15% to 20% of patients, and at least 4 tumors have metastasized to intraparotid and cervical lymph nodes (3,4). Such behavior indicates that these tumors should be regarded as low-grade malignancies or at least potentially malignant.

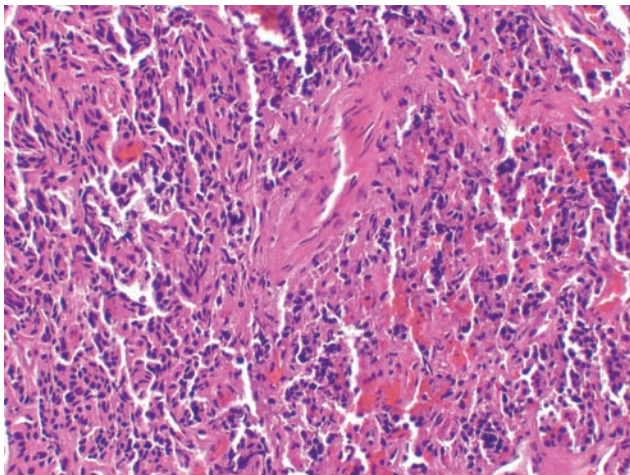


**FIGURE 5.3.8** Some JTPGs are received crushed and distorted, which may interfere with diagnosis or result in confusion with other entities. Synaptophysin and cytokeratin stains are helpful in this instance.

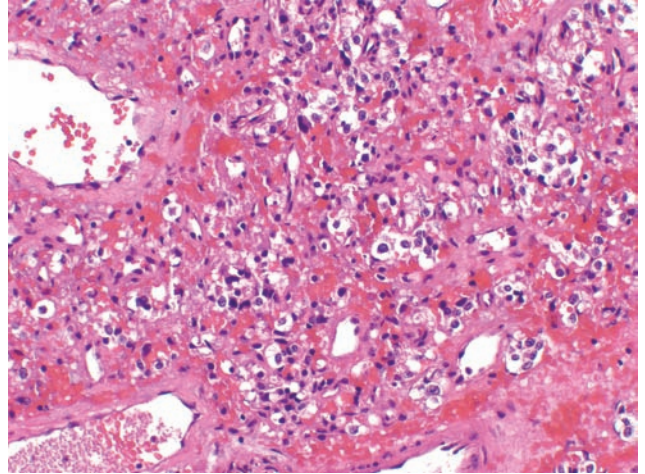


**FIGURE 5.3.9** Distorted, hemorrhagic JTPG that might be confused with granulation tissue or a hemangioma.

When we encounter one of these lesions, we currently use the term MEA, as recommended by the World Health Organization, and add the comment as listed above.

Middle ear adenomas are rare tumors that occur over a broad age range (20–80 years; mean, 45 years) and exhibit a slight male predominance (1). Conductive hearing loss, aural fullness, and tinnitus are the most common manifestations. Facial nerve weakness

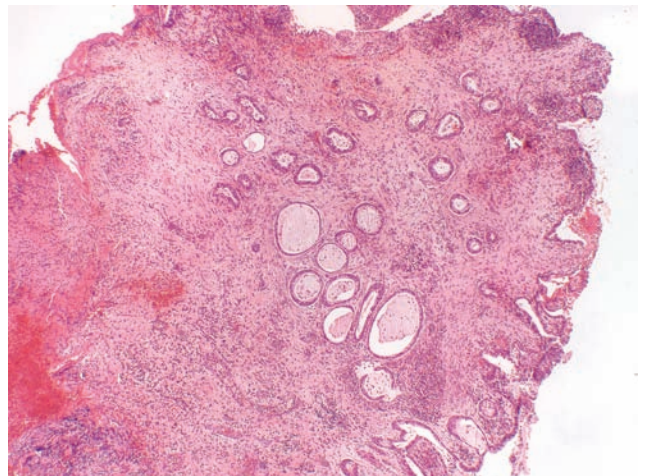


**FIGURE 5.3.10** Otitis media with glandular metaplasia. The glands are derived from invagination and sequestration of the overlying epithelium.



## 5.3

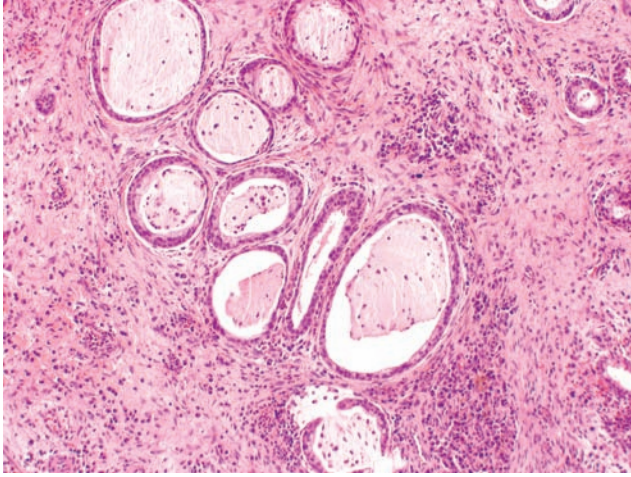


**FIGURE 5.3.11** Otitis media with glandular metaplasia. Note the inflammatory and fibrotic background.

is unusual. Exceptionally, a patient may manifest signs and symptoms of a carcinoid syndrome (3,4).

The differential diagnosis includes a jugulotympanic paraganglioma (JTPG) and otitis media with glandular metaplasia (OMGM).

The JTPG has a zellballen arrangement of tumor cells and is devoid of glands (Figure 5.3.5). Although both tumors (MEA and JTPG) are positive for synaptophysin, only the MEA is positive for cytokeratin; the JTPG is negative (Figures 5.3.6 and 5.3.7) (5).

Frequently, JTPGs are received in the surgical pathology laboratory as small, crushed, and distorted biopsies with no recognizable zellballen pattern and may be confused, in addition to a MEA, with a hemangioma or granulation tissue (Figures 5.3.8 and 5.3.9). The fact that a JTPG is positive for synaptophysin and negative for cytokeratin should allow one to distinguish among these entities.

The middle ear is lined by a modified respiratory mucosa. When it becomes stimulated, as by infection, the mucosa starts to proliferate, invaginates into the stroma, and eventually becomes sequestered from its mucosal attachment and gives rise to glands within the stroma (Figures 5.3.10, 5.3.11, and 5.3.12) (6,

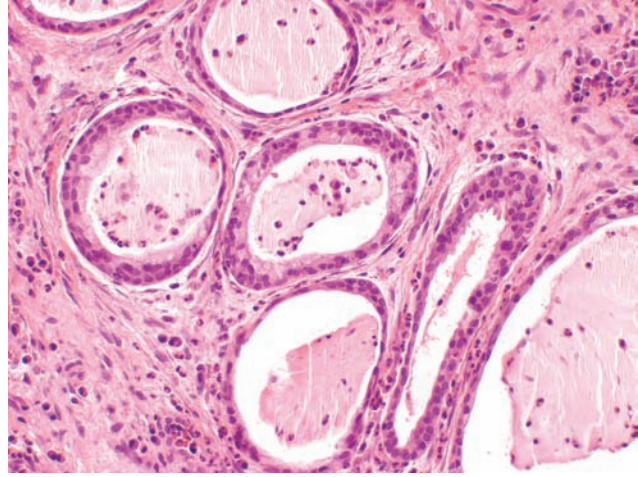


**FIGURE 5.3.12** Otitis media with glandular metaplasia. Higher magnification of Figure 5.3.11 showing benign glands containing luminal secretions and inflammatory cells. The glands are negative for synaptophysin.

7). Middle ear adenoma can be distinguished from OMGM by the absence of significant inflammation in MEA and its prominence in OMGM. Moreover, the glands in OMGM are negative for synaptophysin.

### References

1. Torske KR, Thompson LDR. Adenoma versus carcinoid tumor of the middle ear: a study of 48 cases and review of the literature. *Mod Pathol.* 2002;15:543–555.
2. Michaels L, Soucek S. Adenoma of the middle ear. In: Barnes L, Eveson JW, Reichart P, Sidransky D, eds. *World Health Organization Classification of Tumours. Pathology and Genetics, Head and Neck Tumours.* Lyon: IARC Press; 2005:345.
3. Ramsey MJ, Nadol JB Jr, Pilch BZ, et al. Carcinoid tumor of the middle ear: clinical features, recurrences, and metastases. *Laryngoscope.* 2005;115:1660–1666.
4. Ferlito A, Devaney KO, Rinaldo A. Primary carcinoid tumors of the middle ear: a potentially metastasizing tumor. *Acta Otolaryngol.* 2006;126:228–231.
5. Michaels L, Soucek S, Beale T, et al. Jugulotympanic paraganglioma. In: Barnes L, Eveson JW, Reichart P, Sidransky D, eds. *World Health Organization Classification of Tumors, Pathology and Genetics, Head and Neck Tumours.* Lyon: IARC Press; 2005:366–367.
6. Sade J. Pathology and pathogenesis of serous otitis media. *Arch Otolaryngol.* 1966;84:79–87.
7. Luntz M, Levit I, Sade J. The histologic patterns of normal and inflamed middle ear mucosa. *Eur Arch Otorhinolaryngol.* 1991;248:127–128.

## 5.4

*Mixed Olfactory Neuroblastoma-Adenocarcinoma***CLINICAL INFORMATION**

“An 83-year-old woman with a right nasal cavity mass.”

**OPINION**

Microscopically, the tumor consists of a nested/lobular proliferation of round blue cells embedded in a fibrovascular stroma (Figure 5.4.1). The cells are monomorphic with scant cytoplasm and “salt-and-pepper” chromatin (Figure 5.4.2). However, in several areas, small angulated glands with luminal secretions are noted within and at the periphery of the round cell nests composed of a single layer of monomorphic cuboidal cells with scant eosinophilic cytoplasm (Figure 5.4.3). Immunohistochemical staining for synaptophysin shows positivity in the round cell component and negativity in the glandular component (Figure 5.4.4), whereas a cytokeratin 7 immunostain shows

the opposite with staining in the glandular component and absence of staining in the round blue cell component (Figure 5.4.5). An S100 immunostain highlights a sustentacular pattern of staining around the round blue cell component and faint positivity in the glandular cells (Figure 5.4.6).

**DIAGNOSIS**

Nasal cavity, right, biopsy: Mixed olfactory neuroblastoma-adenocarcinoma.

**COMMENT**

This represents a mixed olfactory neuroblastoma-adenocarcinoma, an extremely rare tumor with both

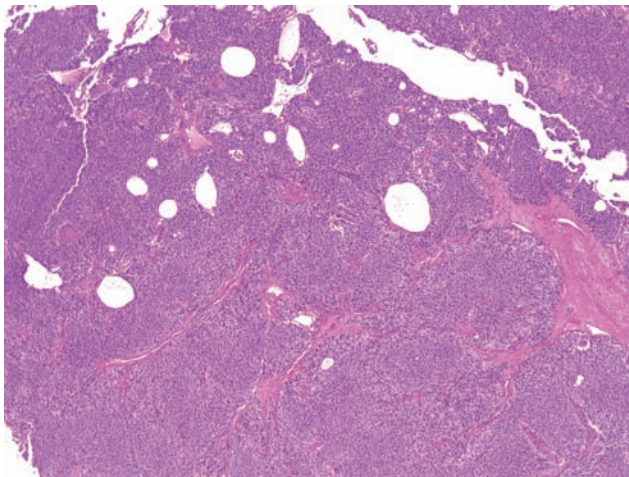


**FIGURE 5.4.1** Lobular nested round blue cell tumor.

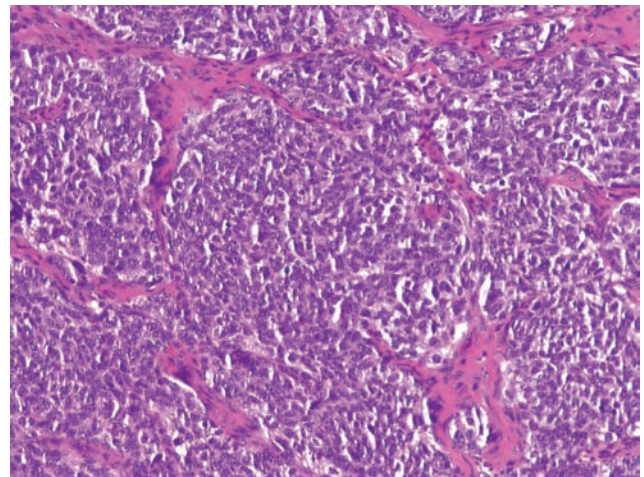


**FIGURE 5.4.2** Monomorphic tumor cells with speckled chromatin.

## 5.4

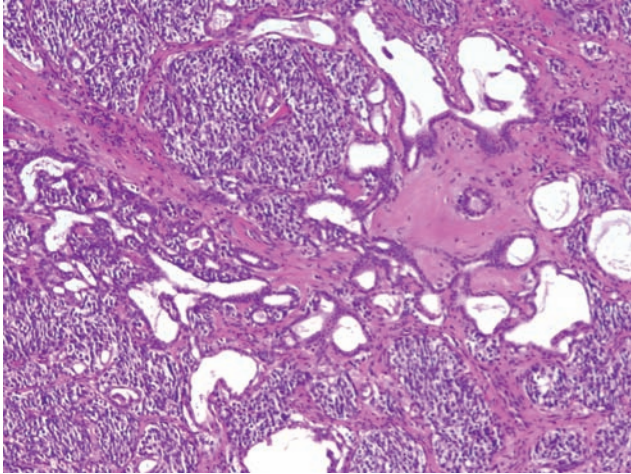


**FIGURE 5.4.3** Bland glandular elements within and at the periphery of round blue cell tumor nests.

glandular and olfactory neuroblastoma components. Only rare cases of this entity have been described.

This tumor is composed of mostly olfactory neuroblastoma (80%) with a minor well-differentiated adenocarcinoma component (20%).

## DISCUSSION

Olfactory neuroblastoma is a malignant tumor of the nasal cavity derived from the olfactory neuroepithe-

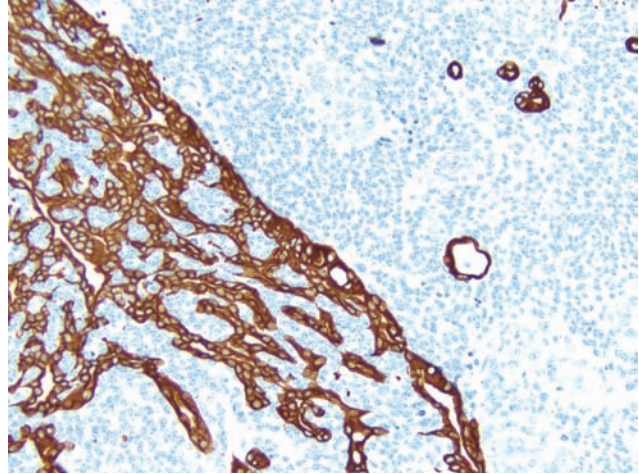


**FIGURE 5.4.5** Cytokeratin 7 positivity in the glandular component (left) and negativity in the round blue cell component.

lium that lines the superior aspect of the nasal cavity. Typically, these tumors are composed of lobular arrangements of round blue cells with a salt-and-pepper neuroendocrine chromatin distribution. The stroma is characteristically fibrovascular. Immunophenotypically, these cells show a neuroendocrine phenotype strongly positive for markers such as synaptophysin. Cytokeratin may occasionally be expressed in olfactory

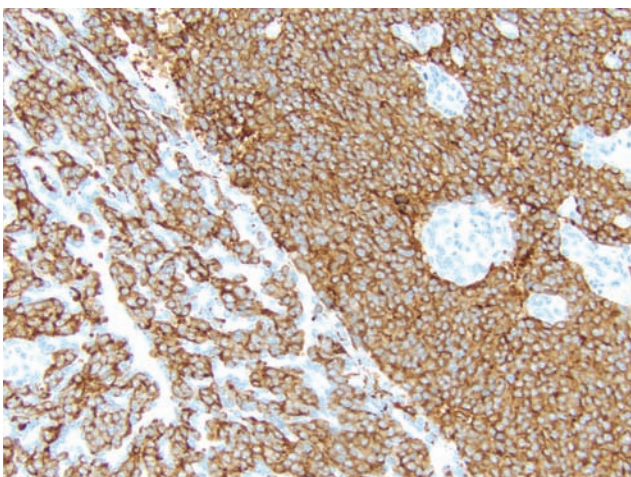


**FIGURE 5.4.4** Synaptophysin positivity in the round blue cell component with negativity in the glandular component (left).

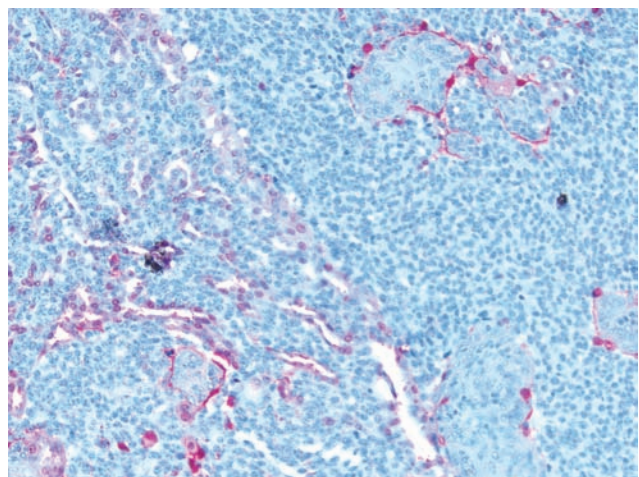


**FIGURE 5.4.6** Sustentacular S100 reactivity with weaker staining of the glandular component.

neuroblastoma, particularly using the CAM 5.2 pan-keratin; however, staining is typically patchy and focal (1) and a sustentacular S100-positive component.

Unlike peripheral neuroblastomas, olfactory neuroblastomas only occasionally show ganglionic differentiation or epithelial glandular elements by light microscopy (2–4). Olfactory neuroblastomas may rarely show truly heterologous elements as well as melanocytes (5) or rhabdomyoblasts (6). Because these are rare tumors, it is not clear whether these tumors behave any differently from typical olfactory neuroblastomas. However, there is a suggestion that tumors with epithelial differentiation (ie, adenocarcinoma or squamous cell carcinoma) tend to be more aggressive than those with ganglioneuronal differentiation (4).

## References

1. Frierson HF Jr, Ross GW, Mills SE, Frankfurter A. Olfactory neuroblastoma. Additional immunohistochemical characterization. *Am J Clin Pathol*. 1990;94(5):547–553.
2. Miller DC, Goodman ML, Pilch BZ, Shi SR, Dickersin GR, Halpern H, et al. Mixed olfactory neuroblastoma and carcinoma. A report of two cases. *Cancer*. 1984;54(9):2019–2028.
3. Sugita Y, Kusano K, Tokunaga O, Mineta T, Abe M, Harada H, et al. Olfactory neuroepithelioma: an immunohistochemical and ultrastructural study. *Neuropathology*. 2006;26(5):400–408.
4. Seethala RR, Wenig BM, Barnes EL, Hunt JL. Olfactory neuroblastoma with divergent differentiation: from ganglioneuroblastoma to carcinoma. *Mod Pathol*. 2007;20(S2):229A.
5. Curtis JL, Rubinstein LJ. Pigmented olfactory neuroblastoma: a new example of melanotic neuroepithelial neoplasm. *Cancer*. 1982;49(10):2136–2143.
6. Miyagami M, Katayama Y, Kinukawa N, Sawada T. An ultrastructural and immunohistochemical study of olfactory neuroepithelioma with rhabdomyoblasts. *Med Electron Microsc*. 2002;35(3):160–166.

## 5.5

*Mucosal Melanoma***CLINICAL INFORMATION**

“A 78-year-old woman presented with difficulty breathing progressively worsening over the period of 2 months. A CT scan of the neck and chest showed an obstructing subglottic tumor and no evidence of metastatic disease. Tracheostomy and laryngoscopic biopsies were performed. Is this a metastatic cutaneous melanoma or a primary mucosal melanoma? Dermatologic examination showed no evidence of primary cutaneous disease.”

**OPINION**

Histologic examination shows polypoid tumor covered by squamous mucosa (Figure 5.5.1). The neoplastic epithelioid cells are discohesive, show solid growth pattern, and have abundant cytoplasm and pleomorphic hyperchromatic nuclei (Figure 5.5.2).

Enlarged prominent nucleoli are identified (Figure 5.5.3). Focal deposits of dark brown nonrefractile pigment are present (Figure 5.5.3). The tumor surface is focally ulcerated, and the preserved squamous epithelium showed numerous intramucosal nests of neoplastic cells (Figure 5.5.4). Immunohistochemically, the neoplastic cells are positive for HMB45 (Figure 5.5.5), tyrosinase, and S100. Cytokeratin and p63 immunostains are negative.

**DIAGNOSIS**

Subglottic tumor, biopsy: Ulcerated nodular malignant melanoma, favor primary mucosal melanoma.

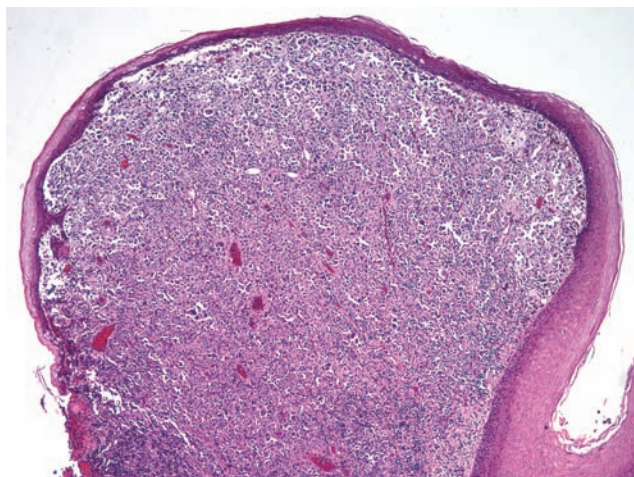


**FIGURE 5.5.1** Polypoid tumor covered by squamous mucosa.

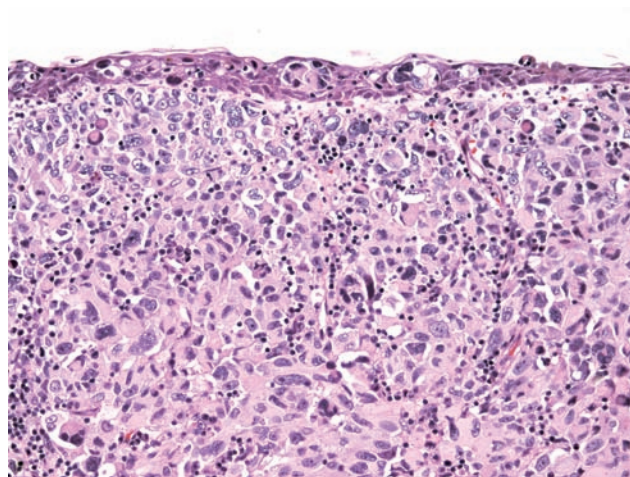


**FIGURE 5.5.2** Epithelioid pleomorphic discohesive neoplastic cells with solid growth.

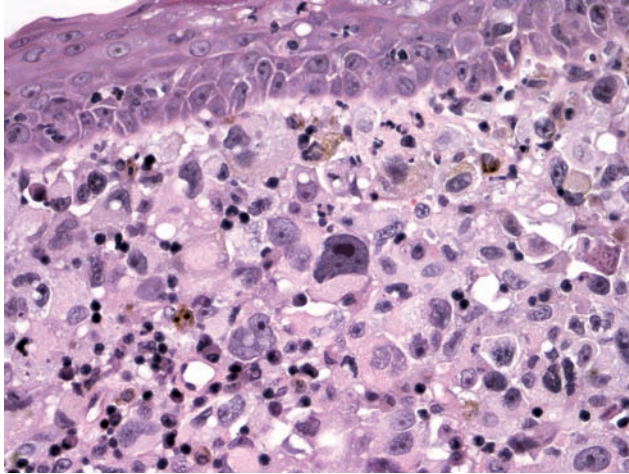


**FIGURE 5.5.3** Neoplastic cells with abundant cytoplasm, pleomorphic nuclei, prominent nucleoli. Dark brown non-refractile pigment.

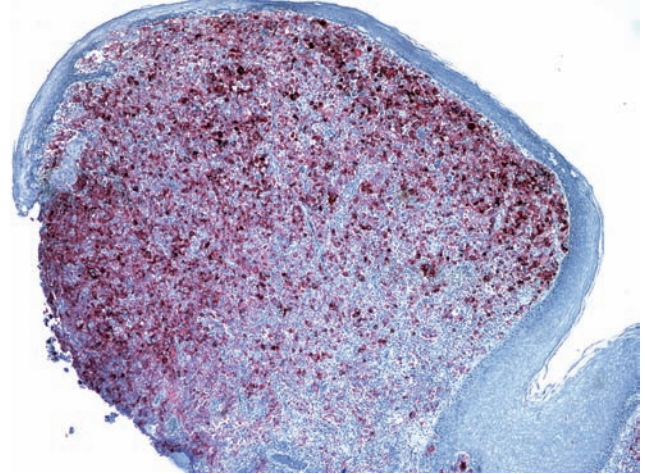


**FIGURE 5.5.5** The neoplastic cells are positive for HMB45. HMB45 is predominantly expressed by more superficial/submucosal cells.

#### COMMENT

The primary mucosal malignant melanoma (MMM) is favored for the following reasons. First, the negative dermatologic examination is reassuring. Second, an in situ component is quite extensive. Although epidermotropic (“mucosotropic”) variants of metastatic melanoma have been described, they usually arise close to the primary lesion and uncommonly are present at distant metastases. Third, HMB45 and tyro-

sinase immunostains show stronger staining in more superficial/submucosal tumor cells. This gradient of expression is suggestive of a possible preexisting melanocytic nevus. At least 1 case of laryngeal melanocytic nevus has been reported (1).

Finally, molecular analysis showed no *BRAF* or *NRAS* mutations. When compared to melanomas of the skin, the incidence of *BRAF* and *NRAS* mutations is lower in melanomas arising in non-sun-exposed anatomic sites (2,3).

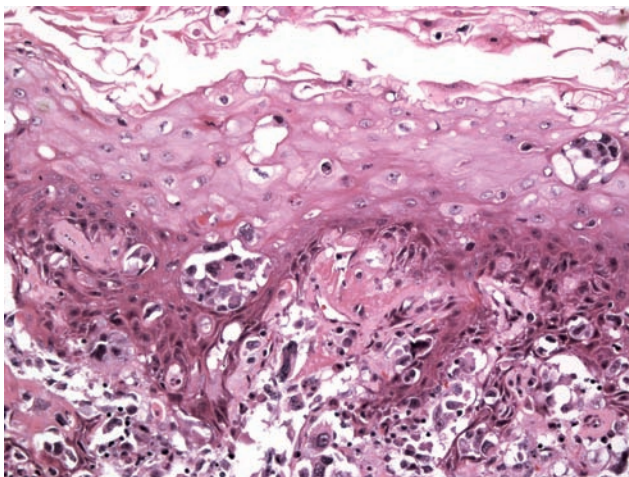


**FIGURE 5.5.4** Intraepithelial nests of neoplastic cells.

#### DISCUSSION

Mucosal malignant melanomas are most common in the sinonasal tract and oral cavity (4). Primary laryngeal mucosal melanomas are very rare. Only about 50 cases have been reported (5,6), and about 80% of patients are men in the sixth or seventh decades of life. In contrast, cutaneous melanoma affects women more frequently than men.

The current case may be the first case of MMM arising in the subglottic region (6).

In general, the practical significance of in situ component remains unclear. First, the surface

## 5.5

of MMM is commonly ulcerated, and the overlying mucosa is missing. Second, melanocytes are normally present within minor salivary glands. These submucosal (in addition to intramucosal) melanocytes may also give rise to primary melanocytic neoplasms.

Dermatologic evaluation remains an important part of clinical management.

### References

1. Seals JL, Shenefelt RE, Babin RW. Intralaryngeal nevus in a child. A case report. *Int J Pediatr Otorhinolaryngol.* 1986; 12(1):55–58.
2. Cohen Y, Rosenbaum E, Begum S, Goldenberg D, Esche C, Lavie O, et al. Exon 15 BRAF mutations are uncommon in melanomas arising in nonsun-exposed sites. *Clin Cancer Res.* 2004;10(10):3444–3447.
3. Wong CW, Fan YS, Chan TL, Chan AS, Ho LC, Ma TK, et al. BRAF and NRAS mutations are uncommon in melanomas arising in diverse internal organs. *J Clin Pathol.* 2005; 58(6):640–644.
4. Thompson LD, Wieneke JA, Miettinen M. Sinonasal tract and nasopharyngeal melanomas: a clinicopathologic study of 115 cases with a proposed staging system. *Am J Surg Pathol.* 2003;27(5):594–611.
5. Amin HH, Petruzzelli GJ, Husain AN, Nickoloff BJ. Primary malignant melanoma of the larynx. *Arch Pathol Lab Med.* 2001;125(2):271–273.
6. Weniag BM. Laryngeal mucosal malignant melanoma. A clinicopathologic, immunohistochemical, and ultrastructural study of four patients and a review of the literature. *Cancer.* 1995;75(7):1568–1577.

## 5.6

*Secretory Meningioma***CLINICAL INFORMATION**

“A 60-year-old man presented with conductive hearing loss in the right ear. He has undergone a tympanoplasty with ossicular reconstruction. Right middle ear contents (4 fragments, 0.1 to 0.3-cm) were submitted for histologic evaluation.”

**OPINION**

Histologic sections demonstrate middle ear mucosa with fibrosis and nests/whorls of tumor cells (Figure 5.6.1). The tumor cells have moderately abundant basophilic cytoplasm and small oval and angulated nuclei (Figure 5.6.2). Flattened tumor cells surround gland-like spaces. Discrete, Periodic Acid Schiff (PAS)-positive, and diastase-resistant intraluminal secretions are noted (Figure 5.6.2, periodic acid-Schiff stain with diastase). Mitoses, intranuclear inclusions,

and psammoma bodies are absent. The neoplastic cells are positive for vimentin, cytokeratin AE1/3 (Figure 5.6.3), and progesterone receptor (Figure 5.6.4) and weakly positive for epithelial membrane antigen and monoclonal carcinoembryonic antigen (carcinoembryonic antigen with pattern similar to AE1/3). Immunostains for synaptophysin and S100 are negative. Ki67 proliferative index is low, less than 2%.

**DIAGNOSIS**

Right middle ear contents, tympanoplasty and ossicular reconstruction: Secretory meningioma.

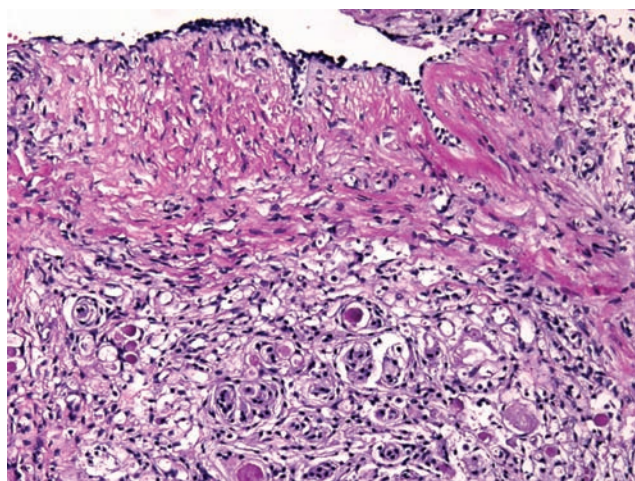


**FIGURE 5.6.1** Middle ear mucosa with fibrosis and tumor.

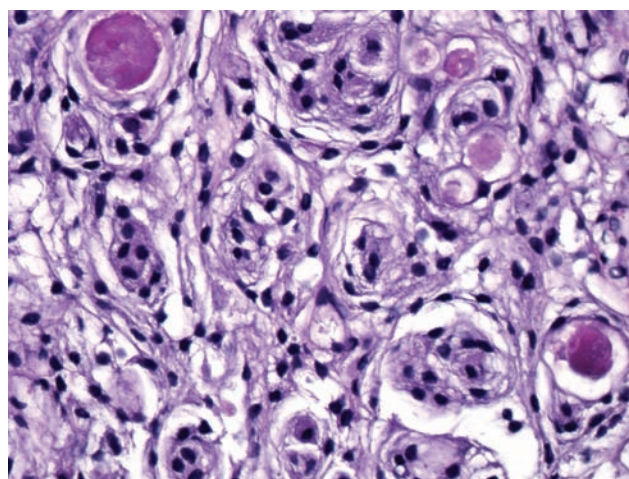


**FIGURE 5.6.2** Whorls of tumor cells. Intraluminal secretions are highlighted by periodic acid-Schiff stain with diastase.



## 5.6

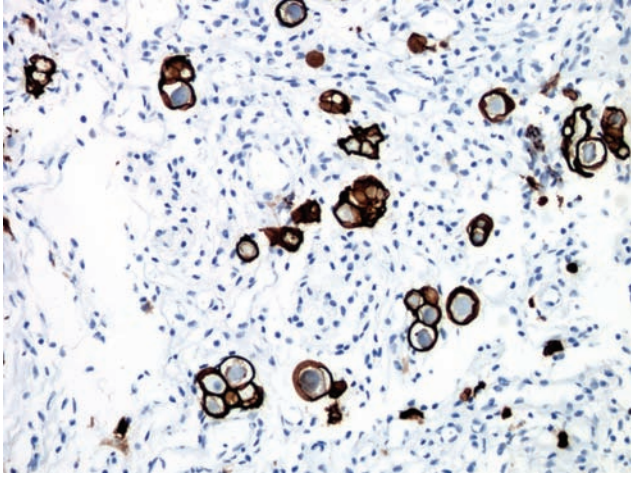


**FIGURE 5.6.3** Immunostaining for cytokeratin AE1/3 highlights neoplastic cells.

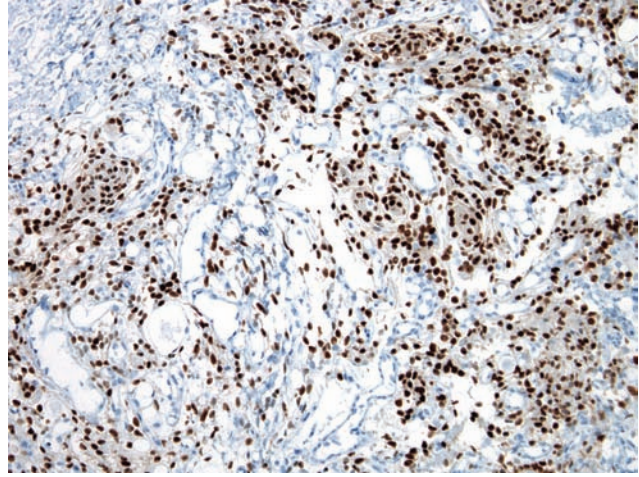


**FIGURE 5.6.4** Neoplastic cells of meningioma are positive for progesterone receptor.

## COMMENT

As indicated above, we believe that this lesion represents a secretory meningioma. This interpretation is supported by the results of immunohistochemical stains.

Although meningiomas may arise in the middle ear, the possibility of a primary intracranial meningioma extending to the middle ear cannot be excluded. Correlation with imaging studies is suggested.

## DISCUSSION

Secretory variant comprises up to 3% of meningiomas (1) and is of no additional prognostic value (World Health Organization grade I).

Intracranial meningiomas rarely extend into the middle ear and mastoid cavity—only about 100 cases are reported to date (2–4). Only 3 cases of primary middle ear secretory meningiomas are documented in the literature (5–7).

Clinically, patients typically present with symptoms of otitis media. However, these cases are resistant to conventional therapy: myringotomy does not yield expected serous fluid, and the biopsy is often performed at that time.

The apparent extracranial location, gland-like structures, and intraluminal secretions (hyaline bodies) of secretory meningioma may pose diagnostic difficulties. Histologically, differential diagnosis includes paraganglioma, middle ear adenoma, schwannoma, mucoepidermoid carcinoma, and adenocarcinomas. In our case, S100 staining was negative, essentially ruling out the possibility of paraganglioma (expect sustentacular cells pattern) or schwannoma. Furthermore, the lack of synaptophysin immunoreactivity is against the diagnosis of middle ear adenoma. The pattern of cytokeratin staining does not support the diagnosis of carcinoma. In combination with other immunohistochemical results, immunoreactivity for progesterone receptor is highly specific for meningiomas (8).

## References

1. Probst-Cousin S, Villagran-Lillo R, Lahl R, Bergmann M, Schmid KW, Gullotta F. Secretory meningioma: clinical, histologic, and immunohistochemical findings in 31 cases. *Cancer*. 1997;79(10):2003–2015.
2. Chang CY, Cheung SW, Jackler RK. Meningiomas presenting in the temporal bone: the pathways of spread from an intracranial site of origin. *Otolaryngol Head Neck Surg*. 1998;119(6):658–664.

3. Civantos F, Ferguson LR, Hemmati M, Gruber B. Temporal meningiomas presenting as chronic otitis media. *Am J Otol.* 1993;14(4):403–406.
4. Ayache D, Tralbalzini F, Bordure P, Gratacap B, Darrouzet V, Schmerber S, et al. Serous otitis media revealing temporal en plaque meningioma. *Otol Neurotol.* 2006;27(7):992–998.
5. Cenacchi G, Ferri GG, Salfi N, Tarantino L, Modugno GC, Rinaldi Ceroni A, et al. Secretory meningioma of the middle ear: a light microscopic, immunohistochemical and ultrastructural study of one case. *Neuropathology.* 2008;28(1):69.
6. Ereño C, Izquierdo AP, Basurko JM, Bilbao FJ, López JI. Temporal bone secretory meningioma presenting as a middle ear mass. *Pathol Res Pract.* 2006;202(6):481–484.
7. Marcelissen TAT, de Bondt RBJ, Lammens M, Manni JJ. Primary temporal bone secretory meningioma presenting as chronic otitis media. *Eur Arch Otorhinolaryngol.* 2008;265(7):843–846.
8. Omulecka A, Papierz W, Nawrocka-Kunecka A, Lewy-Trenda I. Immunohistochemical expression of progesterone and estrogen receptors in meningiomas. *Folia Neuropathol* 2006;44(2):111–5.



## 6 Soft Tissue Tumors

Approximately 10% to 15% of all soft tissue tumors occur in the head. Compared to other sites, the diagnosis and management of these tumors in the head and neck pose several problems: (1) Because they are relatively uncommon, the diagnosis of such is often unexpected or not considered when these tumors occur in the sinonasal tract, the larynx, or the middle ear; (2) when they occur in natural drainage sites (middle ear, sinonasal tract), they often masquerade as inflammatory conditions, both clinically and pathologically; (3) spindle cell squamous carcinoma is especially common in the head and neck and may be mistaken for a soft tissue sarcoma, especially fibrosarcoma or “malignant fibrous histiocytoma”; (4) likewise, mucosal melanomas are often spindled and amelanotic and may be confused with a sarcoma; (5) pleomorphic adenomas and myoepithelial tumors are frequently labeled as leiomyomas or neurofibromas; (6) extracranial meningiomas presenting in the middle or sinonasal tract may also confuse the unwary; (7) sinonasal polyps with stromal atypia, pleomorphic lipomas, spindle cell lipomas, and nodular fasciitis are

additional benign lesions that are often considered malignant; (8) radiation, one of the prime treatments for squamous cell carcinoma of the head and neck, can result in a tissue response that simulates a sarcoma; (9) lastly, the complex anatomy of the head and neck often precludes a desirable wide open resection of a neoplasm.

Although soft tissue neoplasms may occur in virtually any area of the head and neck, there are sites of predilection. For instance, angiofibroma predilects the nasopharynx; spindle-pleomorphic lipomas the posterior neck; glomangiopericytoma the nasal cavity; angiosarcoma the skin of the face and scalp; rhabdomyosarcoma the orbit, the middle ear, and the sinonasal tract–nasopharynx; and synovial sarcoma the neck.

### Selected Readings

1. Fanburg-Smith JC, Lasota J, Auerback A, Foss RD, Laskin WB, Murphey MD. Tumors and tumor-like lesions of soft tissues. In: Barnes L, ed. *Surgical Pathology of the Head and Neck*. 3rd ed. New York: Informa Healthcare; 2009: 773–949.
2. Fletcher CDM, Unni KK, Mertens F. *World Health Organization Classification of Tumours. Pathology and Genetics. Tumours of Soft Tissue and Bone*. Lyon: IARC Press; 2002.

## 6.1

*Angiosarcoma***CLINICAL INFORMATION**

“A 37-year-old woman presented with a left infratemporal skull base mass, 2 cm, and clinical history of ‘hemangioendothelioma.’ CT scan showed expansile lesion involving the base of the left pterygoid bone, pterygoid plates, pterygopalatine fossa, sphenopalatine foramen, and masticator space. The left foramen rotundum was expanded. Also, imaging studies showed perineural spread of tumor by the left maxillary nerve.”

**OPINION**

Histologic sections show fragments of tumor infiltrating the skeletal muscle (Figure 6.1.1) and bone (Figure 6.1.2). The lesion is undermining the mucosa of

the maxillary sinus (Figure 6.1.3). Perineural invasion (Figure 6.1.4) is identified. Within the mass, there are irregular anastomosing open spaces and foci of tumor necrosis (Figure 6.1.5). Closer examination of the open spaces reveals that they contain red blood cells and are lined by plump cells in numbers greater than typically seen in a vessel of this size (Figure 6.1.6). The majority of the tumor is represented by spindle (Figure 6.1.7) and epithelioid cells (Figure 6.1.8). Occasional mitoses (5 in 10 high-power fields) are identified. Some tumor cells show intracytoplasmic “vacuoles” or lumens with erythrocytes (Figure 6.1.9). Immunohistochemically, the irregular branching open spaces are strongly positive for CD31 (Figure 6.1.10). The neoplastic cells are focally positive for cytokeratin AE1/3 (Figure 6.1.11).

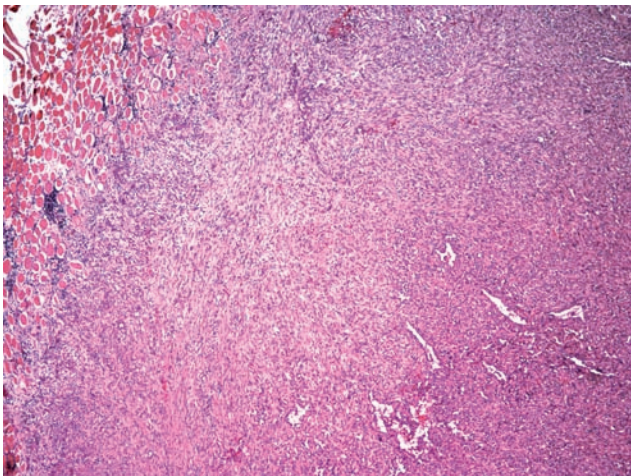


**FIGURE 6.1.1** Tumor infiltrating skeletal muscle (left upper corner). Note irregular anastomosing open spaces in the lower right corner.

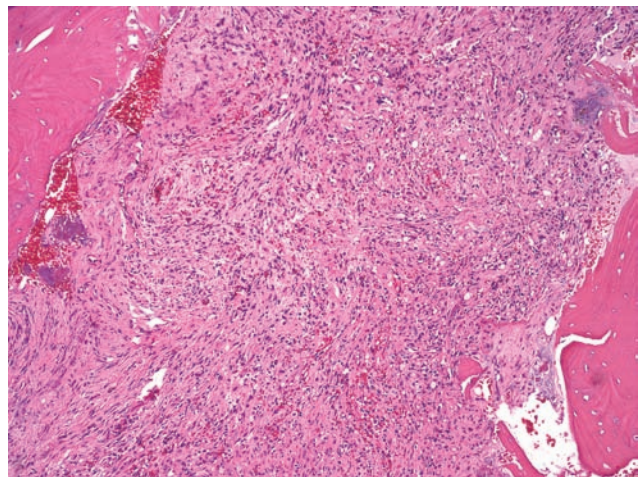


**FIGURE 6.1.2** Tumor cells between bone trabeculae.

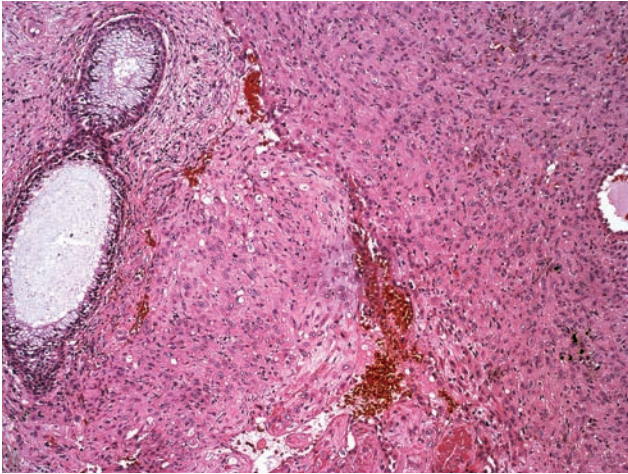


**FIGURE 6.1.3** Tumor undermining mucosa of the maxillary sinus.

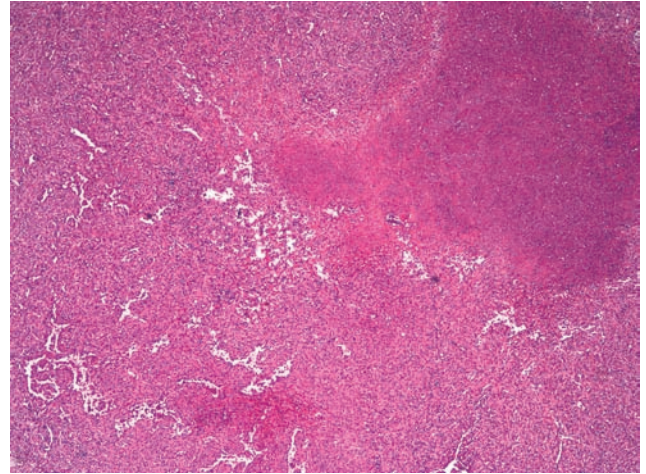


**FIGURE 6.1.5** Tumor necrosis and anastomosing irregular open spaces.

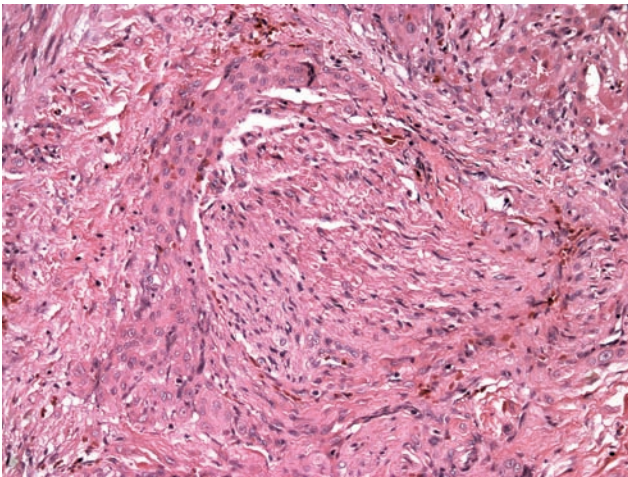


**FIGURE 6.1.4** Perineural invasion.

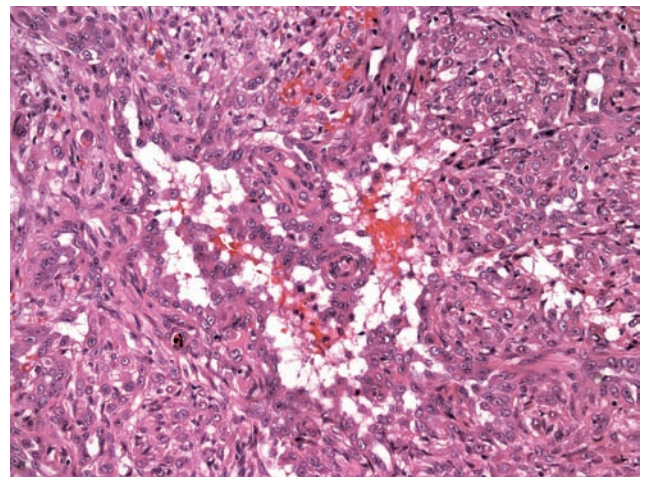


**FIGURE 6.1.6** Open irregular spaces contain red blood cells and are lined by “crowded” plump cells.

#### DIAGNOSIS

Left temporal bone, pterygoid, excision with endoscopic transpterygoid approach and medial maxillectomy: Epithelioid angiosarcoma.

#### COMMENT

Most of the material is diagnostic of epithelioid angiosarcoma (EAS). However, areas with unequivocal features of epithelioid hemangioendothelioma (EH)

are also identified. This case highlights the histologic heterogeneity of vascular tumors: features of both EH and EAS are present, and one diagnosis may be favored over the other depending on the sampled area.

#### DISCUSSION

The differential diagnosis of EAS includes EH (1), carcinoma, and epithelioid sarcoma (ES).

Distinct well-formed vascular channels are rarely seen in EH. Instead, EH tumor cells show more

## 6.1

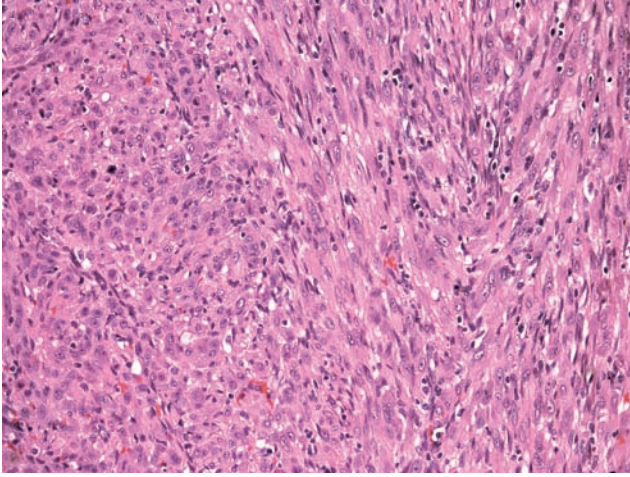


**FIGURE 6.1.7** Spindle neoplastic cells.

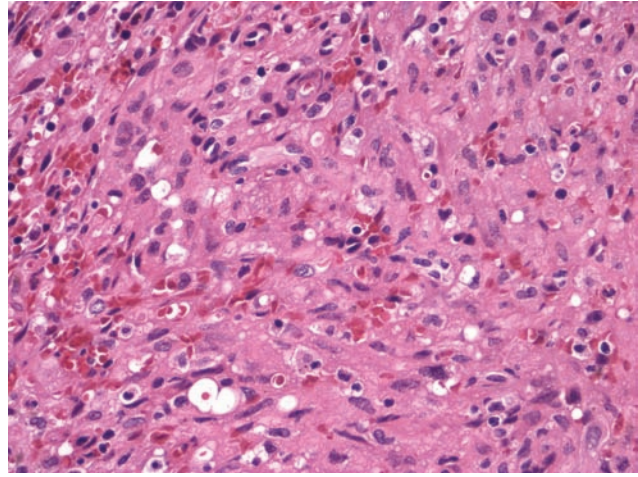


**FIGURE 6.1.9** Neoplastic cells with intracellular lumens containing erythrocytes.

rudimentary vascular differentiation—intracytoplasmic lumens. In our case, vascular canals are seen on hematoxylin and eosin (Figure 6.1.6) and are highlighted by the immunostain for CD31 (Figure 6.1.10). There is a higher intensity of CD31 staining in the irregularly branching vascular channels as compared to the spindle cell component of the tumor. About half of EH are associated with a large vein (2). In this case, no adjacent large vessels are seen. In addition, readily identifiable necrosis, high mitotic activity, and perineural invasion favor the diagnosis of EAS.

The intracytoplasmic lumens and patchy cytokeratin expression by EH may be confused with a carcinoma (2). However, focal cytokeratin expression in epithelioid vascular neoplasms has been well described (3). Cytokeratin coexpression with CD31/CD34 is not typical of an epithelial neoplasm and should prompt the consideration of ES. The ES presents primarily as a distal extremity mass and is characterized by

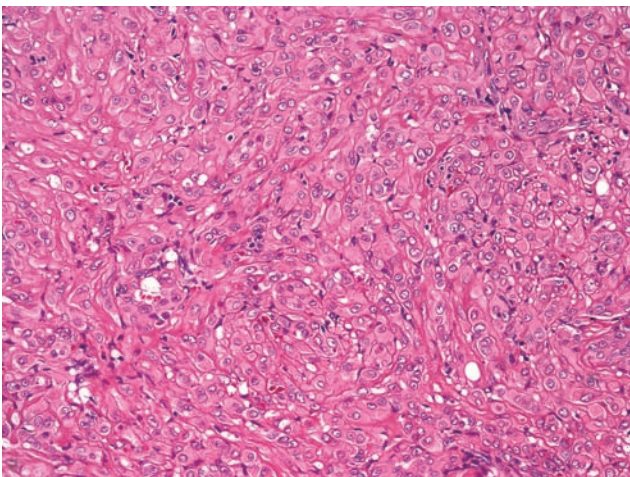


**FIGURE 6.1.8** Epithelioid neoplastic cells.

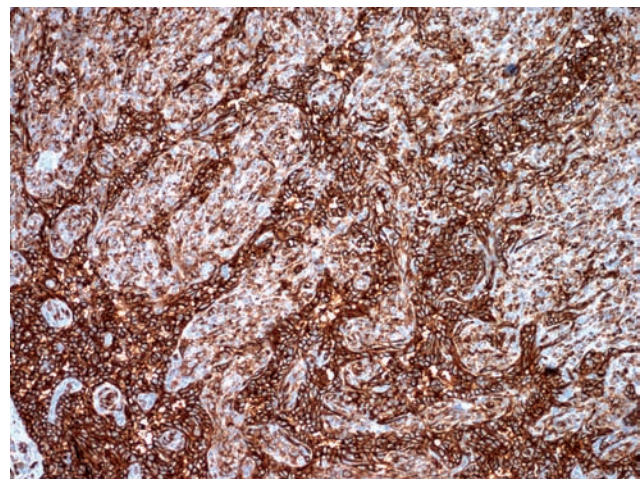


**FIGURE 6.1.10** Neoplastic cells are strongly positive for CD31. Staining is accentuated around the canal-like structures, confirming their endothelial/vascular origin.

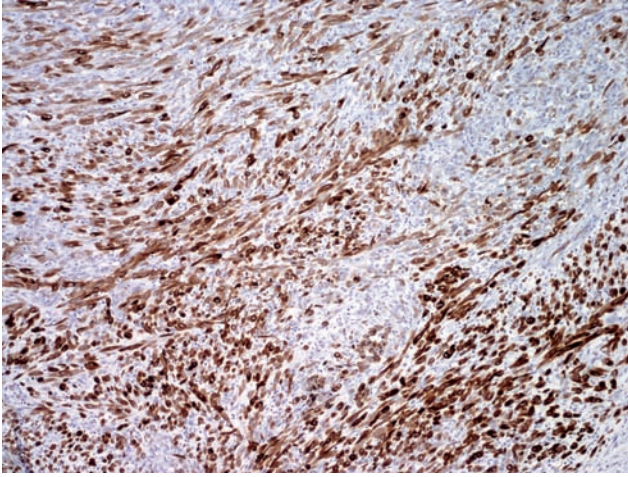


**FIGURE 6.1.11** Positive immunostain for cytokeratin AE1/3.

neoplastic cells palisading around necrotic debris. The ES lacks the anastomosing vascular channels of angiosarcoma (AS) and intracytoplasmic lumens of EH.

### References

1. Stout AP. Hemangio-endothelioma: a tumor of blood vessels featuring vascular endothelial cells. *Ann Surg.* 1943;118(3):445–464.
2. Weiss SW, Enzinger FM. Epithelioid hemangioendothelioma: a vascular tumor often mistaken for a carcinoma. *Cancer.* 1982;50(5):970–981.
3. Miettinen M, Fetsch JF. Distribution of keratins in normal endothelial cells and a spectrum of vascular tumors: implications in tumor diagnosis. *Hum Pathol.* 2000;31(9):1062–1067.



## 6.2

*Glomangiopericytoma—Solitary Fibrous Tumor***CLINICAL INFORMATION**

“Enclosed please find slides of a nasal lesion removed from a 78-year-old man. I believe that this represents an intranasal glomus tumor; however, I have never seen one arise in this anatomic site. Your opinion is greatly appreciated.”

**OPINION**

Sections show a well-circumscribed, cellular, and highly vascular stromal tumor covered by an intact metaplastic squamous mucosa (Figure 6.2.1). The cells have pink, poorly defined cytoplasm and round to short, spindle-shaped hyperchromatic nuclei devoid of mitotic activity (Figures 6.2.2 and 6.2.3). Blood vessels, predominately sinusoidal, are numer-

ous. A few scattered vessels, however, are larger and surrounded by hyalined collagen (Figure 6.2.4). Necrosis and cellular pleomorphism are not seen nor is there any evidence of a significant fibrous stromal component. A CD34 stain highlights the blood vessels, whereas the tumor cells are negative (Figure 6.2.5). The vast majority of the tumor is positive for smooth muscle actin and negative for desmin, CD99, and bcl-2.

**DIAGNOSIS**

Nasal lesion, excision: Glomangiopericytoma.

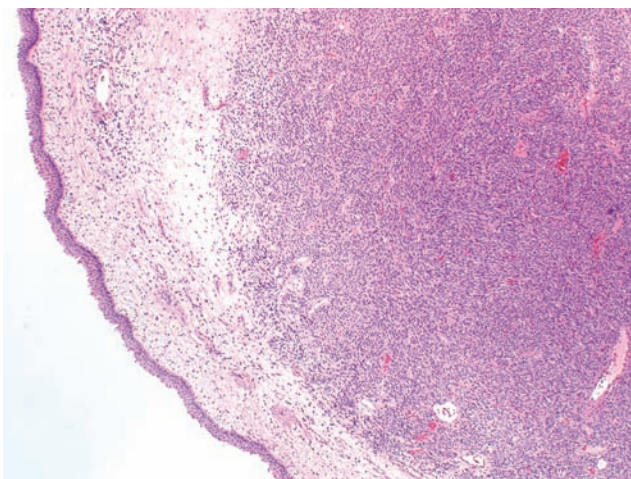


**FIGURE 6.2.1** Glomangiopericytoma. Well-circumscribed, cellular stromal tumor. The overlying respiratory mucosa has undergone extensive squamous metaplasia.

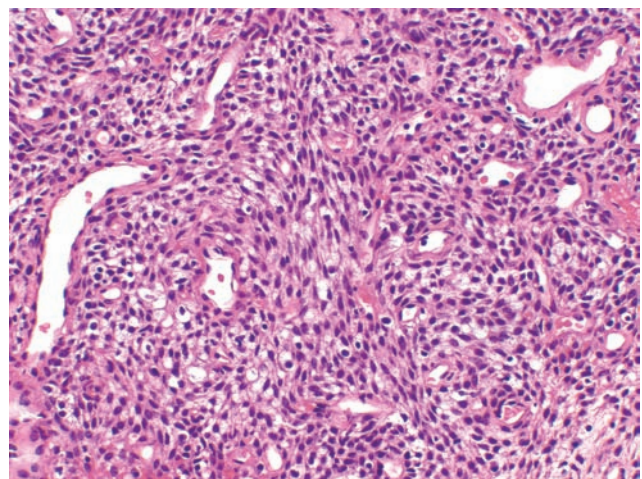


**FIGURE 6.2.2** Glomangiopericytoma. The tumor is highly vascular and composed of cells with uniform round to short spindle-shaped nuclei and pink cytoplasm.

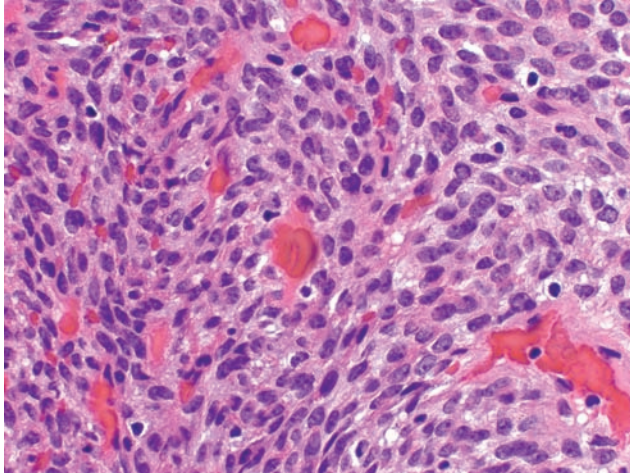


**FIGURE 6.2.3** Glomangiopericytoma. Higher magnification of Figure 6.2.2.

#### COMMENT

I essentially agree with your diagnosis. Over the years, this neoplasm has undergone several name changes including hemangiopericytoma-like tumor and glomus tumor. The current preferred term is *glomangiopericytoma* (GPC).

#### DISCUSSION

In 1976, Compagno and Hyams (1) reported 23 tumors of the sinonasal tract that bore some resem-

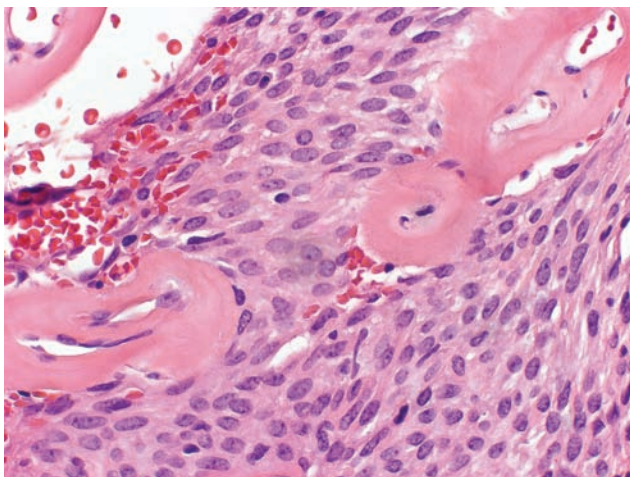


**FIGURE 6.2.4** Glomangiopericytoma. Small blood vessels are sometimes surrounded by hyalinized collagen.

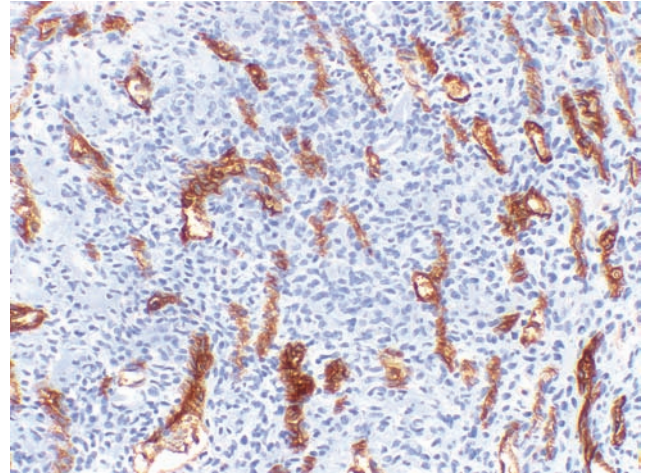


**FIGURE 6.2.5** Glomangiopericytoma. A CD34 immunohistochemical stain highlights the blood vessels. Tumor cells are negative.

blance to the soft tissue hemangiopericytoma but had a decidedly better prognosis. They coined the term *hemangiopericytoma-like tumor* for these lesions (1). Subsequently, “like” was deleted from the name, and the tumors were simply referred to as *hemangiopericytomas*. More recently, it has been shown that these tumors exhibit perivascular myoid differentiation and are more akin to either glomus tumors or hybrid neoplasms with mixed glomus-pericytic features. As such,

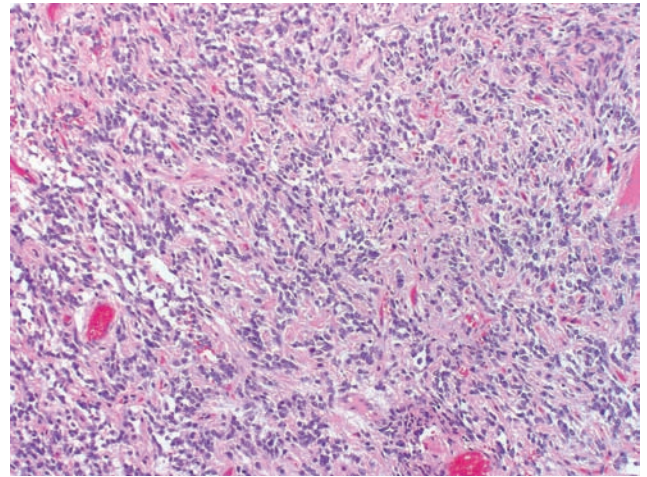


**FIGURE 6.2.6** Solitary fibrous tumor. Cellular area with few blood vessels.

## 6.2

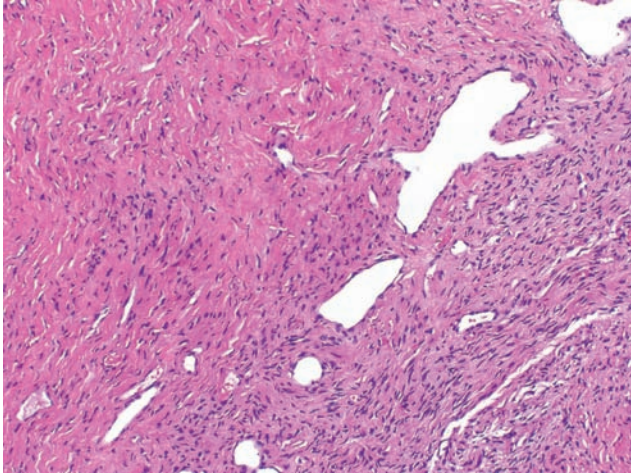


**FIGURE 6.2.7** Solitary fibrous tumor. “Hemangiopericytoma-like area” on right alternating with large fibrous area on left.

the term *glomangiopericytoma* has been proposed and accepted by the World Health Organization as the preferred designation (2). For historical reasons, some still prefer retaining *hemangiopericytoma* and advocate the term *sinonasal-type hemangiopericytoma* (3).

Glomangiopericytoma can occur at any age. Most patients, however, are adults with a mean age at presentation between 55 and 65 years. Most studies indicate an equal gender distribution or a slight female predominance of 1.2:1.

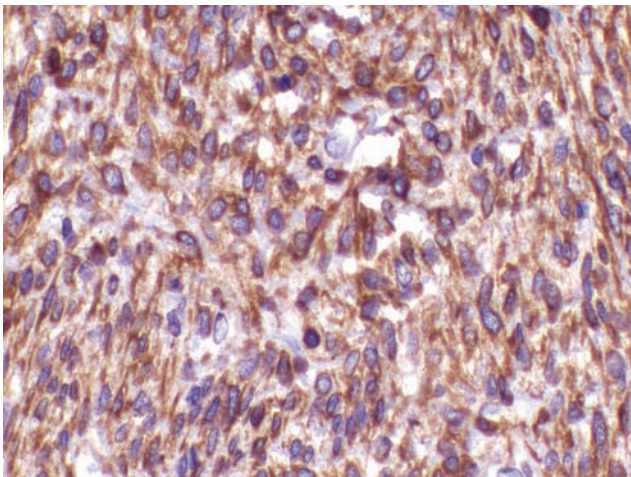


**FIGURE 6.2.8** Solitary fibrous tumors are positive for CD34.

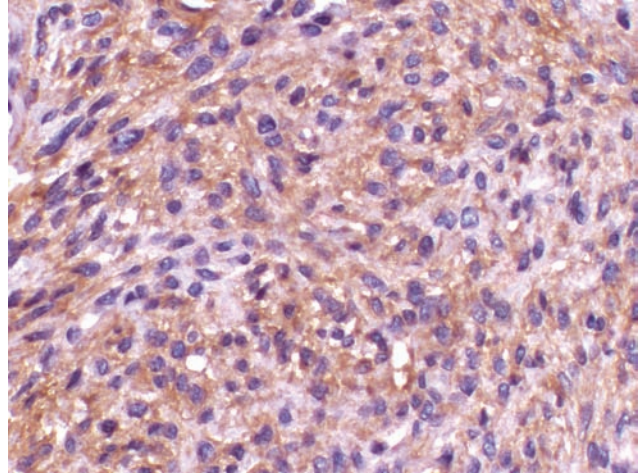


**FIGURE 6.2.9** Solitary fibrous tumors may be positive for CD99.

The tumor typically presents as a unilateral, intranasal, 0.8-cm to 8.0-cm, soft to firm, tan, gray, or white polypoid mass that is often confused with an ordinary nasal polyp. There is no significant lateralization to either side of the nose and no site of predilection within the nasal cavity. The tumor may also arise within a paranasal sinus or involve both nasal cavity and adjacent sinus.

Unilateral nasal obstruction and epistaxis are by far the most frequent complaints. Pain is exceptional.

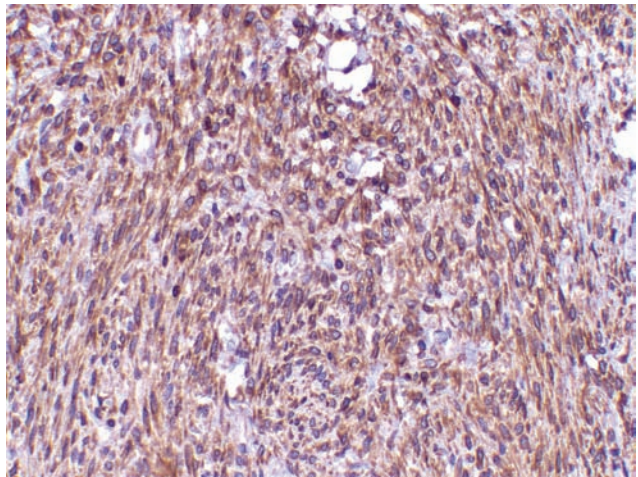


**FIGURE 6.2.10** Solitary fibrous tumors may be positive for bcl-2.

Imaging studies show only a soft tissue density at times associated with a background of obstructive sinusitis. Bone erosion and/or sclerosis are uncommon.

Most patients with GPC of the sinonasal tract are treated by simple polypectomy, and the prognosis is good. Approximately 15% to 20% of patients experience local recurrence, and less than 3% develop metastasis (3–5). Most recurrences appear within 5 years and often within 1 year. Lungs and bones are the most frequent sites of metastases. Lymph nodes are rarely involved. Potential signs of malignancy include large size (>5 cm), bone invasion, nuclear pleomorphism, greater than 4 mitoses per 10 high-power fields, necrosis, and a proliferative index in excess of 10% (2).

Glomangiopericytoma must be distinguished from other richly vascular soft tissue tumors, most notably solitary fibrous tumor (SFT) and mesenchymal chondrosarcoma.

Solitary fibrous tumors have been described in multiple sites in the head and neck, including the sinonasal tract (6–8). Although it is thought by some that hemangiopericytoma and SFT are variants of the same tumor, this is not so in the head and neck. Glomangiopericytoma and SFT are 2 separate and distinct tumors in this anatomic site. Solitary fibrous tumors may contain “hemangiopericytoma-like areas”; however, these areas are not uniformly present throughout

the tumor as seen in GPC but typically alternate with more fibrous or collagenized foci (Figures 6.2.6 and 6.2.7). Moreover, GPC and SFT also differ immunohistochemically (Table 6.2.1) (Figures 6.2.8, 6.2.9, and 6.2.10).

The presence of cartilage separates mesenchymal chondrosarcoma from GPC.

## References

1. Compagno J, Hyams VJ. Hemangiopericytoma-like intranasal tumors. A clinicopathologic study of 23 cases. *Am J Clin Pathol.* 1976;66:672–683.
2. Thompson LDR, Fanburgh-Smith JC, Wenig BM. Glomangiopericytoma (sinonasal-type hemangiopericytoma). In: Barnes L, Eveson JW, Reichert P, Sidransky D, ed. *World Health Organization Classification of Tumours. Pathology and Genetics. Head and Neck Tumours.* Lyon: IARC Press; 2005:43–44.
3. Thompson LDR, Miettinen M, Wenig BM. Sinonasal-type hemangiopericytoma. A clinicopathologic and immunophenotypic analysis of 104 cases showing perivascular myoid differentiation. *Am J Surg Pathol.* 2003;27:737–749.
4. Catalano P, Brandwein M, Shah DK, et al. Sinonasal hemangiopericytoma: a clinicopathologic and immunohistochemical study of seven cases. *Head Neck.* 1996;18:42–53.
5. Marianowski R, Wassef M, Herman P, et al. Nasal hemangiopericytoma: Report of two cases with literature review. *J Laryngol Otol.* 1999;113:199–206.
6. Zukerberg LR, Rosenberg AE, Randolph G, et al. Solitary fibrous tumor of the nasal cavity and paranasal sinuses. *Am J Surg Pathol.* 1991;15:126–130.
7. Witkin GB, Rosai J. Solitary fibrous tumor of the upper respiratory tract. A report of six cases. *Am J Surg Pathol.* 1991;15:842–848.
8. Ganly I, Patel SG, Stambuk HE, et al. Solitary fibrous tumors of the head and neck. A clinicopathologic and radiologic review. *Arch Otolaryngol Head Neck Surg.* 2006;132:517–525.

**TABLE 6.2.1** GPC vs SFT

Stain	GPC	SFT
CD34	8% (focal)	90%–95%
Bcl-2	2%	20%–35%
CD99	?	70%
EMA	0%	20%–35%

EMA indicates epithelial membrane antigen.

## 6.3

*Inflammatory Myofibroblastic Tumor***CLINICAL INFORMATION**

“A 47-year-old woman with maxillary and ethmoid sinusitis and multiply recurrent right nasal mass. There was no history of prior irradiation.”

**OPINION**

Microscopically, the tumor is a polypoid myxoid proliferation with overlying epithelial attenuation and squamous metaplasia (Figure 6.3.1). The tumor cells are arranged in loose fascicles and are composed of bland spindle cells with long, slender tapered ends and moderate amounts of cytoplasm. Nuclei are somewhat plump with vesicular nuclei and noticeable nucleoli, but no pleomorphism, mitoses, or necrosis was noted (Figure 6.3.2). Inflammation was actually quite sparse.

Immunohistochemically, the tumor cells were actin-positive (Figure 6.3.3) and anaplastic lymphoma

kinase 1 (ALK1)-positive (Figure 6.3.4). Focal calponin positivity was noted as well. The tumor was negative for desmin, p63, S100, melanocytic markers, and various cytokeratins.

**DIAGNOSIS**

Nasal mass, right, excision: Inflammatory myofibroblastic tumor.

**COMMENT**

This represents an inflammatory myofibroblastic tumor (IMT) with a myxoid predominant pattern. The morphology is typical of this entity, and the immunostains, notably ALK1, are supportive of the diagnosis.

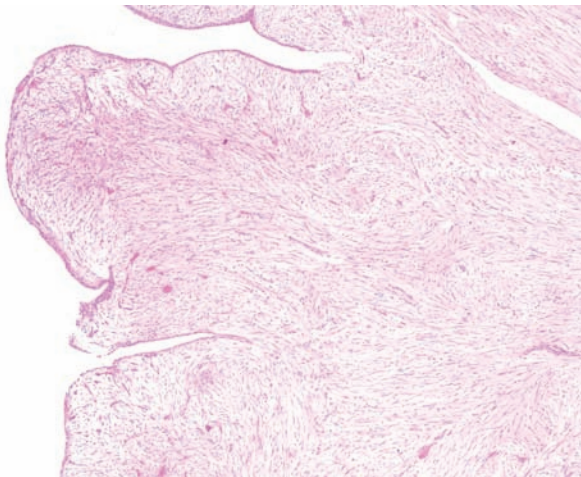


**FIGURE 6.3.1** Polypoid myxoid proliferation lined by metaplastic squamous epithelium.

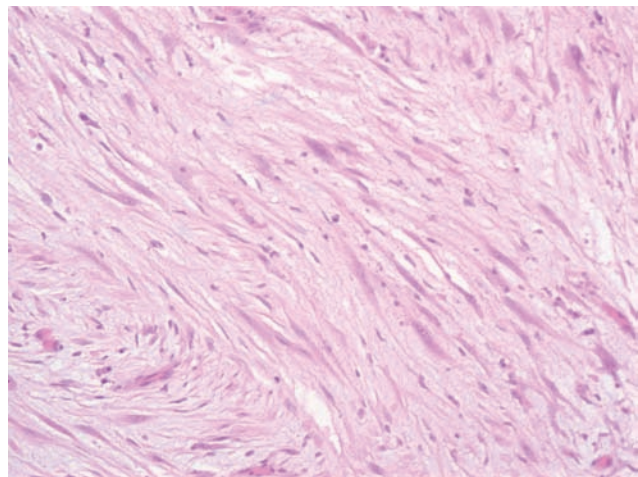


**FIGURE 6.3.2** Bland spindled cells with long tapering processes and sparse inflammation.

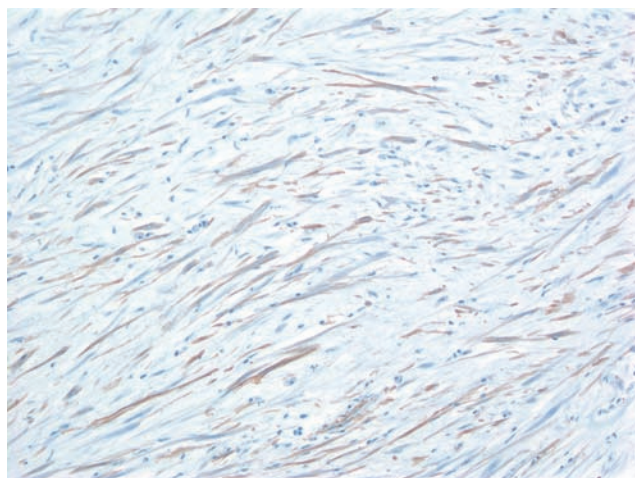


FIGURE 6.3.3 Actin positivity.

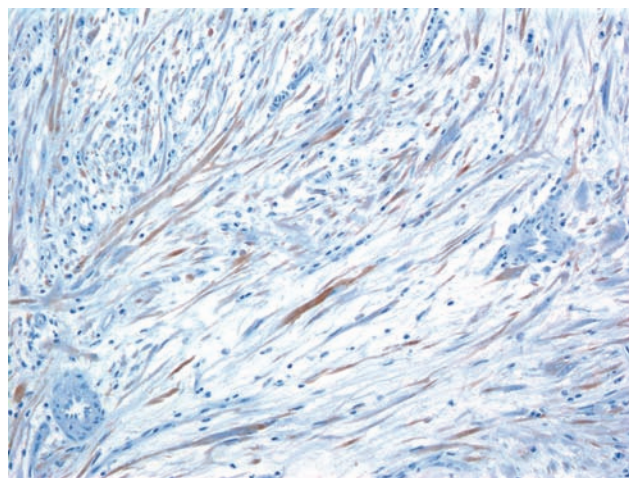


FIGURE 6.3.4 Anaplastic lymphoma kinase 1 positivity.

### DISCUSSION

Inflammatory myofibroblastic tumors were originally considered a reactive pseudotumoral process. However, the description of *ALK* gene rearrangements in many of these tumors suggests that at least a subset are clonal neoplasms. Inflammatory myofibroblastic tumors of the head and neck are uncommon and comprise approximately 20% of all extrapulmonary IMT (1). Within the head and neck, IMT has been most frequently reported in the larynx (2), although tumors of the sinonasal tract have been described (3).

Inflammatory myofibroblastic tumors of mucosal sites typically present as polypoid masses. Unlike visceral IMT, head and neck IMTs are not frequently associated with systemic inflammatory findings (hyperglobulinemia, elevated sedimentation rate) or anemia and thrombocytopenia. The morphologic features of IMT of the head and neck are similar to those of other sites, ranging from myxoid to fibrous with varying amounts of inflammation ranging from sparse (as in this case) to abundant. The *ALK* gene rearrangements, which can be detected by fluorescent in situ hybridization, are found in a subset of IMT, particularly in patients younger than 40. Immunohistochemical

overexpression of ALK1 serves as a surrogate marker for these rearrangements as well (4).

Aggressive head and neck IMTs are uncommon, comprising less than 15% of “aggressive IMT” in one study. Histologic features such as mitoses, necrosis, and pleomorphism, including ganglion-like cells, may predict a more aggressive course (5).

The differential diagnostic considerations for IMT in the sinonasal tract will vary depending on the predominance of the inflammatory component. In tumors with prominent inflammatory components, lymphoma- and IgG4-associated pseudotumoral processes may be considered. Lymphomas may be excluded by the use of immunohistochemical panels and/or molecular techniques. In addition, unlike IgG4-associated pseudotumors, IMT will not have an increase in IgG4 plasma cell infiltrates or obliterative phlebitis (6).

Tumors that have sparse inflammation may have morphologic overlap with spindle cell squamous carcinoma, melanoma, and true mesenchymal neoplasms, such as spindle cell rhabdomyosarcoma, myofibroma, and leiomyosarcoma. The absence of a surface dysplastic component and immunonegativity

## 6.3

for keratins and p63 will exclude spindle cell squamous carcinoma, whereas negativity for melanocytic markers will exclude spindle cell melanomas. Both leiomyosarcoma and spindle cell rhabdomyosarcoma may show overlap with IMT. A careful assessment will show “strap” cells in rhabdomyosarcoma. In addition, IMT tends to have more long tapered cytoplasmic processes than either rhabdomyosarcoma or leiomyosarcoma. Finally, most IMT will be desmin-negative excluding these considerations. Myofibroma is common in the head and neck but is characterized morphologically by paucicellular nodular growth patterns with interspersed hypercellular areas with curvilinear almost “hemangiopericytoma-like” vasculature.

### References

1. Coffin CM, Watterson J, Priest JR, Dehner LP. Extrapulmonary inflammatory myofibroblastic tumor (inflammatory pseudotumor). A clinicopathologic and immunohistochemical study of 84 cases. *Am J Surg Pathol.* 1995;19(8):859–872.
2. Wenig BM, Devaney K, Bisceglia M. Inflammatory myofibroblastic tumor of the larynx. A clinicopathologic study of eight cases simulating a malignant spindle cell neoplasm. *Cancer.* 1995;76(11):2217–2229.
3. Wenig BM. Inflammatory myofibroblastic tumor. In: Barnes EL, Eveson JW, Reichart P, Sidransky D, eds. *Pathology and Genetics: Head and Neck Tumors.* Lyons: IARC; 2005.
4. Freeman A, Geddes N, Munson P, Joseph J, Ramani P, Sandison A, et al. Anaplastic lymphoma kinase (ALK 1) staining and molecular analysis in inflammatory myofibroblastic tumours of the bladder: a preliminary clinicopathological study of nine cases and review of the literature. *Mod Pathol.* 2004;17(7):765–771.
5. Coffin CM, Hornick JL, Fletcher CD. Inflammatory myofibroblastic tumor: comparison of clinicopathologic, histologic, and immunohistochemical features including ALK expression in atypical and aggressive cases. *Am J Surg Pathol.* 2007;31(4):509–520.
6. Yamamoto H, Yamaguchi H, Aishima S, Oda Y, Kohashi K, Oshiro Y, et al. Inflammatory myofibroblastic tumor versus IgG4-related sclerosing disease and inflammatory pseudotumor: a comparative clinicopathologic study. *Am J Surg Pathol.* 2009;33(9):1330–1340.

## 6.4

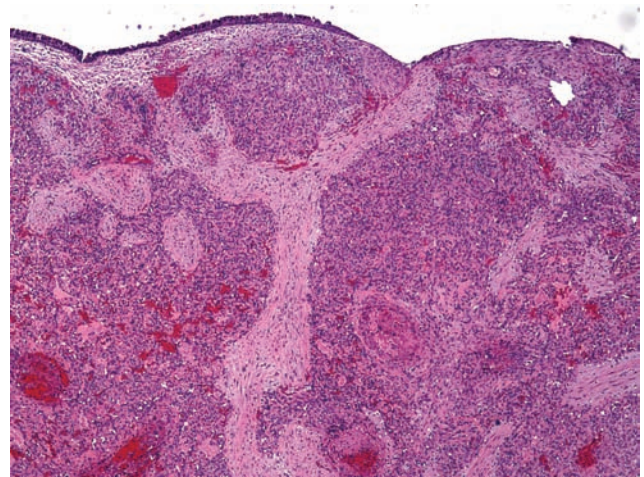
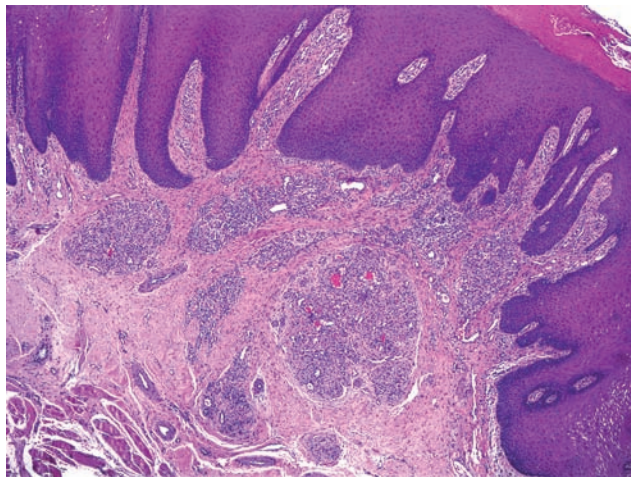
*Lobular Capillary Hemangioma*

## CLINICAL INFORMATION

“A 34-year-old healthy woman presented with a suddenly developed nasal obstruction. CT scan showed a  $4 \times 4 \times 1.7$ -cm left nasal mass which pushed into the left maxillary sinus with erosion of bone, but without radiographic evidence of bone invasion. Prior to surgery, the mass was biopsied and extensive bleeding was noted. The mass was removed piecemeal. Intraoperatively, the lesion was found to be unilateral and attached to the mid septum. Histologically, the lesion is polypoid, vascular, and shows surface ulceration and stromal myxoid change. I feel this is a benign vascular lesion consistent with angiofibroma. My concern is that the location and patient’s gender are unusual for this diagnosis. Also, I have considered the diagnosis of capillary hemangioma; however, I have not seen it in this location or of this size.”

## OPINION

Histologic sections demonstrate a polypoid lesion covered by keratinizing squamous (Figure 6.4.1) and respiratory epithelium (Figure 6.4.2). Superficial ulceration with fibrinopurulent exudate is noted (Figure 6.4.3). Subepithelial parts of the lesion show well-circumscribed compact lobules of capillaries (Figure 6.4.4). In other areas, the capillary clusters are smaller and surrounded by paucicellular fibrous stroma devoid of inflammation. Dilated capillaries and interlobular gaping vessels resembling small veins and arteries without smooth muscle layer are seen (Figure 6.4.5). In other aspects of the lesion, capillaries are inconspicuous, and the thin-walled vessels are dominant (Figure 6.4.6). Focal endothelial hyperplasia is noted (Figure 6.4.7). The endothelial cells are bland and show no mitotic activity.



**FIGURES 6.4.1 AND 6.4.2** Polypoid lesion covered in areas by keratinizing squamous epithelium (Figure 6.4.1) and respiratory epithelium (Figure 6.4.2). Note well-circumscribed lobular clusters of capillaries.



## 6.4

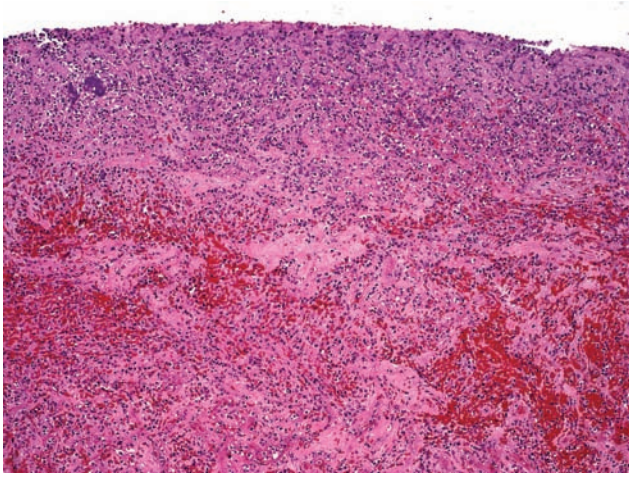


**FIGURE 6.4.3** Superficial ulceration corresponding to the traumatized/biopsied area.

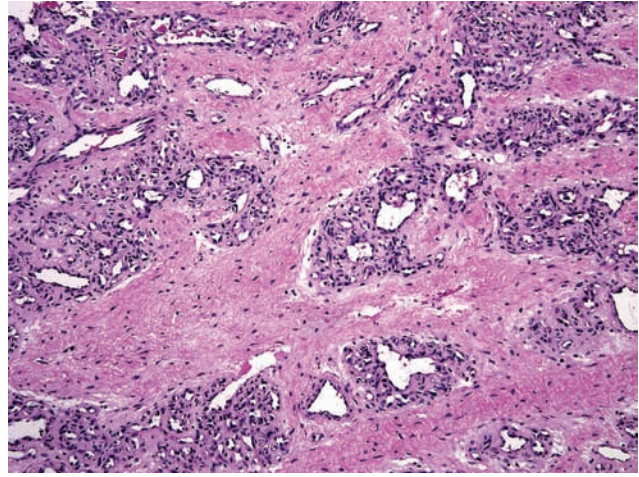


**FIGURE 6.4.5** Fibrous tissue between the lobules. Note gaping thin-walled small vessels and dilated capillaries.

**DIAGNOSIS**

Left nasal mass, excision: Lobular capillary hemangioma.

**COMMENT**

We believe this lesion represents a lobular capillary hemangioma (LCH). This diagnosis is based on the presence of a unique lobular arrangement of

well-formed compact capillaries. Areas with capillary dilatation, obscured lobular pattern, endothelial hyperplasia, and thin-walled vessels most likely represent superimposed alterations due to trauma, biopsy, and vascular compromise (infarct) commonly seen in polypoid nasal lesions of large size.

**DISCUSSION**

The lip is the most common location for mucosal LCH. Nasal cavity, especially nasal septum, is the sec-

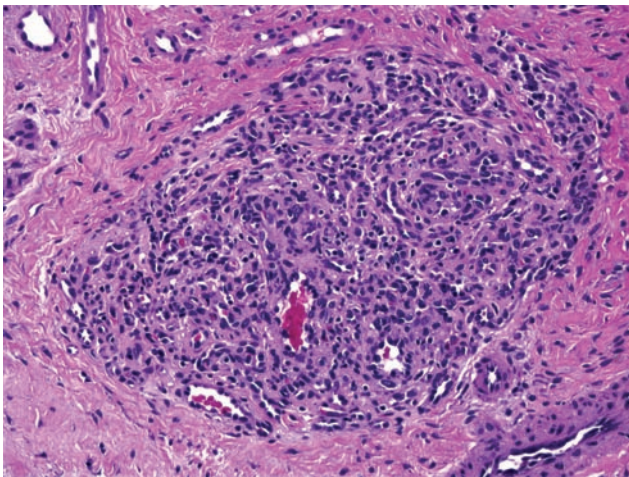


**FIGURE 6.4.4** The diagnostic histologic feature of LCH—well-defined lobules of capillary proliferations.

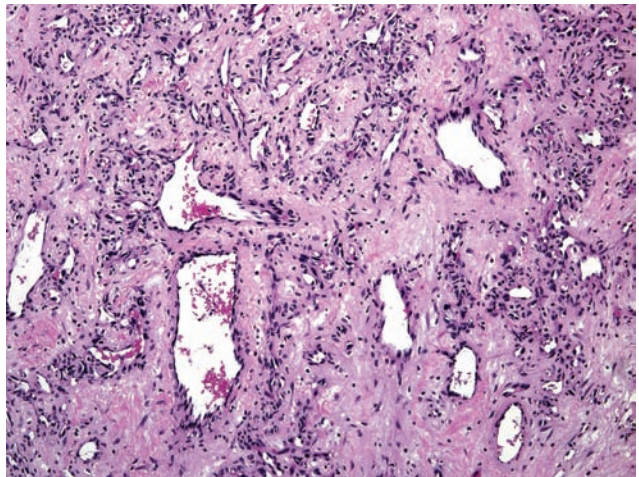


**FIGURE 6.4.6** Areas of the lesion with thin-walled vessels as the dominant histologic feature.

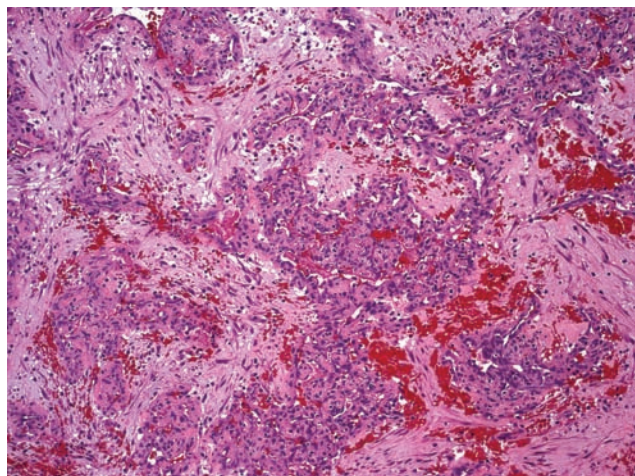


FIGURE 6.4.7 Endothelial hyperplasia.

ond most common site (1). Clinically, LCHs of the nose are often confused with polyps, papilloma, and even angiofibroma (1). Histologically, the differential diagnosis includes granulation tissue; antrochoanal polyp (ACP); rarely, angiofibroma; and sinonasal-type hemangiopericytoma. Granulation tissue practically never shows capillary lobules. On the other hand, ulcerated surface of the LCH may show granulation tissue underlying fibrinopurulent exudate. These areas comprise only a minor component of the LCH and show capillaries that tend to be oriented perpendicular to the surface.

The ACP usually arises in the maxillary sinus and extends in dumbbell fashion through the antral ostium and middle meatus into the posterior choana (2,3). The length of the stalk connecting ACP to the maxillary sinus predisposes it to infarction. When resulting vascular proliferation is exuberant, ACP are referred to as angiomatous polyps (4). Antrochoanal polyp does not show lobular arrangement of the vessels.

Fibrotic stroma and irregular gaping thin-walled vessels can be seen in LCH. These findings raise the possibility of angiofibroma. However, angiofibroma occurs only in males and originates in the posterior lateral wall of the nasal cavity (5). Extensive capillary proliferation is rarely seen in angiofibroma. Even when present, capillary proliferation is never lobular and is usually associated with other secondary vascular changes induced by tumor embolization. In these cases, foreign embolization material can be seen within the vessels.

Sinonasal-type hemangiopericytomas are composed of ovoid short spindle cells forming fascicles and whorls. The vascular channels are fewer than in LCH and have “staghorn” configuration. Furthermore, the vessels of hemangiopericytoma are characterized by prominent hyalinization. Unlike LCH and soft tissue hemangiopericytomas, sinonasal-type hemangiopericytomas are negative for CD34 and other vascular markers (6).

## References

1. Mills SE, Cooper PH, Fechner RE. Lobular capillary hemangioma: the underlying lesion of pyogenic granuloma. A study of 73 cases from the oral and nasal mucous membranes. *Am J Surg Pathol.* 1980;4(5):470–479.
2. Heck WE, Hallberg OE, Williams HL. Antrochoanal polyp. *AMA Arch Otolaryngol.* 1950;52(4):538–548.
3. Sirola R. Choanal polyps. *Acta Otolaryngol.* 1966;61(1):42–48.
4. Batsakis JG, Sneige N. Choanal and angiomatous polyps of the sinonasal tract. *Ann Otol Rhinol Laryngol.* 1992;101(7):623–625.
5. Harrison DF. The natural history, pathogenesis, and treatment of juvenile angiofibroma. Personal experience with 44 patients. *Arch Otolaryngol Head Neck Surg.* 1987;113(9):936–942.
6. Thompson LD, Miettinen M, Wenig BM. Sinonasal-type hemangiopericytoma: a clinicopathologic and immunophenotypic analysis of 104 cases showing perivascular myoid differentiation. *Am J Surg Pathol.* 2003;27(6):737–749.

## 6.5

*Synovial Sarcoma*

## CLINICAL INFORMATION

“A 27-year-old woman presented with a 2-month history of the left neck mass. The mass is 3 × 3–cm, firm, painless, and with well-defined margins. CT scan showed the mass medial to the carotid artery sheath. Fine-needle aspiration of the mass showed dual population of epithelioid and spindle cells, raising the possibility of a cellular pleomorphic adenoma and an epithelial myoepithelial carcinoma. The surgical specimen was labeled as a *minor salivary gland tumor*. We have considered malignant adnexal tumor, possibly of eccrine glands or an unusual salivary gland tumor, such as a peculiar variant of an adenoid cystic carcinoma.”

## OPINION

Microscopically, the entire specimen is represented by the tumor, and the relationship between the tumor

and normal tissue is unclear. The neoplasm is biphasic. The predominant epithelial component is represented by cribriform glands with comedo-type necrosis (Figure 6.5.1). Some of the epithelial cells are columnar with sharp apical borders (Figure 6.5.2). The intraluminal material is mucicarminophilic (Figure 6.5.3). The spindled component consists of streaming cells with clear to eosinophilic cytoplasm and elongated wavy nuclei (Figure 6.5.4). Three mitoses per 10 high-power fields are identified. The reticulin stain easily differentiates between the epithelial and spindled components: the epithelioid component is essentially devoid of reticulin fibers (Figure 6.5.5). Immunohistochemically, the epithelial component is positive for cytokeratin CAM5.2 (Figure 6.5.6), epithelial membrane antigen, and pan-keratin, and the spindled part is highlighted by vimentin (Figure 6.5.7).

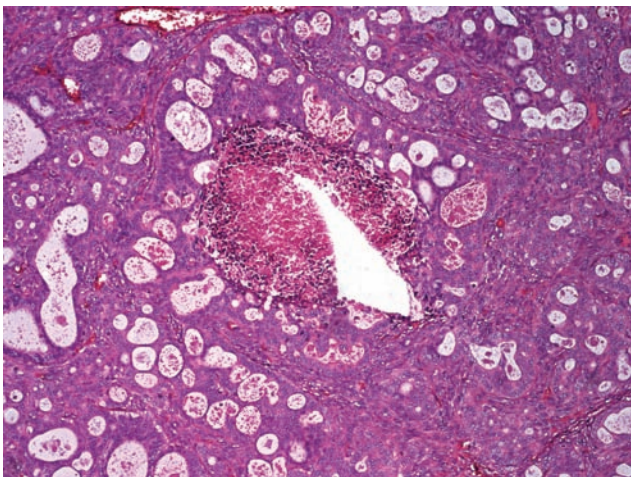


**FIGURE 6.5.1** Epithelioid component—cribriform glands with comedo-type necrosis.

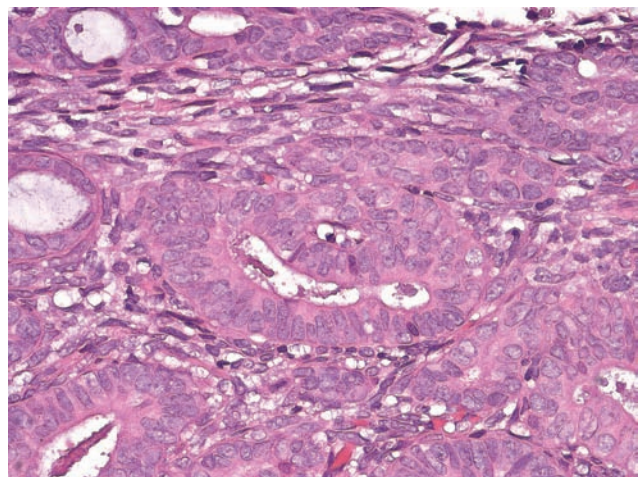


**FIGURE 6.5.2** Columnar cells forming gland structures surrounded by spindle cells.

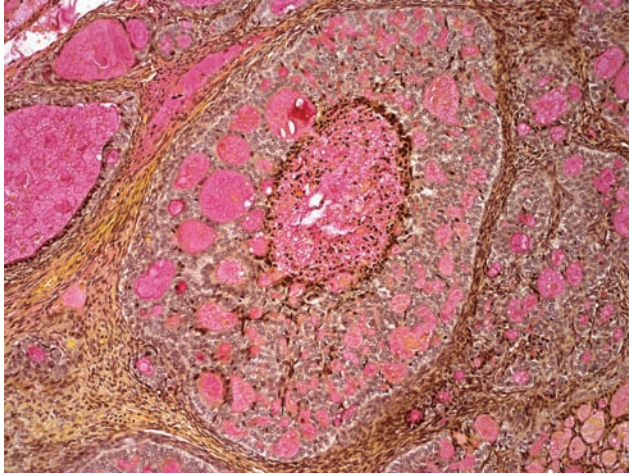


**FIGURE 6.5.3** Mucicarmophilic intraluminal secretions.

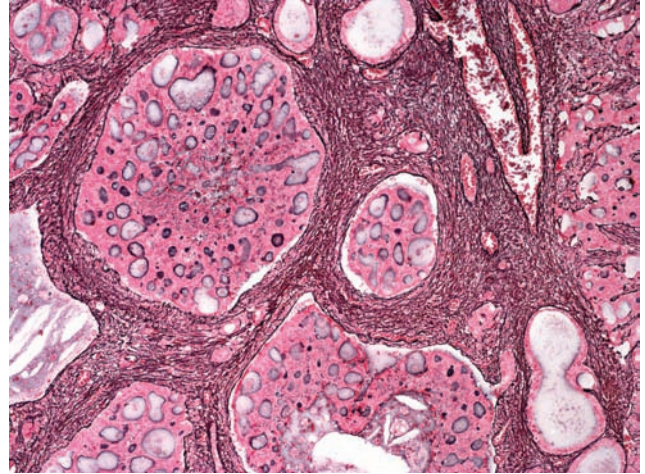


**FIGURE 6.5.5** Epithelioid component is devoid of reticulin fibers.

Immunostains for androgen receptor, S100, C-kit, cytokeratin 5/6, and p63 are all negative. Finally, in situ hybridization with dual-color break-apart probe for 18q11.2 region is positive for translocation in 97% of neoplastic cells.

### DIAGNOSIS

Neck mass, excision: Synovial sarcoma, biphasic.

### COMMENT

We believe the lesion is a synovial sarcoma (SS), biphasic type. Immunohistochemical stains and results of fluorescence in situ hybridization support the diagnosis of SS.

### DISCUSSION

The cribriform epithelioid component mimics some salivary type tumors and, more specifically, tumors

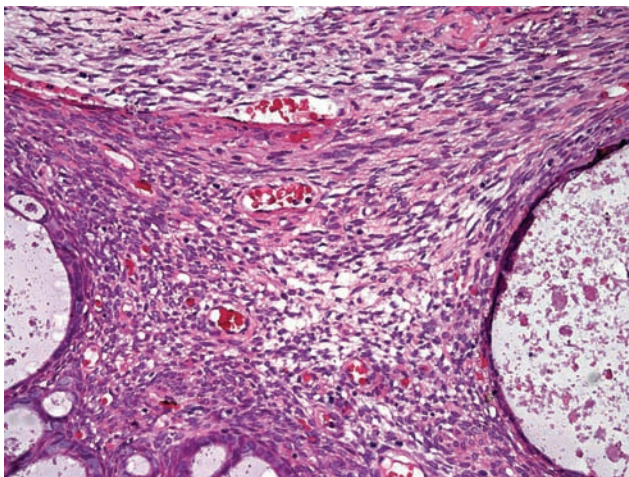


**FIGURE 6.5.4** Spindled component of the neoplasm.

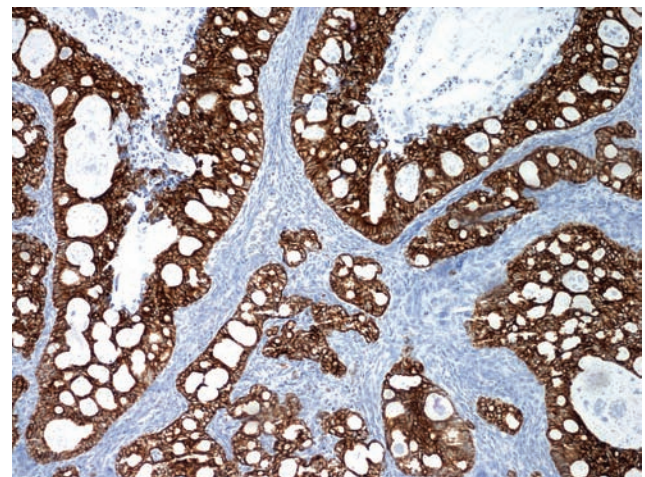


**FIGURE 6.5.6** Epithelial component highlighted by cytokeratin CAM5.2, immunohistochemistry.

## 6.5

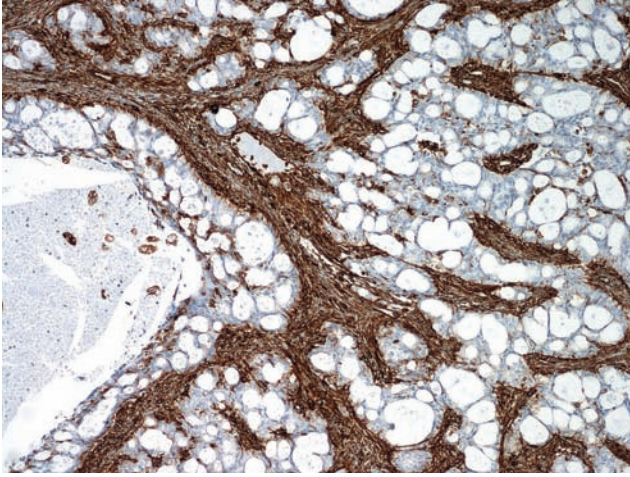


**FIGURE 6.5.7** Spindled component outlined by vimentin, immunohistochemistry.

with inner/luminal cell layer surrounded by an outer myoepithelial/basal layer. First, the cribriform pattern is associated with an adenoid cystic carcinoma (1). However, unlike adenoid cystic carcinoma, SS lacks the outer myoepithelial/basal layer with smaller hyperchromatic angulated nuclei. Accordingly, p63 is negative. The lack of basal/myoepithelial cells is

helpful in excluding another salivary-type neoplasm with dual cellular composition—epithelial-myoepithelial carcinoma. Secondly, back-to-back glands and comedo-type necrosis raise the possibility of a salivary duct carcinoma. However, salivary duct carcinoma is characterized by the cytologic changes of higher grade and generally lacks a spindled component. In addition, about 90% of salivary duct carcinomas are positive for androgen receptor.

Finally, the combination of histologic appearance, results of immunohistochemical studies, and the presence of t(x:18) is diagnostic of a biphasic SS (2,3).

### References

1. Chiosea SI, Peel R, Barnes EL, Seethala RR. Salivary type tumors seen in consultation. *Virchows Arch*. 2009;454(4):457–466.
2. Limon J, Dal Cin P, Sandberg AA. Translocations involving the X chromosome in solid tumors: presentation of two sarcomas with t(X;18)(q13;p11). *Cancer Genet Cytogenet*. 1986;23(1):87–91.
3. van de Rijn M, Barr FG, Collins MH, Xiong QB, Fisher C. Absence of SYT-SSX fusion products in soft tissue tumors other than synovial sarcoma. *Am J Clin Pathol*. 1999;112(1):43–49.

## 7 Bone Tumors

Essentially any lesion observed in long bones can also be found in the craniofacial-cervical skeleton. Among the more common ones seen in the head and neck include the various types of osteomyelitis, osteomas, fibrous dysplasia, ossifying fibroma, giant cell (reparative) granuloma, osteosarcoma chondrosarcoma, and chordoma.

Some of these lesions share overlapping histologic features, and, for this reason, one should never make a diagnosis without first reviewing the imaging studies. In some instances, the images may be more diagnostic than the histology and, especially so, when dealing with low-grade osteosarcomas.

Occasionally, both the biopsy and imaging studies are nondiagnostic, and a diagnosis of “benign or atypical fibro-osseous lesion” will be required. If the term *fibro-osseous lesion* is used as a diagnostic term, the pathologist should state in a comment what the problem is and what the differential diagnosis

includes. This is essential since some pathologists and clinicians often equate the term *fibro-osseous lesion* as synonymous to one of the following three lesions—fibrous dysplasia, cemento-osseous dysplasia, or ossifying fibroma.

Lastly, one must always be aware of chordoma. It is an epithelioid neoplasm that commonly involves the head and neck. Because it is positive for cytokeratin and epithelial membrane antigen, it can easily be confused for a carcinoma.

### Selected Readings

1. Atkins KA, Mills SE. Diseases of the bones and joints. In: Barnes L, ed. *Surgical Pathology of the Head and Neck*. 3rd ed. Informa Healthcare; 2009:951–996.
2. Regezi JA. Odontogenic cysts, odontogenic tumors, fibro-osseous, and giant cell lesions of the jaws. *Mod Pathol*. 2002; 15:331–341.
3. Slootweg PJ. Maxillofacial fibro-osseous lesions: classification and differential diagnosis. *Semin Diagn Pathol*. 1996; 13: 104–112.

## 7.1

## Central Giant Cell Granuloma

## CLINICAL INFORMATION

“26-year-old woman with a 2.5 × 5.0-cm radiolucent mandibular lesion crossing midline and eroding teeth.”

## OPINION

Radiographically, the tumor is a well-demarcated, round, radiolucent lesion of the left-mid anterior mandible with a scalloped rim showing tooth displacement and focal resorption (Figure 7.1.1). There is a fairly homogeneous fibrocellular proliferation that is fairly delineated from bony trabeculae (Figure 7.1.2). However, periphery of the lesion demonstrates secondary bone formation with pronounced osteoblastic activity (Figure 7.1.3). Microscopically, there are several embedded multinucleated giant cells containing approximately 2 to 10 nuclei. The mononuclear

cells in between the giant cells have more elongated tapered nuclei (Figure 7.1.4).

## DIAGNOSIS

Mandible, anterior, excision: Central giant cell granuloma.

## COMMENT

This represents a central giant cell granuloma (CGCG), historically designated as giant cell reparative granuloma and more recently labeled as *central giant cell lesion*. This is a radiolucent, well-demarcated giant cell–rich spindle cell proliferation of the anterior mandible.

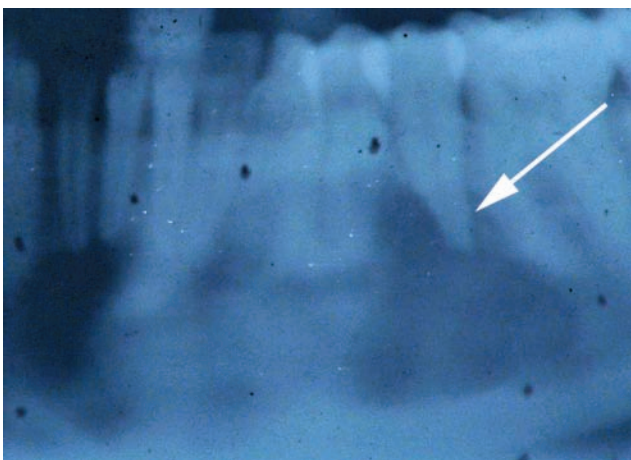


**FIGURE 7.1.1** Panoramic radiograph showing a well-circumscribed lytic lesion with a scalloped border. Tooth resorption is noted (arrow).

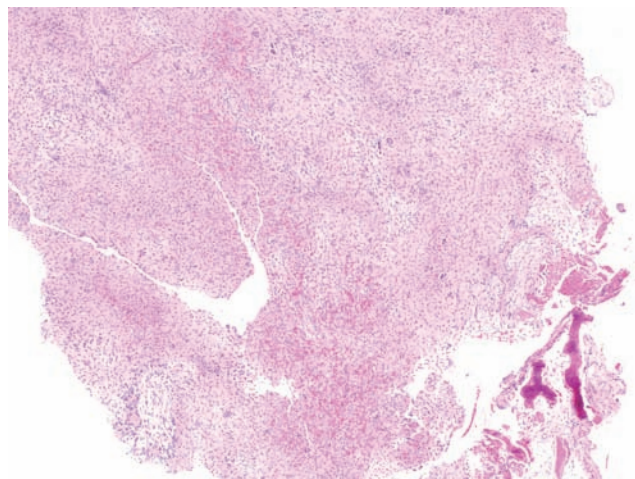


**FIGURE 7.1.2** The lesion is a fairly homogeneous spindle cell proliferation with scattered bony trabeculae on the periphery.

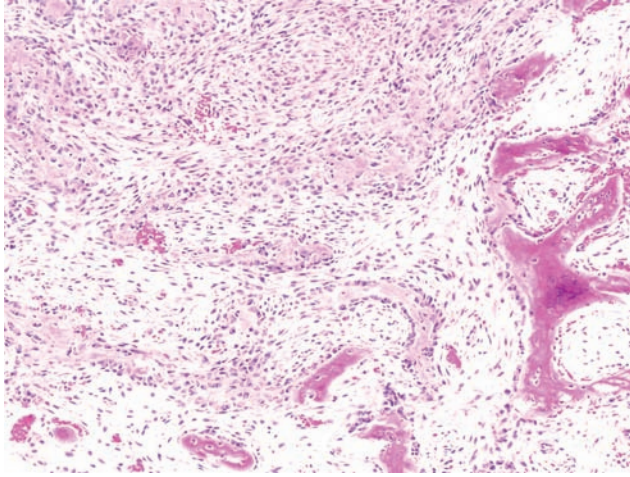


**FIGURE 7.1.3** Osteoblastic activity and secondary bone formation are noted in the periphery of the lesion.

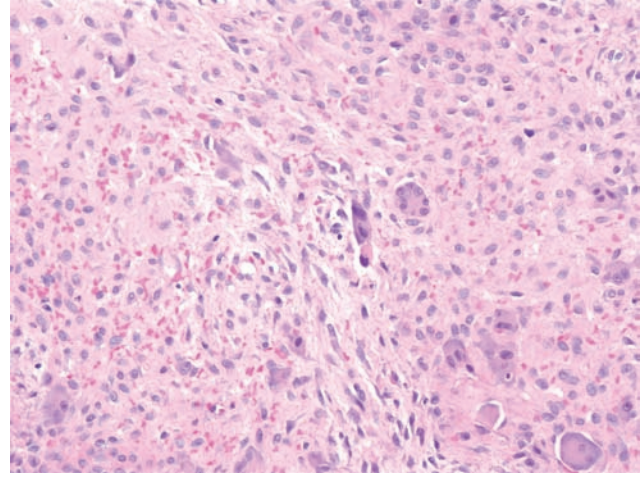


**FIGURE 7.1.4** Embedded within the lesion are numerous osteoclast-like giant cells containing approximately 2 to 10 nuclei per cell. The stroma contains a bland mononuclear spindle cell proliferation with longer more tapered nuclei.

## DISCUSSION

Central giant cell granuloma is considered a reactive osteolytic fibroproliferative growth containing numerous osteoclast-like giant cells. Secondary changes such as hemorrhage and reactive bone formation are quite common.

Central giant cell granuloma typically occurs in individuals between the second and fourth decades with a slight female predilection. The mandibular bones are more frequently involved. Grossly, CGCG consist of friable brown tissue with varying degrees of grittiness depending on the amount of secondary ossification. Histologically, the lesion consists of a mononuclear spindle cell proliferation with small osteoclast-like giant cells, typically with no more than 10 nuclei. There are also varying degrees of hemosiderin deposition, mixed inflammation, and ossification (1,2).

Several entities with histologic findings identical to CGCG need to be excluded clinically. These conditions often show multiple or multifocal giant cell lesions, which may be a useful discriminating factor from primary CGCG. Although currently rare, the so-called brown tumor of hyperparathyroidism is a form of secondary CGCG that needs to be correlated with ele-

vated parathormone and/or calcium levels. Cherubism is a childhood hereditary autosomal dominant disease (with *SH3BP2* mutations) characterized by symmetric swelling of all four jaw quadrants. Here, perivascular collagen cuffing has been noted to be unique to cherubism (1,2). Finally, neurofibromatosis type 1 has been reported in association with CGCG-like lesions, some of which can be quite aggressive (3).

Another perhaps controversial distinction is between CGCG and true giant cell tumor of the jaw. Giant cell tumors are quite rare in the jaw craniofacial region. Classically, these are distinguished by the larger giant cells with more nuclei, a more even distribution, and a mononuclear stromal cell component that has more ovoid vesicular nuclei morphologically similar to those of the multinucleated cells. Giant cell tumors of the bone have also recently been reported to be p63-positive (4). However, some CGCGs show considerable overlap with true giant cell tumor (GCT), suggesting that there may be a spectrum of disease in the jaw (5).

Treatment is primarily surgical, ranging from curettage to resection. However, the recurrence rate



## 7.1

is considerable ranging from 15% to 25% (5–7). It has been suggested that these recurrent tumors share morphologic features with true giant cell tumors of the bone, namely, larger giant cells and fraction of surface area occupied by giant cells, although in general, it is difficult to predict outcome based on histologic features alone (6,7).

### References

1. Regezi JA. Odontogenic cysts, odontogenic tumors, fibroosseous, and giant cell lesions of the jaws. *Mod Pathol*. 2002; 15(3):331–341.
2. Slootweg PJ. Lesions of the jaws. *Histopathology*. 2009; 54(4):401–418.
3. Edwards PC, Fantasia JE, Saini T, Rosenberg TJ, Sachs SA, Ruggiero S. Clinically aggressive central giant cell granulomas in two patients with neurofibromatosis 1. *Oral Surg Oral Med Oral Pathol Oral Radiol Endod*. 2006;102(6):765–772.
4. Dickson BC, Li SQ, Wunder JS, Ferguson PC, Eslami B, Werier JA, et al. Giant cell tumor of bone express p63. *Mod Pathol*. 2008;21(4):369–375.
5. Auclair PL, Cuenin P, Kratochvil FJ, Slater LJ, Ellis GL. A clinical and histomorphologic comparison of the central giant cell granuloma and the giant cell tumor. *Oral Surg Oral Med Oral Pathol*. 1988;66(2):197–208.
6. Chuong R, Kaban LB, Kozakewich H, Perez-Atayde A. Central giant cell lesions of the jaws: a clinicopathologic study. *J Oral Maxillofac Surg*. 1986;44(9):708–713.
7. Whitaker SB, Waldron CA. Central giant cell lesions of the jaws. A clinical, radiologic, and histopathologic study. *Oral Surg Oral Med Oral Pathol*. 1993;75(2):199–208.

## 7.2

## Chordoma

## CLINICAL INFORMATION

“A 41-year-old woman with a clival mass.”

## OPINION

Microscopically, tumor consists of a proliferation of clear, epithelioid cells embedded in a myxoid stroma (Figure 7.2.1). The cells are arranged in cords and have heavily microvacuolated or “physaliferous” appearance (Figure 7.2.2). In some areas, these cells show a macrovacuolated “signet ring” appearance (Figure 7.2.3).

The tumor cells are positive for cytokeratin AE1/AE3 (Figure 7.2.4), S100 protein (Figure 7.2.5), and brachyury (Figure 7.2.6).

## DIAGNOSIS

Clivus, biopsy: Chordoma, conventional type.

## COMMENT

This represents a chordoma of the clivus. Although many, if not most, chordomas are of the chondroid type in this region, this tumor is of the “classic” or conventional type that is typically seen in the sacral region. Mitoses are absent, and solid areas comprise less than 5% of this specimen. Cytologic atypia is only mild.

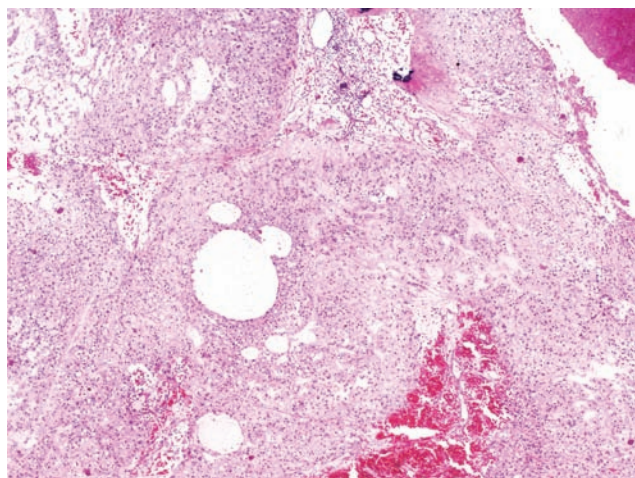


**FIGURE 7.2.1** Epithelioid proliferation of clear cells in myxoid stroma.

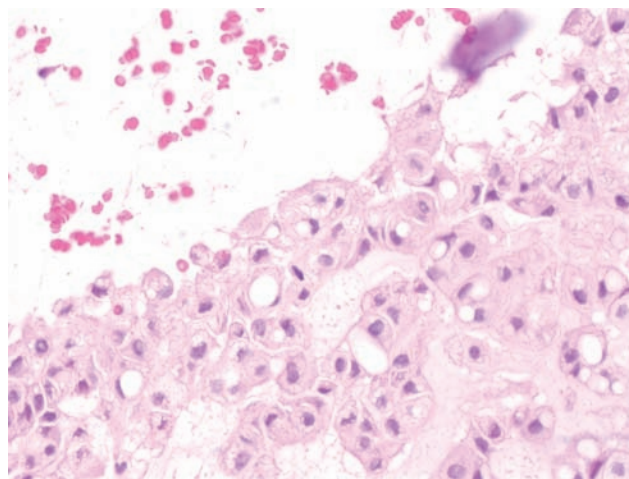


**FIGURE 7.2.2** Cells are arranged in cords and have a microvacuolated physaliferous appearance.

## 7.2

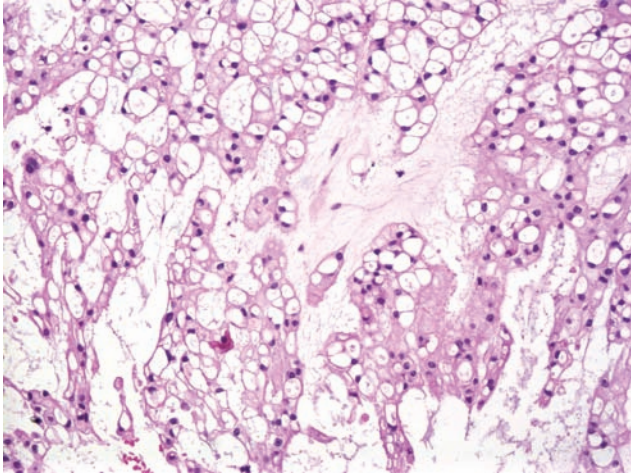


**FIGURE 7.2.3** Other cells have a macrovacuolated signet ring appearance.

## DISCUSSION

Skull base chordomas comprise about one third of all chordomas (1). As in their sacral counterparts, these tumors are composed of lobules of cells arranged in chords with microvacuolated physaliferous cytoplasm. When a specimen is relatively intact, fibrous septation of the lobules may be noted, although this is not as frequent a finding in clival tumors because they are often fragmented and tend to be much smaller. The stroma is very myxoid and often illicit a mixed inflammatory response.

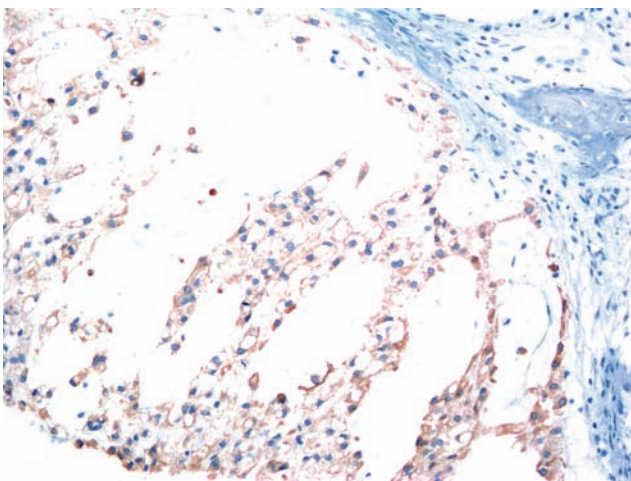


**FIGURE 7.2.4** Cytokeratin AE1/AE3 positivity.

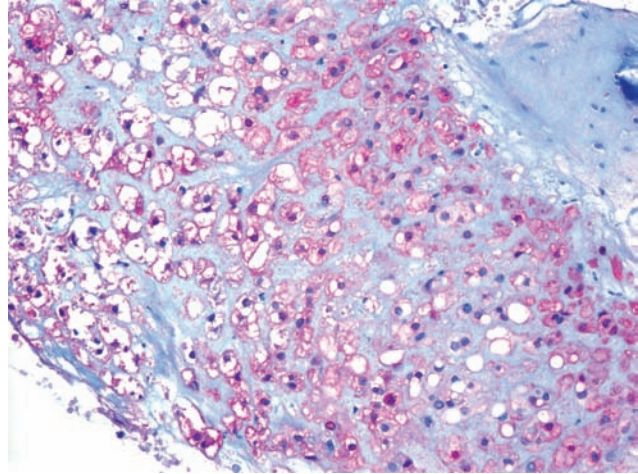


**FIGURE 7.2.5** S100 positivity.

Chordomas have a few variant morphologies, most notable of which is the chondroid subtype. The current consensus is that this histologic subtype is not related to chondrosarcoma and actually behave in a similar fashion to the conventional type (2). In the skull base region, the chondroid variant is frequent and in fact may predominate, present in 25% to 55% of all skull base lesions (3,4). Thus, this case is somewhat unusual in that it is purely of the conventional type on this biopsy.

Differential diagnostic considerations will vary depending on the histologic subtype. When the tumor

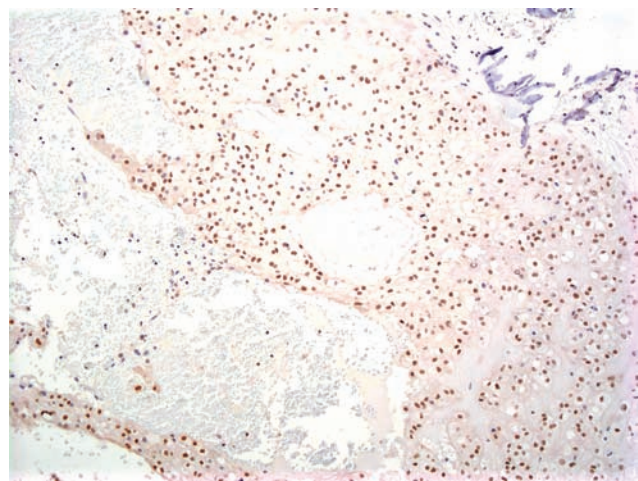


**FIGURE 7.2.6** Brachyury positivity.

is chondroid predominant, the main entity in the differential diagnosis is chondrosarcoma, particularly of the myxoid type. Skull base chondrosarcomas are far more indolent; thus, it is important to distinguish this from a chordoma (4,5). Unlike chordomas, chondrosarcomas typically have tumor cells with hyperchromatic nuclei with scant cytoplasm. Although they may show a lobular accentuation of cellularity, they do not have the corded appearance of chordomas. In addition, they do not have the same fibrous septation or inflammatory response seen in chordomas.

In difficult cases, immunohistochemical staining is helpful. Although both tumor types are S100-positive and SOX-9-positive, chordomas, which have notochordal phenotype, are also cytokeratin, epithelial membrane antigen, and brachyury (newly described transcription factor seen in notochord) expressions (4).

Occasionally, chordomas may have areas that are devoid of stroma, with tumor cells arranged in solid areas. Solid growth raises other differential diagnostic considerations, particularly clear cell tumors, such as myoepithelial carcinoma, metastatic renal cell carcinoma, and perhaps even a signet ring cell

adenocarcinoma, primary or metastatic. Although cytokeratin alone is sufficient to distinguish a chordoma from a chondrosarcoma, it would not be as useful in this setting. Thus, brachyury becomes quite useful because it will be negative in all the other entities. In addition, other phenotypic specific markers (ie, p63 and actin in myoepithelial carcinoma, RCC antigen in renal cell carcinoma) would be useful in the differential diagnosis (4).

### References

1. McMaster ML, Goldstein AM, Bromley CM, Ishibe N, Parry DM. Chordoma: incidence and survival patterns in the United States, 1973-1995. *Cancer Causes Control*. 2001;12(1):1-11.
2. Rosenberg AE, Brown GA, Bhan AK, Lee JM. Chondroid chordoma—a variant of chordoma. A morphologic and immunohistochemical study. *Am J Clin Pathol*. 1994;101(1):36-41.
3. Hoch BL, Nielsen GP, Liebsch NJ, Rosenberg AE. Base of skull chordomas in children and adolescents: a clinicopathologic study of 73 cases. *Am J Surg Pathol*. 2006;30(7):811-818.
4. Oakley GJ, Fuhrer K, Seethala RR. Brachyury, SOX-9, and podoplanin, new markers in the skull base chordoma vs chondrosarcoma differential: a tissue microarray-based comparative analysis. *Mod Pathol*. 2008;21(12):1461-1469.
5. Pamir MN, Ozduman K. Analysis of radiological features relative to histopathology in 42 skull-base chordomas and chondrosarcomas. *Eur J Radiol*. 2006;58(3):461-470.

## 7.3

*Ossifying Fibroma (Conventional Type)***CLINICAL INFORMATION**

“46-year-old woman with a right mid posterior intraosseous mandibular mass.”

**OPINION**

Radiographically, the tumor is a well-demarcated, round, radiolucent lesion with a sclerotic rim (Figure 7.3.1). The tumor appeared to have “shelled out” as 1 fragment (Figure 7.3.2). Microscopically, the tumor is composed of bland spindle cells with a fascicular to storiform growth pattern and focal calcifications (Figure 7.3.3). The calcifications are noted to be acellular, round, and lamellated compatible with cementicles (Figure 7.3.4).

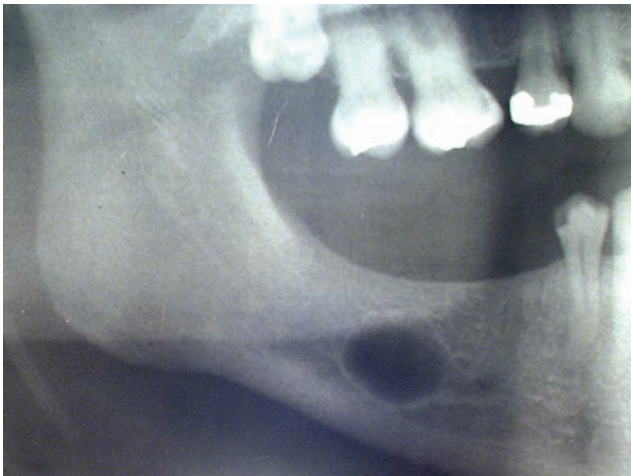


**FIGURE 7.3.1** Panoramic radiograph showing a well-circumscribed lytic lesion with a sclerotic rim.

**DIAGNOSIS**

Mandible, right mid posterior, excision: **Ossifying fibroma, conventional.**

**COMMENT**

This represents an ossifying fibroma (OF). This is a radiographically well-demarcated, radiolucent lesion with a sclerotic rim. The specimen appears as if it shelled out with ease, as it is largely intact. This is a storiform spindle cell proliferation with scattered cementicles and scant vasculature. The combination of radiographic, gross, and histologic findings supports

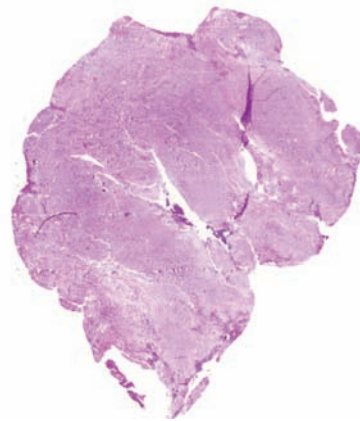


**FIGURE 7.3.2** The tumor was removed intact in 1 fragment.

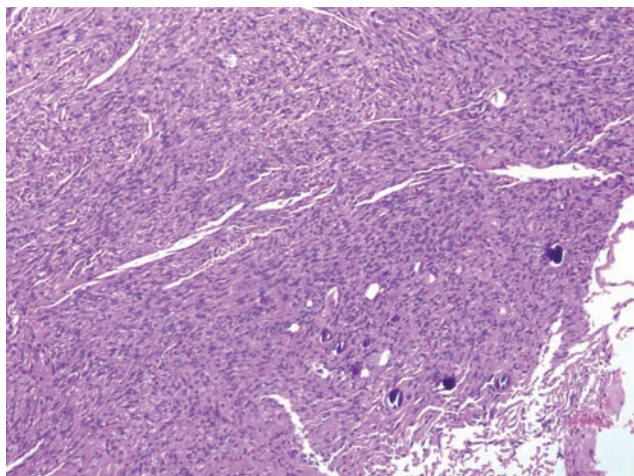


**FIGURE 7.3.3** The tumor is composed of spindle cells arranged in fascicles with calcifications (bottom right).

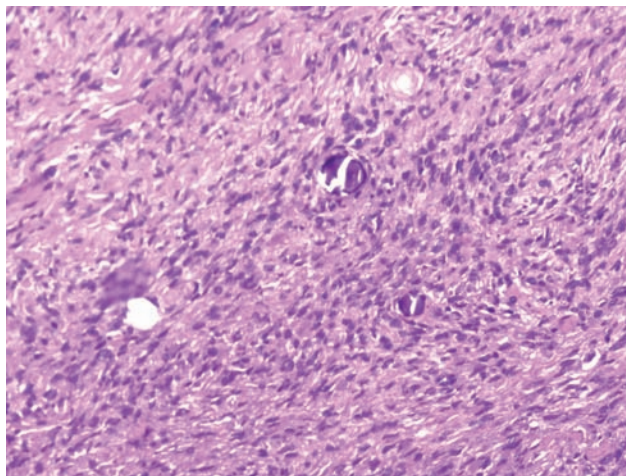


**FIGURE 7.3.4** The spindle cells are bland and monomorphic, and the calcifications are lamellar and acellular.

the above diagnosis. Based on location, size, age, and also histology, this is best considered a conventional OF or alternatively designated as a cementifying or cemento-ossifying fibroma.

### DISCUSSION

Ossifying fibroma is the neoplastic category of the benign fibro-osseous lesion (BFOL). The terms *OF*, *cementifying fibroma*, and *cemento-ossifying fibroma* are now considered to simply represent the histologic spectrum seen in OF (1,2).

Conventional OF typically occurs in individuals between the second and fourth decades with a female predilection of approximately 2.3:1. The classic presentation is that of a slow-growing, painless mass. These lesions are often sizeable (3–4 cm) on presentation. The mandible is the most common site (77%), specifically the molar and premolar regions. *The radiologic impression is critical to the diagnosis of all OFs.* On x-ray and computed tomography, conventional OF is a well-circumscribed, expansile mass that is distinct from the surrounding bone. For the mandibular lesion, there is often “bowing” of the inferior border. There is

often a rim of sclerotic bone. The center of the lesion ranges from lytic to mixed to sclerotic (1,2).

Intraoperatively, this lesion is typically quite easy to enucleate. Surgeons often describe the lesion as having shelled out in 1 piece, which is also an important diagnostic clue because other BFOLs will not typically do this. Grossly, conventional OFs are lobular with whorled homogenous tan, occasionally gritty cut surfaces with varying degrees of calcification. They are not characteristically hemorrhagic. Histologically, the stroma of conventional OF is mild to moderately cellular composed of bland relatively uniform fibroblast/myofibroblasts with ovoid to elongated nuclei with delicate smooth nuclear membranes and vesicular chromatin. The cells are often arranged in a storiform or whorled pattern. Mitoses are scarce to absent. Embedded in the stroma are deposits of matrix that range from well-formed bony trabeculae to acellular cementum-like deposits. Osteoblastic rimming is often present but not a requisite for the diagnosis. Osteoclasts/Osteoclast-like giant cells can be present but are not a prominent finding. Juvenile OF tend to be more aggressive and more cellular than conventional OF. There are two major histologic

## 7.3

subtypes: juvenile trabecular OF, which is characterized by delicate woven trabeculae of bone and osteoid merging with the surrounding fibrous stroma, and juvenile psammomatoid OF, which is characterized by numerous acellular lamellated “cementum-like” calcifications.

The main differential diagnostic considerations include other BFOL, namely, fibrous dysplasia and osseous dysplasia. *It is critical to note that none of these BFOL can be resolved by histologic features alone—these require incorporation of radiographic and clinical data.* Fibrous dysplasia is distinguished from OF by its “ground glass” radiographic appearance and lack of concentric (rounded) growth or demarcation. Histologically, fibrous dysplasia shows characteristic C- or S-shaped delicate woven trabeculae. However, unlike classic long bone fibrous dysplasia, craniofacial fibrous dysplasia may show osteoblastic rimming and cementum-like ossification, thus histologically mimicking other BFOLs (3). One useful histologic feature in fibrous dysplasia is that it merges with the adjacent surrounding normal cortex.

Osseous dysplasia, particularly focal osseous dysplasia, may overlap with OF because they occur

in similar locations and both are well demarcated. However, focal osseous dysplasia is typically a disease of African American women in their fourth to fifth decade. In addition, these lesions rarely grow more than 2 cm and are often incidental findings. Intraoperatively, unlike OF, these lesions are adherent to the adjacent normal bone and are quite hemorrhagic and usually extirpated as multiple fragments. Histologically, there is significant overlap with OF precluding definitive distinction without radiographs and clinical data; however, osseous dysplasias tend to be more vascular than OF (4).

### References

1. Alawi F. Benign fibro-osseous diseases of the maxillofacial bones. A review and differential diagnosis. *Am J Clin Pathol.* 2002;118 Suppl:S50–S70.
2. Brannon RB, Fowler CB. Benign fibro-osseous lesions: a review of current concepts. *Adv Anat Pathol.* 2001;8(3):126–143.
3. Jundt G. Fibrous dysplasia. In: Barnes EL, Eveson JW, Reichart P, Sidransky D, eds. *World Health Organization Classification of Tumours: Pathology & Genetics. Head and Neck Tumours.* Lyon: IARC Press; 2005:321–322.
4. Su L, Weathers DR, Waldron CA. Distinguishing features of focal cemento-osseous dysplasia and cemento-ossifying fibromas. II. A clinical and radiologic spectrum of 316 cases. *Oral Surg Oral Med Oral Pathol Oral Radiol Endod.* 1997;84(5):540–549.

---

## 8 Endocrine Tumors

The thyroid is the third most frequent specimen that we receive for second opinion. The problems associated with the interpretation of follicular-derived thyroid neoplasms are legendary, and the diagnoses rendered are often opinionated, subjective, controversial, and lack consensus.

Another book in the Consultant Pathology Series will be devoted to endocrine organs, only a few cases are presented in this section.

### Selected Readings

1. Ghossein R. Problems and controversies in the histopathology of thyroid carcinomas of follicular cell origin. *Arch Pathol Lab Med* 2009; 133: 683–691.
2. Nikiforov YE, Biddinger PW, Thompson LDR. *Diagnostic Pathology and Molecular Genetics of the Thyroid. A Comprehensive Guide for Practicing Thyroid Pathology*. Wolters Kluwer/Lippincott Williams and Wilkins, Philadelphia, 2009.
3. DeLellis RA, Lloyd RV, Heitz PU. *World Health Organization Classification of Tumours. Pathology and Genetics. Tumours of Endocrine Organs*. IARC Press, Lyon, 2004.



## 8.1

*Carcinoma Metastatic to the Thyroid Gland***CLINICAL INFORMATION**

“A 77-year-old woman presented with a 2.5-cm right thyroid mass. The fine-needle aspirate showed atypical follicular cells and clusters of lymphocytes. Right thyroid lobectomy was performed. Two foci suspicious for medullary carcinoma with unusual immunoprofile are identified. We would appreciate your opinion.”

**OPINION**

Histologic sections demonstrate 2 foci of solid and micropapillary growth, 0.3-cm and 0.4-cm, infiltrating between thyroid follicles (Figure 8.1.1). The neoplastic cells are enlarged and have abundant oncocyctic/apocrine cytoplasm and single prominent nucleolus (Figure 8.1.2). Areas of desmoplastic fibrosis mimic amyloid

deposits (Figure 8.1.3). Together with amphophilic (purple) cytoplasm and solid growth pattern (Figure 8.1.3), this appearance imitates medullary carcinoma.

Several additional intravascular tumor deposits are noted (Figures 8.1.4 and 8.1.5). Intravascular invasion is seen both in the perithyroidal soft tissue and within the thyroid gland. Most of the foci of vascular invasion are seen in sections away from the 2 main tumor deposits. The following features are identified in this case and help to differentiate true vascular invasion from “knife floaters”: (a) the clusters of tumor cells conform to the shape of invaded vessels; (b) tumor cells are attached to the endothelial lining and are intermingled with red blood cells, fibrin, and neutrophils; and (c) intravascular tumor deposits

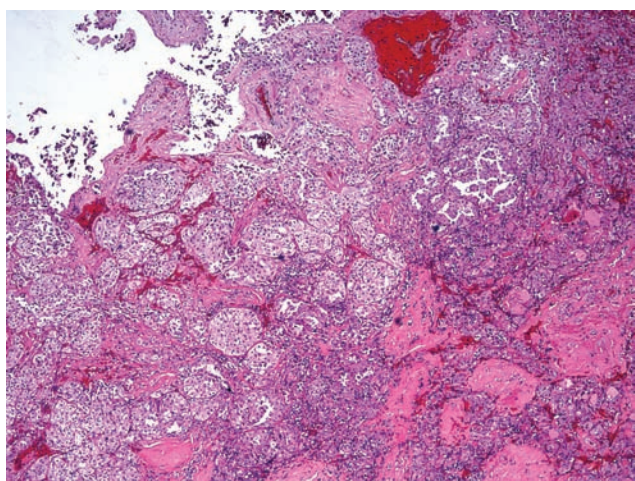


**FIGURE 8.1.1** Focus of neoplastic cells, forming solid nests and micropapillae and infiltrating thyroid tissue.

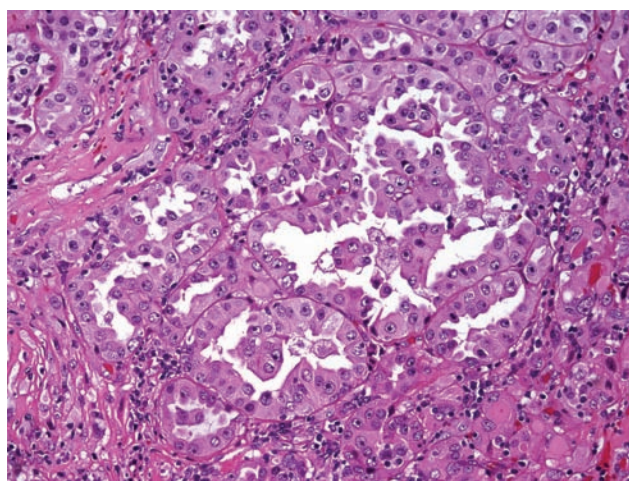


**FIGURE 8.1.2** Micropapillary and acinar-like growth of cells with prominent single nucleolus and abundant oncocyctic/apocrine cytoplasm.

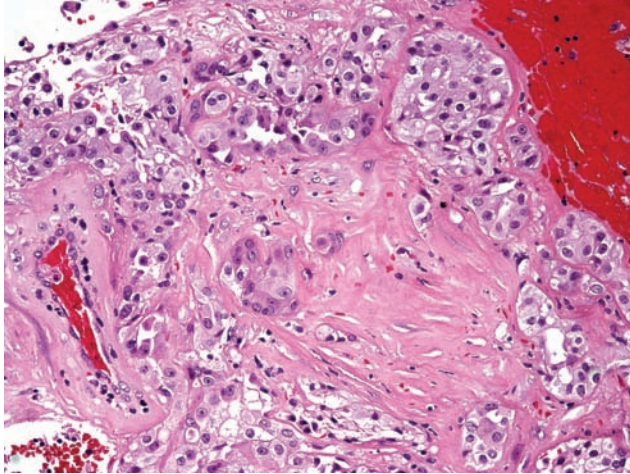


**FIGURE 8.1.3** Areas of fibrosis mimic amyloid deposits.

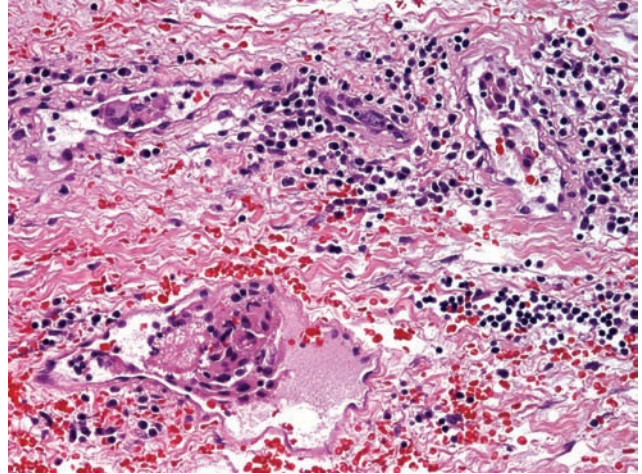


**FIGURE 8.1.5** Additional foci of vascular invasion.

are present in several tissue blocks/sections and are unrelated to the main tumor deposits. The pattern of invasion of the smaller vessels (Figure 8.1.5) may be described as “lymphangitic.”

Congo red histochemical stain is negative for amyloid. Immunohistochemically, the main (infiltrating) tumor foci are positive for thyroid transcription factor 1 (TTF-1), cytokeratin 7, and carcinoembryonic antigen and are negative for calcitonin, synaptophysin, chromogranin, and thyroglobulin (Figs 8.1.6,

8.1.7, and 8.1.8). The calcitonin immunostain shows no C-cell hyperplasia. The hematoxylin and eosin presentation (ie, acinar-like structures, lymphangitic distribution) and immunoprofile are highly unusual for a primary carcinoma of the thyroid gland (including medullary carcinoma) and are suggestive of a metastatic carcinoma.

In an attempt to distinguish between primary thyroid carcinoma and metastatic lung adenocarcinoma, PAX-8 immunostain was performed (Figure

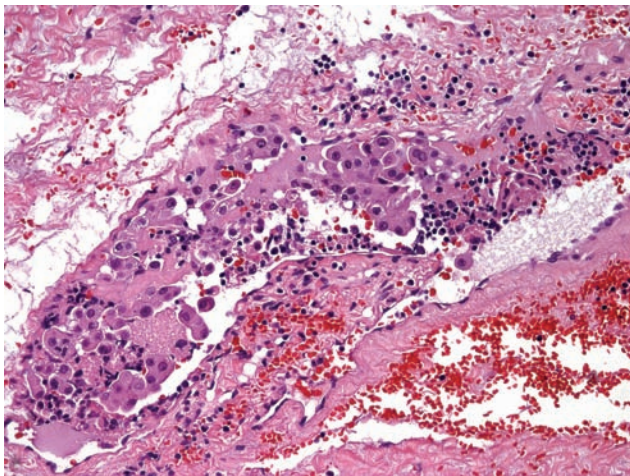


**FIGURE 8.1.4** The largest focus of vascular invasion is seen in perithyroidal soft tissue and is away from the main tumor deposits.

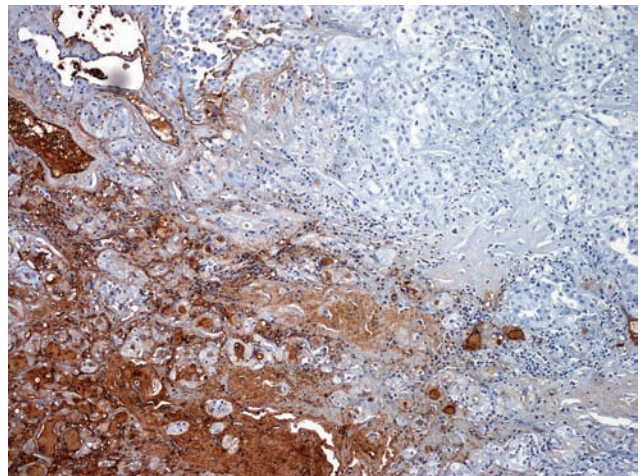
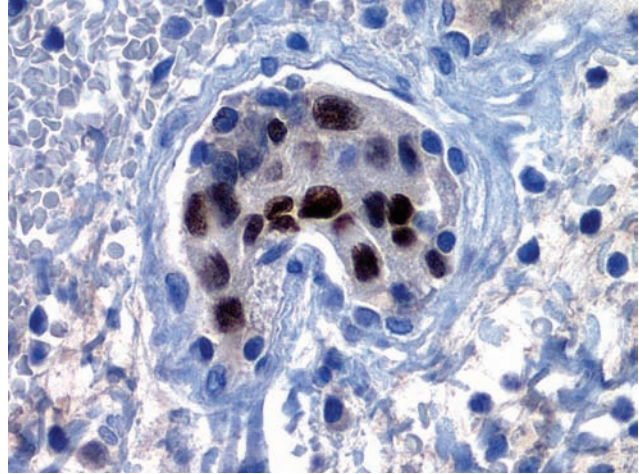
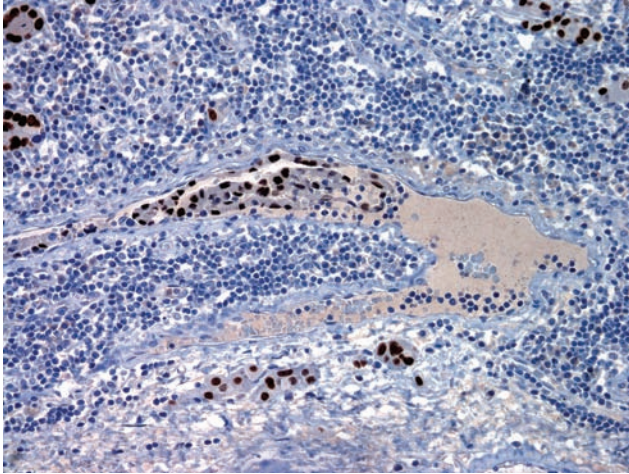


**FIGURE 8.1.6** Immunostain for thyroglobulin highlights normal thyroid tissue (left lower corner) and is negative in neoplastic cells (right upper corner).

## 8.1



**FIGURES 8.1.7 AND 8.1.8** Immunostain for thyroid transcription factor 1 highlights foci of vascular invasion.

8.1.9). PAX-8 was very weak in the neoplastic cells, suggesting a nonthyroidal origin. Surfactant protein A (SPA) (Figures 8.1.10 and 8.1.11) immunostain was positive. In contrast to normal adjacent thyroid tissue, the neoplastic cells were strongly positive for cytokeratin 20 (Figure 8.1.12). In addition, cytokeratin 7+/20+ immunoprofile raises the possibility of a metastatic ovarian carcinoma.

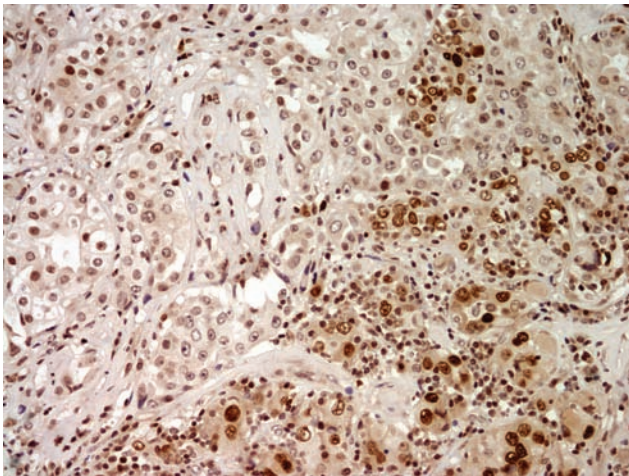


**FIGURE 8.1.9** Immunostain for PAX-8 highlights normal thyroid follicles (right half) and admixed lymphocytes (smaller nuclei, right half). The neoplastic cells (left half) are stained significantly weaker than normal adjacent thyroid tissue.

### DIAGNOSIS

Thyroid gland, right lobe, lobectomy: Multifocal intrathyroidal metastatic carcinoma, highly suspicious for metastatic lung or ovarian adenocarcinoma; chronic lymphocytic thyroiditis and nodular thyroid hyperplasia, with nodules up to 2.5-cm.

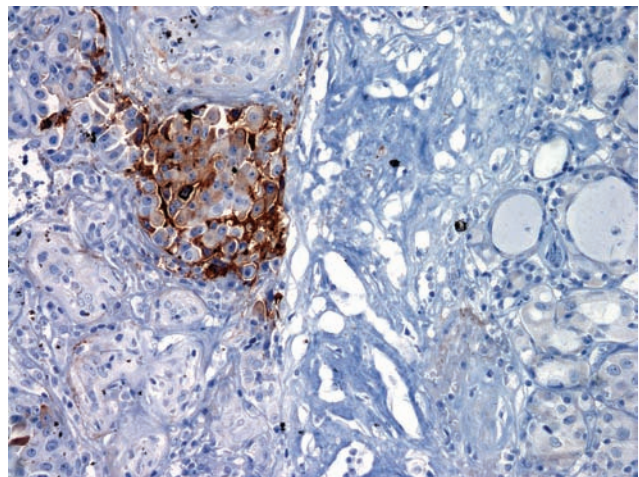


**FIGURE 8.1.10** Tumor cells express SPA.

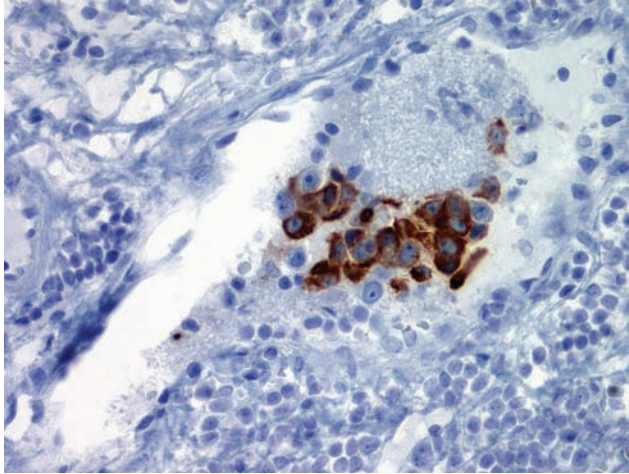


**FIGURE 8.1.11** Surfactant protein A immunostain highlights focus of vascular invasion.

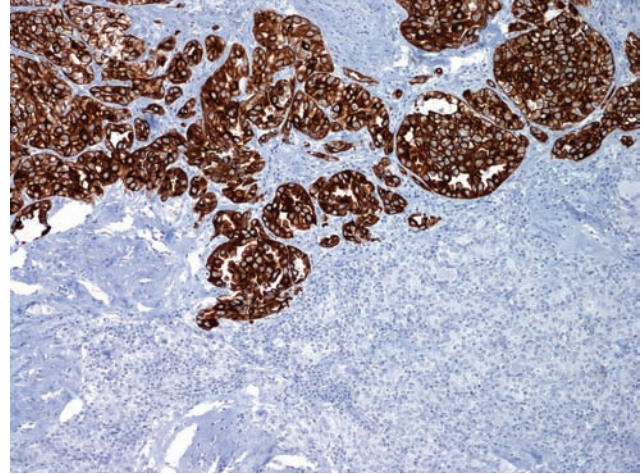


**FIGURE 8.1.12** Immunostain for cytokeratin 20 is strongly positive in tumor cells. Cytokeratin 20 positivity alone may be used as a strong argument against primary thyroid neoplasm.

### COMMENT

The diagnosis of an intrathyroidal metastatic carcinoma is based on the presence of multifocal vascular invasion, lack of hematoxylin and eosin features of any primary thyroid carcinoma, and immunoprofile of the neoplastic cells (positive for TTF-1, cytokeratin 7 and 20, carcinoembryonic antigen, and SPA, combined with negative thyroglobulin and very weak PAX-8). Negative calcitonin, chromogranin, and Congo red stains essentially rule out the diagnosis of medullary thyroid carcinoma.

The overall presentation is highly suspicious for intrathyroidal metastases from the lung primary adenocarcinoma. Positivity for cytokeratin 20 also raises the possibility of an ovarian primary adenocarcinoma. Clinical correlation with imaging studies of the thorax and pelvis is essential.

### DISCUSSION

Although the rich vascularity of the thyroid gland is predisposing it to metastases, metastases to the thyroid gland are still rare in clinical practice. In a review of all thyroidectomies performed at 1 institution of a

10-year period, Papi et al (1) showed the 0.13% prevalence of metastases to the thyroid. Elderly females are more frequently affected. Metastases to the thyroid have the same impact on prognosis as nonthyroidal metastases. The three most common primary sites are the kidney, the lung, and the breast.

The TTF-1 positivity can be seen in the thyroid gland and adenocarcinomas of the lung and ovary (2). Although SPA can be expressed in adenocarcinomas of the breast and colon (3), the combination of positive TTF-1 and SPA, along with negative thyroglobulin, is highly suggestive of lung primary.

More recently, PAX-8 was added to the list of immunostains distinguishing thyroid carcinomas (usually positive) from lung carcinomas (usually negative) (4).

### References

1. Papi G, Fadda G, Corsello SM, Corrado S, Rossi ED, Radighieri E, et al. Metastases to the thyroid gland: prevalence, clinicopathological aspects and prognosis: a 10-year experience. *Clin Endocrinol (Oxf)*. 2007;66(4):565–571.

---

## 8.1

2. Zhang PJ, Gao HG, Pasha TL, Litzky L, Livolsi VA. TTF-1 expression in ovarian and uterine epithelial neoplasia and its potential significance, an immunohistochemical assessment with multiple monoclonal antibodies and different secondary detection systems. *Int J Gynecol Pathol.* 2009;28(1):10–18.
3. Bejarano PA, Baughman RP, Biddinger PW, Miller MA, Fenoglio-Preiser C, al-Kafaji B, et al. Surfactant proteins and thyroid transcription factor-1 in pulmonary and breast carcinomas. *Mod Pathol.* 1996;9(4):445–452.
4. Nonaka D, Tang Y, Chiriboga L, Rivera M, Ghossein R. Diagnostic utility of thyroid transcription factors Pax8 and TTF-2 (FoxE1) in thyroid epithelial neoplasms. *Mod Pathol.* 2008;21(2):192–200.

## 8.2

*Mixed Medullary–Papillary Thyroid Carcinoma***CLINICAL INFORMATION**

“A 41-year-old man with a familial history of medullary thyroid carcinoma with thyroid enlargement and lymphadenopathy. Sixteen years later, the patient presents with additional lymphadenopathy.”

**OPINION**

Microscopically, the tumor consists of a predominantly solid infiltrative proliferation with abundant sclerosis and “waxy” refractile matrix compatible with amyloid (Figure 8.2.1). In most areas, the solid growth is composed of dyshesive cells with amphophilic cytoplasm and delicate nuclei (Figure 8.2.2). In other areas, the proliferation shows spindled morphology (Figure 8.2.3). Focally, there is an inter-

persed follicular pattern with colloid. The nuclei here are enlarged with cytoplasmic clearing and nuclear membrane irregularities (Figure 8.2.4). The lymph nodes excised 16 years later (Figure 8.2.5) show a metastasis with dual population of tumor cells as well (Figure 8.2.6).

A thyroglobulin stain shows positivity in the follicular patterned areas but not the solid areas (Figure 8.2.7). Conversely, the calcitonin stain shows positivity in the solid areas and not the follicular patterned areas (Figure 8.2.8). A PAX-8 stain is strongly positive in the follicular patterned areas and only focally weakly positive in the solid areas (Figure 8.2.9). An HBME-1 immunostain highlights apical membranous staining in the follicles (Figure 8.2.10).

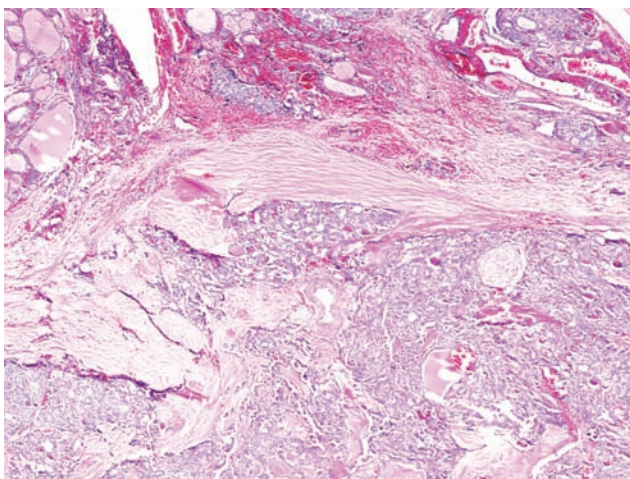


**FIGURE 8.2.1** An infiltrative predominantly solid tumor with sclerotic stroma and more eosinophilic “refractile” amyloid (bottom).

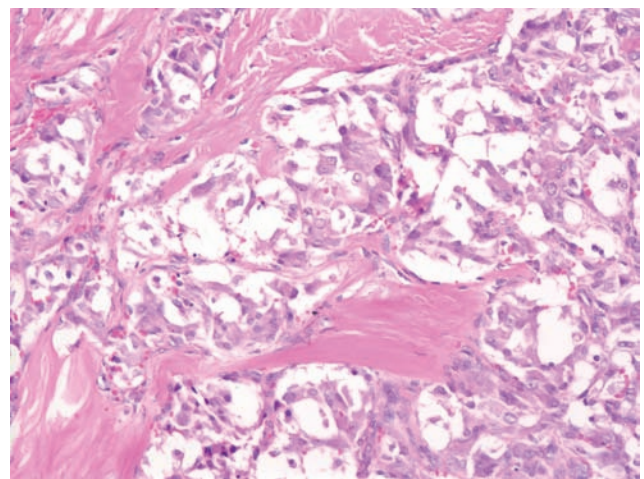


**FIGURE 8.2.2** Tumor nests consist of dyshesive cells with amphophilic cytoplasm.

## 8.2

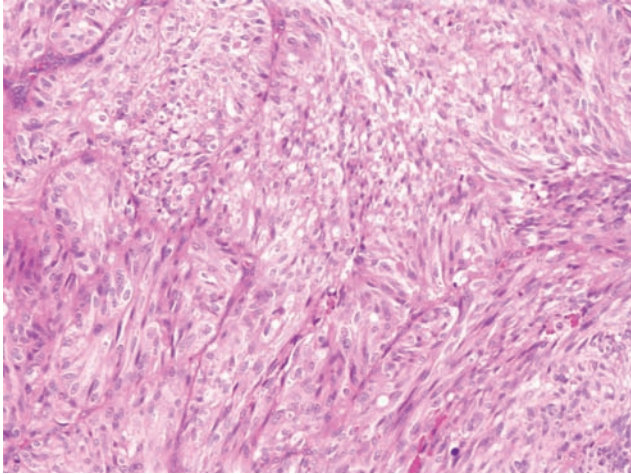


FIGURE 8.2.3 Spindled areas are present.

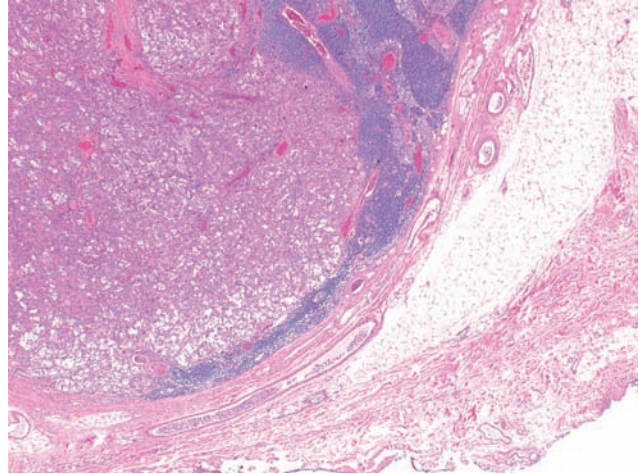


FIGURE 8.2.5 Lymph node metastasis 16 years later.

### DIAGNOSIS

Thyroid, total thyroidectomy: Mixed medullary-papillary thyroid carcinoma.

Lymph nodes, selective dissection: Metastatic mixed medullary-papillary thyroid carcinoma.

### COMMENT

This represents a mixed medullary-papillary thyroid carcinoma (MTC-PTC). Although many medullary thyroid carcinomas will contain thyroid follicles because of entrapment, the metastasis of both components to the lymph node confirms a true dual phenotype. In addition, the follicular patterned component had nuclear features of papillary thyroid carcinoma as confirmed by the HBME-1 immunostain.

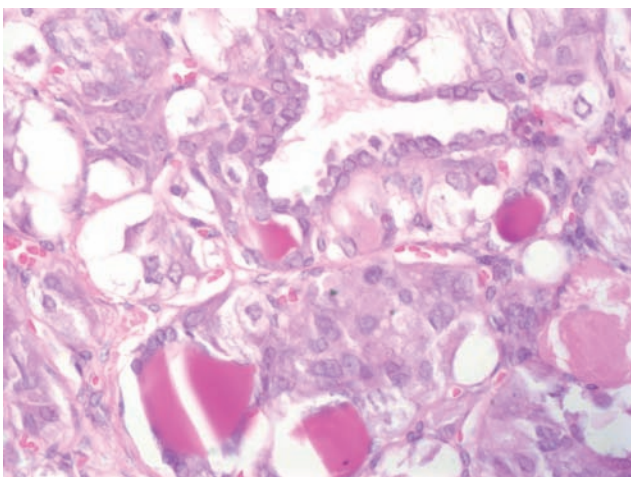


FIGURE 8.2.4 Admixed within these nests are follicular patterned areas with colloid. The nuclei show enlargement, clearing, overlap, and membrane irregularities.

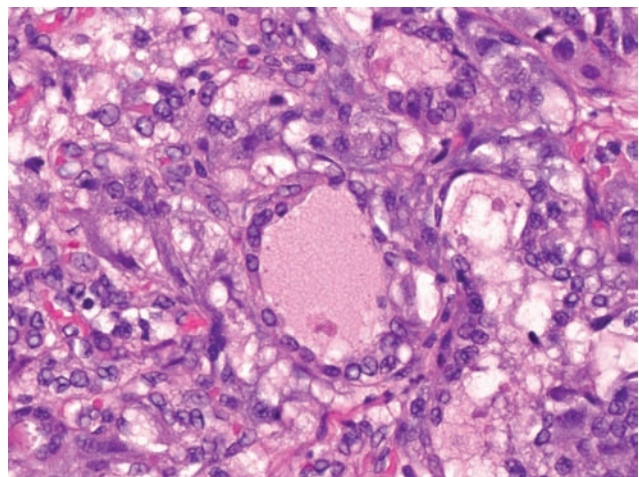
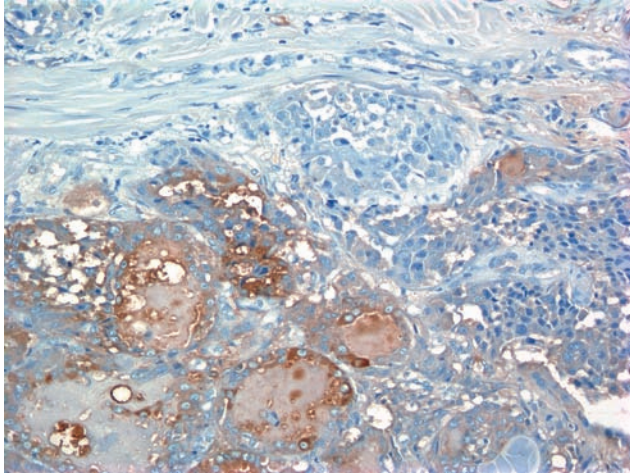


FIGURE 8.2.6 The metastasis also shows a dual population of cells with a follicular patterned component present.



**FIGURE 8.2.7** Follicular patterned areas (bottom) are thyroglobulin-positive.

### DISCUSSION

Thyroid tumors with mixed follicular and parafollicular cell differentiation are rare and poorly characterized. Most of these tumors are designated as mixed medullary-follicular carcinomas, although even within this category, the follicular component has nuclear features that are more compatible with follicular variant of papillary carcinoma (1).

The major differential diagnostic consideration is simple medullary thyroid carcinoma with normal

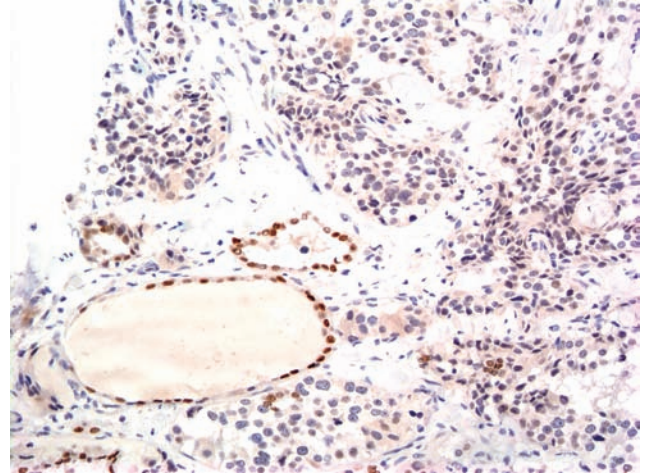


**FIGURE 8.2.9** Follicular patterned areas are more strongly PAX-8-positive than the solid areas.

or reactive thyroid follicle entrapment. However, the presence of both components in the metastasis, as well as the primary, is required to confirm the diagnosis of MTC-PTC. In addition, here, the follicles show nuclear features of papillary thyroid carcinoma and HBME-1 immunostaining to support this designation.

Another minor differential diagnostic consideration includes papillary thyroid carcinoma with

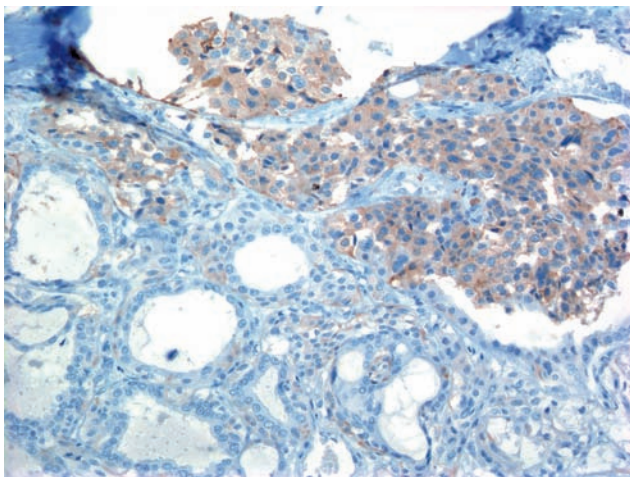


**FIGURE 8.2.8** Solid areas (top) are calcitonin-positive.

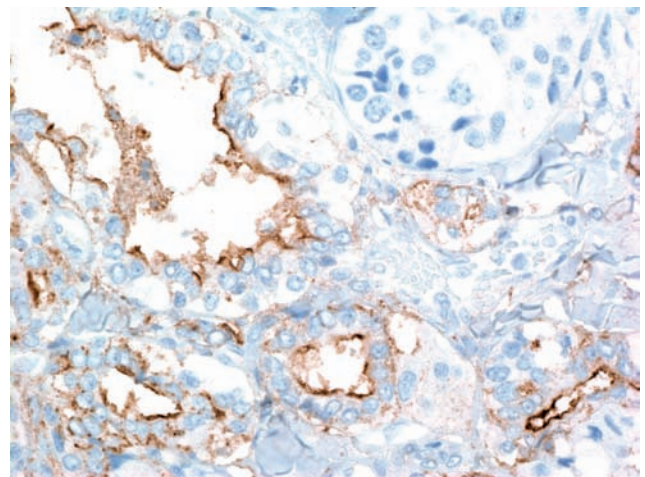


**FIGURE 8.2.10** Follicular areas show apical and membranous HBME-1 staining.



## 8.2

progression to poorly differentiated thyroid carcinoma. Poorly differentiated thyroid carcinoma, characterized by solid, trabecular, and insular growth, may show some overlap with medullary thyroid carcinoma; thus, when both a well-differentiated and poorly differentiated component are present, there may be some resemblance to MTC-PTC (2). However, poorly differentiated thyroid carcinomas tend to have scant cytoplasm, do not show as much single cell dyshesion, and do not show stromal amyloid. Furthermore, these tumors would not be positive for calcitonin but tend to be more strongly positive for PAX-8.

The nature or pathogenesis of MTC-PTC and other thyroid carcinomas of mixed phenotype is widely debated. Some believe that these tumors are truly biphenotypic and have suggested a stem cell derivation from ultimobranchial bodies (solid cell nests) because these have the potential to give rise to both C-cells and follicular cells (3,4). Others believe that these are “collision” tumors that happen to juxtaposed to one another. Support for this hypothesis stems from the observation that a medullary thyroid carcinoma and papillary thyroid carcinoma that are spatially distinct in the thyroid can show intermin-

gled metastases appearing as a mixed tumor. Molecular evidence to date suggests that both components are indeed clonally separate (5,6).

### References

1. Michal M, Curik R, Macak J, Ludvikova M, Dedic K. Mixed medullary-follicular and medullary-papillary carcinoma of the thyroid: one or two entities? *Zentralbl Pathol.* 1993;139(4-5): 333-335.
2. Volante M, Collini P, Nikiforov YE, Sakamoto A, Kakudo K, Katoh R, et al. Poorly differentiated thyroid carcinoma: the Turin proposal for the use of uniform diagnostic criteria and an algorithmic diagnostic approach. *Am J Surg Pathol.* 2007;31(8):1256-1264.
3. Williams ED, Toyn CE, Harach HR. The ultimobranchial gland and congenital thyroid abnormalities in man. *J Pathol.* 1989;159(2):135-141.
4. Lax SF, Beham A, Kronberger-Schonecker D, Langsteger W, Denk H. Coexistence of papillary and medullary carcinoma of the thyroid gland-mixed or collision tumour? Clinicopathological analysis of three cases. *Virchows Arch.* 1994;424(4):441-447.
5. Papotti M, Volante M, Komminoth P, Sobrinho-Simoes M, Bussolati G. Thyroid carcinomas with mixed follicular and C-cell differentiation patterns. *Semin Diagn Pathol.* 2000;17(2):109-119.
6. Volante M, Papotti M, Roth J, Saremaslani P, Speel EJ, Lloyd RV, et al. Mixed medullary-follicular thyroid carcinoma. Molecular evidence for a dual origin of tumor components. *Am J Pathol.* 1999;155(5):1499-1509.

## 8.3

*Paraganglioma of Thyroid*

## CLINICAL INFORMATION

“A 40-year-old man presented with a 2-year history of dyspnea on exertion. Imaging studies revealed a 5.7-cm left thyroid mass invading the trachea. Family history, clinical and biochemical data (thyroid function tests and serum calcium) are not available. Fine-needle aspiration was bloody and nondiagnostic. Total thyroidectomy with segmental tracheal resection with primary anastomosis was performed. Intraoperatively, a malignant process was favored. Immunohistochemically, thyroid transcription factor and calcitonin stains are negative. Thyroglobulin appears to be focally positive. Is this a poorly differentiated thyroid carcinoma or a medullary carcinoma?”

## OPINION

Histologic sections show a mass invading through the tracheal wall (Figure 8.3.1) and involving the thyroid gland (Figure 8.3.2). The border between the tumor and the thyroid is well defined. There is no capsule. About one fifth of the tumor is characterized by irregular fibrous bands (Figure 8.3.3). The permanent hematoxylin and eosin section of the frozen section remnant shows a solid growth of neoplastic cells (Figure 8.3.4). The neoplastic cells have abundant eosinophilic cytoplasm and random nuclear enlargement (Figure 8.3.5). Other aspects of the tumor show a “zellballen” arrangement typical of paraganglioma (PG) (Figure 8.3.6). There is no necrosis or mitoses. Immunohistochemically, the tumor is negative for cytokeratin. Thyroid transcription factor, PAX-8, and

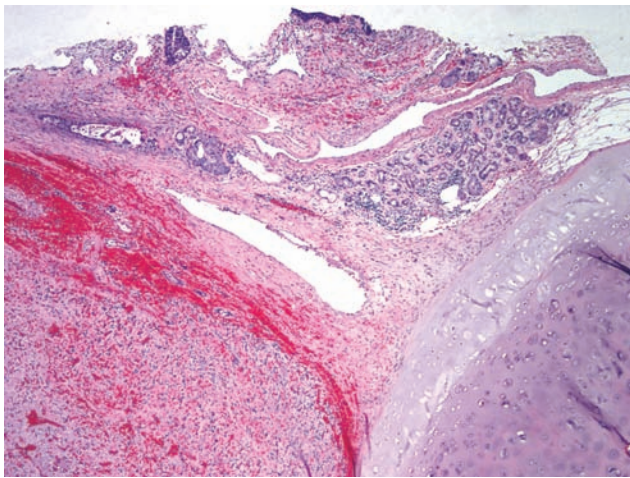


**FIGURE 8.3.1** Tumor invasion through the tracheal wall. Tracheal cartilage is in the right lower corner, and the tumor is in the left lower corner.

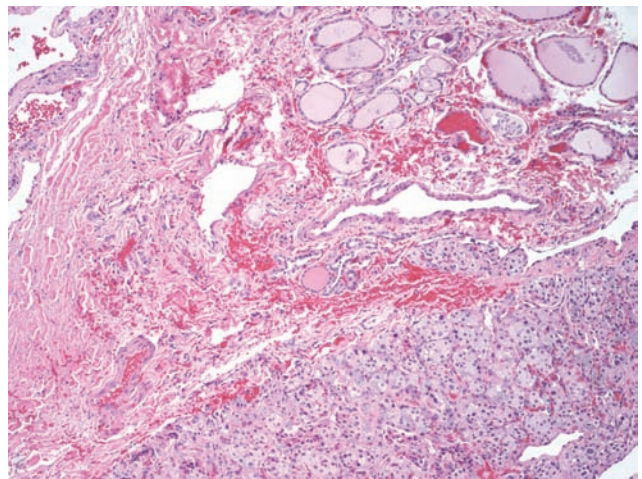


**FIGURE 8.3.2** Tumor involves the thyroid gland.

## 8.3

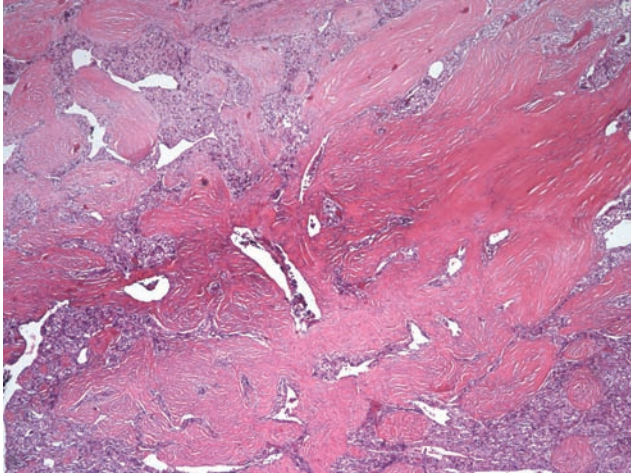


**FIGURE 8.3.3** Sclerosing areas of the tumor.

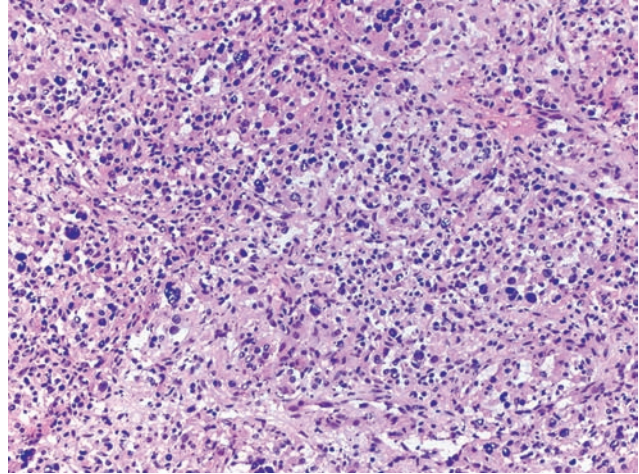


**FIGURE 8.3.5** Random nuclear atypia.

calcitonin are also negative. Thyroglobulin is positive in entrapped follicular thyroid cells. S100 highlights sustentacular cells and perineural invasion (Figure 8.3.7).

#### DIAGNOSIS

Total thyroidectomy (23 g) and segmental tracheal resection: Paraganglioma, 5.7-cm, with sclerosing features.

#### COMMENT

The diagnosis of thyroid PG is based on the presence of areas with characteristic zellballen pattern and results of immunostains. Negative stains for cytokeratin, thyroid transcription factor 1, and PAX-8 are against the possibility of a poorly differentiated thyroid carcinoma and medullary carcinoma.

#### DISCUSSION

Usually, PGs present at predictable anatomic locations, such as the carotid body, the jugulotympanic, or

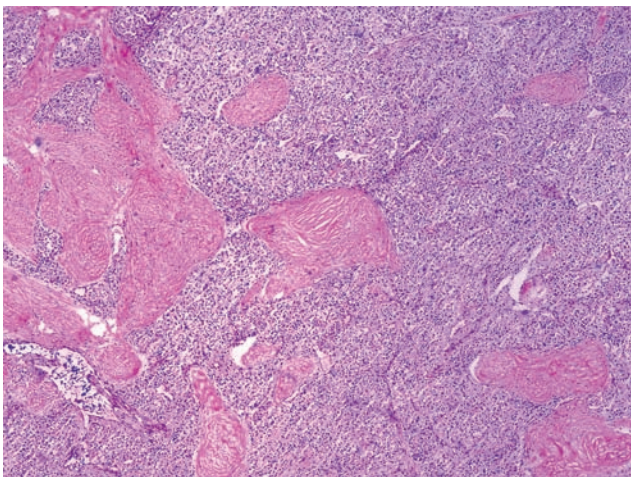


**FIGURE 8.3.4** Solid growth of neoplastic cells.

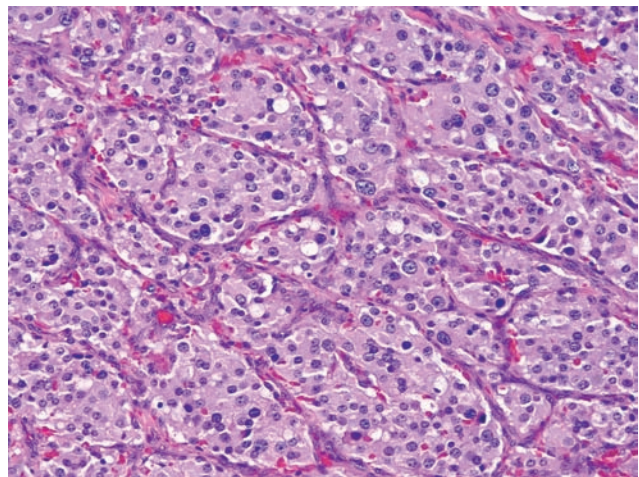


**FIGURE 8.3.6** Zellballen arrangement of PG.

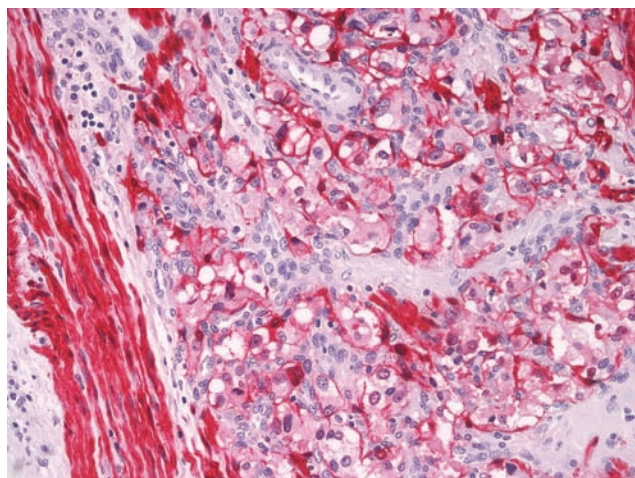


**FIGURE 8.3.7** The S100 immunostain highlights sustentacular cells.

the vagal ganglia. Paraganglioma involving the thyroid gland is rare with about only 20 cases reported in the English literature (1,2). Thyroid PG is especially rare in male patients—the present case may be only the fourth published case of a thyroid PG in a man.

This case highlights the following diagnostic challenges. Clinically, PGs are usually slow-growing and asymptomatic. Exceptionally, PGs are locally aggressive and may cause airway obstruction (3).

Paraganglioma are characterized by rich vascularity, and preoperative fine-needle aspirates are often

bloody and nondiagnostic. When lesional cells are present, they may be misinterpreted as primary thyroid neoplasm (2).

The PGs of the head and neck frequently show sclerosing foci (4). At the time of intraoperative evaluation, the combination of infiltrative growth, sclerosis, random nuclear pleomorphism, and lack of a zellballen arrangement may lead to the preliminary diagnosis of a malignant neoplasm.

Generous microscopic sampling and immunohistochemical studies are essential for rendering the correct diagnosis of PG.

### References

1. González Poggioli N, López Amado M, Yebra Pimentel MT. Paraganglioma of the thyroid gland: a rare entity. *Endocr Pathol.* 2009;20:62–65.
2. Yano Y, Nagahama M, Sugino K, Ito K, Kameyama K, Ito K. Paraganglioma of the thyroid: report of a male case with ultrasonographic imaging, cytologic, histologic, and immunohistochemical features. *Thyroid.* 2007;17(6):575–578.
3. Mukhopadhyay S, Naqvi AH, Su W, Landas SK. Airway-occlusive sclerosing paraganglioma presenting with dyspnea. *Am J Surg Pathol.* 2006;30(9):1206–1207.
4. Plaza JA, Wakely PE Jr, Moran C, Fletcher CD, Suster S. Sclerosing paraganglioma: report of 19 cases of an unusual variant of neuroendocrine tumor that may be mistaken for an aggressive malignant neoplasm. *Am J Surg Pathol.* 2006;30(1):7–12.

## 8.4

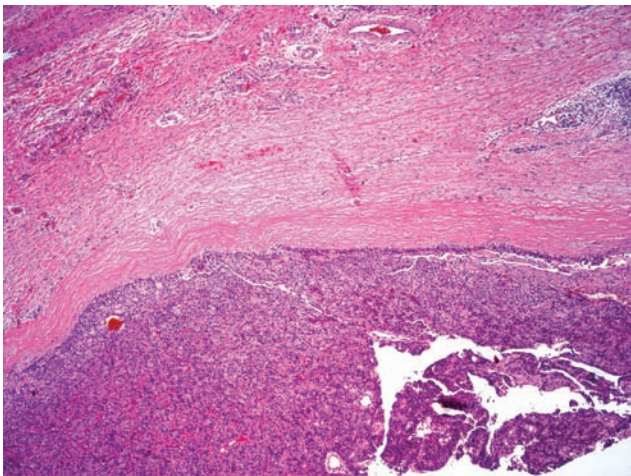
*Parathyroid Adenoma***CLINICAL INFORMATION**

“A 23-year-old woman presented with a 3-cm right lower neck mass. The fine-needle aspirate showed clusters of benign-appearing cells compatible with parathyroid tissue. Calcitonin immunostain is negative.” Additional clinical and functional (eg, serum calcium, parathyroid hormone levels) data were not available.

**OPINION**

Histologic sections demonstrate a well-circumscribed, enlarged, and hypercellular parathyroid gland. The entire gland is surrounded by a well-developed thick fibrotic capsule (Figure 8.4.1). Pericapsular areas of

hemosiderin deposits with reactive fibroblastic and endothelial cell proliferation are also seen (Figure 8.4.2). There is a single linear smooth defect in the capsule mimicking capsular invasion (Figures 8.4.3 and 8.4.4). Immunohistochemical stains for CD31 (Figure 8.4.5) and S100 show no evidence of vascular or perineural invasion. The protrusion of the parathyroid cells through the capsular defect is accentuated by the immunostain for parathyroid hormone (Figure 8.4.6). Otherwise, the overall contour of the parathyroid gland is smooth (no evidence of infiltrative growth pattern). The proliferative index (Ki67 immunostain) is mildly elevated (3% to 5%). No mitoses are identified.



**FIGURES 8.4.1** Well-circumscribed encapsulated parathyroid mass.

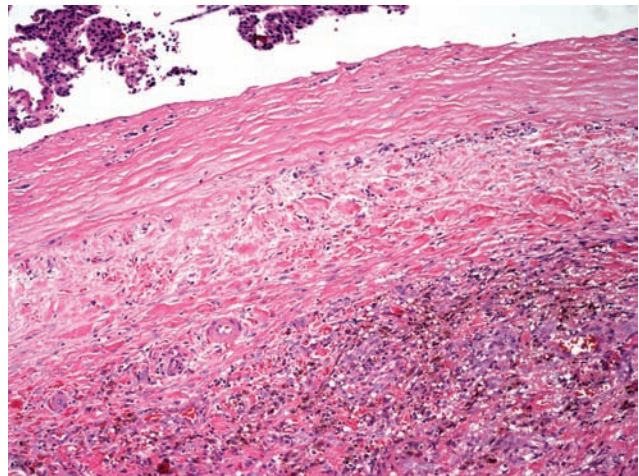


**FIGURE 8.4.2** Areas of hemosiderin deposition and vascular proliferation (granulation-like tissue) adjacent to the capsule.

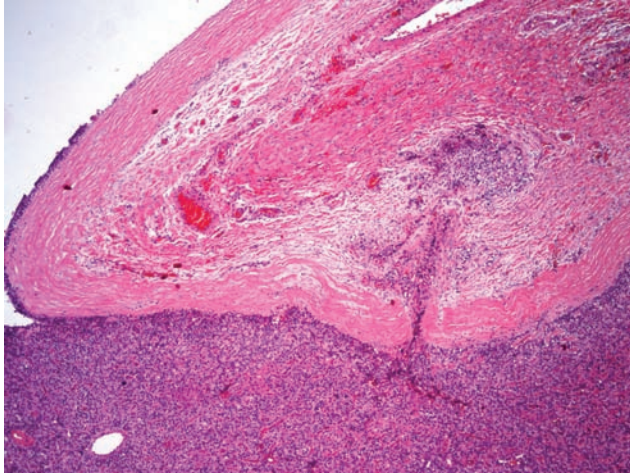


**FIGURE 8.4.3** Capsular pseudo-invasion induced by the FNA.

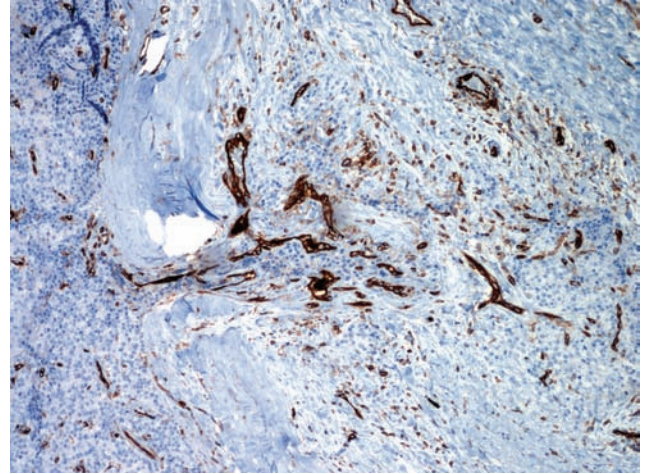


**FIGURE 8.4.5** CD31 immunostain highlights reactive vascular proliferation associated with the FNA-induced capsular perforation. Note linear arrangement of the vessels crossing the capsule.

#### DIAGNOSIS

“Right inferior parathyroid adenoma,” parathyroidectomy (1900 mg): Enlarged hypercellular parathyroid gland with solitary focus of capsular distortion, hemosiderin deposits, reactive fibroblastic and vascular proliferation, consistent with fine needle aspiration induced changes.

#### COMMENT

Histologic sections demonstrate an enlarged hypercellular encapsulated parathyroid gland. Because no other parathyroid glands are available for histologic examination, we are unable to distinguish between single-gland disease (ie, parathyroid adenoma) and multiglandular parathyroid hyperplasia. Correlation

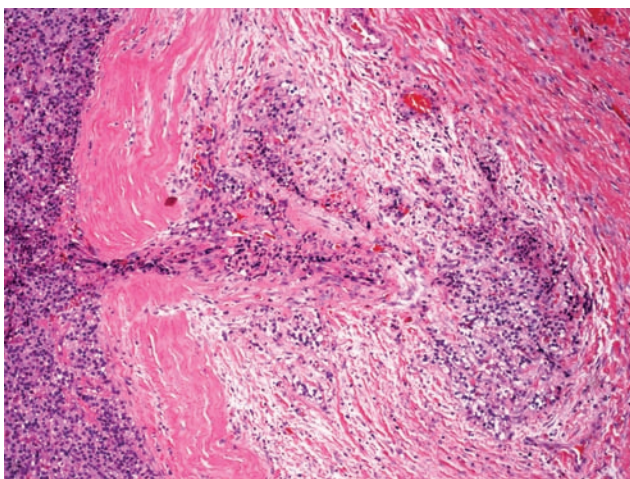


**FIGURE 8.4.4** Smooth, linear, narrow capsular defect.

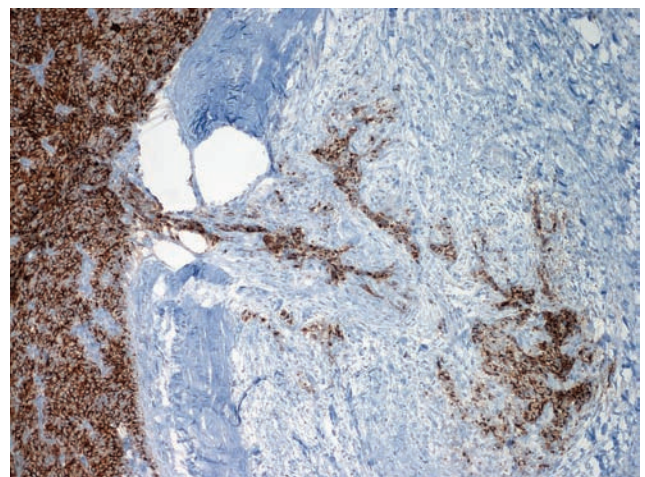


**FIGURE 8.4.6** Immunostain for parathyroid hormone highlights parathyroid cells protruding through the capsular defect.

## 8.4

with intraoperative parathyroid hormone levels is suggested.

We believe the solitary capsular defect represents the fine-needle penetration site. There is no evidence of true capsular, vascular, or perineural invasion.

### DISCUSSION

Although fine-needle aspiration (FNA) is a common diagnostic tool for evaluation of thyroid nodules, it is rarely used for preoperative workup of the parathyroid lesions. Worrisome histologic alterations fol-

lowing FNA of the thyroid (1) are well described in the thyroid gland, for example, mimics of capsular or vascular invasion, reactive fibroblastic proliferation, infarction. This case illustrates that the histologic criteria used to distinguish true capsular invasion from FNA-induced capsular “pseudo-invasion” in follicular lesions of the thyroid are also applicable to encapsulated parathyroid lesions.

### Reference

1. LiVolsi VA, Merino MJ. Worrisome histologic alterations following fine-needle aspiration of the thyroid (WHAFFT). *Pathol Annu.* 1994;29(Pt 2):99–120.

---

## 9 Miscellaneous Lesions

**A**lthough most of our consults deal with tumors, either primary or secondary, we also see a wide assortment of nonneoplastic lesions. These include hamartomas, cysts, systemic diseases manifesting in the head and neck, and a variety of inflammatory-

infectious conditions. Some of these cases are presented in this section.

### Selected Reading

1. Barnes L. *Surgical Pathology of the Head and Neck*. 3rd ed. New York: Informa Healthcare; 2009.



## 9.1

*Branchial Cleft Cyst—Carcinoma*

## CLINICAL INFORMATION

“Please find enclosed slides from a mass removed from the left neck of a 50-year-old man. This gentleman presented with a solitary mass in a location characteristic of a branchial cleft cyst; it was anterior to the sternocleidomastoid. He reportedly has no evidence of a mucosal lesion of the nasopharynx or oropharynx on careful examination, and this is the only lesion identified by CT scan. The scan showed an approximately 2.5-cm solid and cystic mass. Prior fine-needle aspiration was negative for malignancy. I would be most grateful if you could help me with classification of this lesion. To me it has features of a fairly poorly differentiated squamous cell carcinoma. Given the history of a lack of a primary elsewhere, I wonder if this could be arising as a primary tumor in a branchial cleft remnant.”

## OPINION

Sections show a lymph node almost totally replaced by a metastatic, non-keratinizing squamous cell carcinoma. The tumor is arranged in ribbons and solid aggregates with interspersed cysts, some of which contain intracystic papillary projections of tumor (Figures 9.1.1, 9.1.2, 9.1.3, and 9.1.4).

The tumor cells are mitotically active throughout all layers and are frequently permeated by mature lymphocytes (Figures 9.1.5 and 9.1.6).

The cells contain mildly vesicular to hyperchromatic nuclei with occasionally small nucleoli. The cytoplasm varies from light pink to basophilic. Large, round, vesicular nuclei with prominent “viral-like” nucleoli, which are characteristic of undifferentiated nasopharyngeal carcinoma, are not seen.

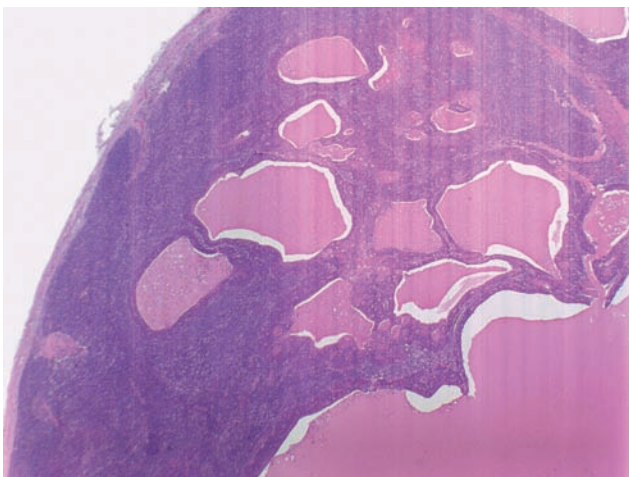


**FIGURE 9.1.1** The lymph node contains a cystic nonkeratinizing squamous cell carcinoma.

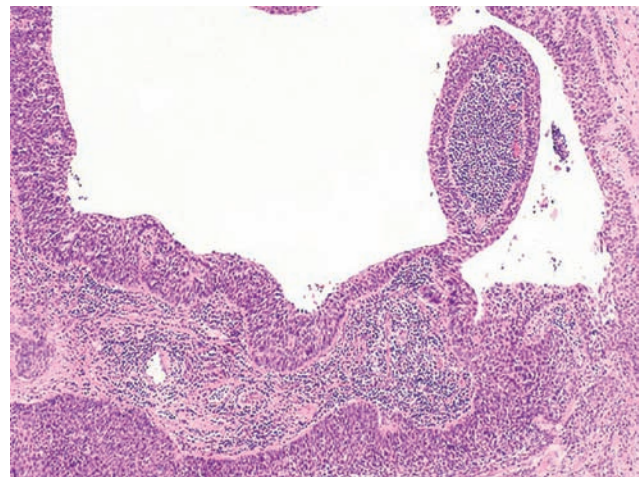


**FIGURE 9.1.2** Intracystic papillary projections of tumor are common.

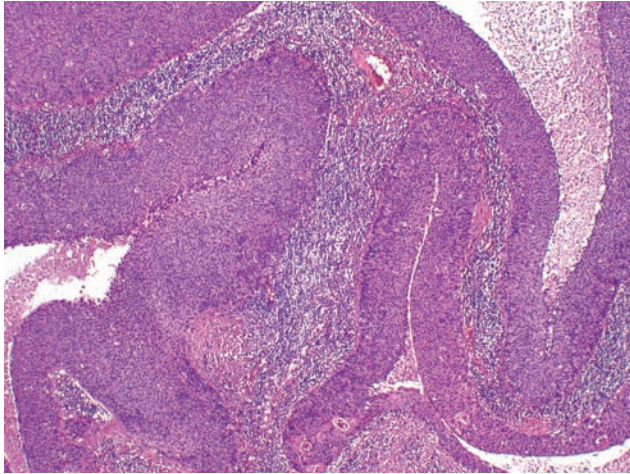


**FIGURE 9.1.3** Ribbon-like arrangement of tumor cells.

In some areas, the tumor cells “line” the cystic spaces and are well demarcated from the stroma creating the false impression that this may be an in situ carcinoma arising in a cyst (Figure 9.1.4). Closer inspection, however, reveals there are no basement membranes separating the tumor from the stroma. Moreover, solid aggregates of tumor can be seen in the stroma adjacent to the cysts (Figure 9.1.4). See “Comment” section for additional features.

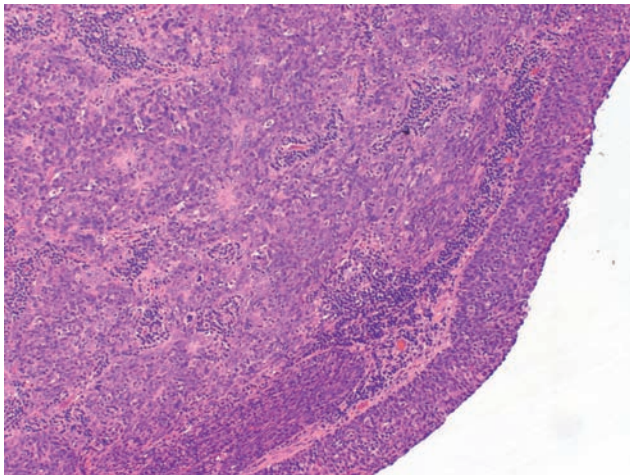


**FIGURE 9.1.4** Solid aggregates of tumor cells adjacent to cyst. Tumor cells lining the cysts are often well demarcated from the stroma creating the false impression of in situ carcinoma arising in a cyst.

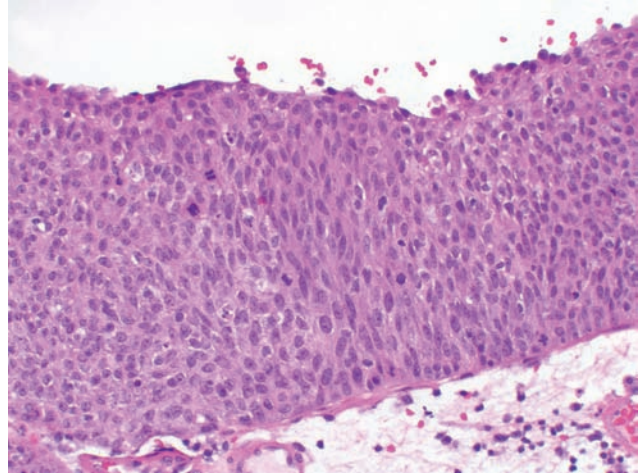


**FIGURE 9.1.5** High-power of cyst lining shows nonkeratinizing squamous cell carcinoma. Note mitoses throughout all layers.

#### DIAGNOSIS

Mass, left neck, excision: Lymph node with metastatic squamous cell carcinoma, nonkeratinizing type, with cystic changes.

#### COMMENT

We believe that this lesion represents a lymph node with metastatic squamous cell carcinoma of the

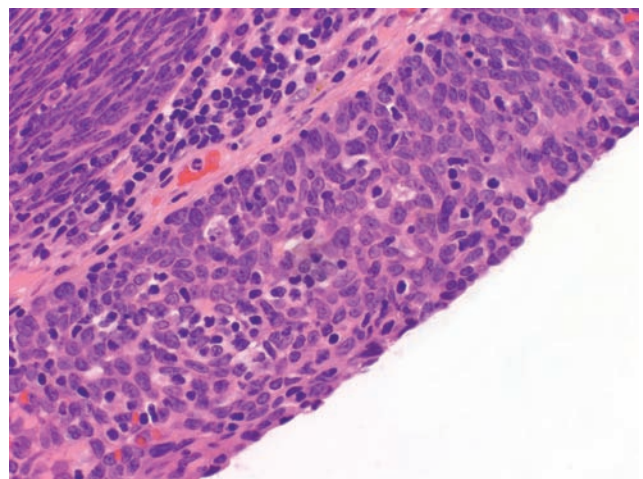


**FIGURE 9.1.6** Lymphocytes often permeate the tumor.

## 9.1

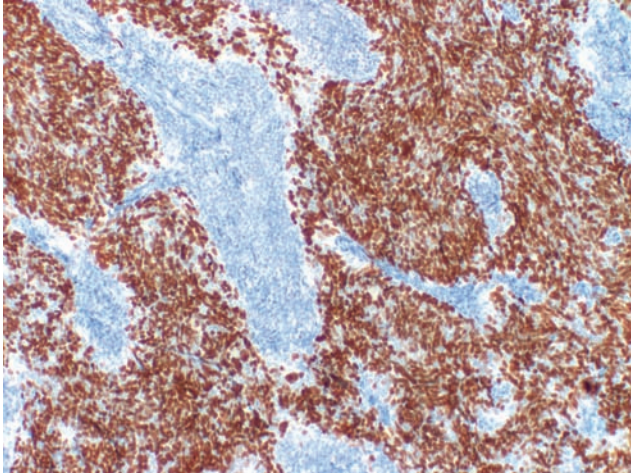


**FIGURE 9.1.7** Solid aggregates of tumor cells in wall of cysts are strongly positive for cytokeratin (CAM 5.2).

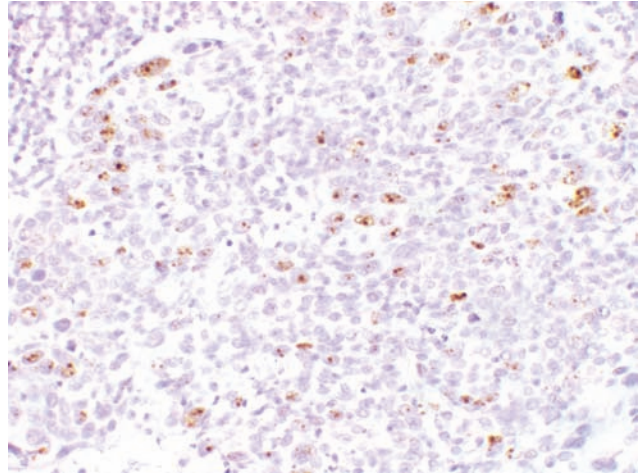


**FIGURE 9.1.9** Tumor is positive for human papillomavirus by in situ hybridization.

nonkeratinizing type. The tumor is positive for p63, CAM 5.2, pan-keratin, and p16 (Figures 9.1.7 and 9.1.8). By in situ hybridization, it is also positive for human papillomavirus and negative for Epstein-Barr virus (Figure 9.1.9).

These findings strongly suggest a squamous cell carcinoma arising in the oropharynx. We recommend a diagnostic tonsillectomy on the same side as the patient's adenopathy. Tonsillar biopsies are virtually useless given that these tumors tend to arise

deep within the tonsillar crypts. It is also incumbent upon the pathologist to entirely submit the tonsillar tissue, as these tumors are often very small and may be missed by routine sections.

Although the tonsil is the most likely site of origin, the base of the tongue should also be considered as a potential primary site.

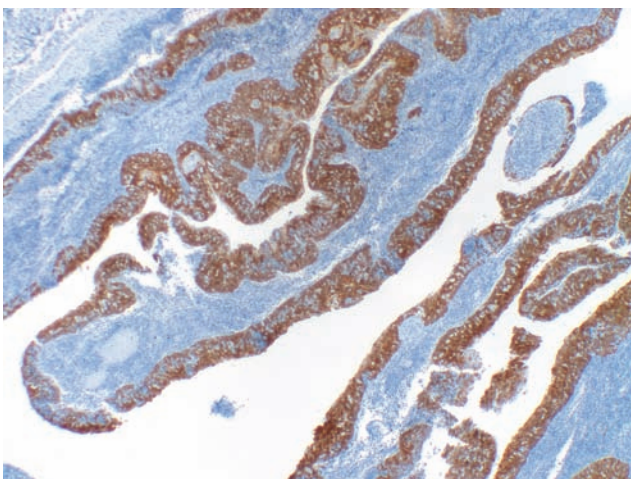


**FIGURE 9.1.8** Tumor is strongly positive for p16.

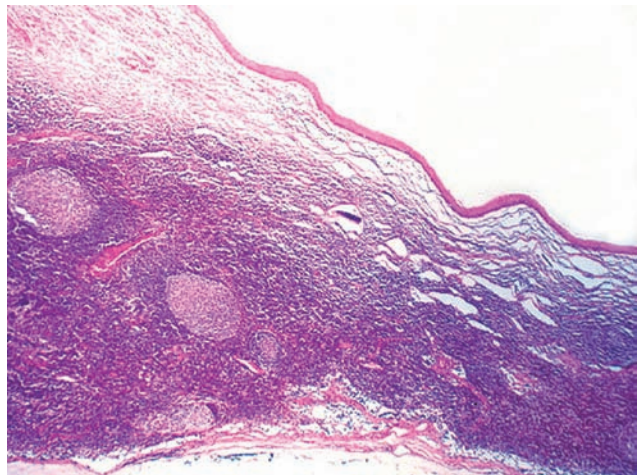


**FIGURE 9.1.10** Branchial cleft cyst. Note capsule of lymph node, subcapsular sinus, lymphoid component with germinal centers, areas of fibrosis, attenuated squamous epithelial lining, and lack of intracystic papillary projections.

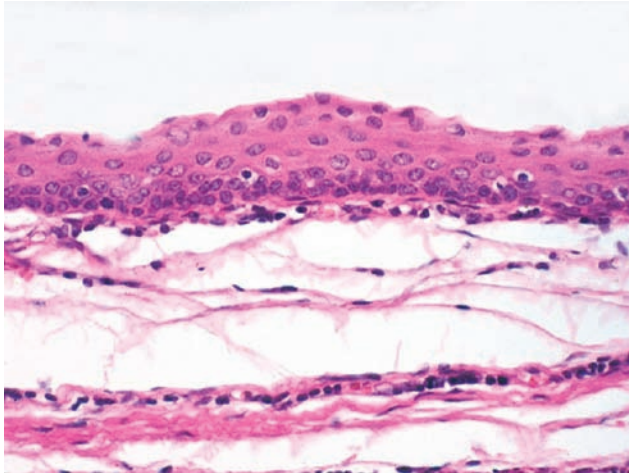


**FIGURE 9.1.11** Branchial cleft cyst. Squamous epithelial lining is thin and histologically bland.

### DISCUSSION

Carcinoma arising in a branchial cleft cyst (CBCC), so-called branchiogenic carcinoma, has been a source of confusion ever since it was first proposed by Von Volkman in 1882 (1). In 1950, Martin et al (2) reviewed almost 250 cases of CBCCs reported in the literature and excluded almost all as being vague and poorly documented. To qualify as a CBCC, they proposed the following four criteria: (1) the cervical tumor must have occurred somewhere along a line extending from a point just anterior to the tragus of the ear, downward along the anterior border of the sternomastoid muscle to the clavicle; (2) the histologic appearance of the growth must be consistent with an origin from tissue known to be present in branchial vestiges; (3) the patient must have survived and have been followed by periodic examinations for at least 5 years without the development of any other lesion, which could possibly have been the primary tumor; (4) the best criterion of all would be the histologic demonstration of a cancer developing in the wall of an epithelial-lined cyst situated in the lateral aspect of the neck.

Although hypothetical, the current opinion is that from a practical point of view, CBCC does

not exist and that all alleged cases are unrecognized examples of metastatic squamous cell carcinoma (3-8). Branchial cleft cysts are uncommon in patients older than 50 years and a diagnosis of such in this population should be made with caution, as this is the age in which squamous cell carcinomas of the head and neck become more apparent.

The 2 tumors that are notorious for producing cystic lymph nodes metastasis that masquerade as a branchial cleft cyst are those that arise in the tonsillar crypts and those that arise from the base of the tongue. The tumors are typically small and metastasize early without producing any significant gross abnormality. As a result, when the tonsil is suggested as a possible primary site of origin, the clinician often responds, “Impossible, the tonsils are of normal size, symmetrical, and free of mucosal ulceration.”

When no clinically apparent site of origin can be detected, the myth of a CBCC starts to be entertained.

Clues to recognizing tumors from the tonsillar crypts and base of tongue (so-called Waldeyer ring carcinomas) include the following: (1) clinically, the lymph node is unilateral, enlarged, and solitary and presents in the neck at levels II or III; (2) they are typically nonkeratinizing squamous cell carcinomas; (3) metastases are uni- or multicystic; (4) intracystic papillary projections of the tumor are common; (5) the tumor in the wall of the cyst often has a ribbon-like arrangement; (6) mitoses are frequent; (7) lymphocytes permeate the tumor; and (8) the tumor is often (not always) positive for p16 and the human papillomavirus.

Branchial cleft cysts, in turn, are unicystic with smooth inner cyst walls devoid of papillary projections and lined by an attenuated “more keratinized” squamous epithelium without mitoses (Figures 9.1.10 and 9.1.11). Fibrosis from previous bouts of infection is common, and tests for human papillomavirus are negative. Nonkeratinizing carcinoma of the nasopharynx, at times, may also enter the differential diagnosis.

## 9.1

These tumors, however, usually (not always) do not produce cystic metastasis and are positive for the Epstein-Barr virus.

It should be emphasized that not all tonsillar and base of tongue squamous cell carcinomas are nonkeratinized. Some are keratinized. It is the nonkeratinized variants that most often masquerade as branchial cleft cysts or CBCCs. If the cystic metastases are keratinized, then the primary site may be anywhere in the head and neck (or even below the clavicles).

See the “Comment” section to see how one should proceed if a tonsillar crypt or base of tongue carcinoma is suspected.

### REFERENCES

1. Von Volkman R. Das tefe branchiogene Halskarzinom. *Zentralbl Chir.* 1882;9:49–63.
2. Martin H, Morfit HM, Ehrlich H. The case for branchiogenic cancer (malignant branchioma). *Ann Surg.* 1950;132:867–887.
3. Compagno J, Hyams VJ, Safavian M. Does branchiogenic carcinoma really exist? *Arch Pathol Lab Med.* 1976;100:311–314.
4. Micheau C, Klijanienko J, Luboinski B, Richard J. So-called branchiogenic carcinoma is actually cystic metastases in the neck from a tonsillar primary. *Laryngoscope.* 1990;100:878–883.
5. Foss RD, Warnock GR, Clark WB, et al. Malignant cyst of the lateral aspect of the neck: branchial cleft carcinoma or metastasis? *Oral Surg Oral Med Oral Pathol.* 1991;71:214–217.
6. Flanagan PM, Roland NJ, Jones AS. Cervical node metastases presenting with features of branchial cysts. *J Laryngol Otol.* 1994;108:1068–1071.
7. Thompson LDR, Heffner DK. The clinical importance of cystic squamous cell carcinomas in the neck. A study of 136 cases. *Cancer.* 1998;82:944–956.
8. Goldenberg D, Begum S, Westra HH, et al. Cystic lymph node metastasis in patients with head and neck cancer: an HPV-associated phenomenon. *Head Neck.* 2008;30:898–903.

## 9.2

*Eosinophilic Angiocentric Fibrosis***CLINICAL INFORMATION**

“This 60-year-old man presented in 2004 with a widened nasal septum, which was excised. The lesion has now recurred and involves both nares. There is no adenopathy or history of systemic disease. In addition, he has recently developed a 3-cm skin lesion of the right frontotemporal scalp that was first noticed several months ago. I would appreciate your opinion of this unusual case.”

**OPINION**

Sections show a fibroinflammatory lesion composed of numerous eosinophils with admixed lymphocytes and plasma cells (Figures 9.2.1 and 9.2.2). In some areas, blood vessels, ranging from capillaries to arterioles, are surrounded by concentric layers of collagen (so-called onion-skin fibrosis) (Figures 9.2.3 and 9.2.4).

In other areas, the lesion becomes less inflammatory and more fibrous (Figures 9.2.5, 9.2.6, and 9.2.7).

The skin lesion shows an intact epidermis with a prominent Grenz zone (Figure 9.2.8). The mid and lower dermis contain a mixed inflammatory infiltrate centered around blood vessels (Figure 9.2.9). Some blood vessels are associated with fibrin exudation and are surrounded by neutrophils with an element of leukocytoclasia (Figure 9.2.10). Eosinophils are prominent (Figure 9.2.11).

**DIAGNOSIS**

Lesions of the nasal septum and right frontotemporal scalp: Eosinophilic angiocentric fibrosis associated with granuloma faciale.

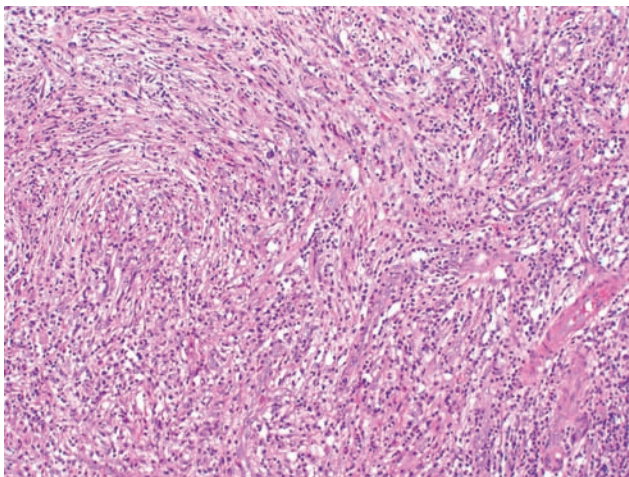


**FIGURE 9.2.1** Eosinophilic angiocentric fibrosis. Note the fibrous background and diffuse inflammation.

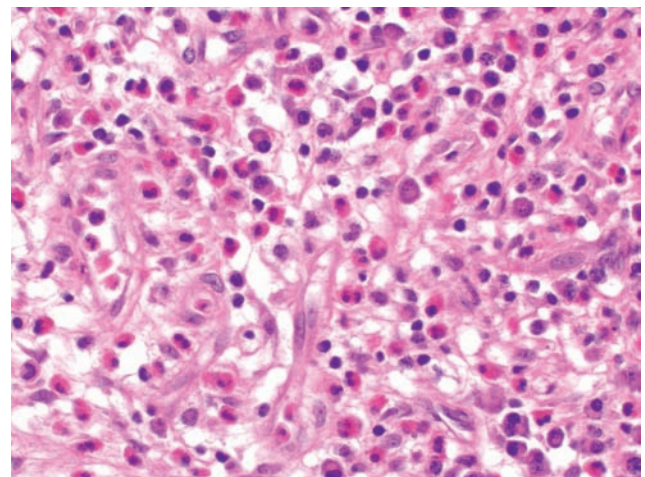


**FIGURE 9.2.2** Eosinophilic angiocentric fibrosis. The lesion contains abundant eosinophils.

## 9.2

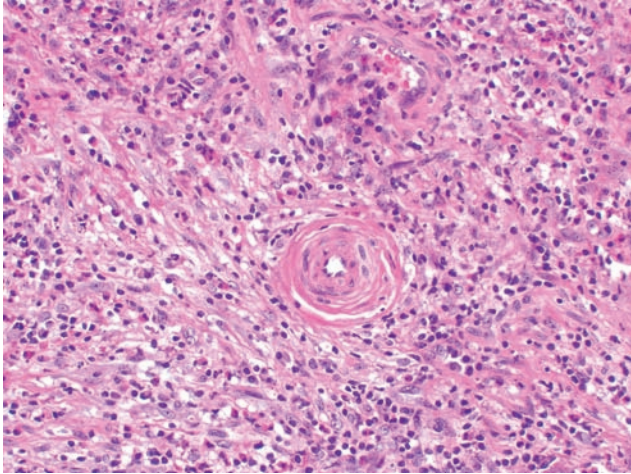


**FIGURE 9.2.3** Eosinophilic angiocentric fibrosis. An arteriole with concentric layers of collagen.

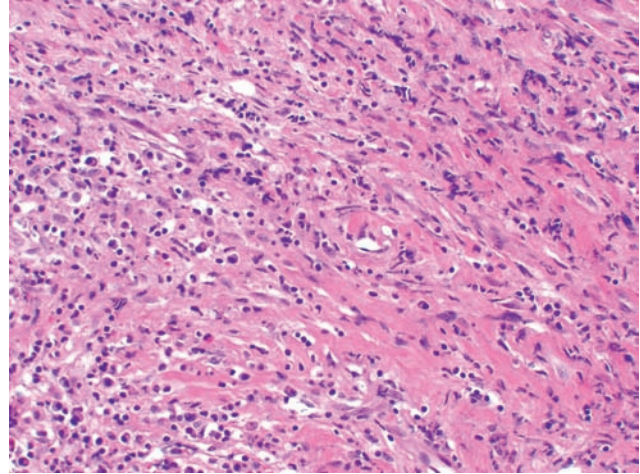


**FIGURE 9.2.5** Eosinophilic angiocentric fibrosis. As the lesion matures, it becomes more fibrous and less inflammatory.

**COMMENT**

Eosinophilic angiocentric fibrosis (EAF) is a very rare condition of unknown etiology that predilects the nasal septum, usually as a fibroinflammatory mass that leads to nasal obstruction. Some cases are associated with granuloma faciale.

**DISCUSSION**

Eosinophilic angiocentric fibrosis is an exceedingly rare, slowly progressive, obstructive, fibroinflammatory disorder of unknown etiology that predilects the nasal cavity and occasionally the paranasal sinuses, larynx, orbit, and gingival (1).

It is slightly more common in women (60%) than men and occurs in patients averaging 48 years

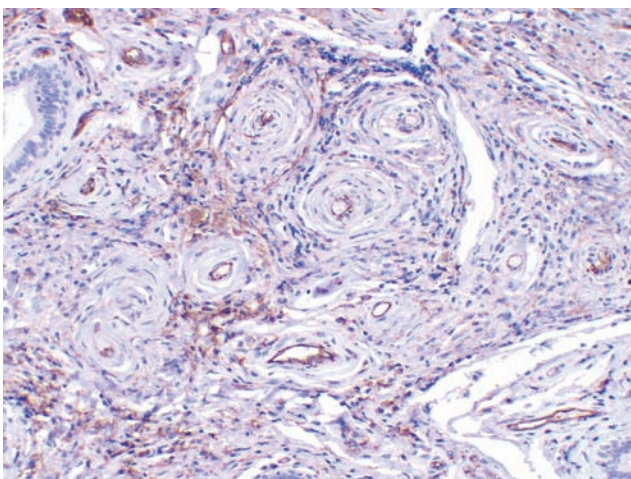


**FIGURE 9.2.4** Eosinophilic angiocentric fibrosis. A CD34 immunohistochemical stain accentuates the blood vessel in each area of concentric fibrosis.

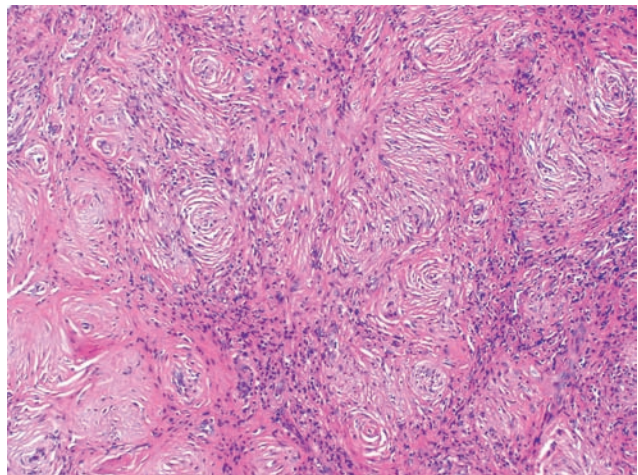


**FIGURE 9.2.6** Eosinophilic angiocentric fibrosis. More mature lesion showing extensive perivascular fibrosis.

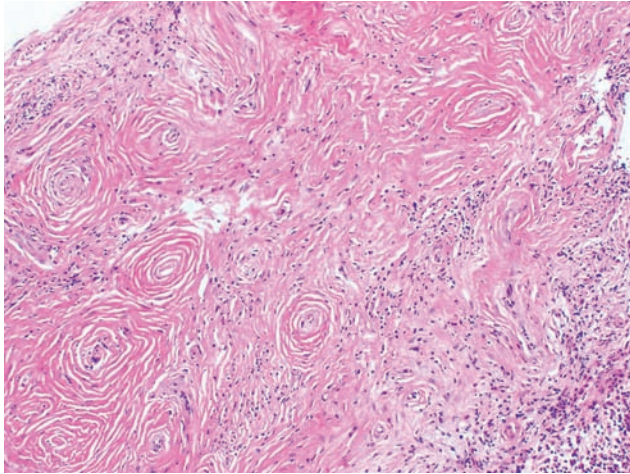


**FIGURE 9.2.7** Eosinophilic angiocentric fibrosis. Another view of a mature lesion. Although it is more scar-like, perivascular fibrosis is still apparent.

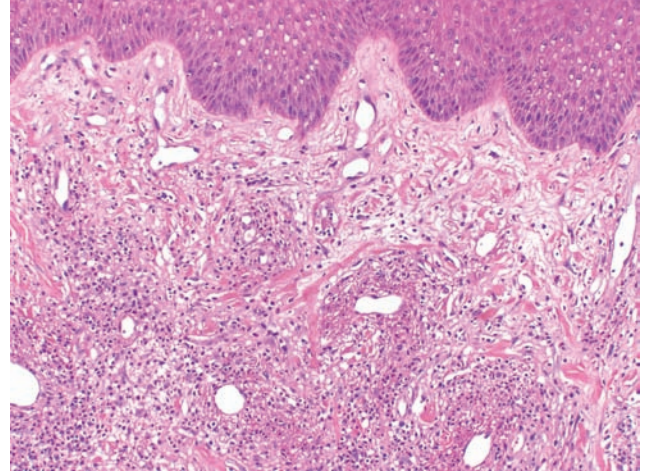


**FIGURE 9.2.9** Granuloma faciale. Higher magnification of Figure 9.2.8. Note the inflammation is centered around blood vessels.

of age (range, 19-79 years). It evolves slowly over the course of many years and, in the nasal cavity, typically involves the septum and/or lateral cartilaginous wall, resulting in a tumor-like expansion with progressive unilateral or bilateral obstruction. No cases, thus far, have been described below the clavicles.

The etiology is unknown. Some have suggested that it may represent the mucosal variant of granuloma faciale, and indeed, 25% of cases are associated

with cutaneous granuloma faciale. When this occurs, the skin lesion may precede, coincide, or follow the diagnosis of EAF. Allergy and trauma have also been proposed.

The pathology of EAF consists of 2 phases—early and late—both of which may be seen in a single biopsy, suggesting that the condition is continually evolving.

The early lesion is more “inflammatory” than “fibrous” and consists of numerous eosinophils with

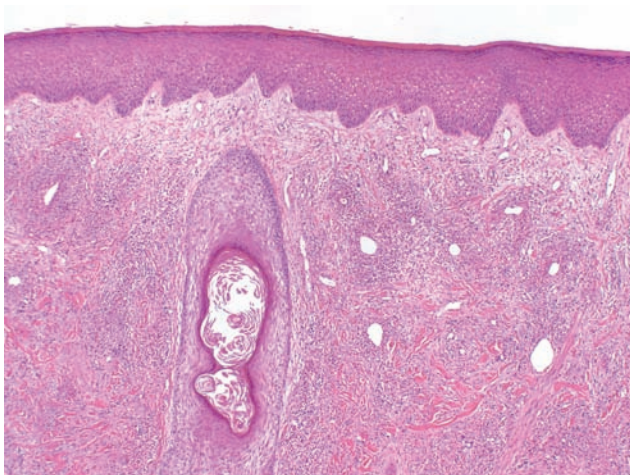


**FIGURE 9.2.8** Granuloma faciale. Note the Grenz zone and the perivascular inflammation.

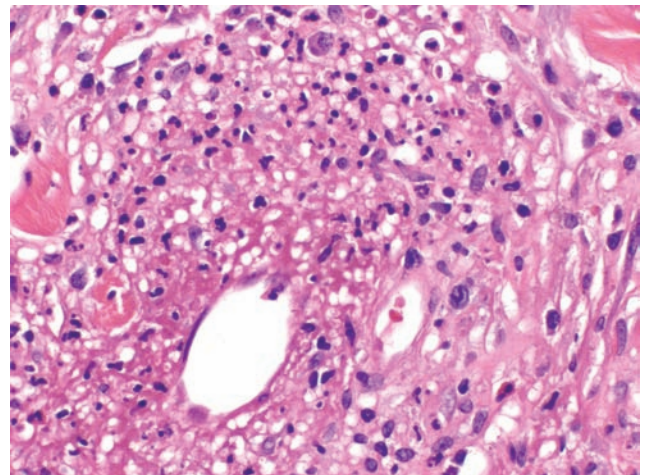


**FIGURE 9.2.10** Granuloma faciale. Note the fibrin exudate and neutrophils with some evidence of leukocytoclasia.



## 9.2

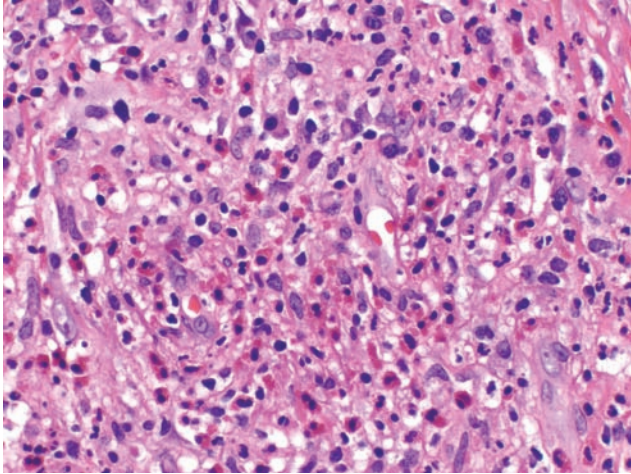


**FIGURE 9.2.11** Granuloma faciale. Eosinophils are prominent.

admixed lymphocytes, plasma cells, and occasionally neutrophils arranged in a nodular and/or diffuse pattern. At times, the cellular infiltrate extends into the walls of small blood vessels with or without leukocytoclasia. As the lesion matures, inflammation becomes less intense, stromal fibrosis ensues, and small blood vessels acquire a characteristic onion skin type of perivascular fibrosis. Stromal necrosis is uncommon, and granulomas and giant cells are not seen. The process typically involves soft tissue but may also involve cartilage and/or bone. Lymphoid aggregates are sparse to absent. The involved blood vessels are predominantly capillaries, venules, and arterioles.

Surgical debulking and/or excision are the treatment of choice and recurrence and/or persistence of disease are frequent. Oral and intralesional steroids, immunosuppressive agents, dapsone, laser therapy, cryotherapy, and radiation have been tried with variable but usually poor results.

The differential diagnosis includes inflammatory myofibroblastic tumor (IMT, inflammatory pseudotumor), Churg-Strauss syndrome, and Wegener granulomatosis. Of these, IMT may be the most problematic. Inflammatory myofibroblastic tumor can occur in any site, including mucous membranes, and may contain eosinophils. Perivascular onion skin fibrosis, however, is usually not seen in IMT. The presence of a large component of spindle cells positive for smooth muscle actin, muscle-specific actin, and/or desmin would also favor IMT. Anaplastic lymphoma kinase is positive in some cases of IMT but has not been evaluated in EAF.

Churg-Strauss syndrome is characterized by a diagnostic triad of (1) asthma, often severe; (2) systemic vasculitis that varies from granulomatous to nongranulomatous; and (3) peripheral and tissue eosinophilia. It is also associated with P-ANCA in 40% to 80% of cases. The presence of these findings and the absence of perivascular onion skin fibrosis should allow one to distinguish Churg-Strauss syndrome and EAF.

Wegener granulomatosis may be localized or generalized and is characterized by necrosis, granulomatous inflammation, vasculitis, absence of significant eosinophilia (about 5% of Wegener granulomatosis may be associated with eosinophilia), and an elevated and rising titer of C-ANCA.

### Reference

1. Barnes L. Eosinophilic angiocentric fibrosis and granuloma faciale presented at The Head and Neck/Endocrine Pathology Conference, United States and Canadian Academy of Pathology Meeting, Boston, Massachusetts, March 12, 2009 (review of 40 cases, unpublished material).

## 9.3

*Follicular Dendritic Cell Sarcoma***CLINICAL INFORMATION**

“I have enclosed the slides of a right tonsillar mass from a 47-year-old man. We initially believed this to be a poorly differentiated carcinoma; however, the immunohistochemical stains do not suggest this diagnosis. We now believe that we are dealing with a sarcoma; however, of our available stains, only vimentin and S100 protein are focally positive. We are considering a malignant peripheral nerve sheath tumor, but the morphology is not classic. We would appreciate your review and suggestion.”

**OPINION**

Sections show a neoplasm with a variegated pattern of growth composed of round to spindle-shaped cells with poorly defined cytoplasm and large round

to oval vesicular nuclei and small nucleoli (Figures 9.3.1, 9.3.2, and 9.3.3). In some areas, the tumor is arranged in small closely packed lobules, whereas in others, large bands of collagen divide the tumor into irregular, interconnecting clusters (Figures 9.3.4 and 9.3.5). Scattered lymphocytes of both T- and B-cell types permeate the tumor (Figure 9.3.6). Mitoses are few, and necrosis is not seen. There is no connection to the overlying squamous mucosa of the tonsil.

**DIAGNOSIS**

Tonsil, right, tonsillectomy: Follicular dendritic cell sarcoma.

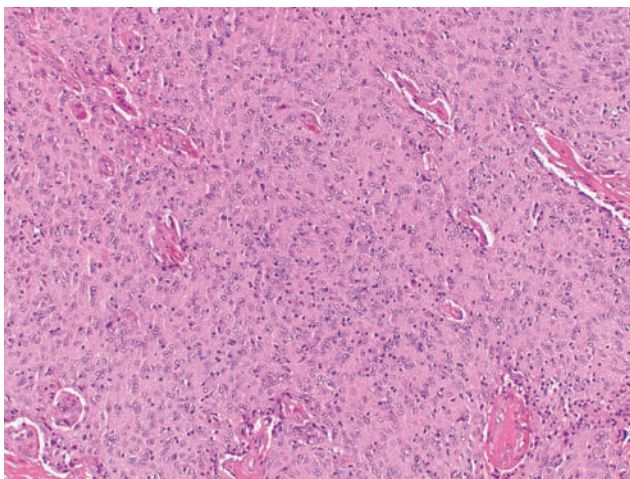


**FIGURE 9.3.1** Follicular dendritic cell sarcoma composed of sheets of round, epithelioid cells.

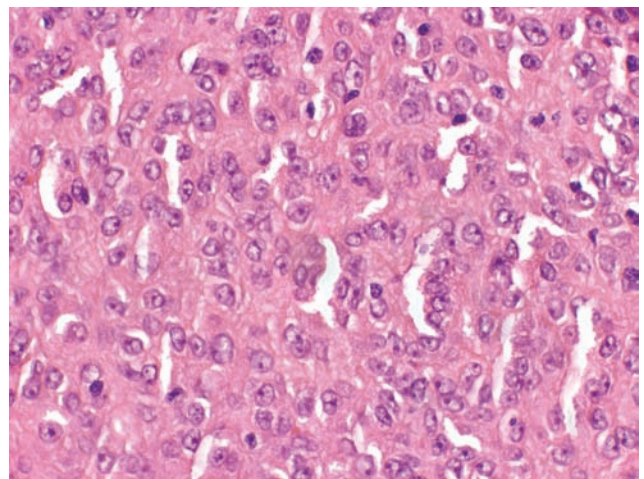


**FIGURE 9.3.2** High-power magnification of Figure 9.3.1. The cells have poorly defined cytoplasm and round vesicular nuclei with small nucleoli.

## 9.3

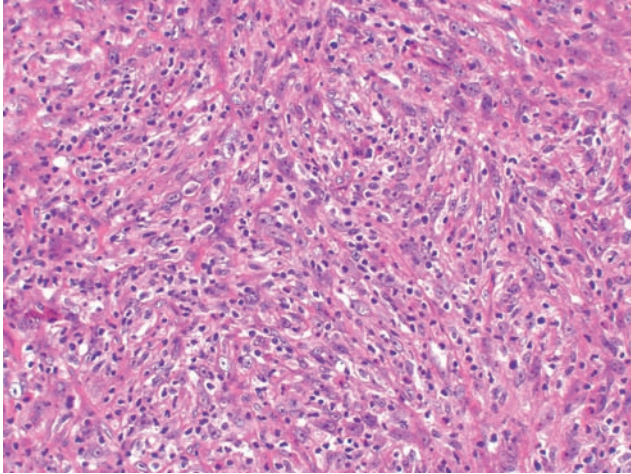


**FIGURE 9.3.3** Follicular dendritic cell sarcoma composed of spindle cells. Note the admixed lymphocytes.

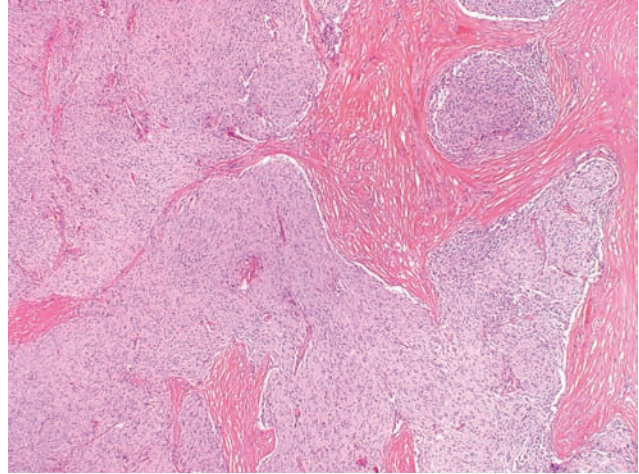


**FIGURE 9.3.5** Follicular dendritic cell sarcoma composed of large bands of collagen.

## COMMENT

As noted above, we believe this is a follicular dendritic cell sarcoma. In support of this diagnosis is strong and diffuse immunoreactivity for CD21 and focal positivity for CD68 (Figure 9.3.7). In addition, stains for CD1a, S100 protein, CD3, CD20, and numerous cytokeratins (pancytokeratin, cytokeratin 5/6, CAM 5.2) are negative (Figure 9.3.8).

## DISCUSSION

Dendritic cells are a heterogeneous group of non-lymphoid, nonphagocytic immune accessory cells found in lymphoid and nonlymphoid tissues that are involved in antigen presentation to lymphocytes (1–9). Three types of dendritic cells are recognized: follicular, interdigitating, and Langerhans. Interdigi-

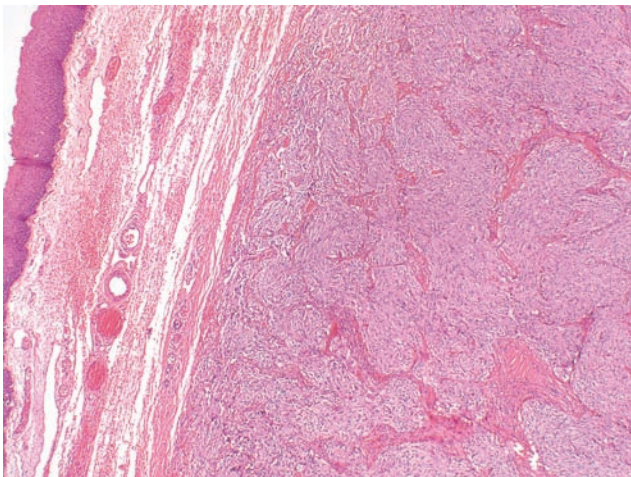


**FIGURE 9.3.4** Follicular dendritic cell sarcoma focally composed of small, closely packed lobules.

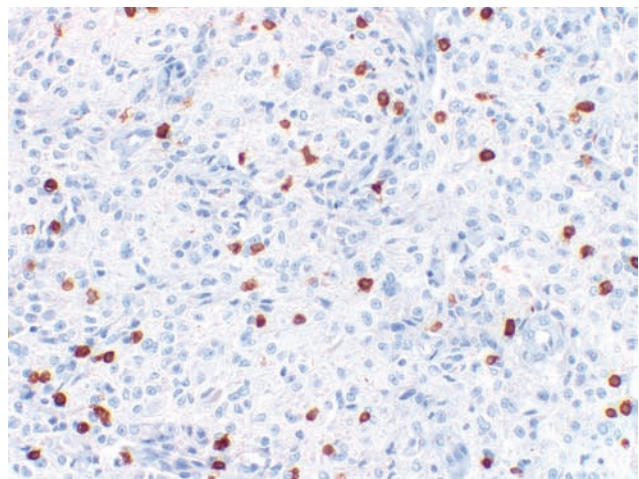


**FIGURE 9.3.6** Follicular dendritic cell sarcoma stained with common leukocyte antigen accentuating the permeation by lymphocytes. See Figure 9.3.3.

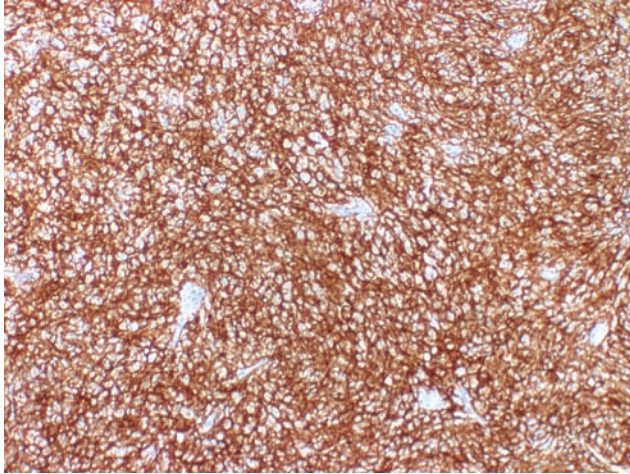


**FIGURE 9.3.7** Follicular dendritic cell sarcoma strongly positive for CD21.

tating follicular cells (IDCs) and Langerhans cells are bone marrow–derived. The origin of the follicular dendritic cell (FDC) is controversial but may be derived from mesenchymal stem cells.

The FDCs are associated with B-cells and are found in germinal centers of primary and secondary lymphoid follicles (Figure 9.3.9). The IDCs are associated with T-cells and, accordingly, are located in the paracortical areas of lymph nodes. Langerhans cells

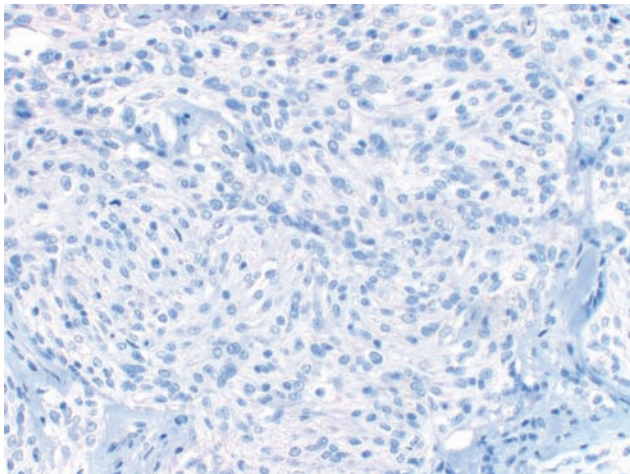


**FIGURE 9.3.8** Follicular dendritic cell sarcoma negative for CD1a.

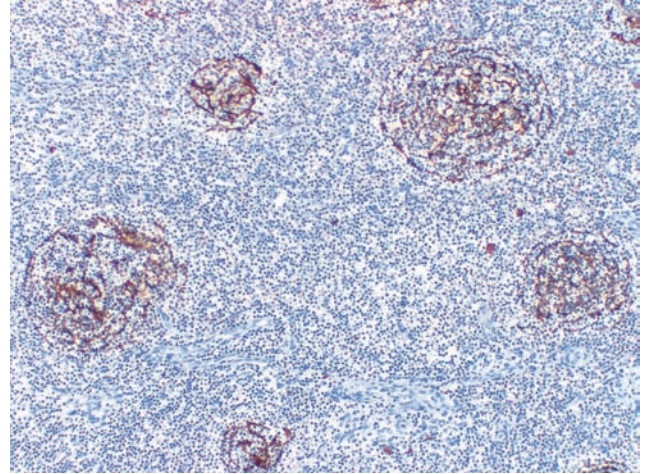


**FIGURE 9.3.9** Normal lymph node stained for CD21. Note that the follicular dendritic cells are confined to the germinal centers.

are also associated with T-cells but are located primarily in the skin.

Tumors of dendritic cells are rare but are being recognized more frequently with the availability of more specific commercial markers. A proposed classification is shown in Table 9.3.1. These tumors, according

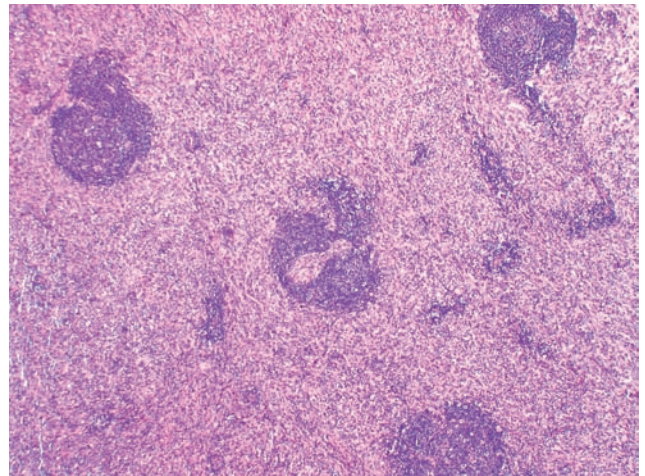


**FIGURE 9.3.10** Interdigitating dendritic cell sarcoma. Note the preserved germinal centers where the follicular dendritic cells are located. The abnormal cells involve the paracortical region of the lymph node. (Courtesy of Kathryn L. Lane, MD, Pathology Associates, Huntsville, AL).

## 9.3

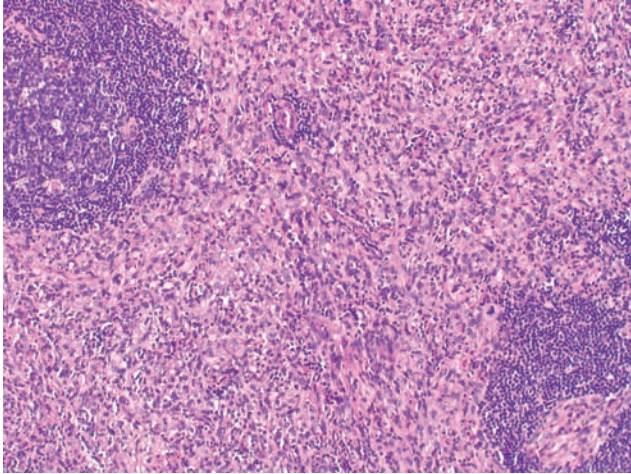


**FIGURE 9.3.11** Interdigitating dendritic cell sarcoma. The tumor cells are also spindled with admixed lymphocytes.

to Pileri et al (5), can be further subclassified in more than 90% of the time using the 6 immunostains seen in Table 9.3.2. The one that is seen most often in the head and neck is the FDC sarcoma and is the focus of this discussion.

The possible existence of a tumor arising from FDCs was first postulated by Lennert in 1978. It was, however, not until 1986 that an actual tumor composed of FDCs was first recognized by Monda et al (8). The tumor occurs over a broad age range (9–77 years),

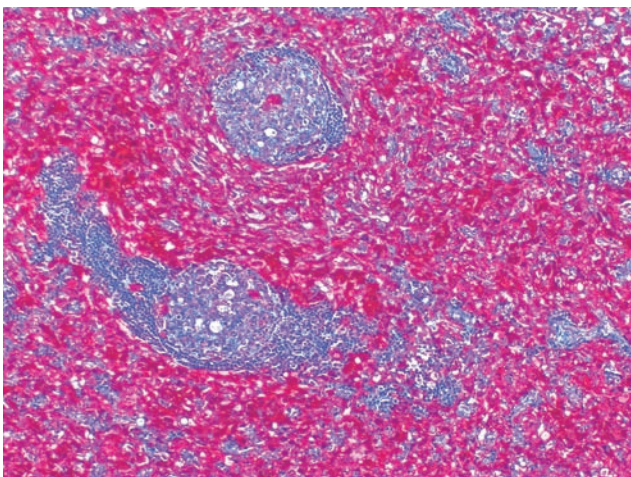


**FIGURE 9.3.12** Interdigitating dendritic cell sarcoma. The tumor cells are strongly positive for S100 protein.

**TABLE 9.3.1** Classification of Dendritic Cell Neoplasms

I. Follicular dendritic cell sarcoma
II. Interdigitating dendritic cell sarcoma
III. Langerhans cell lesions
A. Langerhans cell tumor (cytologically benign)
B. Langerhans cell sarcoma (cytologically malignant)
IV. Dendritic cell sarcoma, unclassified type (indeterminant)

with an average of about 45 years and an equal gender distribution. Most patients present with an asymptomatic mass without systemic manifestations. About 50% of cases arise in lymph nodes, 35% involve extranodal areas, and in 15%, both nodal and extranodal sites are involved simultaneously.

Ten to twenty percent of FDCs have been associated with the hyaline-vascular variant of Castleman disease, and a few have also been positive for the Epstein-Barr virus, especially those that involve the liver and spleen (2).

Treatment is not standardized and continues to evolve. Most patients have been managed by surgical excision, whereas others have received radiation and/or chemotherapy. About 40% to 50% of patients have experienced local recurrence and 25% distant metastasis, mainly to the lungs, liver, and lymph nodes. Death from disease occurs in 10% to 20% of patients.

The FDC sarcomas larger than 6 cm and exhibit significant cytologic atypia, extensive coagulative necrosis, and more than 5 mitoses per 10 high-power fields tend to be more aggressive.

**TABLE 9.3.2** Immunoprofile of Dendritic Cell Neoplasms

Stain	FDC	IDC	LH
CD68	+/-	+/-	+
Lysozyme	-	-	-/+
CD1a	-	-	+
S100	-/+	+	+
CD21	+	-	-
CD35	+	-	-

\*Data derived from Reference (5).

The differential diagnosis is broad and includes other dendritic neoplasms (Table 9.3.2), ectopic meningioma, melanoma, spindle cell carcinoma, nasopharyngeal carcinoma, ectopic thymoma, CASTLE (carcinoma showing thymus-like differentiation), inflammatory myofibroblastic tumor, and a variety of sarcomas (Figures 9.3.10, 9.3.11, and 9.3.12). The clue to recognizing FDC sarcoma is simply considering it in the differential diagnosis and observing its strong affinity for CD21 and CD35. The tumor is positive for vimentin and, in about 40% of cases, may decorate with epithelial membrane antigen. A few are also positive for muscle-specific action. It is otherwise negative for cytokeratin, HMB-45, and the thymic marker CD5.

### References

1. Perez-Ordóñez B, Erlandson RA, Rosai J. Follicular dendritic cell tumor: report of 13 additional cases of a distinctive entity. *Am J Surg Pathol.* 1996;20:944–955.
2. Chan JKC. Proliferative lesions of follicular dendritic cells: an overview, including a detailed account of follicular dendritic cell sarcoma, a neoplasm with many faces and uncommon etiologic associations. *Adv Anat Pathol.* 1997;4:387–411.
3. Fonseca R, Yamakawa M, Nakamura S, et al. Follicular dendritic cell sarcoma and interdigitating reticulum cell sarcoma: a review. *Am J Hematol.* 1998;59:161–167.
4. Choi PCL, To KF, Lai FMM, et al. Follicular dendritic cell sarcoma of the neck. Report of two cases complicated by pulmonary metastases. *Cancer.* 2000;89:664–672.
5. Pileri SA, Grogan TM, Harris NL, et al. Tumours of histiocytes and accessory dendritic cells: an immunohistochemical approach to classification from the International Lymphoma Study Group based on 61 cases. *Histopathology.* 2002;41:1–29.
6. Biddle DA, Ro JY, Yoon GS, et al. Extranodal follicular dendritic cell sarcoma of the head and neck region: three new cases, with a review of the literature. *Mod Pathol.* 2002;15:50–58.
7. Kairouz S, Hashash J, Kabbara W, et al. Dendritic cell neoplasms: an overview. *Am J Hematol.* 2007;82:924–928.
8. Chera BS, Orlando C, Villaret DB, et al. Follicular dendritic cell sarcoma of the head and neck: case report and literature review. *Laryngoscope.* 2008;118:1607–1612.
9. Rezh SA, Spagnolo DV, Brynes RK, et al. Indeterminate cell tumor: a rare dendritic neoplasm. *Am J Surg Pathol.* 2008;32:1868–1876.

## 9.4

*Histoplasmosis***CLINICAL INFORMATION**

“This 53-year-old man from the Mississippi River Valley area presents with hoarseness. At laryngoscopy, a nodule of the right true vocal cord was found and removed. Could this be a squamous cell carcinoma?”

**OPINION**

Sections show fragments of intact and ulcerated squamous mucosa with a marked infiltrate of acute and chronic inflammatory cells in the lamina propria (Figures 9.4.1 and 9.4.2). A few multinucleated giant cells are also seen (Figure 9.4.3). The intact mucosa is hyperplastic and show evidence of atypia probably related to the inflammation. A periodic acid-Schiff (PAS) stain shows numerous organisms within the giant cells with a small red dot-like configuration surrounded by a clear halo (Figures 9.4.3 and 9.4.4). A

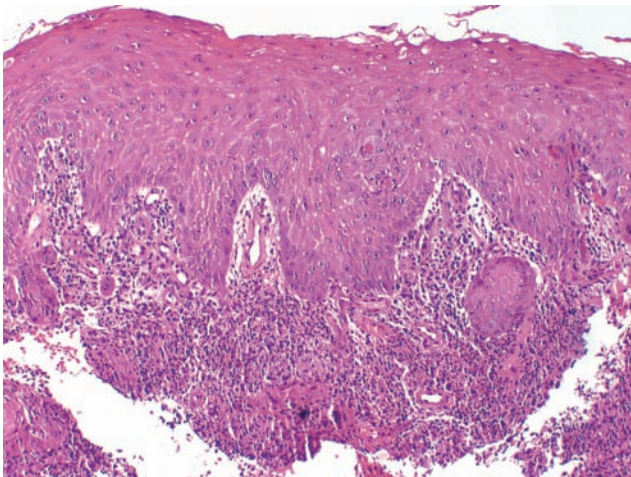


**FIGURE 9.4.1** The squamous mucosa is hyperplastic, and the stroma is markedly inflamed.

Grocott stain shows numerous yeasts about 3 microns in diameter (Figure 9.4.5).

**DIAGNOSIS**

Lesion, right true vocal cord: Histoplasmosis associated with pseudoepitheliomatous hyperplasia, ulceration, granulation tissue and reactive atypia.

**COMMENT**

The biopsy contains organisms morphologically compatible with histoplasmosis. The fact that the patient resides in a known endemic area is also supportive of this diagnosis.

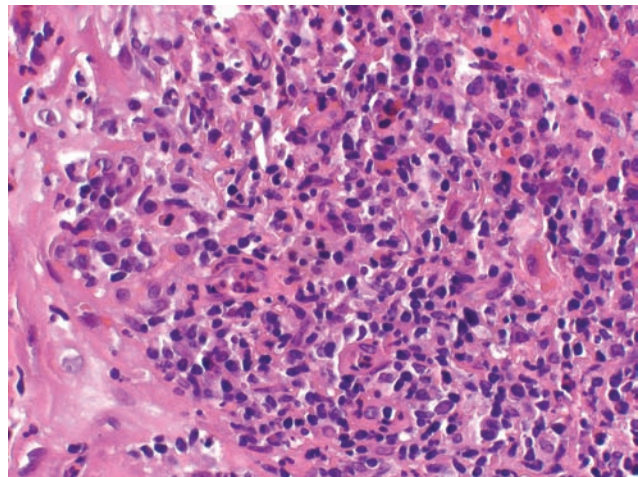


**FIGURE 9.4.2** The inflammatory infiltrate consists mainly of acute and chronic inflammatory cells.

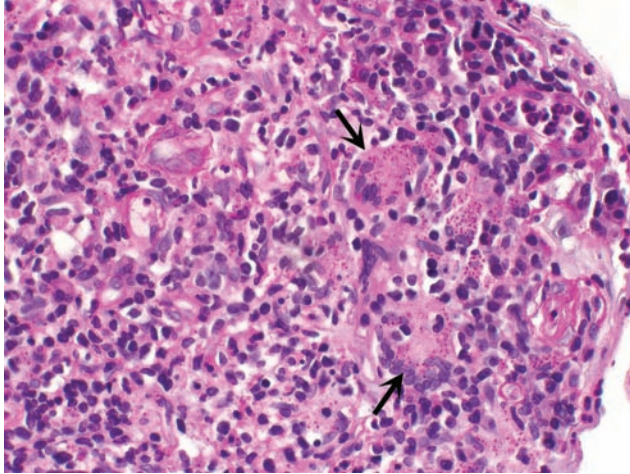


**FIGURE 9.4.3** A few giant cells are seen that contain numerous intracytoplasmic organisms appearing as red round dots surrounded by a small clear halo (arrows) (PAS).

### DISCUSSION

Histoplasmosis is a disease caused by the dimorphic fungus, *Histoplasma capsulatum*. It occurs in temperate zones worldwide but is particularly endemic in the Ohio and Mississippi River Valleys in the United States (1).

The organism resides in the soil, often contaminated with chicken, bird, and bat excrement. The infection is acquired by inhalation of the fun-

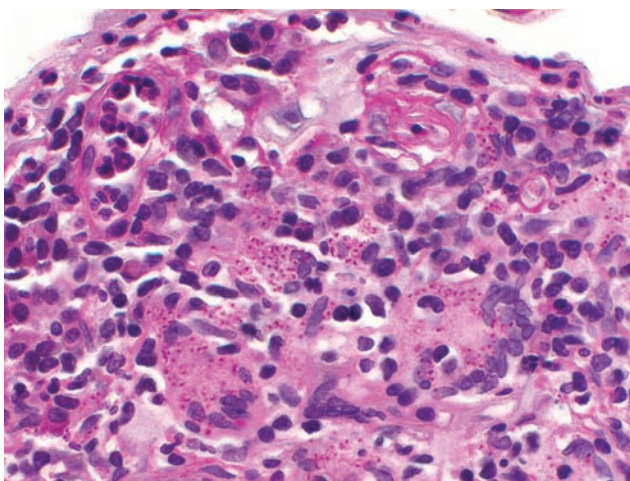


**FIGURE 9.4.4** Higher magnification of Figure 9.4.4 (PAS).

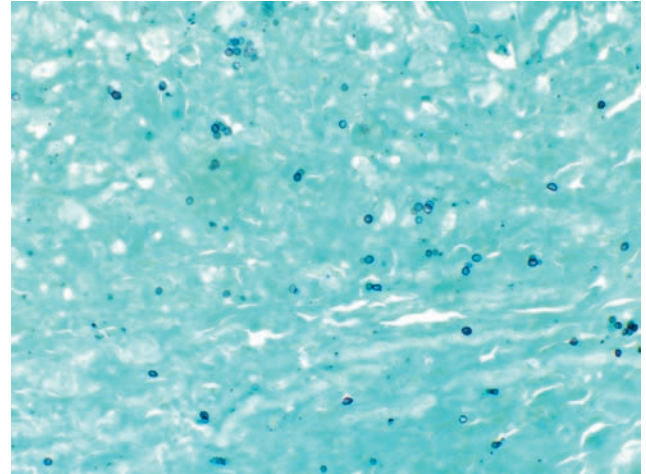


**FIGURE 9.4.5** A Gomori silver stain also shows numerous small extracellular yeasts.

gus and not by person-to-person contact. Individuals who work around bird-chicken roosts, old houses, and barns and those whose activities involve disruption of soil, such as farming and excavating, are especially at risk (1).

The disease has a broad spectrum of manifestations ranging from asymptomatic to life-threatening. Factors that impact on disease activity include the size of the initial inhaled inoculum, competency of the immune system, and extremes of age (the very young and old individuals are more at risk).

Histoplasmosis of the larynx is uncommon and is most often part of systemic disease, although disease limited to the larynx and/or other adjacent upper aerodigestive mucosal sites have been described (2-6). It may involve any site in the larynx and typically presents as a mucosal irregularity and/or ulceration accompanied by pain, dysplasia, and hoarseness. Clinically it is often confused with a neoplasm or tuberculosis. Once the disease is confirmed, the extent of the disease should be addressed and treated with antifungal medication.



---

## 9.4

### References

1. Kurowski R, Ostapchuk M. Overview of histoplasmosis. *Am Fam Physician*. 2002;66:2247–2252.
2. Gerber ME, Rosdeutscher JD, Seiden AM, Tami TA. Histoplasmosis: the otolaryngologist's perspective. *Laryngoscope*. 1995;105:919–923.
3. Sataloff RT, Wilborn A, Prestipino A, Hawkshaw M, Heuer RJ, Cohn J. Histoplasmosis of the larynx. *Am J Otolaryngol*. 1993;14:199–205.
4. Gulati SP, Gupta A, Wadhwa R, et al. Histoplasmosis of larynx in immunocompetent patients mimicking carcinoma: report of two cases. *J Infect Dis Antimicrob Agents*. 2008;25:145–149.
5. Pochini Sobrinho F, Della Negra M, Queiroz W, Ribeiro UJ, Bittencourt S, Klautau GB. Histoplasmosis of the larynx. *Braz J Otorhinolaryngol*. 2007;73:857–861.
6. O'Hara CD, Allegretto MW, Taylor GD, Isotalo PA. Epiglottic histoplasmosis presenting in a nonendemic region: a clinical mimic of laryngeal carcinoma. *Arch Pathol Lab Med*. 2004;128:574–577.

## 9.5

## Median Rhomboid Glossitis

## CLINICAL INFORMATION

“A 52-year-old woman, nonsmoker, presented with a 0.5-cm area of leukoplakia on the midline dorsum of the tongue anterior to the circumvallate papillae. Excisional biopsy was performed. Although we favor pseudoepitheliomatous hyperplasia, we would like to exclude a well-differentiated squamous cell carcinoma.”

## OPINION

Histologic sections show hyperplastic squamous mucosa with elongated “psoriasiform” rete ridges (Figure 9.5.1). In other areas, the rete ridges are more rounded and “bulbous” (Figure 9.5.2). Squamous mucosa is further characterized by keratosis (Figure 9.5.3), acute mucositis, and submucosal lymphoplasmacytic infiltrate (Figure 9.5.4). Intraepithelial microabscesses are

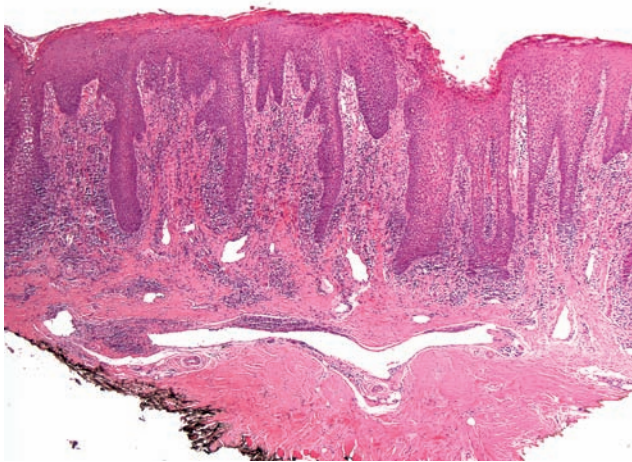


**FIGURE 9.5.1** Hyperplastic squamous mucosa with psoriasiform rete ridges.

noted (Figure 9.5.5). *Candida hyphae* are identified in the keratotic layer (Figure 9.5.6). Filiform and fungiform papillae are absent. There is no evidence of epithelial dysplasia or mitoses.

## DIAGNOSIS

Tongue, midline, excisional biopsy: Hyperplastic squamous mucosa with acute mucositis and keratosis, consistent with median rhomboid glossitis.

## COMMENT

The diagnosis of median rhomboid glossitis (MRG) is based on the combination of mucosal hyperplasia and acute mucositis identified at the characteristic site—midline dorsal tongue. Median rhomboid

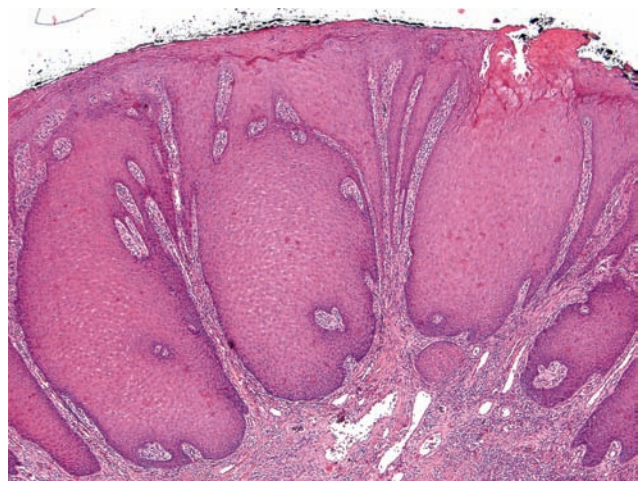


**FIGURE 9.5.2** Rounded bulbous rete ridges.

## 9.5

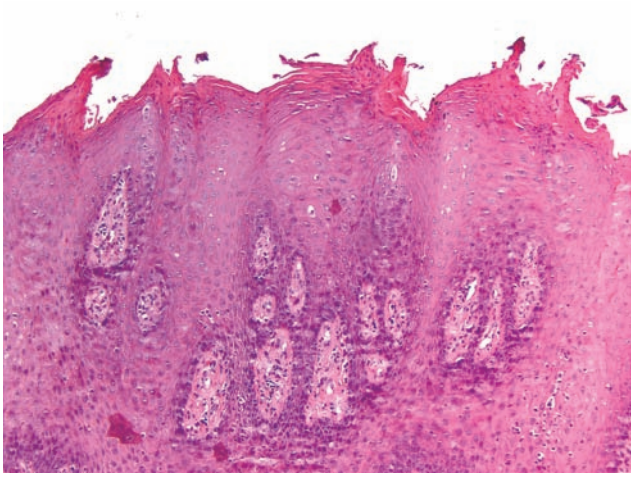


FIGURE 9.5.3 Keratosis.

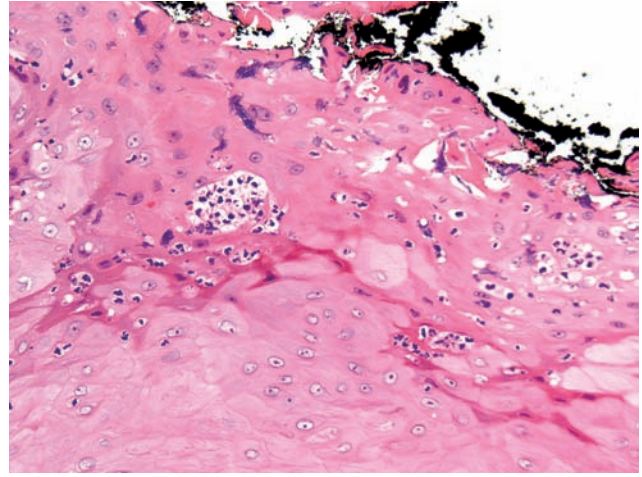


FIGURE 9.5.5 Intraepithelial microabscess.

glossitis is also known as central (or posterior) papillary atrophy and posterior midline atrophic candidiasis. It is believed that MRG represents a chronic reaction to *Candida*, although *Candida* organisms may not be histologically identifiable in all cases.

### DISCUSSION

Clinically, MRG is diagnosed in about 1% of the population (1,2). It usually presents as an oval or rhomboid

smooth erythematous area less than 2 cm located on the midline dorsal tongue anterior to the circumvallate papillae. The erythematous appearance of MRG may mimic erythroplakia. When clinical presentation is atypical (eg, large size), it may be biopsied.

Histologically, the main differential diagnosis is pseudoepitheliomatous hyperplasia versus squamous dysplasia and squamous cell carcinoma. The location of the lesion and the lack of dysplastic changes are

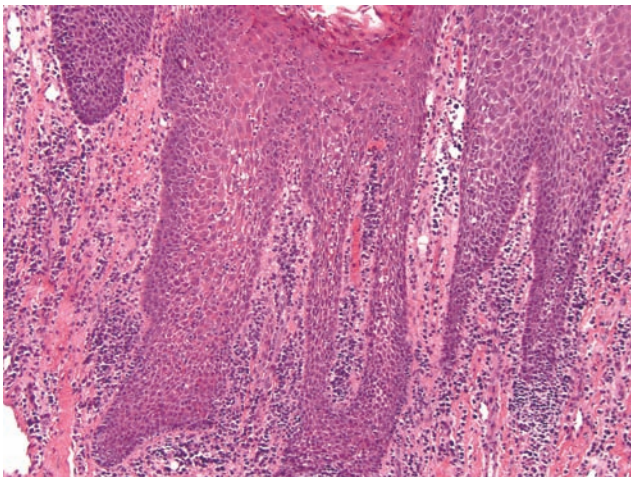


FIGURE 9.5.4 Acute mucositis and submucosal lymphoplasmacytic infiltrate.

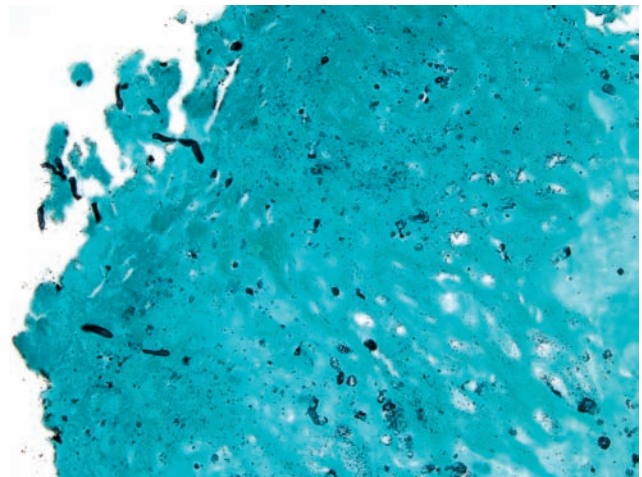


FIGURE 9.5.6 Grocott stain highlights *C* hyphae.

helpful in excluding squamous dysplasia/carcinoma. Only about 3% to 5% of squamous cell carcinomas of the tongue involve its dorsal surface (3). The midline dorsal surface of the tongue would be a most unusual site for a squamous cell carcinoma.

### References

1. Pentenero M, Broccoletti R, Carbone M, Conrotto D, Gandolfo S. The prevalence of oral mucosal lesions in adults from the Turin area. *Oral Dis*. 2008;14(4):356–366.
2. Mathew AL, Pai KM, Sholapurkar AA, Vengal M. The prevalence of oral mucosal lesions in patients visiting a dental school in Southern India. *Indian J Dent Res*. 2008;19(2):99–103.
3. Goldenberg D, Ardekian L, Rachmiel A, Peled M, Joachims HZ, Laufer D. Carcinoma of the dorsum of the tongue. *Head Neck*. 2000;22(2):190–194.

## 9.6

*Rosai-Dorfman Disease–Rhinoscleroma***CLINICAL INFORMATION**

“This 23-year-old woman presented with frequent headaches, allergies, and sinusitis. She underwent a Caldwell-Luc procedure for removal of tissue from her right maxillary sinus and nasal cavity. The histologic features are unusual. I look forward to your opinion.”

**OPINION**

Sections show respiratory mucosa containing poorly defined aggregates of mature lymphocytes with admixed plasma cells alternating with large sheets and/or small clusters of histiocytes with voluminous clear cytoplasm and round to oval vesicular nuclei and single nucleoli (Figure 9.6.1). Neutrophils are sparse to absent. Lym-

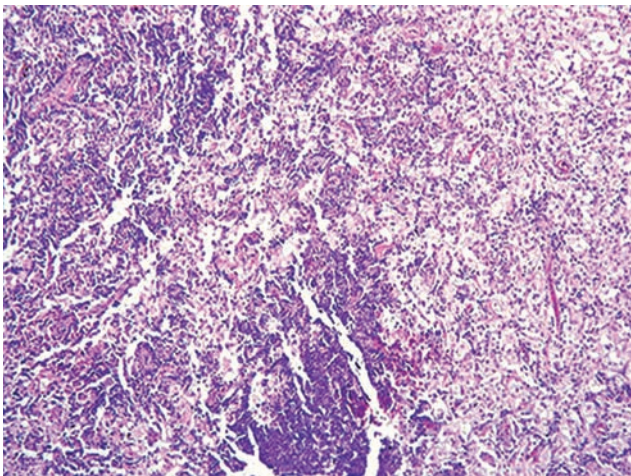


**FIGURE 9.6.1** Extranodal RDD involving the sinonasal tract. Note the aggregates of lymphocytes and sheets of clear cells (histiocytes).

phocytes and plasma cells are occasionally seen in the cytoplasm of the histiocytes (emperipolesis) (Figure 9.6.2). In other areas, fibrosis is prominent, as well as small hemosiderin granules (Figure 9.6.3). No granulomas, multinucleated giant cells, necrosis, nuclear pleomorphism, or significant mitotic activity is seen.

The histiocytes are strongly positive for S100 protein and CD68 and are negative for CD1a (Figure 9.6.4). Stains for bacteria, fungi, and acid fast bacilli are negative.

**DIAGNOSIS**

Contents of right nasal cavity and maxillary sinus:  
Rosai-Dorfman disease.

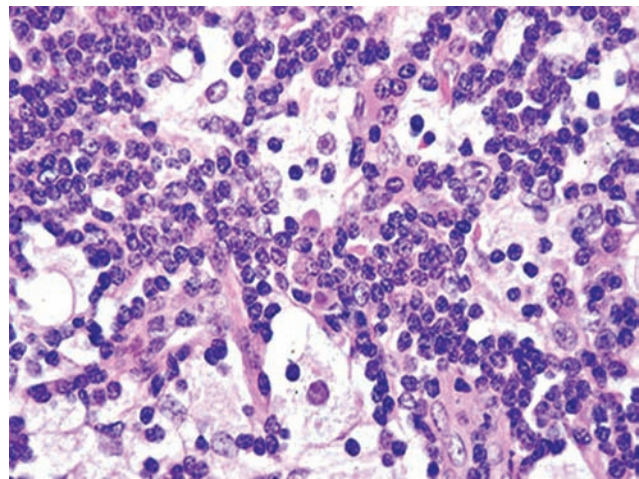


**FIGURE 9.6.2** Higher magnification of Figure 9.6.1 showing lymphocytes in the cytoplasm of the histiocytes (emperipolesis).

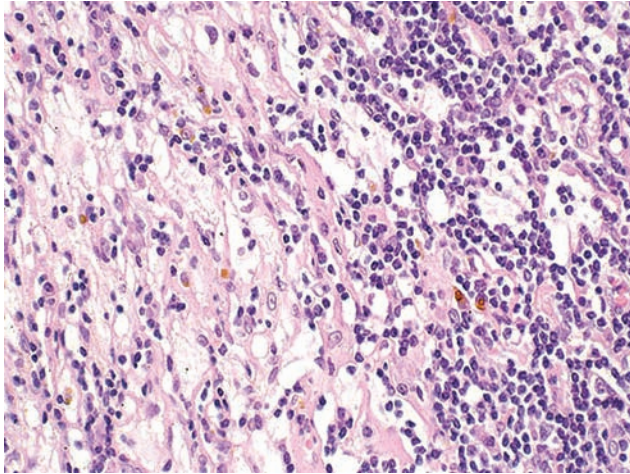


**FIGURE 9.6.3** Areas of fibrosis were also apparent.

#### COMMENT

Extranodal Rosai-Dorfman disease (RDD) is now being recognized more frequently. One of the most common extranodal sites is the sinonasal tract, where it usually manifests as chronic rhinosinusitis.

#### DISCUSSION

Rosai-Dorfman disease (sinus histiocytosis with massive lymphadenopathy) is an idiopathic, histiocytic disorder that was first described by Destombes in 1965

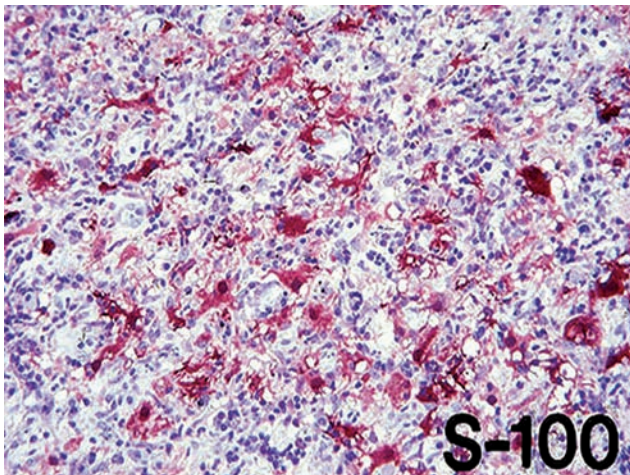


**FIGURE 9.6.4** The clear histiocytes are strongly positive for S100 protein.

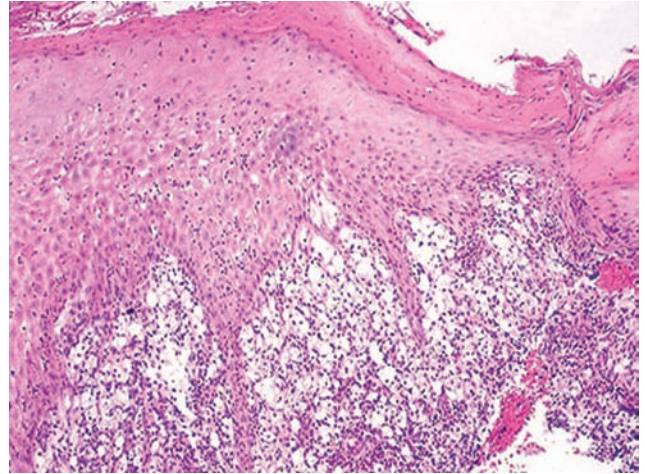


**FIGURE 9.6.5** Rhinoscleroma of the trachea (tracheal scleroma). Normal respiratory mucosa is replaced by hyperplastic, keratinizing squamous epithelium. Note the large sheets of clear cells.

but was recognized as a distinct clinicopathologic entity by Rosai and Dorfman in 1969 (1,2). In its classic form, the disease manifests as a massive, bilateral, painless cervical lymphadenopathy associated with fever, leukocytosis, elevated erythrocyte sedimentation rate, and polyclonal hypergammaglobulinemia (3–8).

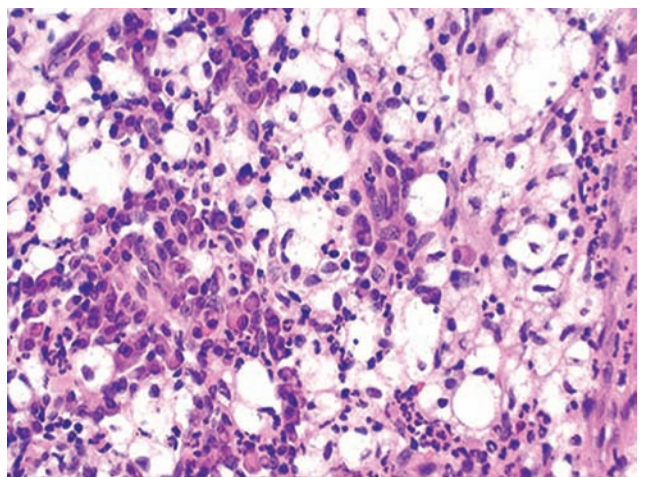


**FIGURE 9.6.6** Higher magnification of Figure 9.6.5. Note the clear cells with admixed lymphocytes, plasma cells, and neutrophils.

## 9.6

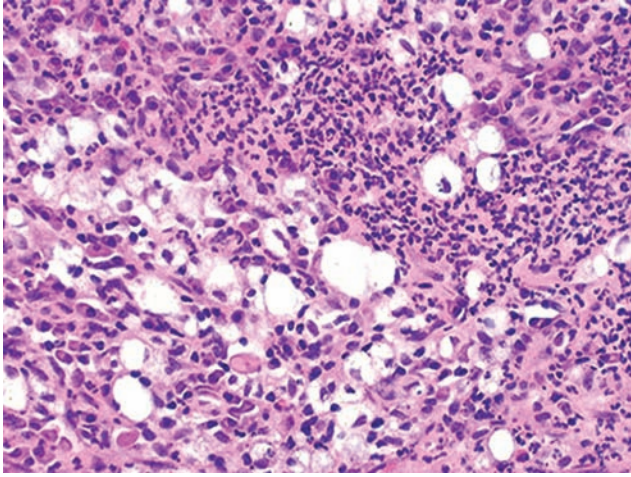


**FIGURE 9.6.7** In other areas of Figure 9.6.5, neutrophilic microabscesses are apparent.

Forty to fifty percent of cases, however, involve extranodal sites, either independent of or in association with lymph nodes. The most common extranodal sites are the skin, sinonasal tract, eyelid-orbit, soft tissue, and bone.

Regardless of site of origin, the pathology is basically similar and consists of a proliferation of histiocytes with clear cytoplasm intimately associated with lymphocytes and plasma cells and occasionally fibrosis. The histiocytes are thought to be of

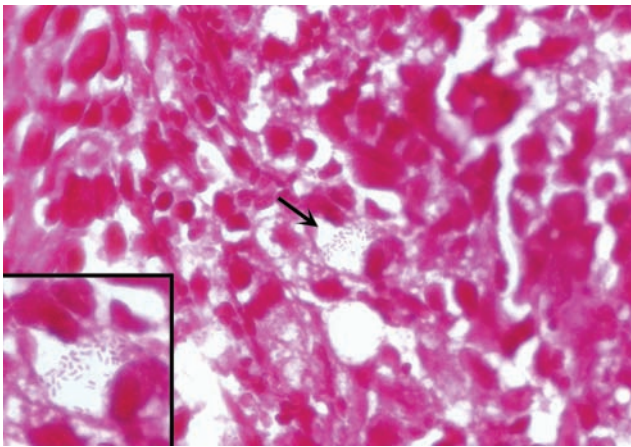


**FIGURE 9.6.8** A tissue Gram stain of Figure 9.6.5 shows Gram-positive coccobacilli within the cytoplasm of the histiocytes (clear cells, Mikulicz cells). See arrow and inset.

monocyte/macrophage lineage and frequently show emperipolesis. They are typically S100 protein–positive and generally immunoreactive for alpha-1-antitrypsin, CD68, lysozyme, and MAC-387. They are negative for CD1a and lack Birbeck granules by electron microscopy.

When the disease involves the sinonasal tract, it often presents as polyps and, as such, is easily mistaken, both clinically and histologically, for a routine case of chronic polypoid rhinosinusitis.

Rhinoscleroma is a chronic, progressive infectious disease with a predilection for the upper aerodigestive tract caused by the Gram-negative coccobacillus *Klebsiella rhinoscleromatis* (9,10). Although uncommon in the United States, the histology can be confused with RDD. The disease is characterized by a diffuse cellular proliferation composed of neutrophils, lymphocytes, plasma cells, and large, foamy macrophages (Mikulicz cells), with eventual fibrosis (Figures 9.6.5, 9.6.6, and 9.6.7). The Mikulicz cells are S100 protein–negative and do not show emperipolesis. Depending on the stage of the disease, the organisms can be identified by a Gram or Warthin-Starry silver stain. Cultures are positive in only about 50% to 60% of cases (Figure 9.6.8).

Leprosy and atypical mycobacterial infections, especially in immunocompromised individuals, may also contain a prominent component of foamy histiocytes. These can be excluded with appropriate stains for organisms.

### References

1. Destombes P. Adenitis with lipid excess, in children or young adults, seen in the Antilles and Mali (4 cases) [in French]. *Bull Soc Pathol Exot Filiales*. 1965;58:1035–1039.
2. Rosai J, Dorfman RF. Sinus histiocytosis with massive lymphadenopathy: A newly recognized benign clinical entity. *Arch Pathol*. 1969;87:63–70.
3. Foucar E, Rosai J, Dorfman RF. Sinus histiocytosis with massive lymphadenopathy. Ear, nose, and throat manifestations. *Arch Otolaryngol*. 1978;104:687–693.

4. Foucar E, Rosai J, Dorfman RF (guest editors). Sinus histiocytosis with massive lymphadenopathy (Rosai-Dorfman disease): A review of the entity. *Semin Diagn Pathol.* 1990;7:19–73 (whole issue devoted to this disorder).
5. Goodnight JW, Wang MB, Sercarz JA, et al. Extranodal Rosai-Dorfman disease of the head and neck. *Laryngoscope.* 1996;106:253–256.
6. Paulli M, Rosso R, Kindl S, et al. Immunophenotypic characterization of the cell infiltrate in five cases of sinus histiocytosis with massive lymphadenopathy (Rosai-Dorfman disease). *Hum Pathol.* 1992;23:647–654.
7. Wenig BM, Abbondanzo SL, Childers EL, et al. Extranodal sinus histiocytosis with massive lymphadenopathy (Rosai-Dorfman disease) of the head and neck. *Hum Pathol.* 1993;24:483–492.
8. Gaitonde S. Multifocal extranodal histiocytosis with massive lymphadenopathy. An overview. *Arch Pathol Lab Med.* 2007;131:1117–1121.
9. Andraca R, Edson RS, Kern EB. Rhinoscleroma: A growing concern in the United States? Mayo Clinic Experience. *Mayo Clin Proc.* 1993;68:1151–1157.
10. Montone KT. Infectious diseases of the head and neck. A review. *Am J Clin Pathol.* 2007;128:35–67.



## 9.7

*Wegener's Granulomatosis*

## CLINICAL INFORMATION

"I am writing to you in consultation with a septal biopsy from a 60-year-old man with a history of chronic nasal congestion. The surgeon noted an ulcer on the septum. The patient has no known past history of vasculitis and no serologic studies. The biopsy demonstrates ulceration with granulation tissue formation and focal granulomatous inflammation. Stains for organisms are negative. The elastic stain shows some disruption of one vessel. The question of Wegener's granulomatosis is raised. I would appreciate your opinion as to whether these changes are diagnostic of such a diagnosis."

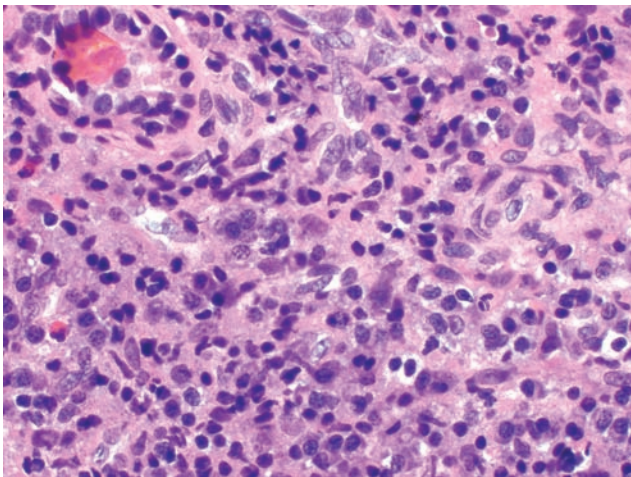


**FIGURE 9.7.1** The cellular infiltrate in Wegener granulomatosis is composed of lymphocytes, histiocytes, neutrophils, and plasma cells. Eosinophils are not prominent. No atypia is seen.

## OPINION

Sections show fragments of respiratory mucosa with focal squamous metaplasia. The lamina propria contains a marked infiltrate of lymphocytes, plasma cells, and neutrophils with a few admixed widely scattered multinucleated giant cells (Figures 9.7.1 and 9.7.2). A rare neutrophilic microabscess surrounded by epithelioid histiocytes and multinucleated giant cells (granulomatous microabscess) is seen, as well as a few areas of stromal necrosis (Figures 9.7.3 and 9.7.4). Blood vessels range from normal to those that show either perivascular fibrosis or luminal obliteration by fibrous tissue with admixed chronic inflammatory cells (Figures 9.7.5 and 9.7.6). No cellular atypia

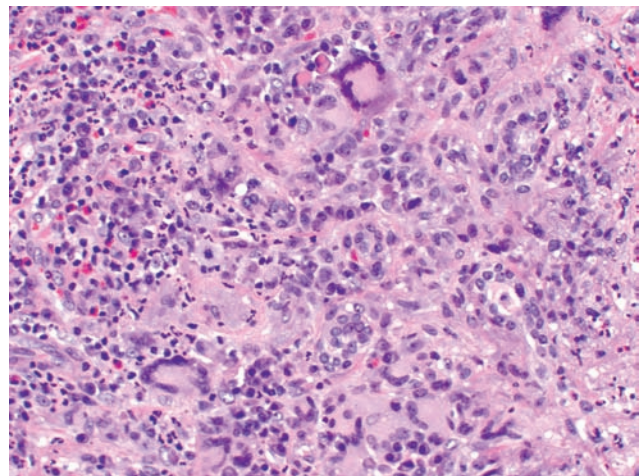


**FIGURE 9.7.2** Scattered multinucleated giant cells.

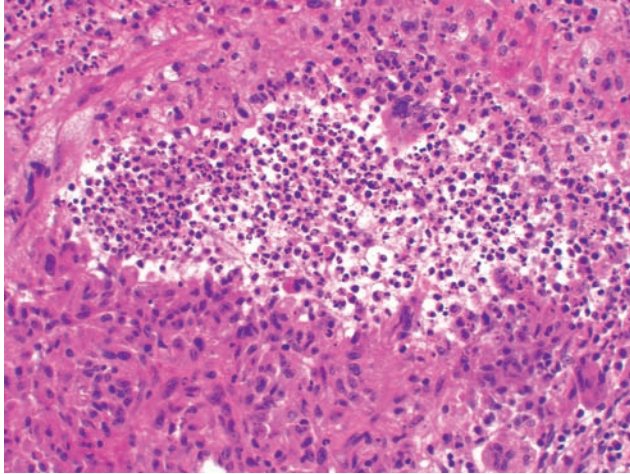


**FIGURE 9.7.3** Granulomatous microabscess composed of a central collection of neutrophils surrounded by epithelioid histiocytes and few multinucleated giant cells.

pia, malignant changes, or foreign material is seen. Special stains for bacteria, fungi, and acid fast bacilli are negative.

#### DIAGNOSIS

Nasal septum, biopsy: Histologic changes suspicious for Wegener granulomatosis.

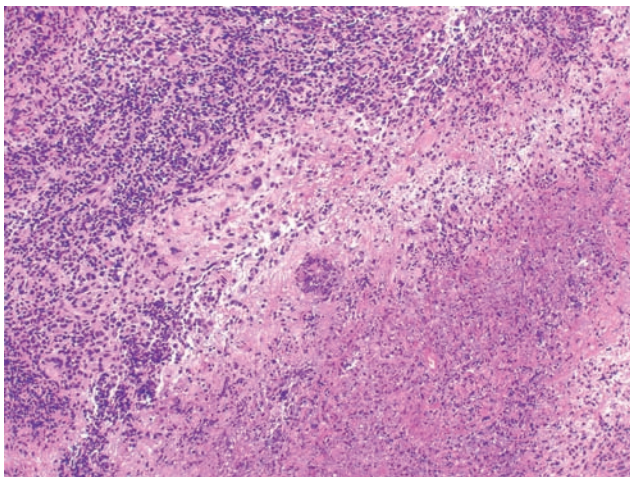


**FIGURE 9.7.4** Area of stromal necrosis.

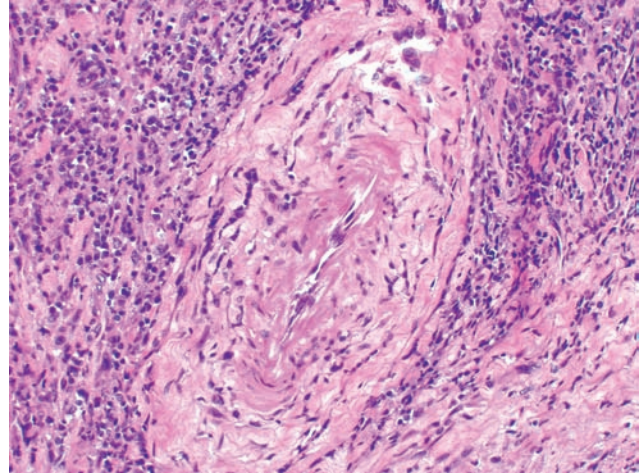


**FIGURE 9.7.5** Blood vessel with perivascular fibrosis.

#### COMMENT

I believe that the histologic changes are suspicious for Wegener granulomatosis. The patient has not yet undergone serologic evaluation for this diagnosis. Clinical correlation and further staging are suggested.

#### DISCUSSION

Wegener granulomatosis is a distinct clinicopathologic entity consisting of a diagnostic triad: (1) Necrotizing granulomatous inflammation and vasculitis of the upper respiratory tract and lungs; (2) systemic vasculitis

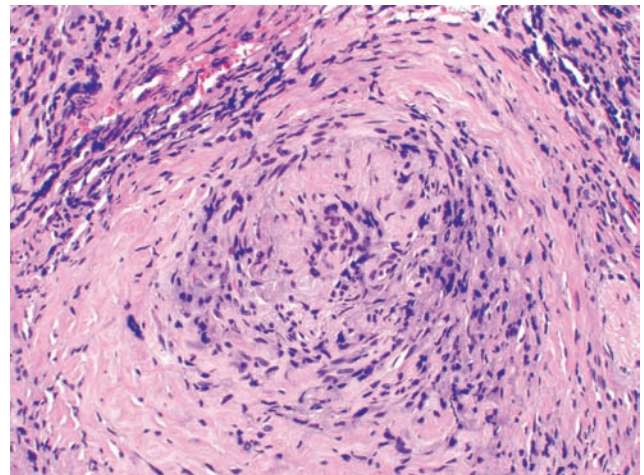


**FIGURE 9.7.6** Another occluded blood vessel with chronic inflammatory cells in the wall.

## 9.7

involving primarily small arteries; and (3) glomerulonephritis (1,2). The disease generally starts with granulomatous inflammation and vasculitis of the upper respiratory tract and lungs, spreads in varying degrees to other organs, and, if left untreated, often fatally terminates in a necrotizing glomerulonephritis.

Just as Wegener granulomatosis consists of a clinical triad of findings, there is also a characteristic histologic triad of findings that consists of (1) vasculitis, (2) necrosis, and (3) granulomatous inflammation (1). The vasculitis may be fibrinoid, granulomatous, acute, or chronic; typically involves small arteries and sometimes veins; and may show varying temporal stages of development (Figures 9.7.5 and 9.7.6). The necrosis is also highly variable. In the classic biopsy, one sees large geographic zones of necrosis (often granular and blue as a result of nuclear fragmentation) surrounded by palisading histiocytes and fibroblasts, multinucleated giant cells, and granulation tissue (Figure 9.7.4). In other instances, one may see fibrinoid necrosis of collagen or microabscesses composed of collections of neutrophils. Sometimes, the microabscesses are surrounded by multinucleated giant cells and/or epithelioid histiocytes (granulomatous microabscesses) (Figure 9.7.3). The granulomas in Wegener granulomatosis range from scattered giant cells to somewhat organized granulomas (but never as “tight” as those seen in sarcoid).

When the diagnosis of Wegener granulomatosis is suspected, a biopsy of the sinonasal mucosa is usually obtained, since this is such a readily accessible site. For adequate biopsy, it is essential that the nasal crust be removed first followed by thorough sampling of the underlying tissue. If the crust is not removed, the biopsy will almost assuredly be returned by the pathologist as “acute and chronic nonspecific inflammation, necrosis, and granulation tissue.”

The frequency of finding the complete histologic triad of vasculitis, necrosis, and granulomas in sinonasal biopsies ranges from 15% to 50% and

depends on the size of the biopsy, the number of sections examined, and the diligence of the pathologist.

Once the diagnosis of Wegener granulomatosis is suspected, serologic studies for antineutrophil cytoplasmic autoantibodies (ANCA) should be obtained, and the patient staged for localized or systemic disease. Wegener granulomatosis is characteristically associated with cytoplasmic (C)-ANCA and only infrequently with perinuclear (P)-ANCA. The sensitivity of this test however varies with the extent of the disease. Cytoplasmic ANCA is found in about 65% of patients with localized disease and 90% or more in patients with systemic disease.

The threshold for the diagnosis of Wegener granulomatosis varies according to the pathologist and the clinician. Knowledge of the ANCA status, however, may convert a “compatible with biopsy” into a firm diagnosis of Wegener granulomatosis.

In this consult case, I believe the histologic changes are suspicious (even diagnostic according to some) of Wegener granulomatosis, but I am unwilling to make a firm diagnosis without further corroborating evidence, including ANCA status and additional clinical signs and symptoms. I believe this conservative approach is warranted because treatment includes powerful medication (corticosteroids and cyclophosphamide), which may not only have potential harmful side effects but may also mask histologic and serologic findings if the disease is not firmly established before therapy.

The differential diagnosis of Wegener granulomatosis includes fungal and mycobacterial infectious agents (excluded by appropriate stains), other ANCA-associated vasculitides (microscopic polyangiitis and Churg-Strauss syndrome), NK/T-cell lymphoma, and drug abuse. Microscopic polyangiitis only infrequently involves the sinonasal tract, does not contain granulomas, and is usually associated with P-ANCA (3,4). Churg-Strauss syndrome commonly involves the sinonasal tract, but unlike Wegener

granulomatosis, it is characteristically associated with asthma, eosinophilia (both peripheral and tissue), and P-ANCA (5). NK/T-cell lymphoma may involve blood vessels but does not contain granulomas. It is also negative for ANCA, positive for the Epstein-Barr virus, and exhibits atypia of the cellular infiltrate (6). Biopsies of patients who abuse drugs intranasally may contain polarizable foreign material with foreign body giant cell reaction (adulterants are often used by “street vendors” to dilute the drug). Vasculitis and ANCA however are not seen (7).

### References

1. Devaney KD, Travis WD, Hoffman G, et al. Interpretation of head and neck biopsies in Wegener's granulomatosis. A pathologic study of 126 biopsies in 70 patients. *Am J Surg Pathol.* 1990;14:555–564.
2. Hoffman GS, Kerr GS, Leavitt RY, et al. Wegener's granulomatosis. An analysis of 158 patients. *Ann Int Med.* 1992;116:488–498.
3. Gal AA, Valasquez A. Antineutrophil cytoplasmic autoantibody in the absence of Wegener's granulomatosis or microscopic polyangiitis: implications for the surgical pathologist. *Mod Pathol.* 2002;15:197–204.
4. Ko Kan N, Hosomi Y, Inamoto S, et al. Microscopic polyangiitis histologically confirmed by biopsy from nasal cavity and paranasal sinuses: a case report. *Rheumatol Int.* 2006;26:936–938.
5. Bacciu A, Bacciu S, Mercante G, et al. Ear, nose and throat manifestations of Churg-Strauss syndrome. *Acta Otolaryngol.* 2006;126:503–509.
6. Chan ACL, Chan JKC, Cheung MMC, et al. Hematolymphoid tumours. In: Barnes L, Eveson JW, Reichart P, Sidransky D, eds. *World Health Organization Classification of Tumours. Pathology and Genetics. Head and Neck Tumours.* Lyon: IARC Press; 2005:58–64.
7. Becker GD, Hill S. Midline granuloma due to illicit cocaine use. *Arch Otolaryngol Head Neck Surg.* 1988;114:90–91.



---

# INDEX

- ACC. *See* acinic cell carcinoma.
- ACC. *See* adenoid cystic carcinoma.
- ACC-HGT, carcinoma ex pleomorphic adenoma, 26  
dedifferentiated epithelial-myoepithelial carcinoma, 26  
immunostains, 26
- ACC-salivary duct carcinoma hybrid tumor, 25
- Acini, 52  
cytokeratins, 52
- Acinic cell carcinoma (ACC), 21–23  
high-grade transformation (HGT), 25  
basophilic zymogen granules, 21  
components, 24  
infiltrative bilayered tubular proliferation, 24  
myxoid acellular matrix, 24  
diagnostics, 25  
ACC-salivary duct carcinoma hybrid tumor, 25  
carcinoma ex pleomorphic adenoma, 25  
dedifferentiated epithelial myoepithelial carcinoma, 25  
monomorphic component, 25  
evaluation, 22–23  
cuboidal intercalated duct-type cells, 23  
cystic salivary lesions, 22  
finely vacuolated cytoplasm, 22  
fibrous pseudocapsule, 21  
high-grade transformation, 24–26  
diagnostics, 25  
pleomorphic tumor cells, 24  
pleomorphic mitotically active high-grade carcinoma, 25  
staining patterns, 24
- ACP. *See* antrochoanal polyp.
- Adenocarcinoma, 47, 67
- Adenoid cystic carcinoma (ACC), 8, 31, 43, 128  
basaloid squamous cell carcinoma vs., 9  
cribriform pattern, 8
- Adenoid squamous cell carcinoma, 2
- Adenomatoid odontogenic tumor, 77
- Adenosquamous carcinoma (AdSC), 3–5  
apical intraluminal mucous secretions, 4  
cervical lymph node, 5  
clinical background, 3  
discussions, 4  
glandular component, 4  
invasive cell, 3 F  
opinion, 3  
prognosis, 4
- Androgen receptor, 26
- AdSC. *See* adenosquamous carcinoma
- Ainic cell carcinoma, androgen receptor, 26
- ALK gene rearrangement, 29
- Ameloblastoma, 74, 92
- Amphophilic cytoplasm focal tubule formation, 41
- Amyloid stroma, 75
- ANCA. *See* antineutrophil cytoplasmic autoantibodies
- Androgen receptor, 35
- Angiofibroma, 59, 125
- Angiolymphatic invasion, 43
- Angiosarcoma (AS), 112–115  
bone trabeculae, 112  
epithelioid, 13  
epithelioid cells, 112  
immunostains, 112  
skeletal muscle, 112  
spindle cells, 112
- Angulated hyper-chromatic cells, 24
- Antineutrophil cytoplasmic autoantibodies (ANCA), 182
- Antrochoanal polyp (ACP), 125

- Apical Intraluminal mucous secretions, 4
- Apple-green firefingence, 76
- AS. *See* angiosarcoma
- Autoimmune disease process, 28
- Basaloid cells, 72
- Basaloid squamous carcinoma, 2
- Basaloid squamous cell carcinoma (BSCC), 6–9, 65
- adenoid cystic carcinoma, 8, 9
  - biphasic pattern, 7
  - distant metastasis, 9
  - human papilloma virus 16, 8
  - hyaline cylinders, 7
  - locations of, 7
    - head and neck, 7
  - metastasis, 9
    - lymph nodes, 9
  - size, 8
  - squamous differentiation, 8
- Basal cell adenocarcinoma, polymorphous low-grade adenocarcinoma vs., 43
- Basophilic zymogen granules, 21
- Bcl-2, 118
- Benign cyst, 86
- Benign fibro-osseous lesion (BFOL), 137
- BFOL. *See* benign fibro-osseous lesion, 137
- Biopsy evaluation, 1
- adenoid squamous cell carcinoma, 2
  - basoloid squamous carcinoma, 2
  - mucoepidermoid carcinoma, 2
  - papillary squamous carcinomas, 1
  - spindle cell lesion, 1
  - keratinizing dysplasias, 1
  - lymphoepithelial carcinoma, 2
- Biphasic pattern, 7
- Biphasic Spindle cell squamous carcinoma, 15
- Biphasic tumor, 31
- Bone trabeculae, 112
- Bone tumors, 129–138
- central giant cell granuloma, 130–132
  - chordoma, 129, 133–135
  - fibro-osseous lesion, 129
  - ossifying fibroma, 136–138
- BRAF mutations, 105
- Branchial cleft cyst (CBCC), 156–160
- age group, 159
  - carcinoma, 156–160
  - cystic lymph nodes metastasis, 159
  - cystic metastasis, 160
  - cystic nonkeratinizing squamous cell carcinoma, 156
  - intracystic papillary tumor projections, 156
  - lymphocytes, 157
  - tonsillar crypts, 159
  - treatment, 158
  - tumor cell arrangement, 157
  - Waldeyer ring carcinomas, 159
- Brown tumor of hyperparathyroidism, 131
- BSCC. *See* basaloid squamous cell carcinoma
- Buccal mucosa, 58
- Calcifying cystic odontogenic tumor (CCOT), 72–74
- adenomatoid odontogenic tumor, 77
  - amyloid stroma, 75
  - apple-green birefringence, 76
  - basaloid cells, 72
  - characteristics, 76–77
  - diagnosis, 74, 77
    - ameloblastoma, 74
  - distinguishing characteristics, 74
  - frequency, 73, 76
  - Gorlin cyst, 73
  - intraosseous, 73
  - lamellar calcification, 76
  - matrix congophilia, 76
  - misdiagnosis, 77
  - myoepithelial subpopulation, 77
  - Pindborg tumor, 75
    - squamous cell carcinoma, 77
- Calcifying epithelial odontogenic tumor (CEOT), 75–77
- Candida hyphae*, 173
- Capsular invasion, 30
- Carcinoids, 98

- Carcinoma, 47, 114  
 adenosquamous, 3–5
- Carcinoma ex pleomorphic adenoma, 25, 26
- Carcinoma metastatic to the thyroid gland, 140–143  
 cytokeratin, 142  
 immunostain, 141  
 intravascular invasion, 140  
 metastases, 143
- Carcinosarcoma, 13–14, 15  
 osteosarcoma, 14
- Castleman disease, 168
- CBCC. *See carcinoma branchial cleft cyst*, 159
- CD34, 118
- CD99, 118
- Cellular pleomorphic adenoma, 31  
 invasiveness of, 31
- Cemento-ossifying fibroma, 137
- Central giant cell granuloma (CGCG), 130–132  
 brown tumor of hyperparathyroidism, 131  
 cherubism, 131  
 giant cell tumor, 131  
 osteoblastic activity, 130, 131  
 patient age, 131  
 reactive osteolytic fibroproliferative growth, 131  
 recurrence rate, 132  
 treatment, 132
- Central mucoepidermoid carcinoma (CMEC), 84
- CEOT. *See calcifying cystic odontogenic tumor*
- Cervical lymph node, 5
- CGCG. *See central giant cell granuloma*
- Cherubism, 131
- Chordoma, 129, 133–135  
 clivus, 133  
 cytokeratin, 135  
 differential diagnostics, 134–135  
 chondrosarcoma, 135  
 immunohistory, 135  
 morphologies, 134  
 myxoid stroma, 133  
 skull base, 134  
 stroma, 135  
 cystic neoplasm, 33–34  
 clearing, 44  
 sarcoma, 135
- Chronic sclerosing sialadenitis (CSS), 27–29, 54, 55  
 diagnosis, 28–28  
 autoimmune disease process, 28  
 IgG4 plasma cell infiltrates, 28  
 inflammatory myofibroblastic tumors, 28, 29  
 lymphoma, 29  
 obliterative phlebitis, 28  
 pseudotumoral inflammatory process, 28  
 serum IgG4 levels, 29  
 sialadenitis, 28  
 Sjogren syndrome, 29  
 submandibular gland, 28  
 granulomatous inflammation, 27, 28  
 obliterative phlebitis, 28  
 periductal lymphoplasmacytic infiltrates, 27  
 submandibular gland, 27
- Churg-Strauss syndrome, 164
- Ciliated epithelium, 87
- Clear cell mucoepidermoid carcinoma, 51
- Clivus chordoma, 133
- Clonal neoplasms, 121
- CMEC. *See central mucoepidermoid carcinoma*.
- Collagen, 161
- Collagenized stroma, 93
- Collision tumor, 13–14
- Comedonecrosis, 24
- Comedo-type necrosis, 45
- Compact capillaries, 124
- CP. *See craniopharyngioma*
- Craniopharyngioma (CP), 90–92  
 Cytokeratin, 90  
 Epstein-Barr virus, 91  
 frequency, 92  
 histological differential diagnosis, 92  
 ameloblastoma, 92  
 odontogenic classifications, 92  
 respiratory nasopharyngeal mucosa, 90  
 wet keratin, 90



- Cribriform growth pattern, 45
- Cribriform pattern, 8
- CSS. *See* chronic sclerosing sialadenitis
- Cuboidal intercalated duct-type cells, 23
- Cutaneous papillomas, 62
- Cystadenocarcinomas, 37, 48
- Cystic change, 36
- Cystic low grade tumors
- oncocytic cystadenoma, 39
  - Warthin tumor, 39, 40
- Cystic lymph nodes metastasis, 159
- Cystic metastasis, 160
- keratinized, 160
- Cystic neoplasm, 33–34
- Cystic nonkeratinizing squamous cell carcinoma, 156
- Cystic salivary lesions, 22
- Cysts, 61
- Cytokeratin, 52, 90, 97, 100, 135, 142
- Cytokeratin 5/6, 14
- Cytokeratin CA 5.2, 30–31
- Cytology, 46
- Dedifferentiated epithelial myoepithelial carcinoma, 25–26
- Dendritic cells, 166–168
- follicular, 166
  - interdigitating, 166
  - Langerhans, 166
  - neoplasms, 168
- Dental follicle, 78–81
- fibromyxoid matrix, 78
  - odontogenesis, 79
  - odontogenic fibroma vs., 80
  - odontogenic keratocyst, 85–87
- Dental lesions, 71–87
- calcifying cystic odontogenic tumor, 72–74
  - calcifying epithelial odontogenic tumor, 75–77
  - dental follicle, 78–81
  - dental papilla, 78–81
  - dentigerous cyst, 80
  - glandula odontogenic cyst, 82–84
  - hematoxylin and eosin, 71
  - keratocystic odontogenic tumor, 85–87
  - myxoma, 78–81
  - odontogenic fibroma, 80
  - odontogenic myxoma, 80
- Dental papilla, 78–81
- odontogenic myxoma vs., 81
- Dentigerous cyst, 80–81, 83
- Dermatologic evaluation, 106
- Desquamated keratin, 85
- Dimorphic fungus, *Histoplasma capsulatum*, 171
- Ductal proliferation, 58
- Ducts
- cytokeratins, 52
  - impact of sclerosing polycystic adenosis, 52
- Dysplasia, 11
- verrucous carcinoma diagnosis and, 18
- Dysplasia/carcinoma in situ, 58
- Dyskeratotic cells, 17
- EAF. *See* eosinophilic angiocentric fibrosis
- EAS. *See* epithelioid angiosarcoma
- EH. *See* epithelioid hemangioendothelioma
- EMCa. *See* epithelial-myoepithelial carcinoma
- Endocrine tumors, 139–154
- carcinoma metastatic to the thyroid gland, 140–143
  - mixed medullary-papillary thyroid carcinoma, 145–148
  - paraganglioma thyroid, 149–151
  - parathyroid adenoma, 152–154
- Endophytic pattern of growth, 68
- Eosinophilic angiocentric fibrosis (EAF), 161–164
- collagen, 161
  - differential diagnosis
    - inflammatory myofibroblastic tumor, 164
    - Churg-Strauss syndrome, 164
    - Wegener granulomatosis, 164  - epidermis, 161
  - etiology, 163
  - frequency, 162
  - granuloma faciale, 162

- pathology, 163–164
- treatment, 164
- Eosin-stained sections, 89
- Epidermis, Grenz zone, 161
- Epithelial attenuation, 120
- Epithelial glandular elements, 103
- Epithelial membrane antigen, 50
- Epithelial myoepithelial carcinomas (EMCa), 30–32, 43
  - capsular invasion, 30
  - cytokeratin CAM 5.2, 30–31
  - diagnosis, 31–32
    - adenoid cystic carcinoma, 31
    - biphasic tumor, 31
    - cellular pleomorphic adenoma, 31
    - Myoepithelial carcinoma, 31
    - occurrences of, 31
  - sites, 31
  - solid nests, myxoid stroma, 30
  - survival rate, 32
  - tubulotrabeular basal
    - adenocarcinoma, 31
    - adenoma, 31
  - tumor description, 30
- Epithelial-stromal interface, 17
- Epithelioid angiosarcoma, 13
  - epithelioid hemangioendothelioma, 113
- Epithelioid cells, 165
- Epithelioid component, 126
- Epithelioid hemangioendothelioma (EH), 113
  - angiosarcoma, 115
  - carcinoma, 114
  - differential diagnosis, 113–114
  - epithelioid sarcoma, 113
  - immunostains, 114
- Epithelioid pleomorphic discohesive neoplastic cells, 104
- Epithelioid sarcoma (ES), 113
- Epithelium, 59, 83
- Epithelioid cells, 112
- Epstein-Barr virus, 64, 91, 168
- ES. *See* epithelioid sarcoma.
- ESP. *See* exophytic Schneiderian papilloma
- Exophytic Schneiderian papilloma (ESP), 60–63
  - cutaneous papillomas vs., 62
  - cysts, 61
  - focal surface keratinization, 61, 62
  - nasal septum, 62
  - nonkeratinized squamous epithelium, 60
  - resected lesion examination, 61
  - Schneiderian membrane, 61
  - sinonasal tract, 61–63
- Exophytic squamous papillary surface, 56
- Exophytic superficial papillomatous squamous component, 58
- FDC. *See* follicular dendritic cells
- Fibromyxoid matrix, 78
- Fibro-osseous lesion, 129
- Fibrotic stroma, 33
- Fibrous pseudocapsule, 21
- Fibrous stroma, 49, 97
- Fine needle aspiration (FNA), 154
- Finely vacuolated cytoplasm, 22
- First branchial cleft abnormalities, 34
  - type I variants, 34
  - type II variants, 34
- FNA. *See* fine needle aspiration
- Focal surface keratinization, 61, 62
- Follicular dendritic cell (FDC) sarcoma, 165–169
  - Castleman disease, 168
  - dendritic cells, 166–168
  - differential diagnosis, 169
  - epithelioid cells, 165
  - Epstein-Barr virus, 168
  - frequency, 167
  - spindle cells, 166
  - treatment, 168
- Follicular dendritic cells (FDC), 166
- Fungus, *Histoplasma capsulatum*, 171
- Ganglionic differentiation, 103
- GCT. *See* giant cell tumor
- Giant cell tumor (GCT), 131

- Glandula odontogenic cyst (GLOC), 82–84  
 age group, 83  
 cure rate, 84  
 dentigerous cysts, 83  
 diagnosis, 84  
   central mucoepidermoid carcinoma, 84  
 epithelium, 83  
 frequency, 82  
 intraepithelial ductile formation, 83
- Glandular component, Adenosquamous carcinoma  
 and, 4
- GLOC. *See* glandular odontogenic cyst.
- Glomangiopericytoma (GPC), 116–119  
 age groups, 118  
 epistaxis, 118  
 glomus tumors, 117  
 hemangiopericytoma-like tumor, 117  
 hyalinized collagen, 117  
 hybrid neoplasms, 117  
 perivascular myoid differentiation, 117  
 physiology, 116  
 recurrences, 119  
 solitary fibrous tumor, 117, 119  
   comparison of, 119  
   bcl-2, 118  
   CD34, 118  
   CD99, 118  
   treatment, 119  
 unilateral nasal obstruction, 118  
 World Health Organization, 118
- Glomus tumors, 117
- Gorlin cyst, 73
- GPC. *See* Glomangiopericytoma
- Gram-negative coccobacillus *Klebsiella rhinoscleromatis*,  
 178
- Granuloma faciale, 162
- Granulomatous inflammation, 27, 28, 182
- Grenz zone, 161
- H & E. *See* hematoxylin and eosin
- Hard palate, 58
- HC. *See* hybrid verrucous carcinoma
- Head and neck carcinoma, basaloid squamous cell, 7
- Head and neck sarcomas, 94
- Head and the neck tumors, 121
- Hemangiopericytoma-like tumor, 117
- Hemangiopericytomas, 125
- Hematoxylin and eosin, 71
- Hematoxylin sections, 89
- Hemosiderin deposition, 152
- HGT. *See* high-grade transformation
- HIradenocarcinoma, 51
- Histoplasma capsulatum*, 171
- Histoplasmosis, 170–172  
 larynx, 171  
 manifestations, 171  
 origins, dimorphic fungus, 171  
 stromal, 170
- HPV 16. *See* human papilloma virus, 16
- Human papilloma virus 16 (HPV 16), 8
- Hyaline cylinders, 7
- Hyalinized collagen, 117
- Hyalinosis, 7
- Hybrid carcinoma, 18
- Hybrid neoplasms, 117
- Hybrid verrucous carcinoma (HC), 10–12  
 evaluation of, 12  
 features of, 10  
 frequency of, 12  
 mild dysplasia, 11  
 pleomorphism, 11  
 prognostic variables, 12  
 stromal inflammatory reaction, 11
- Hyperplastic squamous mucosa, 173
- IDCs. *See* interdigitating dendritic cells
- IgG4 plasma cell infiltrates, 28
- Immunohistochemistry, 95
- Immunostains, 105, 107, 112, 114, 120, 127, 141  
 keratins, 96
- IMT. *See* inflammatory myofibroblastic tumor
- Immunostains, 26

- In situ component, 105  
     salivary duct carcinoma and, 47
- Infiltrative bilayered tubular  
     angulated hyper-chromatic cells, 24  
     proliferation, 24
- Infiltrative solid tumor, 49
- Inflammatory myofibroblastic tumor (IMT), 15, 28, 29, 120–122, 164  
     ALK gene rearrangement, 29  
     clonal neoplasms, 121  
     differential diagnostic, 121  
     epithelial attenuation, 120  
     head and neck, 121  
     immunostains, 120  
     leiomyosarcoma, 122  
     myofibroma, 122  
     spindle cell rhabdomyosarcoma, 122  
     squamous metaplasia, 120  
     systemic inflammatory findings, 121
- Interdigitating dendritic cells (IDCs), 166
- Intracranial meningiomas, 108
- Intracystic papillary tumor projections, 156
- Intraductal mucoepidermoid carcinoma, 58
- Intraductal, 36
- Intraepithelial ductile formation, 83
- Intraosseous, 73
- Intravascular invasion, 140
- Inverted ductal papilloma, 58
- Inverted papillomas (IP), 70
- Inverted Schneiderian papilloma (ISP), 61, 62, 67
- IP. *See* inverted papillomas
- ISP. *See* inverted Schneiderian papilloma
- JTPG. *See* jugulotypanic paraganglioma
- Jugulotypanic paraganglioma (JTPG), 100  
     cytokeratin, 100  
     synaptophysin, 100
- Juvenile ossifying fibroma, 137
- Keratinizing dysplasias, 1
- KCOT. *See* keratocystic odontogenic tumor
- Keratin filled cysts, 33
- Keratinized  
     cystic metastasis, 160  
     squamous epithelium, 97
- Keratinizing  
     morphology, 51  
     squamous epithelium, 123  
     squamous cell carcinoma, 65
- Keratocystic odontogenic tumor (KCOT), 85–87  
     benign cyst, 86  
     chronic inflammation, 87  
     ciliated epithelium, 87  
     desquamated keratin, 85  
     histopathologic features, 86  
     recurrence, 86
- Keratocystoma, 33–34  
     choristoma, cystic neoplasm, 33–34  
     differential diagnosis, 34  
     first branchial cleft abnormality, 34  
     mucoepidermoid carcinoma, 34  
     pleomorphic adenoma with squamous elements, 34  
     squamous cell carcinoma, 34  
     fibrotic stroma, 33  
     keratin filled cysts, 33  
     occurrences of, 33  
     parotid gland, 33  
     survival rate, 34
- Keratohyalin granules, 17
- Keratosis, definition of, 17
- Klebsiella rhinoscleromatis*, 178  
     culturing of, 178
- Kuttner tumor, 55
- Lamellar calcification, 76
- Langerhans, 166
- Large duct involvement, 45
- Larynx, histoplasmosis and, 171
- LCH. *See* lobular capillary hemangioma
- Leiomyosarcoma, 122
- Lesions, 155–183  
     branchial cleft cyst, 156–160

- Lesions (*continued*)
- eosinophilic angiocentric fibrosis, 161–164
  - follicular dendritic cell sarcoma, 165–169
  - histoplasmosis, 170–172
  - Median rhomboid glossitis (MRG), 173–175
  - Rosai-Dorfman disease, 176–178
  - Wegener's granulomatosis, 180–183
- LGSDC. *See* low-grade salivary carcinoma
- Lip, 124
- Lobular capillary hemangioma (LCH), 123–125
- angiofibroma, 125
  - compact capillaries, 124
  - differential diagnosis, 124
    - antrochoanal polyp, 125
  - fibrotic stroma, 125
  - keratinizing squamous epithelium, 123
  - locations, 124
    - lip, 124
    - nasal cavity, 124
    - respiratory epithelium, 123
    - sinonasal-type hemangiopericytomas, 125
- Lobular nested round blue bell tumor, 101
- Low-grade cribriform cystadenocarcinoma, 35–37
- Low-grade salivary duct carcinoma (LGSDC), 35–37
- androgen receptor, 35
  - cystadenocarcinomas, 37
  - cystic change, 36
  - diagnosis, salivary duct carcinoma, 36
  - frequency of, 36
  - intraductal, 36
  - low-grade cribriform cystadenocarcinoma vs., 35
  - monomorphic tumor nests, 35
  - parotid gland, 36
  - S100, 35
  - sclerotic stroma, 35
- Lymph nodes, 9, 178
- enlargement of, 17
- Lymphocytes, 157
- Lymphoepithelial carcinoma, 2
- Lymphoma, 29
- Lytic lesion, 136
- Macrocystic mass, 38
- Malignancy probability, salivary gland tumors, 19
- Malignant peripheral nerve sheath tumor (MPNST), 93–96
- collagenized stroma, 93
  - differential diagnosis, 95
    - immunohistochemistry, 95
    - immunostains for keratins, 96
    - markers, 96
    - melanocytic markers, 96
    - solitary fibrous tumors, 96
  - head and neck sarcomas, 94
  - parapharyngeal, 94
  - schwannomas, 94
- MAML2 FISH, 51
- Matric congophilia, 76
- MEA. *See* middle ear adenoma
- MEC, salivary duct carcinoma vs., 48
- MEC. *See* mucoepidermoid carcinoma
- Median rhomboid glossitis (MRG), 173–175
- Candida hyphae*, 173
  - classic form, 177
  - differential diagnosis, 174–175
  - extranodal sites, 178
  - frequency, 174
  - hyperplastic squamous mucosa, 173
  - keratosis, 174
  - lymph nodes, 178
  - pathology, 178
  - rhinoscleroma, 178
  - sinonasal tract, 178
  - site, 173
    - midline dorsal tongue, 173, 175
- Melanocytic
- markers, 96
  - nevus, 105
- Metastases, 143
- Metastasis, 47
- basaloid squamous cell carcinoma, 9
  - distant, 9
- Microcystic mass, 38

- 
- Middle ear adenoma (MEA), 97–100
- carcinoids, 98
  - common manifestations, 99
  - cures, 99
  - cytokeratin, 97
  - differential diagnosis, 100
    - jugulotypanic paraganglioma, 100
    - otitis media with glandular metaplasia, 100
  - fibrous stroma, 97
  - frequency, 98, 99
  - keratinized squamous epithelium, 97
  - neuroendocrine
    - adenomas, 98
    - differentiation, 98
  - otitis media with glandular metaplasia, 100
  - recurrence, 99
  - synaptophysin, 97
  - World Health Organization, 99
- Middle ear mucosa, 107
- Midline dorsal tongue, 173, 175
- Mild dysplasia, 17
- Minor salivary glands, 58
- Mixed medullary-papillary thyroid carcinoma (MTC-PTC), 145–148
- differential diagnosis, 147–148
  - metastasis, 146
  - pathogenesis, 148
  - sclerotic stroma, 145
  - thyroglobulin stain, 145
  - thyroid tumors, 147
- Mixed olfactory neuroblastoma-adenocarcinoma, 101–103
- epithelial glandular elements, 103
  - frequency, 103
  - ganglionic differentiation, 103
  - lobular nested round blue cell tumor, 101
  - monomorphic tumor cells, 101
  - olfactory neuroepithelium, 102
  - stroma, 102
- Monomorphic component, acinic cell carcinoma and, 25
- Monomorphic tumor, 43
- cells, 101
  - speckled chromatin, 101
    - nests, 35
- Monophasic spindle cell squamous carcinoma, 15
- MPNST. *See malignant peripheral nerve sheath tumor*
- MRG. *See median rhomboid glossitis*
- MTC-PTC. *See mixed medullary-papillary thyroid carcinoma*
- Mucicarmine, 49, 50
- stain, 40
- Mucinous/sebaceous cells, mimicking of, 22
- Mucoepidermoid carcinoma (MEC), 2, 34, 39, 47
- percentage that are oncocytic mucoepidermoid carcinoma, 39
- Mucosal malignant melanoma (MMM), 104–106
- BRAF mutations, 105
  - dermatologic evaluation, 106
  - frequency, 105
  - immunostains, 105
  - in situ component, 105
  - melanocytic nevus, 105
  - NRAS mutations, 105
  - squamous mucosa, 104
  - subglottic region, 105
- Muir-Torre syndrome, 50
- Myoepithelial
- carcinoma, 31
  - subpopulation, 77
- Myoepithelioma carcinoma, 31
- invasiveness of, 31
- Myofibroma, 122
- Myxoid acellular matrix, 24
- Myxoid stroma, 30, 133
- Myxoma, 78–81
- Nasal septum, 62
- Nasal cavity, 124–125
- Nasopharyngeal carcinoma, 64–66
- basaloid squamous cell carcinoma, 65
  - diagnosis, 66
    - primary lymphoepithelial carcinoma, 66
    - sinonasal undifferentiated carcinoma, 66

- Nasopharyngeal carcinoma (*continued*)  
 Epstein-Barr virus, 64  
 frequency of, 64  
 keratinizing squamous cell carcinoma, 65  
 nonkeratinizing carcinoma, 65–66  
 undifferentiated variant, 66  
   Regaud pattern, 66  
   Schmincke pattern, 66  
 World Health Organization classification, 65
- Nasopharynx, 59–70  
 angiofibroma, 59  
 epithelium, 59  
 physiology, 59
- Neck carcinoma, basoid squamous cells, 7
- Necrosis, 182
- Necrotic foci calcification, 46
- Neoplasms, 168
- Neural-neuroectodermal lesions, 89–109  
 craniopharyngioma, 90–92  
 eosin-stained sections, 89  
 hematoxylin sections, 89  
 malignant peripheral nerve sheath tumor, 93–96  
 malignant peripheral nerve sheath tumor, 93–96  
 middle ear adenoma, 97–100  
 mixed olfactory neuroblastoma-adenocarcinoma, 101–103  
 mucosal malignant melanoma, 104–106  
 secretory meningioma, 107–108  
 sinonasal tract, 89  
 small round cell neoplasms, 89  
 supraglottic larynx, 89
- Neuroendocrine adenomas, 98
- Neuroendocrine differentiation, 98
- Neurofibromatosis, 94
- Nonciliated glands, 69
- Nonkeratinized squamous epithelium, 60
- Nonkeratinizing carcinoma, 65–66
- NRAS mutations, 105
- Obliterative phlebitis, 28
- Odontogenesis, 79
- Odontogenic fibroma, 8, 80  
 dental follicle vs., 80
- Odontogenic keratocyst, 85–87
- Odontogenic myxoma, 80  
 dental papilla vs., 81
- Odontogenic tumors, 76
- OF. *See* ossifying fibroma
- Olfactory Mucosal malignant melanoma, neuroepithelium, 102
- OMEK. *See* oncocytic mucoepidermoid carcinoma
- OMGM. *See* Otitis media with glandular metaplasia
- Oncocytic carcinoma, 39
- Oncocytic cystadenoma, 39
- Oncocytic mucoepidermoid carcinoma (OMEK), 38–40  
 mucoepidermoid carcinoma, 39  
 cystic low grade key features, 40  
   mucicarmine stain, 40  
   oncocytic cystadenoma, 39  
   translocation, 40  
 macrocystic mass, 38  
 microcystic mass, 38  
 mucoepidermoid carcinoma, 39  
 parotid gland, 39  
 prominent lymphoid stroma, 38, 39  
 solid intermediate grade, oncocytic carcinoma, 39  
 Warthin tumor, 39, 40
- Oncocytic Schneiderian papilloma (OSP), 61, 62
- Oncocytoma carcinoma, 39
- OSP. *See* oncocytic Schneiderian papilloma
- Osseous dysplasia, 138
- Ossifying fibroma (OF), 136–138  
 benign fibro-osseous lesion, 137  
 cemento-ossifying fibroma, 137  
 differential diagnosis, 138  
 frequency, 137  
 juvenile, 137  
 lytic lesion, 136  
 osseous dysplasia, 138  
 radiologic impression, 137  
 stroma, 137  
 treatment of, 137

- Osteoblastic activity, 130, 131
- Osteosarcoma, 14, 15
- Otitis media, 108
- Otitis media with glandular metaplasia (OMGM), 100
- Ovoid nuclear contours, 44
- P63, 50
- PAP. *See* prostate acidic phosphate
- Papillary keratosis (PK), 16–18
- hybrid carcinoma, 18
  - keratohyalin granules, 17
  - mild dysplasia, 17
  - rete pegs, 18
  - verrucous carcinoma, distinguishing between, 17–18
- Papillary predominant growth pattern, 43
- Papillary squamous carcinomas, 1
- Paraganglioma (PG), 149–151
- anatomic locations, 150
  - differential diagnosis, 150
  - immunohistory, 149
  - paraganglioma, 149
  - sclerosing foci, 151
- Parapharyngeal malignant peripheral nerve sheath tumor, 94
- frequency, 94
  - neurofibromatosis, 94
- Parathyroid adenoma, 152–154
- fine-needle aspiration, 154
  - histologic sectioning, 153
  - vascular proliferation, 152
  - hemosiderin desposition, 152
- Parotid gland, 19, 33, 36, 39, 49, 54
- PAS. *See* periodic acid Schiff
- PASD, zymogen granules, 21
- Periductal lymphoplasmacytic infiltrates, 27
- Perineural invasion, 50
- Periodic Acid Schiff (PAS), 107
- Perivascular myoid differentiation, 117
- PG. *See* paraganglioma
- Pindborg tumor. *See* calcifying cystic odontogenic tumor
- PK. *See* papillary keratosis
- Plasmacytoid infiltrate, 56
- Plemorphic tumor cells, 24
- comedonecrosis, 24
- Pleomorphic adenoma, 25
- with squamous elements, 34
- Pleomorphic mitotically active high-grade carcinoma, 25
- Pleomorphic nuclei, 49
- Pleomorphism, 11
- PLGA. *See* Polymorphous low-grade adenocarcinoma
- Polycystic disease, 4, 54
- Polymorphous low-grade adenocarcinoma (PLGA), 41–44
- adenoid cystic carcinoma, 43
  - amphophilic cytoplasm focal tubule formation, 41
  - angiolymphatic invasion, 43
  - basal cell adenocarcinoma vs., 43
  - chromatin clearing, 44
  - cytonuclear features, 43
  - epithelial myoepithelial carcinomas, 43
  - markers, 43
  - monomorphic, 43
  - ovoid nuclear contours, 44
  - prognosticators, 43
  - papillary predominant growth pattern, 43
  - recurrence rate, 42
  - recurrent tumor, 42
  - S100 immunostaining, 41
  - stroma, 43
  - submucosal nodule, 41
  - tongue tumors, 43
- Polypoid, 15
- lesion, 67
- Primary lymphoepithelial carcinoma, 66
- Prominent lymphoid stroma, 38, 39
- Prostate acidic phosphate (PAP), 46
- Prostate-specific antigen (PSA), 46
- PSA. *See* prostate-specific antigen
- Psammoma body like calcifications, 46
- Pseudotumoral inflammatory process, 28
- RDD. *See* Rosai-Dorfman disease
- Reactive osteolytic fibroproliferative growth, 131



- Reactive stroma, Spindle cell squamous carcinoma and, 13–14
- Recurrence rate, polymorphous low-grade adenocarcinoma and, 42
- Recurrent tumor, 42
- Regaud pattern, 66
- Resected lesion examination, 61
- Respiratory epithelial adenomatoid hamartoma (REAH), 67–70
- adenocarcinoma, 70
  - appearance, 67
  - appearance, polypoid lesion, 67
  - composition of, 68
  - cure, 67
  - endophytic pattern of growth, 68
  - frequency, 68
  - inverted papillomas, 70
  - inverted Schneiderian papilloma, 67
  - nonciliated glands, 69
  - physiology, 68
  - respiratory epithelium, 69
  - squamous epithelium, 69
  - well-differentiated adenocarcinoma, 67
- Respiratory epithelium, 69, 123
- Respiratory nasopharyngeal mucosa, 90
- Rete pegs, 18
- Rhinoscleroma, 178
- gram-negative coccobacillus *Klebsiella rhinoscleromatis*, 178
- Rosai-Dorfman disease (RDD), 176–178
- S100 immunostaining, 41
- Salivary duct carcinoma (SDC), 36, 37, 45–48, 128
- comedo-type necrosis, 45
  - cribriform growth pattern, 45
  - cystadenocarcinomas, 48
  - cytology, 46
  - diagnosis
    - adenocarcinoma, 47
    - carcinoma, 47
  - frequency of, 47
  - in situ, 37
    - component, 47
  - large duct involvement, 45
  - markers, 47
  - MEC vs., 48
  - mucoepidermoid carcinoma, 47
  - necrotic foci calcification, 46
  - prostate acidic phosphate, 46
  - prostate-specific antigen, 46
  - psammoma body like calcifications, 46
  - diagnosis, metastasis, 47
- Salivary gland sebaceous carcinoma, 49–51
- age distribution, 50
  - clear cell mucoepidermoid carcinoma, 51
  - diagnosis, 51
    - tumor location, 51
  - epithelial membrane antigen, 50
  - fibrous stroma, 49
  - frequency of, 50
  - hidradenocarcinoma, 51
  - infiltrative solid tumor, 49
  - keratinizing morphology, 51
  - MAML2 FISH, 51
  - mucicarmine, 49, 50
  - Muir-Torre syndrome, 50
  - P63, 50
  - parotid lesion, 49
  - perineural invasion, 50
  - pleomorphic nuclei, 49
  - skin adnexal, 50
  - squamous cell carcinoma, 51
- Salivary glands, 19–58
- acinic cell carcinoma, 21–23
    - high-grade transformation, 24–26
  - chronic sclerosing sialadenitis, 27–29
  - epithelial-myoepithelial carcinoma, 30–32
  - keratocystoma, 33–34
  - low-grade salivary duct carcinoma, 35–37
  - malignancy probability, 19
  - oncocytic mucoepidermoid carcinoma, 38–40
  - parotid, 19

- polymorphous low-grade adenocarcinoma, 41–44  
 salivary duct carcinoma, 45–48  
 sclerosing polycystic adenosis, 52–55  
 sialadenoma papilliferum, 56  
 sublingual, 19  
 submandibular, 19  
 tumor, World Health Organization histological classification, 20  
 Sarcomas, head and neck, 94  
 Schmincke pattern, 66  
 Schneiderian membrane, 61  
 Schwannomas, 94  
 Sclerosing foci, 151  
 Sclerosing polycystic adenosis (SPA), 52–55  
   Acini, 52  
     cytokeratins, 52  
   age distribution, 54, 55  
   chronic sclerosing sialadenitis, 55  
   ducts, 52  
     cytokeratins, 52  
   diagnosis, 53–54  
     carcinoma, 54  
     chronic sclerosing sialadenitis, 54  
     parotid gland, 54  
     polycystic disease, 54  
     Kuttner tumor, 55  
     polycystic disease, 54  
     submandibular glands, 54  
   treatment, 53, 55  
 Sclerotic stroma, 35, 145  
 SCSC. *See spindle cell squamous carcinoma*  
 SDC. *See salivary duct carcinoma*  
 Secretory meningioma, 107–108  
   differential diagnosis, 108  
   immunostains, 107  
   intracranial meningiomas, 108  
   middle ear mucosa, 107  
   otitis media, 108  
   Periodic Acid Schiff, 107  
 Serum G4 levels, 29  
 SFT. *See solitary fibrous tumor*  
 Sialadenitis, 28  
 Sialadenoma papilliferum (SP), 56  
   buccal mucosa, 58  
   diagnosis, 58  
   ductal proliferation, 58  
   exophytic superficial papillomatous squamous, 58  
   intraductal mucoepidermoid carcinoma, 58  
   inverted ductal papilloma, 58  
   exophytic squamous papillary surface, 56  
   frequency of, 57  
   hard palate, 58  
   malignant components, 58  
   minor salivary glands, 58  
   plasmacytoid infiltrate, 56  
   recurrence, 57  
   soft palate, 58  
   squamous component, dysplasia/carcinoma in situ, 58  
 Sinonasal tract, 61–63, 89, 178  
   epithelium, 59  
   Nasopharynx, 59–70  
     exophytic Schneiderian papilloma, 60–63  
     nasopharyngeal carcinoma, 64–66  
     respiratory epithelial adenomatoid hamartoma, 67–70  
   papillomas  
     inverted Schneiderian papilloma, 61, 62  
     oncocyctic Schneiderian papilloma, 61, 62  
     physiology, 59  
 Sinonasal type hemangiopericytomas, 125  
 Sinonasal undifferentiated carcinoma (SNUC), 66  
 Sjogren syndrome, 29  
 Skeletal muscle, 112  
 Skin adnexal organs, 50  
 Skull base chordoma, 134  
 Small round cell neoplasms, 89  
 SNUC. *See sinonasal undifferentiated carcinoma*  
 Soft palate, 58  
 Soft tissue tumors, 111–128  
   angiosarcoma, 112–115

- Soft tissue tumors (*continued*)
- glomangiopericytoma, 116–119
  - inflammatory myofibroblastic tumor, 120–122
  - lobular capillary hemangioma, 123–125
  - physiology, 111
  - synovial sarcoma, 126–128
- Solitary fibrous tumor (SFT), 96, 117, 119
- bcl-2, 118
  - CD34, 118
  - CD99, 118
- SP. *See* sialadenoma papilliferum
- SPA. *See* Sclerosing polycystic adenosis
- Speckled chromatin, 101
- Spindle cells, 112, 166
- Lesion, 1
- Spindle cell rhabdomyosarcoma, 122
- Spindle cell squamous carcinoma (SCSC), 1, 13–15, 14
- biphasic, 15
  - carcinosarcoma, 15
  - cytokeratin 5/6, 14
  - diagnosis, 15
  - inflammatory myofibroblastic tumor vs., 15
  - male rate, 15
  - mitoses, 14
  - monophasic, 15
  - osteosarcoma, 15
  - polypoid, 15
  - spindle cells, 14
  - squamous mucosa, 14
  - types, 13–14
    - carcinosarcoma, 13–14
    - collision tumor, 13–14
    - reactive stroma, 13–14
- Squamous cell carcinoma, spindle cell, 13–15
- Squamous cell carcinoma, 34, 51, 77
- basaloid squamous cell carcinoma, 6–9
  - biopsy evaluation, 1
  - hybrid verrucous carcinoma, comparison of, 11
  - pleomorphism, 11
  - spindle cell, 1
    - variants, 1–18
      - verrucous, 1
    - verrucous carcinoma, papillary keratosis, 16–18
- Squamous differentiation, 8
- Squamous metaplasia, 120
- Squamous mucosa, 14, 104
- SS. *See* synovial sarcoma
- Staining patterns, acinic cell carcinoma and, 24
- Stroma, 135, 137
- Stroma, 137
- Stromal inflammatory reaction, 11
- Subglottic region, 105
- Sublingual glands, 19
- Submandibular glands, 19, 28, 54
- Submucosal nodule, 41
- Submandibular gland, 27
- Supraglottic larynx, 89
- Surface squamous dysplasia, 3 F
- Synaptophysin, 97, 100
- Synovial sarcoma (SS), 126–128
- adenoid cystic carcinoma, 128
  - epithelioid component, 126
  - immunostains, 126
  - salivary duct carcinoma, 128
- Systemic inflammatory findings, 121
- Tangential embedding, 1
- Thyroglobulin, stain, 145
- Thyroid gland, carcinoma metastatic to, 140–143
- Thyroid tumors, 43, 147
- Tongue, midline dorsal, 173, 175
- Tonsillar crypts, 159
- Translocation, 40
- Tubulotrabeular basal cell
- adenocarcinoma, 31
  - adenoma, 31
    - invasiveness of, 31
- Tumors
- cells, branchial cleft cyst and, 157
  - salivary gland, 19
  - World Health Organization histological classification of, 20

- Unilateral nasal obstruction, 118
- Vascular nuclei, 6
- Vascular proliferation, 152
- Vasculitis, 182
- VC. *See* verrucous carcinoma
- Verrucous carcinoma (VC)
- diagnosis of, dysplasia, 18
  - dyskeratotic cells, 17
  - early form, 18
  - epithelial-stromal interface, 17
  - lymph node enlargement, 17
  - papillary keratosis, 16–18
    - distinguishing between, 17–18
- Verrucous squamous cell carcinoma, 1
- Waldeyer ring carcinomas, 159
- Warthin tumor, 39, 40
- Wegener's granulomatosis, 164, 180–183
- antineutrophil cytoplasmic autoantibodies, 182
  - beginning symptoms, 181–182
  - Churg-Strauss syndrome, 182
  - differential diagnosis, 182–183
    - antineutrophil cytoplasmic autoantibodies, 182
  - findings, 182
    - necrosis, 182
    - vasculitis, 182
  - frequency, 182
  - granulomatous inflammation, 182
  - treatment, 182
- Wet keratin, 90
- World Health Organization
- glomangiopericytoma, 118
  - histological classification of tumors, 20
  - middle ear adenoma, 99
  - nasopharyngeal carcinoma classification, 65
- Zymogen granules, 21, 23

# HEAD AND NECK PATHOLOGY

Leon Barnes, MD

Simion I. Chiosea, MD

Raja R. Seethala, MD

## Add Expert Analysis of Difficult Cases to Your Practice with Consultant Pathology

Intended for busy practitioners, this text provides the guidance to resolving the real world problems pathologists face when diagnosing head and neck tumors. Examples of fifty head and neck tumors running the gamut from the common to the very rare are included. The wide variety of cases covers the entire scope of head and neck pathology and affords the opportunity to review the basics for the beginning or relatively inexperienced pathologists as well as the chance to examine some of the rare examples of head and neck disease.

Each case features actual consultation reports; a brief clinical history, in-depth review of the expert's analysis and diagnostic process; amplified descriptions and references to the literature; and high-quality photomicrographs.

### All Consultant Pathology Titles Provide:

- ACTUAL consultation cases and expert analysis
- EXPERT analysis provides a detailed discussion of the reasoning behind the diagnosis of each case
- COMPREHENSIVE coverage of challenging diagnoses
- THE CASES are richly illustrated with high-quality photomicrographs

### About the Authors

**Leon Barnes, MD**, Professor of Pathology and Otolaryngology, University of Pittsburgh School of Medicine, and Chief, Division of Head and Neck Pathology, University of Pittsburgh Medical Center, and Professor of Oral and Maxillofacial Pathology, University of Pittsburgh School of Dental Medicine, Pittsburgh, Pennsylvania

**Simion I. Chiosea, MD**, Assistant Professor of Pathology, University of Pittsburgh Medical Center, and Department of Pathology, Presbyterian Hospital, Pittsburgh, Pennsylvania

**Raja R. Seethala, MD**, Assistant Professor of Pathology and Otolaryngology, University of Pittsburgh Medical Center, Pittsburgh, Pennsylvania

Recommended  
Shelving  
Classification  
**Pathology**



**demosMEDICAL**

11 W. 42nd Street, 15th Floor  
New York, NY 10036  
www.demosmedpub.com

